Microneedle assisted percutaneous delivery of lidocaine carboxymethylcellulose with gelatine co-polymer hydrogel

Atul Nayak

A thesis submitted in partial fulfilment of the requirements for the degree of doctor of philosophy

August 2015

Abstract

Local anaesthetic drugs are usually administered as symptom relieving drug formulations for the treatment of pain in superficial skin extremities. The anaesthesia is delivered into skin tissues at the site of pain because of nociceptive receptors. Concerns that exist regarding local anaesthetic drug formulations are low drug encapsulation efficiency, polydispersity of colloidal formulations, chemical interactions of released local anaesthetic drug with skin proteins and bulk viscoelastic properties. Complimenting drug formulation characteristics are the desirable rates of controlled release of drug molecules from chosen formulations pertaining to favourable in vitro skin permeation kinetics are imperative pharmaceutics based research areas because skin percutaneous delivery has distinct barrier property restrictions for passive diffusion (PD) of active molecules. Lidocaine is currently the active anaesthetic molecule of choice in local anaesthesia by clinicians because of minimum toxicity and good potency. It is a low molecular weight drug comprising of electron donating and electron withdrawing functional groups with the capacity to interact by hydrogen bonding and electrostatic interactions with several drug formulation vehicles.

In this work, a naturally occurring bi-polymeric formulation was achieved with lidocaine NaCMC:gelatine hydrogel. Lidocaine NaCMC:gelatine ratio of 1:2.3 was the most favourable formulation because of faster skin permeation kinetics. Lidocaine NaCMC:gelatine 1:2.7 provided the highest drug encapsulation efficiency. This resulted in high, sustained permeation rates after adaptation of the microneedle (MN) “poke and patch” technique, past the stratum corneum layer of skin for quick target delivery in attaining a maximum permeation flux of near 6.0 $\mu g/cm^2/h$ in the hypodermis layer. Mass balance of in vitro studies using an indirect approach to quantify lidocaine permeation showed significant lidocaine permeation

in skin. Subsequent vertical and horizontal (depth averaged) in vitro studies using similar MN techniques resulted in crossing minimum therapeutic level across a 10 mm radius from the epicentre of the skin sample at major reduced lag times of minutes for vertical permeation and within 0.5 hours for horizontal permeation. Furthermore, the spreadability of lidocaine NaCMC:gelatine hydrogel shows favourability in the control of droplet spreading on MN treated skin.

Keywords: Lidocaine, In Vitro drug release, Microneedles, Hydrogel, Polymer, drug permeation, Passive diffusion, Spreadability

Acknowledgements

Firstly, I owe a huge debt of gratitude to my parents Mrs Ashalata Nayak and Dr. Vithal Nayak, a retired associate specialist physician, for encouraging my interest through academia since secondary curricula. I have a lot of hope and dedication from their immense support. Secondly, I owe a huge debt of gratitude to Dr Diganta B. Das, Supervisor, and Dr G.T. Vladisalvijeć, co-supervisor, for supporting and guiding my overall efforts towards bonafide research and development leading to this thesis. I feel that I have strongly acquired substantially improved explanation of the science, innovative concept and technological aspects of my work. They have constantly stimulated my research interests and encouraged me to pay fine attention to detail in all aspects of my research work. I am very pleased with the contribution of Mr Hiten Babla and Mr Liam Short towards this research. They have shown great willingness and determination in learning experimental characterisation, raw data analysis and scientific report writing.

I am very grateful to Mr S. Creedon, Laboratory Supervisor, Mr D. Smith, Snr. Laboratory Technician, Mr Tony Eyre, Experimental Officer, and Ms Monika Peritzek, Bio-analytical Laboratory Technician, for their guidance in experimental methods and techniques. I am equally very grateful to Mr T. Han and Miss K. Cheung for fine discussions and guidance as my respective peers.

Contents

List of figures

List of tables

Abbreviations and acronyms

d	Density
DI	Deionised water
EMLA	Eutectic mixture of local anaesthetics
FDC	Franz diffusion cell
HPLC	High performance liquid chromatography
LC-DA	Liquid chromatography – diode array
LFS	Low frequency sonophoresis
MN	Microneedles
NaCMC	Sodium Carboxymethylcellulose
NIPAAm	N-isoproplacrylamide
PBS	Phosphate buffer solution
PD	Passive diffusion
PDMS	Polydimethylsiloxane
SC	Stratum Corneum
SPAN	Sorbitan mono-oleate
TD	Transdermal delivery
VE	Viable Epidermis
W/O	Water in oil
W/O/W	Water in oil in water

Glossary

Aspect ratio

Scalar dimensional length against width ratio of a micron scale needle, e.g. an aspect ratio of 4:1 means a factor 4 increase in length in relation to the width with a factor of 1.

Auricle

Anatomical name for the external and visible part of the ear located on the head.

B. mori cacoons

Natural silk cocoon fibrons spun by the silkworm, Bombyx mori.

Biodegradable polymer

A polymer which degrades mainly by hydrolysis over time into smaller molecular weight monomer units.

Bipolymer

A polymer vehicle consisting of two polymers chemically bound. For example, NaCMC and gelatine combined are known as a bipolymer.

Bolus

An fast administered quantity of intravenous drug for rapid drug delivery.

Co-drug

Two or more active drugs joined by covalent bonds for the purpose of improving the drug delivery of one or more drugs. A co-drug is pharmaceutically inactive before cleavage of covalent bonds by enzymes in target tissues.

Coat and poke

Technique for coating microneedles in a layer of drug and piercing the microneedles through the skin, the drug coating dissolves into the skin. The coating can be applied by rolling, spraying or dipping the formulation onto the microneedles.

Daltons

A unit of measure of the total molecular weight of biomacromolecules. Permissible values are from hundreds to hundred thousands of daltons.

Diffusion Coefficient (D)

A mass of a compound diffusing into a specified unit surface in a defined unit time at a concentration gradient of unity.

Dissolution

A process in which a solute dissolves in a solvent forming a solution, e.g. saline is a result of sodium chloride dissolving into water.

Dissolving array

The drug formulation is combined with biocompatible excipients and moulded into microneedles in the fabrication process. The principle is that the drug formulation matrix dissolves into the skin compartment; drug acting normally on its target molecules and the excipients degrade as non-toxic metabolites.

Emulsion

An immiscible colloidal system of liquid dispersed in one or two liquid mediums.

Empirical

A source of knowledge acquired by observation and experiment.

Encapsulation

The enclosure or trapping of a core material (solid, liquid or gas) inside a solid or liquid matrix for the purpose of controlled release.

Eutectic mixture

A composition consisting of two or multiple lead components forming a lowest crystal-lisation temperature system.

Fick's law

A theory that describes the diffusion of exogenous/active molecules along a concentration gradient.

Flux (*J*)

The vector quantity of a property of matter, e.g. concentration, permeating through a given area in a given time interval and through a defined surface area for that period of duration. The defined surface area can be a skin section or filter membrane.

Franz diffusion cell (FDC)

An upright glass container shaped like a small teapot with a spout and water jacket. Used in in vitro experimental analysis of drug permeation through a dissected organ, e.g. skin.

Gelatine type A

Animal protein derived from the collagen and tendons of porcine or bovine origin and treated by strong acids in the manufacturing process. The isoelectric point is 7 - 9.

Glutaraldehyde (IUPAC name: 1,5 pentanedial)

A crosslinking molecule used for the hardening and solidifying of biochemical micro-particles such as protein derivatives.

High performance liquid chromatography (HPLC)

An analytical method of separating organic molecules usually on a non-polar, reversed phase column. The inside of a reversed phase column contains carbon molecules of specific molecular size, bonding and stereochemistry such as C_4, C_8, C_{18}.

Homogeneous

A compound or a mixture of substances with a uniform characteristic or composition that is often clearly observable.

Hydrogel

A substance or compound that is immiscible in aqueous solvent with the potential to swell or shrink in specific physicochemical conditions e.g. temperature.

In Vitro

An anatomical segment or component of material in experimentation of a biological sample.

Intercellular

A molecule residing or moving in a region located outside the cell membrane and between cells. N.b. it is outside the cell wall when discussing plant cells.

Intracellular

A molecule residing or moving inside cells. The movement is past cell membranes and inside cells, mainly cell cytoplasm, and into cell membranes.

Lidocaine

A local anaesthetic drug used in the prevention or treatment of localised pain.

Local anaesthetics

A group of drugs which target Na/K ion channels of sensory nerves, blocking superficial nerve impulses and preventing pain.

Liquid chromatography-diode array (LC-DA)

A more specific description of HPLC analysis in particular the diode array (DA) detector component involves detecting specific chromophores of an organic molecule (See HPLC). Distinct chromophore of a molecule are interpreted as a signal peak wavelength (λ_{max}) and correspond to the chosen wavelength peak.

Micelles

A surfactant composed of ampiphilic groups arranged usually as spherical particles. The hydrophobic or hydrophilic region will orientate according to the polarity of the solvent environment, taking the “like dissolves like” rule.

Microneedles

A device composed of a solid base with minute projection of needles. Those minute needles are nearly visible to the naked eye.

Microgel

Hydrogels with particle morphology on a micron scale.

mPEG2000-PLLA

Methoxy poly(ethylene glycol) (mPEG), 2000 Da, Poly-L-lactide.

mPEG5000-PSA

Methoxy poly(ethylene glycol) (mPEG), 5000 Da, Poly(sebacic anhydride). mPEG is hydrophilic region and Poly(sebacic anhydride) is the hydrophobic region.

n-hexane

A colourless volatile organic liquid with a boiling point temperature of 69.0 °C.

n-octanol/water partition coefficient

A measure of substances solubility between a non-polar and polar solvent phase and hence the deduction of the nature of polarity of a substance. A substance of known quantity added to a two phase n-octanol and water mixture with subsequent agitation will eventually concentrate more or less in either the organic or aqueous phase. The n-octanol and water mixture are immisble equal volumes.

Paraffin liquid

A fraction of crude oil consisting of a mixture of alkanes from six carbon chain to twelve carbon chain lengths. The physical property is a low density, non-polar liquid.

Percutaneous

An adjective for administering or absorbing an active molecule in a defined skin layer or organ tissue layer. Alternatively percutaneous absorption is used to describe transdermal delivery.

pH

A measure of substance acidity or alkalinity from a scale of 0 - 14; defined: pH = - log [H+].

PHCL-g-PLLA

Poly(4-hydroxyl-ε-caprolactone-co-ε-caprolactone)-g-poly(L-lactide). A blended polymer to combine degradation and mechanical properties.

Physiological conditions

Biological environment refering to a plasma fluid pH 7 and temperatures of 37°C.

P(LLA-b-εCL)

A diblock co-polymer with a MW 15200 Da. Combines mechanical and degradation properties.

P(LLA-co-εCL)

A diblock random polymer with MW 51000 Da. Combines mechanical and degradation properties.

Poke with patch

Technique in which microneedles penetrate the skin through the SC layer and create pores, followed by the placement of drug on the treated site.

Polymer

A continuously high molecular weight molecule comprising of repeating monomers.

Sirolimus

An immunosuppressant drug.

Sodium carboxymethyl cellulose (NaCMC)

A polyanionic derivative of cellulose with hydrophilic and biodegradable properties.

Stratum Corneum (SC)

A protective and insensitive top layer of the epidermis which is usually 15 - 20μm thick.

SU-8

A high viscosity, negative based photo resist structure for moulding applications.

Suspension

A specific colloidal system of solid particles dispersed in a liquid medium such as water.

Tissues

A group of similar cells in a multicellular organism or dissected body segment.

Topical

The application of medication on the surface of skin or mucous membranes.

Transdermal

Drug delivery into the skin hypodermis and subsequent systemic circulation.

Vehicle

Excipients, additives or reagents temporarily binding with drug molecules for the purpose of bulk handling, physicochemical stability during storage and controlled pharmacokinetics.

W/O

Aqueous droplets dispersed in continuous oil phase.

List of publications

Peer reviewed journals

- Nayak A., Das D.B., (2013). Potential of biodegradable microneedles as a transdermal delivery vehicle for lidocaine, *Biotech Lett*, 35: 1351-1363
- Nayak A., Das D.B., Vladisavljević G.T., (2014) Microneedle-assisted permeation of lidocaine carboxymethylcellulose with gelatine co-polymer hydrogel, *Pharm Res*, 31: 1170-1184
- Nayak A., Babla H., Han Tao., Das D.B., (2014). Lidocaine carboxymethylcellulose with gelatine co-polymer hydrogel delivery by combined microneedle and ultrasound, *Drug Deliv*, 23: 668-679
- Nayak A., Short L., Das D.B., (2015). Lidocaine permeation from a lidocaine NaCMC/gel microgel formulation in microneedle-pierced skin: vertical (depth averaged) and horizontal permeation profiles, *Drug Deliv and Trans Res*, 5: 372-386
- Nayak A., T Chao., Starov V., Das D., (2015). Spreading of a lidocaine formulation on microneedle treated skin, *J Pharm Sci*, 104: 4109-4116

Book chapter

- Nayak A., Olatunji O., Vladisavljević G.T., Das D.B., (2015). Pharmaceutical applications of natural polymers (Chapter 9). Editor: Ololade Olatunji, *Natural Polymers: Industry Techniques and Applications*, Springer publishers, pp. 263-313

Conference presentations

- Third International Conference on Microneedles. Poster presentation held at the University of Maryland, School of Pharmacy. 1st Poster title: Microneedle Assisted Permeation of Lidocaime HCl from a NaCMC:GEL Hydrogel.

  2nd poster title: Lidocaine NaCMC:GEL Hydrogel Delivery using combined Microneedle and Sonophoresis**.** Dates: 19-21 May 2014.

- The Science of Medicines. APS PharmSci, University of Hertfordshire, Hatfield. Poster title: Microneedle and Low Frequency Sonophoresis Permeation of Lidocaine HCL from A NaCMC:GEL Hydrogel. Dates: 8-10th September 2014.

Other research presentations

- Research student seminar. Loughborough University, Loughborough. Presentation title: Optimisation of percutaneous lidocaine delivery through skin by microneedles. Date: January 2014.
- Visiting researcher seminar. Komma Reddy Venkata Sadasiva Rao Siddhartha College of Pharmaceutical Sciences, Vijayawada, India. Presentation title: Optimisation of percutaneous lidocaine delivery through skin by microneedles. Date: April 2015.

Chapter 1

Introduction

Lidocaine is a local anaesthetic for symptomatic pain sensation blockade below the stratum corneum (SC) layer of epidermis. The localised anatomical target for lidocaine are peripheral nerves inherent in cells of skin tissue involved in the nervous system concerning the function of pain and touch in the viable epidermis (VE) and dermis. Local anesthetics are used in symptomatic treatment of dermatological diseases, wound treatment or minor surgery associated with pain in the region of skin. Lidocaine was first synthesised by chemists Holger Erdtman and Nils Löfgren during the early 1940s leading to first clinical trials in 1944 before entering the pharmaceutical market in the 1950s as a bolus solution. Lidocaine's success as a solution based local anesthetic has expanded towards topical based and patch based modes of delivery, i.e., transdermally. However, there is a significant gap in knowledge regarding the percutaneous based delivery of lidocaine. There is also a significant gap in knowledge in the formulation of lidocaine hydrogel using natural polymers and natural excipients encompassing a biocompatible concoction. The focus towards desirable permeation kinetics of lidocaine with the implementation of a microneedle (MN) patch is another significant gap in knowledge.

The aim of this research is to therefore develop a hydrogel based formulation for enhanced lidocaine delivery using a MN patch in balancing ideal formulation and physicochemical properties of a natural bipolymeric hydrogel to achieve increased permeation kinetics below the stratum corneum (SC) layer of skin. Known therapeutic permeation thresholds of lidocaine in the viable epidermis (VE) layer is compared with experimentally derived permeation profiles of lidocaine.

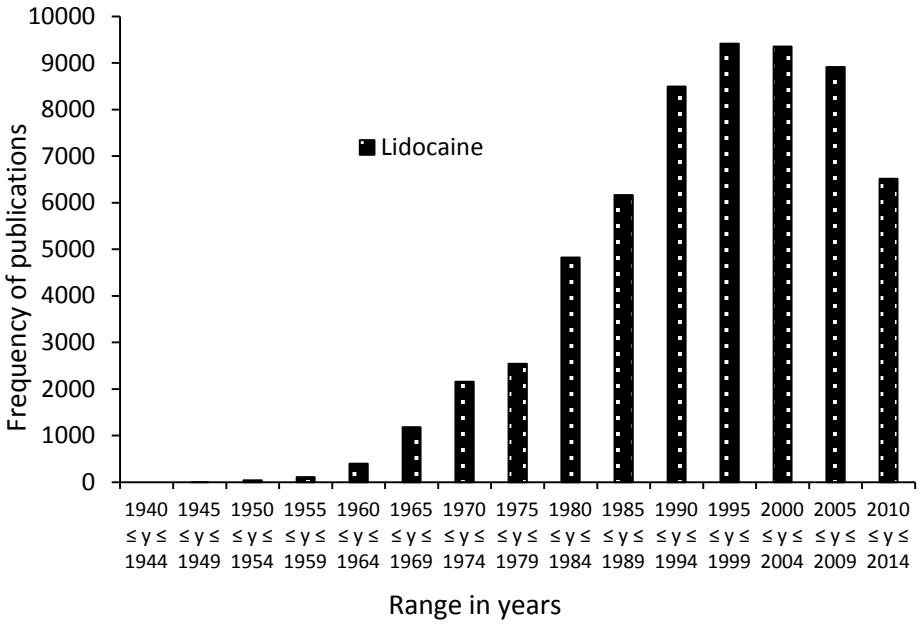

Figure 1.1: The frequency of lidocaine publications during time. (Web of knowledge)

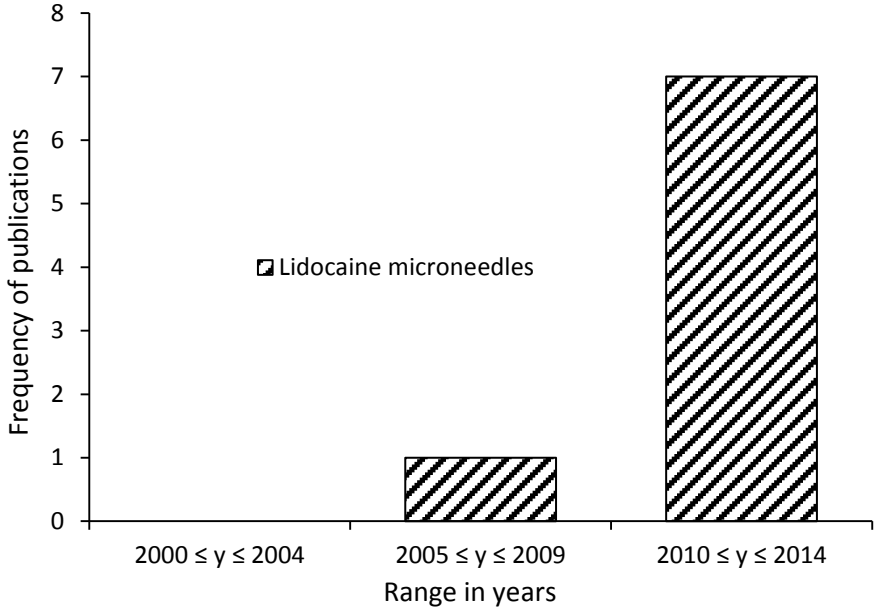

Figure 1.2: The frequency of lidocaine MNs publications during time. (Web of knowledge)

A frequency distribution plot of lidocaine publications (Figure 1.1) outlines an increasing trend for lidocaine before an early stage plateau effect is observed after

1999. The keyword “lidocaine” implies lidocaine, lidocaine HCl and it’s numerous formulations. There is a likelihood that new research interests for lidocaine have decreased significantly after the year 2000. The highest number of lidocaine based publication recorded was approximately 9415 from a year range 1995 till 1999. Unlike the decreasing publication numbers for general lidocaine based publications, there is still a significantly large demand for lidocaine microneedles as a potentially new drug delivery device (Figure 1.2) (Web of knowledge).

A short lag time for bypassing the SC layer in lidocaine permeation and a therapeutic window sustained between 30 to 45 minutes is ideal in emergency treatment of localised lacerations and painful skin wounds. In achieving faster and sustainable lidocaine permeation, the compression forces and MN microcavity depths were compared with the skin permeation rates.

1.1 Specific objectives in formulating a lidocaine hydrogel for MN “poke and patch” delivery

The specific objectives in the current research of a lidocaine NaCMC/gelatine hydrogel are as follows:

1) To determine suitable biocompatible polymers and excipients for the encapsulation of lidocaine that is generally regarded as safe.
2) To attain maximum dispersion of lidocaine microgel microparticles in water from favourable Zeta potentials and particle size distribution analysis.
3) To attain favourable pseudoplasticity of lidocaine NaCMC/gelatine hydrogel from mass ratios.

4) To sustain the percutaneous delivery of lidocaine within or above minimum therapeutic levels from NaCMC/gelatine hydrogel contained in the viable layers of skin by mass transfer with minimum clearance via the blood stream.
5) To compare and enhance the delivery of lidocaine percutaneously by MN "poke and patch" method on skin.
6) To compare and enhance the skin percutaneous delivery of lidocaine vertically and horizontally (depth averaged) above minimum therapeutic levels.
7) To ensure that the skin permeation of lidocaine is sustained within a therapeutic threshold for significantly long periods before drug depletion in the skin.
8) To control the spreading of lidocaine NaCMC/gelatine hydrogels across MN treated skin and compare it with non MN treated skin.

1.2 Structure of thesis

The thesis is divided into a total of seven chapters as discussed below. Chapter 1 outlines the specific aims of this study. Chapter 2 reviews the important areas in the current literature of natural polymers as vehicles and devices in drugs and lidocaine based MNs. This review discusses the success and limitations of current patch based systems and biodegradable lidocaine MNs. Chapter 3 is concerned with the specific areas of formulation development and the 'poke and patch' method of lidocaine hydrogel delivery. Chapter 4 discusses mass transfer of lidocaine in skin and the use of low frequency sonophoresis (LFS) as a technique for lidocaine delivery through skin. The mechanism of LFS as an added permeation enhancer for lidocaine is discussed. Chapter 5 is based on a method that was implemented in determining depth averaged mass transfer of lidocaine in the VE layer of skin. Chapter 6 discusses the control in the spreadability of lidocaine NaCMC/gelatine microgels on skin and artificial membrane. Chapter 7 concludes lidocaine NaCMC/gelatine hydrogel as a potential hydrogel formulation inconjunction to the MN assisted method for superficial pain treatment

on skin. This chapter also discusses possibilities of future work. Chapter 8 lists all references used in this research work.

Chapter 2

Literature review

Chapter overview

There has been an increasing interest in applying biotechnology in formulating and characterising new and innovative drug delivery methods, e.g. Drug loaded biodegradable microneedles within the area of transdermal delivery (TD) technology. Recently, microneedles have been proposed for use in pain management, e.g., post operative pain management through delivery of a local anaesthetic, namely, lidocaine. Lidocaine is a fairly common, marketed prescription-based, local anaesthetic pharmaceutical, applied for relieving localised pain and lidocaine loaded microneedles have been explored. The purpose of this literature review is to evaluate the properties of biodegradable polymers that may allow the preparation of microneedle systems, methods of preparing them and pharmacokinetic conditions in considering the potential use of lidocaine for delivery through the skin. This chapter continues with the pharmaceutical application of natural polymers derived from carbohydrate and protein sources in modified and unmodified forms for pharmaceutical applications such as production of TD and percutaneous drug delivery systems, oral and topical drug delivery systems. Hydrogel and microgel based drug delivery systems are also included due to their increasing impact and potential in the pharmaceutical industry. A detailed overview of the distinctive properties of natural polymers suitable for pharmaceutical applications is provided from the most recent applications reported in literature.

2.1 Introduction

A lidocaine drug vehicle composed of natural polymers and delivered percutaneously by a microneedle patch was researched as a poke and patch

device. Therefore, this chapter aims to provide a comprehensive insight into lidocaine microneedles and natural polymer vehicles, especially hydrogels.

2.2 Microneedles as a drug delivery vehicle for lidocaine

There has been an increasing interest in applying biotechnology in formulating new and innovative drug delivery methods, including biodegradable microneedles within the area of TD drug delivery technology (Orive et al., 2003; Olatunji and Das 2010, 2011). Conventional hypodermic needle delivery causes pain and anxiety, and requires medical personnel for administration. In contrast, the biodegradable microneedle, a drug loaded vehicle moulded into an all-in-one drug formulated micro-structure constructed from either biopolymer or sugar excipients, can be used to deliver drug almost painlessly to humans (e.g., Donnelly et al., 2010; Lhernould and Delchambre, 2011; Olatunji et al., 2014; Olatunji and Das, 2011; Gittard et al., 2012). These microneedles are economical due to using fairly cheap materials (Olatunji et al., 2014), give reproducible results and are generally safe even if microneedle fragments break off after piercing the skin surface as compared to other microneedles made with glass or metal.

Large molecular weight proteins such as bovine serum albumin, growth hormones and vaccines have been successfully loaded into biodegradable microneedles (Lee et al., 2008, 2011a; Raphael et al., 2010). Recently, the microneedles have also been explored for use in post operative pain management through delivery of a local anaesthetic, lidocaine. Lidocaine provides short duration, superficial anaesthesia, to the pain affected area (Kissin. 2012). Lidocaine (Figure 2.1) comprises of a polar tertiary amine and a hydrophobic aromatic group on the opposite ends of the acetamide bond (Costa et al., 2008). It is hydrophobic as the basic drug but it is soluble in water as the ionised form of lidocaine HCl (Figure 2.2) in which the tertiary amine is protonated (Ullah et al. 2012; Rajabi et al., 2011

Shaikh et al., 2011). The physico chemical properties of drug prior to vehicle encapsulation are imperative for relating the structure with function, E.g. solubility effecting the in vitro drug permeation in receptor solvent. The solubility of lidocaine HCl does not equal the solubility of sodium chloride in water thus potentially leading to a saturated solution. Sodium chloride is a known ionic salt. If lidocaine HCl was ionic the saturated concentration would provide inaccurately high cumulative amounts in a known receptor volume of water, thus representing a false positive in IV studies. This is the receptor compartment of a Franz diffusion cell as discussed in Chapter 3. Lidocaine can be encapsulated or dispersed in a drug delivery vehicle which could be either hydrophobic or hydrophilic.

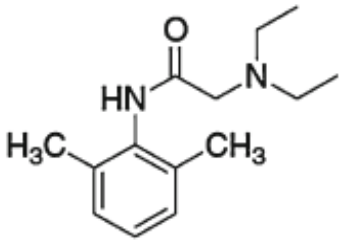

Figure 2.1: The chemical structure of hydrophobic form of local anaesthetic lidocaine (Costa et al., 2008).

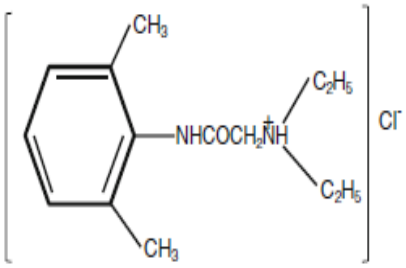

Figure 2.2: The hydrophilic form of lidocaine known as lidocaine hydrochloride (Shaikh et al., 2011).

In the present context, a vehicle for drug delivery is taken as a support material for formulating drugs usually in liquid based or a semi-solid form to remain on the skin surface and facilitate the conditions necessary for TD drug delivery (Allen et al., 2005; Djabri et al., 2012; Subedi et al., 2010). An ideal drug carrier system or

vehicle is sought for identifying optimal conditions in controlled release and TD permeation kinetics of the drug lidocaine. The main objective of using a vehicle is either to allow for fast initial release or permeation in skin with consideration to the suitability of suturing a superficial cut or a slow initial release and longer steady state conditions lasting several hours with an alternative consideration to suturing and treating multiple lacerations at the localised area.

A formulation of lidocaine has been developed by Fiala et al. (2011) for EMLA (eutectic mixture of local anaesthetics) containing lidocaine and prilocaine in hydrofluoroalkane as a propellant enhancer spray. Kaewprapan et al. (2012) studied lidocaine loaded nanoparticles of dextran decanoate esters with varying degrees of substitution for suspension in aqueous medium. Petrisor et al. (2012) mixed lidocaine with silicone elastomer and analysed the controlled release effects of modifiers such as poly(vinylpyrrolidone), PVP, and poly(vinyl alcohol), PVA. Components in drug vehicles have the purpose of mass bulking, preservation of drug, rheological properties and drug release properties in biological target. Compared with injectable and skin surface drug applicants, microneedles are highly beneficial in terms of constant needle lengths being below the length causing epidermal pain stimulation during insertion (Cheung and Das, 2014), while being described as minimally invasive in forming micro-spaces (Cheung and Das, 2014) in conjunction to enhancing the movement of the active compounds through the skin (Ameri et al., 2010; Chu et al., 2010). Besides the laboratory based studies mentioned above, there are a number of proprietary TD delivery systems for lidocaine. These include proprietary medicines in solution, semi-solid and patch delivery system. For example, lidocaine in solution is combined with a bacterially derived hyaluronic acid gel formula to minimise the discomfort of injection as tissue filler in the cosmetics industry (Monheit et al., 2009). The proprietary name of the formulation is Prevelle Silk (Mentor Pharmaceuticals, www.mentorcorp.com).

Lidocaine solution is marketed under the proprietary name of Xylocaine and is also available in an injectable format (www.astrazeneca.co.uk). Clinical research has shown that a 1 % (w/v) lidocaine subcutaneously injected once into the location of a lacerated, injured or tumour affected hand allows for successful local anaesthesia followed by surgical treatment (Tzeng and Chen, 2012). A lidocaine patch for the application to skin is also marketed with the proprietary name Lidoderm (www.Lidoderm.com). A Lidoderm (5 % w/v) patch has been applied for the treatment of postherpetic neuralgia (Katz et al., 2002) and in the reduction of pain during treatment of Dercum's disease (Desai et al., 2008; Martinenghi et al., 2015).

Conceptually, microneedle technology provides an attractive method for delivering lidocaine. For example, it may be possible to apply the drug over a large surface area on the body with no or little pain in contrast to traditional hypodermic injections. With microneedles it may be possible to control the drug delivery rate as well besides reducing wastage of the drug. As far as we know, there is no commercially based FDA approved lidocaine microneedle product available from pharmacies. However, there seems to be some developmental research for lidocaine microneedles. Recently, the 3M Group developed a lidocaine solution mixed with dextran to uniformly coat medical grade, liquid crystalline polymer (class VI) for pre-clinical in vivo studies using biopsy porcine skin of live pigs. This resulted in successful delivery of lidocaine in a faster time compared to EMLA composed of lidocaine and prilocaine as a combined eutectic formulation (Zhang et al., 2012a; Schreiber et al., 2013). A highly significant development was made by Theraject Inc. (Kwon, 2004) with regards to determining the permeation flux of lidocaine through the skin by testing a Theraject MAT dissolvable microneedle system. This vehicle comprised sodium carboxymethyl cellulose (NaCMC) mixed with lidocaine and was cast, compressed and moulded to dryness with a subsequent diffusion characterisation that confirmed the permeation flux had increased up to 12 fold

compared to 10 % (w/v) lidocaine as control (Kwon, 2004). The degree of subsitition, in terms of exchanged hydroxyl groups to carboxymethyl groups in NaCMC, effected solubility, viscosity, gel strength and electro-analytical behaviour as an anionic polymer in solution requires further work in order to aim for a plastic material property (Kundu et al., 2011). Further details on degree of substitution are mentioned in section 2.4.2.

While the above studies show the potential for applying the principles of biotechnology for preparing lidocaine loaded microneedles, there is a clear need to make further progress on the methods of preparation and characterisation of the microneedles for drug delivery. It may also be necessary to learn from what have been done elsewhere while loading and delivering other molecules (e.g., insulin) using biodegradable microneedles. To address these issues, this chapter aims to evaluate critically the current developments in biodegradable microneedle systems for possible applicability in TD lidocaine delivery. In particular, this chapter reviews the methods of preparation and the properties of biodegradable polymers that may allow for the development of a desirable microneedle system for lidocaine delivery. It is expected this would be helpful in preparing biodegradable microneedle for lidocaine delivery.

2.2.1 Preparation of microneedles

The first published paper on microneedles was in 1947 in which soft glass material (30 μm tip diameter and 2.5 cm long) was an example of early microneedles in assisting the isolation of yeast ascospores (Thaysen and Morris, 1947). Gerstel and Place. (1976) were the first to obtain a patent for the architecture of microneedle arrays, outlining a drug solution reservoir to a flow through hollow microneedle. In 1998, a paper on the fabrication of microneedles used silicon layered chromium for ‘coat and poke’ delivery of drugs (Henry et al., 1998). The first published fabrication

of biodegradable microneedles used micromachining technology to mould polycaprolactone polymer into microneedles (Armani and Chang, 2000; Park et al., 2003). At the moment, there is clearly an increasing interest in preparing biodegradable microneedles for a variety of applications. Those applications are considered as drug molecular delivery, cosmoseutical based molecular delivery and adsorption or binding of cellular components for diagnostics.

Preparation and treatment of normal skin surface (e.g. antiseptic wipes) before the application of a microneedle has not been recommended. Most scientific papers suggest that pathogenic infections are not caused by using microneedles (Arora et al., 2008; Donnelly et al., 2009; Han et al., 2012). As long as there is no potential risk of pathogenic infections caused by poor hygiene, it can be assumed that the patient using microneedles has normal immunity to infections. The removal of microneedles leaves indents on the skin and the main factors, such as microneedle length, number in an array and microneedle cross-sectional area, effect the time for natural skin re-sealing (Gupta et al., 2011a). For example, Kalluri and Banga. (2011) have characterised the micro-conduit channels caused by microneedles and pore re-sealing. They show that skin pores close partially in approx. 12 h and completely in approx. 15 h. Micro-conduit re-sealing is shortly discussed in Chapter 5. Considerations on pore re-sealing can affect the controlled drug release over 12 h for a poke and patch system.

A direct thumb application for microneedles allow the drugs encapsulated inside the microneedles to diffuse into the VE layer of the skin as outlined schematically in Figure 2.3a (Shakeel et al., 2011; Kim et al., 2012a). However, in the case of lidocaine, if the drug is concentrated in the middle to lower portion of the microneedle than the tip, the permeation is expected to be near the SC layer of the skin to anaesthetise a superficial cut. As such, one needs to consider where the

drug is loaded in the microneedle. Compared with glass and metal microneedles, biodegradable microneedles have no or little safety concern if they break and become embedded in the skin as a foreign body (Park et al., 2007a). This is due to the brittle properties of glass and malleability of soft metal which can potentially break apart. Usually the manufacturing process and reproducibility of biodegradable microneedles are economical compared with conventional micro-machining manufacture (Donnelly et al., 2010). Figure 2.3b is a scanning electon microscope (SEM) plan view of poly (lactic-co-glycolic acid) (PLGA) microneedles and Figure 2.3c is an image of NaCMC microneedles encapsulated with a dye molecule representing a possible drug, sulforhodamine B (Jeong et al., 2008; Park et al., 2007a).

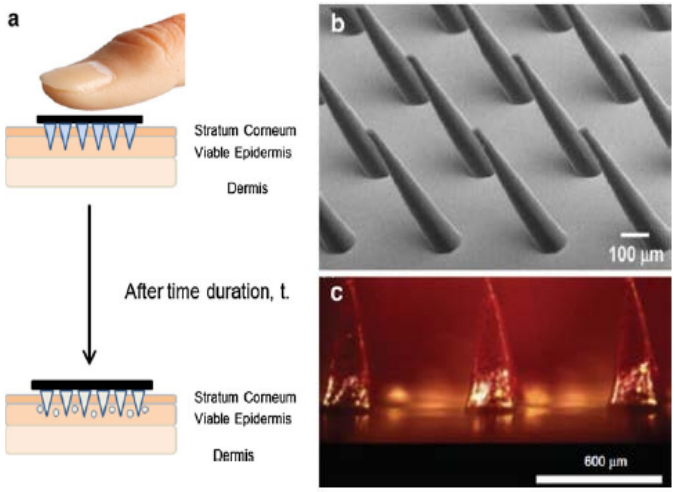

Figure 2.3: Schematic outline of (a) diffusing biodegradable MN after skin insertion. (b) SEM image of conical PLGA microneedles (Park et al., 2007a). (c) Pyramidal NaCMC microneedles containing sulforhodamine B (Jeong et al., 2008).

Microneedles have been fabricated by a variety of means. For example, silicon master substrate is adapted in microelectronic mechanical systems applications and less time consuming, mass producing techniques were researched via operations from the microelectronics industry, known as microelectronic mechanical systems for the fabrication of a master microneedle array prior to micromoulding

(Fujita, 1997; Walraven, 2003; Trautmann et al., 2005). SU-8, 1-methoxy-2-propyl acetate, (Microchem Corp, MSDS) is a negative photoresist material mixed with a sulfonium salt photoinitiator for inducing the mechanism of cationic polymerisation in epoxy groups of SU-8 monomers under UV (Zhang et al., 2001; Qvortrup et al., 2011). It is photosensitive to UV light and a special mask diffraction grating is required to direct a particular wavelength onto the SU-8 (Ami et al., 2011). SU-8 does not always provide accurate structures and cases of bending brought by high residual stress were observed when photoresist and substrate possess incompatible thermal expansion coefficients. As such, the UV exposure time and wavelength range need close monitoring to prevent the distorting structure (Safavieh et al., 2010; Del Camp and Greiner, 2007). Marasso et al. (2011) implemented double spin coating with two different viscosities of SU-8 and observed good adhesion properties between copper substrate and SU-8 in conjunction to an aspect ratio of 7:1 without additional steps such as wafer removal and seed layer introduction, extending production period over 24 h. Also, the viscosity and set thickness of the SU-8 photoresist are dependent on the amount of c-butyrolactone solvent dissolved in producing the solution (Lorenz et al., 1997).

A recent starting material for production of master templates was reported by Viero et al. (2012). They used reactive ion etching on a silicon based master for the construction of microneedles. Chen et al., (2008) also outlined a fabrication process which used silicon oxide layers on silicon followed by a positive photoresist treatment for pattern transfer onto the silicon oxide layer via reactive ion etching and finally producing microneedle tips using an isotropic reactive ion etching process. Lhernould and Delchambre. (2011) arrived at a design fabrication process of implementing laser ablation to create microchannels in polycarbonate material. Matteucci et al. (2009) adapted the micro-fabrication process known in German as Lithographie, Galvanoformung, Abformung (lithography, electroplating and molding)

by Hruby (2001) which produced microneedles by double exposure, deep X-ray lithography (Kim et al., 2004; Miller et al., 2011) using microcrystalline silicon wafers surfaced with Cr/Au bilayer as a template. Even though complicated multi-step processes and specialist resources are required in the production of a large quantity of master microneedles, the production of a single master is economical and time saving when considering the transferability in creating inverse micromould microneedles (Kim et al., 2009, 2012b).

2.2.2 Fabrication of microneedles from moulds

Microneedles have been manufactured from micromoulds that are non-interconnecting micro-well structures (Ryu et al., 2007). There is a lack of publications that outline the micro-moulding fabrication processes methodically. However, the manufacturing processes of casting and hot embossing are common for microneedles and are now discussed briefly. In the casting process, a master template is fabricated to develop a mould template for a molten drug formula to fill the mould contours, solidify under favourable temperature and pressure conditions and finally removal of the mould from the solidified drug formula (Bariya et al., 2011). Polydimethylsiloxane (PDMS) is an ideal material for replica moulding of microneedles because of its non-toxicity, elastic properties and low cost (Saliterman., 2006; Lee and Lee, 2008) and, as such, it has been used in many studies. Laser ablation by focusing a CO_2 laser was used to create conical shaped voids in PDMS material moulds for vacuum setting NaCMC and polyacrylamide solution into solid microneedles (Kim et al., 2009). In another study, a pre-fabricated PDMS mould was used to vacuum set PLGA microneedles containing hydrogels (Kim et al., 2012b). PLGA is composed of D,L-polylactic acid (PLLA) and polyglycolic acid (PGA) monomers (Gabor et al., 1999; Danhier et al., 2012). As a biocompatible polymer, PLGA is used in biotechnology for the goal of preparing microneedles and scaffolds in tissue engineering (Lee et al., 2004). It has been

argued that PLGA with low molecular weights of less than 50 kDa and a D,L-lactide/GA ratio of 50:50 are the most suitable for controlled drug release with respect to faster degradation rates (Fredenberg et al., 2011; Mundargi et al., 2008). PLGA in the context of merchandise is commercially and readily available from many suppliers. Stages in a typical casting process (Figure 2.4a; Chu et al., 2010) start with a PDMS mould (step 1), pre-fabricated from a PDMS male master coated with gold, and the mould is filled with sulforhodamine B (step 2). The residual drug solution is pipette extracted half way to be reused later (step 3) and the remaining drug solution in the mould crevice is dried by centrifugation. The PVA/PVP blend devoid of drug is casted into the mould by vacuum pressure (step 4), the combined polymer is air dried or is centrifuged at a low speed in drying (step 5) and an adhesive backing is used to prise the formed polymer microneedles from the PDMS mould (step 6).

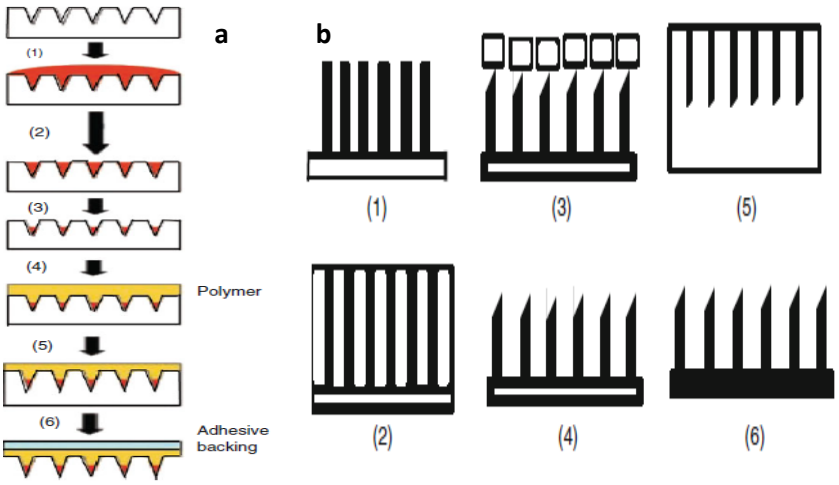

Figure 2.4: Stages in micromoulding of (a) PVP/PVA microneedles (Chu et al., 2010). (b) Stages in micromoulding of PLGA microneedles (Park et al., 2003)

Another polymer system from PLGA, fabricated by Park et al. (2003) (Figure 2.4b) commenced with SU-8 substrate (step 1) by using the same PLGA polymer as a sacrificial filler on SU-8 (step 2) followed by copper coating deposition and acid etching to cover the SU-8 epoxy cylinders as a pattern (step 3) with subsequent

reactive ion etching to asymmetrically etch the tips of epoxy cylinders (step 4) and an inverse PDMS mould was created (step 5) with the prior master structure from reactive ion etching method before casting new PLGA microneedles as the final product (step 6) (Park et al., 2003). Advanced micro-molding components such as copper or SU-8 are either unavailable or very expensive in less industrialised geographical locations. A more economical method using a natural clay, Chinese purple ceramic mould was formed by hydraulic pressing a bed of steel sticks into the soft pliable clay before furnace heating, slow cooling followed by pouring a mixture of PVA, dextran and carboxymethylcellulose polymers into the mould then vacuum setting, freeze thawing and finally drying into microneedles (Yang et al., 2012b). A less common fabrication technique, known as hot embossing, requires the application of heat above the glass transition temperature of the polymer product in contact with the mould followed by force to emboss the mould pattern to the polymer product and then cooling below the glass transition temperature before separation of mould and polymer product (Bodhale et al., 2009).

PLLA is commercially and readily available from many chemical suppliers. It is similar to PLGA. PLLA microneedles were fabricated by a hot embossing technique through a multi-step process via a PDMS replication and then heating and pressuring the PDMS mould and PLLA grains followed by unmoulding at room temperature to obtain the microneedles (Han et al., 2009). A more efficient process was studied by Youn et al. (2008) by fabricating silicon moulds using focused ion beam and then pressing the silicon mould in poly-methylmethacrylate (PMMA) polymer under applied temperatures above the glass transition temperature of PMMA and pressure followed by slow cooling resulted in good reproducibility of replicated structures (Youn et al., 2008). Hot embossing appears only suitable for high temperature stable drugs in a biodegradable polymer vehicle as temperatures of over 100 ˚C are required. As a substantial number of microneedles are classed

polymers, a supposedly third fabrication technique called investment moulding has been used suitably for hollow non-biodegradable polymers in which a drug solution flows through the hollow part of the microneedles into the skin (Lippmann, 2007; Lippmann and Pisano, 2006). Melt injection processes in investment moulding are suitable for thermoplastics because in adaptation of micromoulding, very high shear is required to allow for lower viscous melt and low resistant flow but heat generation can cause degradation of the drug formulation (Zhao et al., 2003). As mentioned earlier, currently there seems to be no lidocaine loaded biodegradable microneedle polymer systems published at present. Table 2.1 outlines the dissolvable or biodegradable materials as a vehicle for the drug and the method and conditions in manufacturing in-conjunction to significant dissolution or permeation results.

Table 2.1: Fabricated MNs according to manufacture, dissolution and permeation of drug

Microneedle materials	Method of manufacture	Conditions and type of manufacture	Results of drug permeation or dissolution of vehicle
Poly (lactic acid) (PLA), Poly (lactic-co-glycolic acid) (PLGA; 50/50) and PEG unmixed initially (Park et al., 2007b).	Casting with PDMS (Park et al., 2007b; Xiangdong et al, 2009) SU-8 photoresist master (Natarajan et al., 2008), gold coating of 500 Å.	Ultrasound pulses to weld polymer micro-particles within mould to create porous structure (Park et al., 2007b). Vacuum pressure and oven heating for microneedle static shaping (Park et al., 2007b).	No publication found.
Silk fibroin from *B. mori* cocoons (You et al., 2011).	Epoxy microneedle master from X-ray lithography to produce female PDMS mould (You et al., 2011). Molten fibroin drug set into PDMS and mould removed (You et al., 2011).	Oven drying and vacuum pressure for shaping and solidifying microneedles (You et al., 2011).	Tetracyline loaded on silk MN. A 10 fold decrease in Staphylococcus aureus growth in nutrient culture at 37˚C overnight (Tsioris et al., 2012).

Table 2.1: Continued

Microneedle materials	Method of manufacture	Conditions and type of manufacture	Results of drug permeation or dissolution of vehicle.
Silk fibroin from *B. mori* cocoons (You et al., 2011).	Epoxy microneedle master from X-ray lithography to produce female PDMS mould (You et al., 2011). Molten fibroin drug set into PDMS and mould removed (You et al., 2011).	Oven drying and vacuum pressure for shaping and solidifying microneedles (You et al., 2011).	Tetracyline loaded on silk MN. A 10 fold decrease in Staphylococcus aureus growth in nutrient culture at 37˚C overnight (Tsioris et al., 2012).
Poly (methyl vinyl ether co-maleic acid) (Garland et al., 2012).	Blulase laser cutting for fabricated silicone elastomer moulds using Aluminium template (Garland et al., 2012).	40°C heat for curing mould and centrifugation at 3500 g for 15 min and microneedles dried for 24 h under ambient temperature (Garland et al., 2012).	In vitro studies with Neonatal procine skin reported 59%, 39% and 23% cumulative release of caffeine, lidocaine and metronidazole respectively for combined concoction microneedles were tested (Garland et al., 2012).
20% (w/w) aqueous blends of co-polymer Gantrez® AN-139 (Donnelly et al., 2011).	Galvanometer controlled excimer laser for variable height and interspacing of microneedle mould setup (Donnelly et al., 2011). Blulase laser cutting for fabricated silicone elastomer moulds using Aluminium template (Donnelly et al., 2011).	40°C heat for curing mould and centrifugation at 3500 g for 15min and microneedles dried for 24hrs under ambient temp. (Donnelly et al., 2011).	83% of the drug, theophylline, contained in microneedles, permeated past the skin compared to 5.5% with patch delivery over a 24hr period (Donnelly et al., 2011) The percentage is out of total drug loaded.
Trehalose/mannitol (50:50w/w), trehalose dihydrate/ sucrose (75:25w/w), trehalose/sucrose (75:25w/w) and trehalose/sucrose (50:50w/w) (Martin et al., 2012).	PDMS mould created from wet etched silicon male master (Martin et al., 2012)	1 h vacuum pressure of (100 mbar) at room temperature conditions followed by 48 h dehydration without vacuum (Martin et al., 2012).	Sugar glass microneedles containing 2% (w/w) methylene blue powder showed complete dissolution between 10 to 20 minutes after insertion into full thickness human skin (Martin et al., 2012).

Table 2.1: Continued

Microneedle materials	Method of manufacture	Conditions and type of manufacture	Results of drug permeation or dissolution of vehicle.
Maltose mono-hydrate (1 g/ml) in DI water (Lee et al., 2011b).	Stainless steel pillars and syringe pump to directly draw molten maltose into conical microneedles (Lee et al., 2011b).	Axial drawing at 400 µm/s for 1 s at 100 °C then 400 µm/s for 3 s at 96 °C, cooling to 60 °C and separation from attached support pillars at 700 µm/s (Lee et al., 2011b).	Optical micro-graphy showed complete dissolution of maltose micro-needle containing sulfor-hodamine B in guinea pig skin after 20 min (Lee et al., 2011b).
Maltose (analytical grade) in water (Kolli and Banga, 2008).	Pre-fabricated inverse moulds formed by etching process (Texmac Inc).	Direct pouring of molten maltose at 95 °C into mould within one minute and gradual cooling to 55 °C to prise out the mould from shaped microneedles (Kolli and Banga. 2008; Miyano et al., 2005).	Nicardipine-hydrochloride loaded maltose micro-needles recorded a mean flux of 7.05 µg/ml/h compared with control value of 1.72 µg/ml/h (Kolli and Banga, 2008).

2.2.2.1 Possible biomaterials for controlled lidocaine release from microneedles

Lidocaine requires controlled release microneedles that allow for initial fast release into skin but reaches the desired plateau levels in which finite dosage is achieved. Therefore, the microneedles have to dissolve or disintegrate in the tissue fluids of physiological conditions at that site near the laceration before medics can treat the area by cleaning and suturing.

Drug molecules directly suspended in a well mixed polymer microneedle matrix contribute to faster recorded time release than those encapsulated in microparticles, followed by suspension in a second matrix vehicle as it is a two stage release mechanism with outer matrix dissolving first. For example, the time of

drug release was 4 h when calcein was released directly from PLGA (85/15) compared with calcein in NaCMC followed by the outer core matrix, PLGA, in which a duration of 4 days' release was observed (Garland et al., 2011; Park et al., 2006). The calcein was obtained commercially in the solid state from pre-processed moulds (Garland et al., 2011). The polymer and co-polymer monomeric ratios are influential in degradation for drug release. For example, single carbohydrate polymer PLLA dichloromethane solution with intrinsic viscosity value 2.38 dL/g was acquired commercially as a solid and processed into films (Loo et al., 2010). This resulted in significantly slower degradation by hydrolysis in the release of lidocaine as compared with PLGA (80:20) films which controlled the release of over 60 % cumulatively from initial loading of lidocaine in 40 days (Loo et al., 2010). PLGA 50:50 microparticles loaded with lidocaine resulted in much faster controlled release of over 50 % from intial loading in 10 days (Klose et al., 2010).

Lidocaine loaded PLGA would be highly suitable for relieving long duration symptoms of skin irritation and discomfort caused by illnesses such as postherpetic neuralgia, previously mentioned for commercially available lidoderm. PLLA's starting monomer, L-lactic acid (LLA), is derived using lactic acid bacteria (Garlotta, 2001; Roy et al., 1982). The distinct synthetic step in the production of PLLA is the condensation polymerisation of LLA in which ester linkages between LLA monomers are formed and water is the by product (Mehta et al., 2005; Garlotta, 2001). PLGA is synthesized by the mechanism of structural ring opening polymerisation of DL-lactide and glycolide by catalysis from stannous 2-ethyl hexanoate in conjunction with a molecular weight regulating additive, triphenylsilanol with the overall objective of consistent chain length and reduction of side branch chains (Ouyang et al., 2011; Mazarro et al., 2009). Biodegradation in the context for polymers is the breakdown of a high molecular weight molecule into smaller components of low molecular weight molecules caused by enzymes from

microorganisms and/or environmental catalysts (Luckachan and Pillai, 2011; Wang et al., 2003). Table 2.2 provides a summary of biodegradable polymer systems with respect of morphological properties and biodegradation measurements while physiological conditions according to plasma fluid are kept constant. The overall trend for Table 2.2 shows that the degradation is faster for PLLA blends than PLLA itself. Also, it seems that PLGA 50:50 is much faster degrading than PLGA 75:25.

Table 2.2: Polymer biodegradation and morphology according to physiological plasma fluid conditions

Polymer	Morphological properties	Degradation studies in physiological conditions
Poly–Ɛ-caprolactone (PCL).	Injection moulded matrix, films and sheets via temperature settings (Wahit et al., 2012).	General long term degradation from weeks to months (Dash and Konkimalla, 2012). In vivo degradation cannot occur readily due to unavailability of desired enzymes and surface erosion caused by hydrolysis is the primary mechanism and the main reason for slow degradation of PCL (Ginde and Gupta, 1987; Woodruff and Hutmaker, 2010).
PLLA.	200 micron and 20 micron films (Mattioli et al., 2012).	5% weight loss by hydrolytic degradation after 49 days (Mattioli et al., 2012).
Mixed mPEG5000–PSA and mPEG2000–PLLA (Lai et al., 2012).	Spherical micelles with hydrophobic matrix and hydrophilic exterior layer (Lai et al., 2012).	Degradation measured from calculation percentage release of curcumin in PBS. Burst release of curcumin near to 40%. Maximum 75% approximate release of curcumin on day 15 (Lai et al., 2012).
P(LLA-*co*-ƐCL) and P(LLA-*b*-ƐCL) (Choi et al., 2002). P(LLA-co-ƐCL) (90/10) (Kalpan et al., 2007). PHCL-g-PLLA (Dai et al., 2009).	240 micon thickness films (Choi et al., 2002). Smooth surface Microspheres (Kalpan et al., 2007). Comb graft polymer films of 110 -120 microns (Dai et al., 2009).	No degradation studies carried out at physiological conditions so far. 60% decrease by hydrolytic degradation in molecular weight after 112 days (Kalpan et al., 2007). 55% weight loss after 70 days (Dai et al., 2009).

Table 2.2: Continued

Polymer	Morphological properties	Degradation studies in physiological conditions
PLGA.	5600 micron diameter Sirolimus loaded films (Ro et al., 2012).	25% weight loss after 13 days for Sirolimus loaded PLGA 50:50 (Ro et al., 2012). 22% mass loss after 55 days for Sirolimus loaded PLGA 75/25 (Ro et al., 2012).

2.2.3 Tensile properties of polymeric microneedles

Dissolvable/biodegradable microneedles require quality testing to determine the maximum direct force required on the base unit before fracturing or crumbling occurs from the tip to the body of the microneedles. Such a test can be done using an axial load testing station which relies on gradually moving the microneedles into a block of metals (e.g. aluminium) until needle breakages are evident (Bariya et al., 2011). A measured section of the metal block contains a pre-determined thickness of skin attached by dual sticky tape and the other section of the block is connected to a compression cell containing microneedles and motorised actuator. The actuator provides a method for constant speed of microneedles insertion into the skin with the output measurement as force (Khanna et al., 2010). A number of components have been used to control tensile strength of dissolving microneedles as shown in Table 2.3.

Table 2.3: Mechanical force properties of microneedle material and force test results of the microneedle system.

Microneedle System	Component with external force tolerance	Results of force tests
PLA (Wang and Jeng, 2009).	Injection grade PLA (Wang and Jeng. 2009).	73.11% impact on structural due to melt temperature variable (Wang and Jeng, 2009).

Table 2.3: Continued

Microneedle System	Component with external force tolerance	Results of force tests
NIPAAm based hydrogel loaded into PLGA (Kim et al., 2012).	Mainly PLGA (Kim et al., 2012).	PLGA microneedles with 18% v/v hydrogel deformed less than the 31% v/v hydrogel ones (Kim et al., 2012).
Sugar glass disaccharide mixture of two sugar components except xylitol (Martin et al., 2012).	Similar molecular weight of two specific disaccharides that formed solid sugar (Martin et al., 2012).	Qualitative skin penetration tests showed most microneedles penetrated skin and complete dissolution in skin after 10 minutes (Martin et al., 2012).
PVP, PLGA, PVA (Ke et al., 2012).	PVP (10000 MW) (Ke et al., 2012).	Microneedles fabricated with 600 mg/ml and 1000 mg/ml PVP were robust as confirmed from SEM images after insertion. The latter PVP concentration showed no geometric change (Ke et al., 2012).
PVP, PVP-MAA poly(vinyl pyrrolidone-co-methacrylic acid (Sullivan et al., 2008).	PVP (8970 MW), MAA (Sullivan et al., 2008).	Displacement force tests proved that 1% MAA in PVP-MAA contributed to nearly double the strength of PVP alone (Sullivan et al., 2008).
PVA/PVP blends (Chu et al., 2010).	PVA (2000 MW) (Chu et al., 2010).	Qualitative skin penetration tests showed 80% of microneedle tips of length 450 μm dissolved in porcine skin after 2 minutes with bright field microscopy (Chu et al., 2010).

2.3 Application of natural polymers for TDD

Polymers are used extensively in TDD drug delivery systems. They control the rate of drug release from the device, act as primary packaging parts, coatings, penetration enhancers and provide ease in drug device handling and structural support to the device in the form of a backing layer. Their unique properties make them ubiquitous component of TDD patches. As petrochemical based resources for the production of synthetic polymers can potentially cause environmental problems; such resources are in short supply and the production of TDD delivery device components from more readily available natural polymers becomes eminent.

Polymers have been in use in TDD delivery as far back as the 1980s. Polymers are used more extensively in TD than any other material as they possess unique properties which are significant to the drug delivery process (Kim, 1996). They are effective in aiding the control of drug release from carrier formulations (Cleary, 1993). Natural polymers are a preferable option in TDD as they are readily available, inexpensive, potentially biodegradable and biocompatible and can undergo various chemical and surface modifications to fit the requirement of the TDD system. A TDD system comprises of a combination of one or more polymers and an embedded drug to be delivered into or through the skin in a controlled and sustained manner (Tojo, 2005).

Polymers used for TDD systems are required to be chemically inert and pure according to high analytical product yields. It should also possess adequate physical properties which correspond with the intended application. The material must not age easily and be suitable for processing. Furthermore biodegradability and safety are paramount properties in the design of a TD patch system due to the long term exposure of the skin in contact withto the patch (Pietrzak et al., 1997; Sonia and Sharma, 2012).

2.4 Hydrogel based drug delivery systems

The need in optimised semi-solid, biocompatible, polymeric formulations in drug loading and routes of entry in the human body is still a growing area in pharmaceutics. Gel and ointment based drug formulations are normally oily and thick in appearance (Mueller et al., 2012). A common purpose of such semi-solid, polymeric gel/ointment formulations are to enhance the viscoelasticity (Teeranachaideekul et al., 2008; Silva et al., 2007) and improve target based pharmacokinetics such as enhanced permeability of luteinizing hormone releasing hormone (LH-RH) from polycarbophil hydrogels inside the vagina compared with solution (Valenta, 2005). Hydrogels can be considered as a semisolid matrix for the purpose of controlled drug release (Jacobs, 2014; York, 1996). A hydrogel is a solid or semi-solid hydrophilic matrix comprising of polymeric macromolecules cross-linked by varying combinations of hydrogen bonding, Van der Waals, ionic electrostatic based and covalent based intermolecular interactions (Laftah et al., 2011; Huang et al., 2007). Hydrogels can change structural configuration during certain temperature or pH induced environments in bodily systems (Cai et al., 2013; Nguyen and Lee, 2010). Usually hydrogels are known to release trapped drug molecules by swelling in watery plasma solvent (Li et al., 2014). A growing demand for hydrogel based drug delivery since 1980 onwards shows increasing treads (Figure 2.5).

This section focuses on hydrogels obtained from natural polymers. It outlines the structure and function of natural polymeric hydrogels in the area of Pharmaceutics based drug delivery. The distinct sub classification of a less common form of hydrogels, known as microgels, explains this difference. Also another area of this review focuses on the physico-chemical properties of hydrogels as a drug delivery system with ideal pharmacokinetic targeting areas.

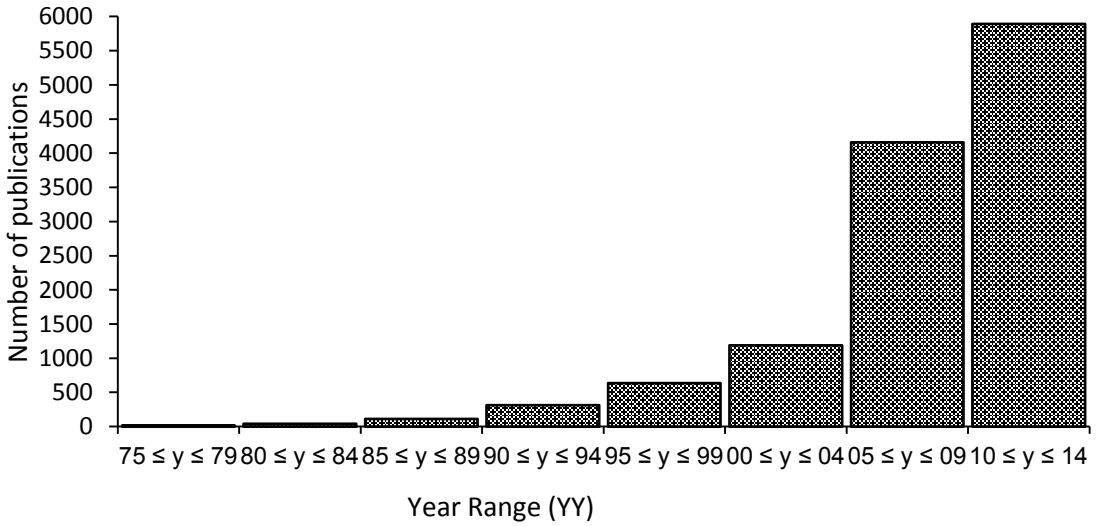

Figure 2.5: The number of hydrogel drug publications according to year range (Web of Science)

Hydrogels possess matrix swelling or shrinkage properties in physico-chemical solvent media such as pH, temperature and ionic strength of electrolytes in solution (Chang et al., 2010; Li et al., 2014). Usually solvent ion concentrations at medium ionic strengths allow for ion exchange between polyelectrolyte gel and solvent ions resulting in osmotic pressure increases inside hydrogel and thus causing swelling (Richter et al., 2008).

The polymeric macromolecules in hydrogels can be cationic, anionic or entirely neutral with regards to interacting with another macromolecule or drug molecules (Van Vlierberghe et al., 2011; Singh and Lee, 2014). The control in the polymeric swelling release rates of drugs with possible subsequent degradation of hydrogels is very much a sought after challenge in matching the duration of drug release across a therapeutic range and target specificity in the body. There are constraints and possible major limitations in stabilising porous combination of polymers in defined mass ratios in attaining desirable controlled release of drug molecules. However the complex chemical structures of hydrogels can pose challenges in synthesis coupled with mass reproducibility and end product purification (Martín del

Valle et al., 2009). Although synthetic polymers seem to have largely dominated over natural polymers in the past decade due to their relatively long service life, high water absorption capacity and gel strength and the possibility of tailored degradation and functionality, natural polymers are highly sort after for their biocompatibility, availability and low cost (Ahmed, 2015). Hydrogels from natural source usually require inclusion of synthetic components as, for example crosslinkers or the hydrogel could be a blend of both natural and synthetic polymers for improved functionality, degradation or biocompatibility (Kamoun et al., 2015).

2.4.1 Polymeric crosslinking in hydrogels

An important characteristic of a hydrogel is the polymeric strand crosslinking. Crosslinking of hydrogels with morphologically cross hatched or entangled macromolecular architecture allows a 3D structure and avoids immediate dissolution of separate macromolecular strands in hydrophilic solvent (Hennick and van Nostrum, 2012). The crosslinking of hydrogels combines highly desirable characteristics such as mechanical strength, pseudoplasticity, drug and macromolecular intermolecular interactions and plasma swelling (Zhao et al., 2014; Kurland et al., 2014). The macromolecule respresents a polymeric drug vehicle and chemical bonding interactions with specific drugs is just as important as release in skin stratra or plasma medium. The porosity of the crosslinked hydrogel matrix determines aqueous solvent adsorption and rate of drug release (Hoare and Kohane, 2008). However, the immiscibility of hydrogels swelling in water is attributed to the networking arrangement of crosslinks between polymer chains thus maintaining physical structure (Gupta et al., 2002). Physical crosslinking of polypeptides are attributed to ionic bonding, hydrogen bonding and hydrophobic interactions in aid of bi-polymeric crosslinking (Nonoyama et al., 2012; Hu et al., 2010). Physically crosslinked hydrogels are inhomogeneous due to more than one type of intermolecular based interaction (Hoffman, 2002). Chemically crosslinked

hydrogels involve covalent linkages in bridging two different polymeric strands and the use of crosslinking agents that can react with specific functional groups in polymeric macromolecules (Hennick and van Nostrum, 2012). Chemically crosslinked hydrogels permit bigger volume increases during sol-gel transition than physically crosslinked hydrogels (Jonker et al., 2012). The use of chemical crosslinking agents to bind specific functional groups for crosslinking polymers is shown in Table 2.4. The process and target application of hydrogel and microgel polymers is outlined in Table 2.5.

Table 2.4: Chemical agents for the chemical crosslinking of functional groups in hydrogels.

Crosslinker	Functional groups	Reaction or functional group interactions	Chemical reaction conditions
Glutaraldehyde (Berger et al., 2004; Costa-Júnior et al., 2009).	di-aldehydes (Berger et al., 2004).	Imine group formed by Schiff base formation. (Berger et al., 2004; Costa-Júnior et al., 2009). Acetal group formation from hydroxyl groups (Costa-Júnior et al., 2009).	No heat required and slow addition is usual (Costa-Júnior et al., 2009).
Poly(ethylene glycol)–propion dialdehyde (PEG–diald) (Luo et al., 2000).	Amine (Luo et al., 2000).	Azide addition (Luo et al., 2000).	Unimolecular addition of PEG-diald and polymer in ambient temperature conditions (Luo et al., 2000).
methylene bis-acrylamide (Berger et al., 2004).	acrylamide, ethylene (Berger et al., 2004; Bhattacharyya and Ray, 2014).	Variable (Berger et al., 2004).	Hydrophobic and therefore solubility in water is low (Yang et al., 2012a).
Genipin (Song et al., 2009; Muzzarelli, 2009).	Amino acid groups and secondary amino group in acidic and neutral pH (Muzzarelli, 2009).	Amino acid groups (Song et al., 2009). Condensation reactions in acidic or neutral conditions and aldol condensation in basic conditions (Muzzarelli, 2009).	Set pH conditions (Muzzarelli, 2009).

Table 2.5: Recent examples of hydrogels developed in drug delivery.

Polymer	Composition	Process	Target/ delivery	Reference(s)
Casein.	100 %.	Temperature based gelation.	Bovine Serum Albumin molecule into buffered solution.	Song et al. (2009).
poly(N-isopropyl-acrylamide-co-Acrylamide) poly(NIPAAm-co-AAm).	NIPAAm and AAm, 83.3:16.7 (% mol ratio).	Poly(NIPAAm-co-AAm) synthesis: free radical copolymerisation with AIBN initiator. Micro-sphere process: W/O emulsification and copolymer solubilised by acidic DI water and crosslinking using glutaraldehyde.	Propranolol and Lidocaine.	Fundueanu et al. (2009).
Alginate (Monomer unit: 1,4-linked b-D-mannuronic acid and a-L-guluronic acid).	Methacrylated alginate (5.7 to 45.3 %).	Photocrosslinking of methacrylated alginate at 365 nm and 0.05 % w/v Irgacure D-2959 photo initiator.	Bovine chondrocytes for cytocompatiblity for cell culture.	Jeon et al. (2009).
NaCMC:Cellulose (Cell).	NaCMC:cell (5:5 to 9:1 by wt). A hydrogel film.	Solubilisation of Cell and NaCMC and crosslinking with Epichlorohydrin (ECH).	In vitro release of Bovine Serum Albumin.	Chang et al. (2010).
poly(ethylene oxide)-poly(propylene oxide)-poly(ethylene oxide) (PF127) and Poly(methy vinyl ether-co-maleic anhydride) (GZ).	GZm/PF127 molar ratio from 1 to 20. (GZm is the monomer, methy vinyl ether-co-maleic anhydride).	Esterification between carboxyl groups of maleic anhydride and hydroxyl groups of PF127. Subsequent solvent evapor- ation of tetra- hydrofuran followed by precipitate copolymer filtration and collection.	Bovine Serum Albumin, glucoprotein rKPM-11 and Dextran in PBS (pH 7.4).	Moreno et al. (2014).

2.4.2 Natural polymers in hydrogels

Polysaccharides such as hyaluronic acid, chondroitin sulfate, chitosan, carboxy-methylcellulose, hydroxypropylmethylcellulose, methycellulose, bacterial cellulose and sodium alginate are common examples of carbohydrate derived polymers in hydrogels (Van Vlierberghe et al., 2011). Examples of proteins used in hydrogels include gelatine, collagen, elastin, ovalbumin, β-lactoglobulin and silk fibroin from both plant and animal sources (Jonker et al., 2012). Polymer strands from natural, synthetic and partially synthetic sources are acquired as drug delivery vehicles (Gupta et al., 2002).

Cellulose is a highly abundant natural polymer in plants, bacteria, algae and fungi phylum. The unbranched chains consist of 1,4 glycosidic linkage of monomer units, D-glucopyranose (DGP) and presence of three hydroxyl groups per DGP monomer (Kamel et al., 2008; Carter Fox et al., 2011). NaCMC is a cellulose derived water soluble polymer (Venkata Prasad et al., 2011). NaCMC is grossly anionic because of the negative electron density with respect to the carboxymethyl substitution region. Hence, polyanionic NaCMC has the potential to electrostatically interact with gelatine below its isoelectric point (Devi and Kumar, 2009). NaCMC and gelatine are biocompatible as NaCMC is biologically excreted and gelatine is degraded by natural enzymes (Rathna and Chatterji, 2003). NaCMC is able to hydrogen bond with water molecules hence hydrogel NaCMC crosslinked gelatine possesses swelling properties which is reported by Tataru et al. (2011). Individual polymers of NaCMC and gelatine have the tendency to swell in ambient temperature water. As far as we know there is no published literature comparing swelling rates of individual NaCMC and gelatine with post bi-polymeric NaCMC/gelatine microgel. Ionic interactions are dominant intermolecular forces in crosslinking polyanionic NaCMC with polycationic polymers such as polyvinylamine (PVAm) (Chang and Zhang, 2011). The degree of substitution defines this structure when hydroxyl

groups in the glycopyranose monomer are replaced with carboxymethyl groups in which the number of substituted hydroxyls accounts to the degree of substitution (Rokhade et al, 2006). The higher the degree of substitution and quite significantly the lower the MW of NaCMC allows for increased in ionic conductivity (Lee and Oh, 2013). The discharge capacity of NaCMC (0.9 degree of substitution and 250 kDa) upto 0.5 current density (C-rate) was 165mAh g^{-1} compared with NaCMC (0.9 degree of substitution and 700 kDa) at 155mAh g^{-1} (Lee and Oh, 2013). Potentiometric titration with hydrochloric acid as a carboxylate proton donor coupled with Infrared spectroscopy in knowing the relative amount of carboxyl groups is implemented in calculating degree of substitution (Pushpamalar et al., 2006).

2.4.3 Preparation techniques of hydrogels

There are numerous engineering techniques for the preparation of natural hydrogels. Natural polymers such as gelatin, κ-carrageenan, agarose and gellan gum in hot solutions undergo random coil to helix transitions with the support of ionic salts such as Na^+ which lowers the repulsive forces between same electrostatic charges, allowing ionic interaction and the polymeric crosslinking to occur (Figure 2.6) (Coutinho et al., 2010; Gulrez et al., 2011).

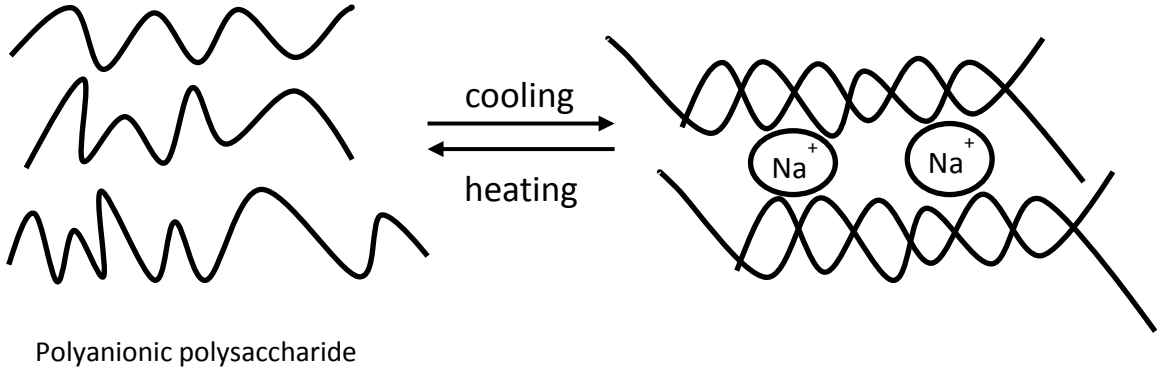

Figure 2.6: Illustration of random coil to helical transition of anionic, natural polymers, eg. gellan gum during the cooling of a hot polymeric solution

A process known as complex coacervation involves the electrostatic attraction of oppositely charged polyelectrolytes such as precipitate or gel in solution because of change of factors such as pH, ionic strength and polymeric mass ratios (Jin and Kim, 2008; Hoffman, 2002). An alginate/β-lactoglobulin lipid droplets contained in hydrogel matrices were complex coacervated with alginate ($-NH_3^+$) and cationic chitosan ($-COO^-$) at acidic pH ranges of 3.5 to 6.5 in the formation of beads for gastrointestinal active molecule delivery (Li and McClements, 2011). An example of a complex coacervate bi-polymer is NaCMC and gelatine in the formation of a complex coacervate.

2.5 Mathemathatical description of percutaneous based pharmacokinetics in targeting the viable epidermis layer

Fick's law of diffusion for molecules is applicable in calculating a concentration gradient from a high concentration area to a concentration low area. The diffusion of molecules across a gradient concentration from a planar surface is outlined from Fick's 2nd law (equation 2.1) (Brazel and Peppas, 2000; Lin and Metters, 2006).

$$\frac{\partial c}{\partial t} = \frac{\partial}{\partial x}\left(D\frac{\partial c}{\partial t}\right) \tag{2.1}$$

Equation 2.1 is a one dimensional, non-steady state, concentration dependent diffusion coefficient. Also equation 2.1 is suitable for a drug system consisting of drug molecules uniformly distributed in the matrix vehicle. The conditions in order to solve the equation according to initial drug distribution and diffusion conditions of delivery system boundary, the boundary conditions are defined as:

$$\text{At } t=0,\ c(x,t) = C_0 \tag{2.1.1}$$

$$\text{At } x = \delta(t),\ C = C_b \tag{2.1.2}$$

$$\text{At } x=0,\ \delta c/\delta x = 0 \tag{2.1.3}$$

C_0 is the uniform, initial drug molecule concentration (equation 2.1.1), δ*(t)* is the drug molecule distance from the centre to the surface which increases when the hydrogel swells (equation 2.1.2), C_b is the bulk loading concentration of the drug in the polymeric surface (equation 2.1.2), it is 0 in perfect sink conditions and *x* is axial plane for drug diffusion (equation 2.1.3). The pharmacokinetics in the permeation of drugs past the SC layer when a reservoir drug system is adopted requires computation using Fick's 1st law of diffusion (equation 2.2) (Couto et al., 2014; Lin and Metters, 2006).

$$J = -D_m \frac{dC}{dx} \tag{2.2}$$

Where *J* is the drug diffusion flux, *C* is the drug concentration, *x* is the thickness of membrane and D_m is the membrane drug diffusion coefficient. The steady state flux of active molecules between vehicle and a skin layer across a concentration gradient mapping one compartment model defined by Fick's 1st law (equation 2.2.1) (Scheuplein et al., 1969; Couto et al., 2014).

$$J_s = k_p \Delta C_{vs} = \frac{K D_m \Delta C_{vs}}{L} \tag{2.2.1}$$

Where *Js* is the steady state diffusion coefficient, k_p is the permeability coefficient comprising of three individual parameters, ΔC_{vs} is the drug concentration gradient between vehicle and skin and *K* is the partition coefficient between drug and skin. For simplicity sake, the VE and Upper dermis will be referred to as VE here and the amount of drug detected can be quantified when the scaler unit of time is outlined in the main equation (2.3).

$$Q = D_m \frac{A}{L} t \Delta C_{vs} \tag{2.3}$$

Where D_m is the diffusion coefficient of a skin layer, *Q* is the amount of active molecule, *A* is the skin surface area, *t* is the time taken for a particular skin path length travelled *L*.

2.6 Chapter summary

Although a number of lidocaine based TD products can be found in the market there is a large gap for lidocaine microneedle products, especially biodegradable microneedles. This implies that considerable amount of new research is required at the developmental and pre-clinical setting in order to achieve the desired controlled release of lidocaine into skin and maintain a steady drug concentration for a short duration of time for the purpose of superficial suturing of a cut. A biodegradable lidocaine microneedle system formulated from carboxymethylcellulose demonstrated the increase in pharmacokinetic permeation flux, thus highlighting further interest in research of other biodegradable materials as drug vehicles for lidocaine with the aim of achieving faster permeation kinetics in skin with the general idea of a minimal delayed therapeutic action. Also, the development of lidocaine microneedles may provide a scope for a cheaper product as compared with current EMLA formulations containing lidocaine in which a second local anaesthetic, prilocaine add to the material costs. Manufacturing of biodegradable microneedles via a casting process with usage of SU-8 or PDMS moulds is economical mainly because these moulds can be reused numerous times in mass production of biodegradable microneedles. The mechanical penetration strengths are a highly important physical challenge seen in biodegradable microneedles. Not only is a sharp tip of microneedle necessary for cutting through skin but the casted, dissolvable material requires adequate resistant to compression forces that mimic finger or thumb pressures. Dissolvable materials with soft solid or brittle physical properties require mucoadhesive co-polymer agents, such as PVA or PVP, in the mixture to provide for mechanical strength.

Natural polymers are very much taken as a substitute to synthetic based petrochemical products because of an environmentally friendly impact. The main criteria is to match the structure with function inconjunction to ideal reproducible

pharmcokinetics in order enhance drug specificity in targeting the disease in a biological system. Nevertheless synthetic petrochemical products cannot be completely removed in the fabrication of certain drug vehicles eg. transdermal patches. This is because certain desirable properties from synthetic products are not observed in common natural polymers hence the adaptation of blended polymeric vehicles. Such petrochemical products can be treated as additives as long as low amounts are permitted to form the polymeric blend.

Chapter 3

Microneedle-assisted permeation of lidocaine carboxymethyl-cellulose with gelatine co-polymer hydrogel

Chapter overview

Lidocaine was formulated in NaCMC/gelatine hydrogel and a 'poke and patch' microneedle delivery method was used to enhance the skin permeation rates and flux parameter of lidocaine. The microparticles were formed by electrostatic interactions between NaCMC and gelatine macromolecules within a water/oil emulsion in paraffin oil and the covalent crosslinking was supported by additional organic molecules, glutaraldehyde. The gelatine to NaCMC mass ratio was varied between 1.6 and 2.7. The lidocaine encapsulation yield in the hydrogel formulation was 1.2 to 7% w/w. Lidocaine NaCMC/gelatine hydrogels was assessed for encapsulation efficiency, Zeta potential, mean particle size and morphology. Subsequent in vitro skin permeation studies were performed via PD and microneedle assisted permeation of lidocaine NaCMC/gelatine to determine the maximum permeation rate through full thickness skin. Lidocaine 2.4% w/w NaCMC/gelatine 1:1.6 and 1:2.3 respectively, possessed optimum Zeta potential. Lidocaine 2.4% w/w NaCMC/gelatine 1:2.3 and 1:2.7 demonstrates higher pseudoplastic behaviour. Encapsulation efficiency (14.9–17.2%) was similar for lidocaine 2.4% w/w NaCMC/gelatine 1:1.6–1:2.3. Microneedle assisted permeation flux was optimum for lidocaine 2.4% w/w NaCMC/gelatine 1:2.3 at 6.1 µg/ml/h. Lidocaine 2.4% w/w NaCMC/gelatine 1:2.3 crossed the minimum therapeutic drug threshold with microneedle skin permeation in less than 70 min.

3.1 Introduction

The delivery of local anaesthesia to lacerated skin regions remains a major challenge for injectable and ointment drugs (Smith and Wilson, 2013). For example,

the subcutaneous injection delivery of local anaesthetics, specifically lidocaine is clinically reported to cause a burning type feeling when infused directly into the skin. Also, lidocaine requires additional active drug molecules in an ointment formulation to compete with injectable lidocaine (Smith and Wilson, 2013; Hogan et al., 2011; Capellan and Hollander, 2003). A bolus dosage of lidocaine by injection is suitable for short duration of action (Smith and Wilson, 2013; Hogan et al., 2011; Capellan and Hollander, 2003; Bekhit, 2011). However, the treatment of multiple lacerations in skin may need co-drugs such as epineprine to aid longer time for lidocaine action, which may be ineffective due to a shorter sustained subcutaneous infiltration or simply a second bolus injection after the first lag time (Bekhit, 2011; Chale et al., 2006; Pregerson, 2007). Lidocaine's characteristic amide functional group (Braga et al., 2013) and its weak base molecule (pKa 7.7) with a lipophilic function while permeating through biological membranes is still a highly attributable choice of local anaesthesia since its first chemical synthesis in 1943 (Braga et al., 2013; Conroy and O' Rourke, 2013). Similarly, the protonated lidocaine is a weakly acidic, hydrophilic molecule which is easily soluble in water at ambient temperature. Injectable lidocaine solution in either the basic or acidic form shares the same local anaesthetic mechanism for the antagonism of nerve signals in cells by inhibiting the influx of sodium ions through the sodium channels of biological cell membranes resulting in a response to temporary pain blockage on the skin surface (Xia et al., 2002; Cepeda et al., 2010; Columb and Ramsaran, 2010). Lidocaine is dependent on a drug vehicle as a support material with respect to viscoelastic bulking and balancing of the encapsulation efficiency with enhanced skin permeation pharmacokinetics. NaCMC polymer and gelatine co-polymer, according to a defined mass ratio are suitable candidates in mapping the crosslinking structure with the functional role of trapping lidocaine and with the goal for optimised skin. The aim of this chapter is to formulate an ideal gelatine to bipolymeric NaCMC mass ratio with lidocaine before determining promising permeation trends for skin based delivery.

NaCMC/gelatine microparticulates form covalent linkages between NaCMC's hydroxyl group lactonisation with the aldehyde of glutaraldehyde's –CHO group in the formation of ether bonds under low pH conditions (Buhus et al., 2009) (Figure 3.1a). A schiff base association between glutaraldehyde and gelatine is formed by covalent linkage in minimising ionic dissociation between NaCMC with gelatine in neutral media (Buhus et al., 2009; Mu et al., 2012) (Figure 3.1a). Also, ionic interactions occur between polyanionic NaCMC, glycine and proline amino acids of a polycationic gelatine and cationic lidocaine with the effect of charge neutralisation (Becker and Reed, 2012; Alvarez-Lorenzo et al., 2013) (Figure 3.1b). Overall, this process forms a pH sensitive hydrogel network of NaCMC intertwined with gelatine crosslinks for trapping active molecules such as lidocaine (Hoare and Kohane, 2008; Matricardi et al., 2013).

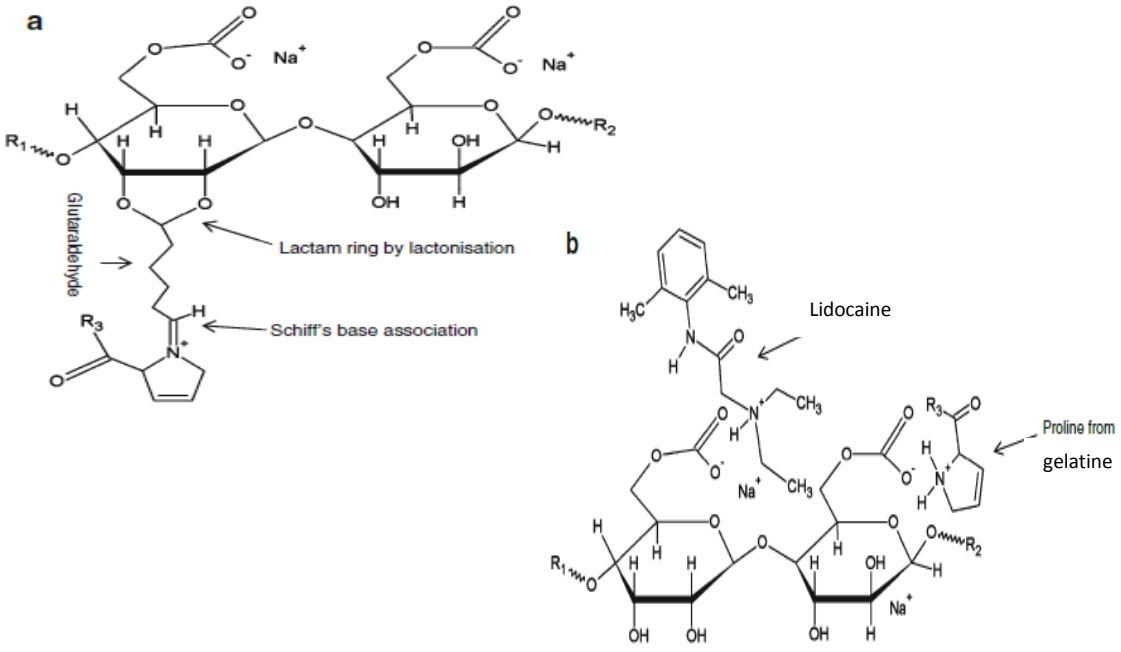

Figure 3.1: (a) Crosslinking between NaCMC and gelatine via ether bonds between NaCMC and glutaraldehyde and schiff's base C=N linkage between glutaraldehyde and proline of gelatine. R_1, R_2, R_3 are repeating monomeric units of each polymer. (b) Ionic interactions between NaCMC, proline of gelatine and lidocaine. R_1, R_2, R_3 are repeating monomeric units of each polymer.

The most ideal pH for electrostatically crosslinking NaCMC with gelatine is at pH 4.0 from the view point of Zeta potential analysis. The lidocaine NaCMC/gelatine vehicles are hydrogel microparticles because of pH sensitivity across a factor of 3.5 which interrupts the electrostatic interactions, allowing the release of trapped drug molecules (Qiu and Park, 2012).

The microparticles in lidocaine NaCMC/gelatine hydrogel alone cannot optimise skin permeation kinetics and a minimally invasive skin puncturing device is essential in aiding the optimisation of skin permeation kinetics. Recent advances in microneedle technology promises to resolve this issue and allow microneedle assisted lidocaine delivery from NaCMC/gelatine hydrogel. Microneedles are minimally invasive micron scale needles protruding perpendicularly from a laterally mounted platform. It is a painless method of micro-injection for not hitting pain receptors concentrated in the dermal layer of skin (Patel et al, 2011). The planar surface and geometrical properties of the MNs, and the texture of skin, which is relatively impermeable to large aqueous, active molecules and drug molecules in a bulk polymeric formulation, can increase permeation through the VE layer of skin via micro-channel cavities created by MNs (Al-Qallaf and Das, 2008; Henry et al., 1998).

Biomedical grade stainless steel is a suitable metallic alloy for MNs as it allows for fast and economical shape cutting to specific dimensions in-conjunction to retaining its highly desirable compressive strength properties (Henry et al., 1998; Donnelly et al., 2010). For example, we find that Type 304 stainless steel has been chosen to prepare MNs in some studies because of its biocompatibility and inherently good compressive and shear force properties (Davis et al, 2003). Recent advances in lidocaine delivery methods involved liquid crystalline polymeric MN arrays which successfully delivered 71% of lidocaine by mass using a coat and poke method with

a therapeutic level maintained for approximately 5 min (Zhang et al., 2012a). Solid MNs were also structured from solution components of lidocaine, mixed with sodium chondroitin sulfate and cellulose acetate as water soluble vehicles (Ito et al., 2013). Skin permeation analysis sustained a therapeutic threshold of lidocaine between 89 and 131 μg/g for an approximate duration of two and a half minutes before crossing the maximum therapeutic level pertaining toxicity greater than 131 μg/g for over 10 min (Ito et al., 2013). A detailed review explaining the current material properties, fabrication process and pharmacokinetic delivery of lidocaine in polymeric microneedles are discussed in detail by Nayak and Das, 2013.

The development of lidocaine NaCMC/gelatine hydrogel coupled with microneedle delivery via a 'poke and patch' method is a promising approach (Nayak and Das, 2013). The approach requires no additional active co-drugs when formulated with NaCMC/gelatine polymeric mass ratios as the most abundant drug vehicle reagents. Co-drugs for lidocaine significantly add to the cost of the final product than NaCMC and gelatine vehicles in abundance. However, at the moment, there is little known about the significance of MN assisted permeation of lidocane from the micro-particles in NaCMC/gelatine hydrogel, and in particular, the relationship of the permeation kinetics with the geometrical parameters of MNs, e.g., the length of the MNs. In addressing these issues, this work aims to develop a lidocaine formulation in NaCMC/gelatine hydrogel and, explore, for the first time, a 'poke and patch' MN delivery method for the purpose of improved drug permeation rates and permeation flux of lidocaine.

The overall goal is towards an optimised cumulative amount of lidocaine in watery plasma media, enhanced lidocaine permeation flux and encapsulation efficiency in-conjunction with a sustained therapeutic permeation range transdermally of over 15 min. As explained in detail previously, lidocaine, as a weak acid, can be bound

electrostatically within soluble drug vehicles consisting of crosslinked NaCMC and gelatine macromolecules. NaCMC, gelatine and glutaraldehyde are cheap, bio-compatible and readily available compounds as potential drug formulas in constructing a carrier for lidocaine. Lidocaine molecules diffuse from the electrostatically formed microparticle to the surrounding DI water, analogous to the watery plasma of the VE layer of skin. The operation of the 'poke and patch' technique allows for lidocaine from hydrogel to permeate through microneedles formed holes on the skin and dissolve into the VE layer. The microparticles in the lidocaine NaCMC/gelatine hydrogel are hydrophilic in nature. A concentration gradient between lidocaine NaCMC/gelatine hydrogel and underlying watery plasma of skin allows for lidocaine to dissociate from NaCMC/gelatine hydrogel and associate as lidocaine into the neutral watery plasma. Skin permeating rates will be compared for PD and MN assisted diffusion of lidocaine NaCMC/gelatine hydrogels.

3.2 Materials and methods

A laboratory scale batch process for the formulation of lidocaine NaCMC/gelatine hydrogel is highly advantageous with respect to low heat treatment and quite efficient preparation times in reaching the desired product. Also laboratory scale processes are essential before devising new process control method plans on a pilot plant scale. A brief mention of pilot plant scale methods does not imply further objectives in this thesis. The high degree of carboxylate substitution of NaCMC of 0.9 enhances the possibility of greater crosslinking with type A, i.e., high bloom gelatine. As explained in the introduction, the crosslinking is electrostatically achievable at pH 4. Lidocaine is a favourable drug molecule in association with NaCMC/gelatine at pH 4 for encapsulation purposes. The glutaraldehyde is necessary in defining spherical microparticles from water in oil (w/o) droplets.

3.2.1 Materials

NaCMC (Degree of substitution: 0.9; MW: 250 kD), sorbitan monooleate (SPAN 80), glutaraldehyde (stock solution of 50% w/w), paraffin liquid (density: 0.859 g/ml), Lidocaine (MW: 288.81 g/mol) and porcine gelatine (type A, Bloom 300) were purchased from Sigma Aldrich Ltd, Dorset, UK. Acetic acid (analytical grade), acetonitrile (HPLC grade), ammonium bicarbonate (analytical grade) and n-hexane (95% w/w) were purchased from Fisher Scientific Ltd, Loughborough, UK. DI water was the common solvent for aqueous solutions unless otherwise stated.

3.2.2 Constant loading of drug lidocaine in hydrogel of different NaCMC/gelatine mass ratios

The mass ratio of NaCMC/gelatine outlines one of the formulation characteristics in relation to lidocaine pharmacokinetics in this study. Therefore, different NaCMC/gelatine mass ratio polymers were encapsulated with a constant lidocaine dosage. The individual reagents/chemicals chosen for this purpose are represented in Table 3.1. The overall batch process for lidocaine NaCMC/gelatine hydrogels is outlined in Figure 3.2. A non-ionic surfactant, Span 80 (0.5% w/w), was dispersed dropwise in 100 ml of light paraffin oil, which was continuously stirred at 400 rpm in a rotating vessel (IKA-Werke, Staufen, Germany) until a slightly cloudy, homogeneous mixture was formed. NaCMC was observed to swell before dissolution in DI water. NaCMC was manually sheared and gently heated (~50˚C) in DI water in order to increase surface area of swollen NaCMC gelly like clumps and accelerate dissolution. Aqueous NaCMC (1.2% w/w) was then dispersed dropwise into the paraffin/surfactant mixture with shear induced at 400 rpm using the same rotating vessel followed by aqueous dropwise dispersion of gelatine (cG,% w/w) until a viscous w/o emulsion was formed (Table 3.1). Prior to gelatine dispersion, gelatine solid was gently heated (~60˚C) to accelerate dissolution until a clear

solution was observed. This gelatine solution was allowed to cool slightly in ambient room temperature to ~40˚C before dropwise dispersion.

The variable mass percentage of the gelatine is denoted by the term cG. In the next step, the pH of the w/o mixture was decreased to pH 4 using acetic acid (~1% w/w). Continuous gentle shear was induced so that the dispersed ionically charged droplets are detected by the pH electrode. The continuous oil component in a w/o immiscible mixture is non-ionic and therefore the pH is not registered. The chosen value, pH 4 was based on Zeta potential as discussed later in this chapter. Lidocaine (2.4% w/w) was then dispersed drop wise into the emulsion and cooled in a refrigerator (4–6ºC) for 30 min. The cooled lidocaine NaCMC/gelatine emulsion was agitated in a rotating vessel (IKA-Werke, Staufen, Germany) at 400 rpm to re-suspend the emerging hydrogel microparticles before the drop wise addition of glutaraldehyde (0.1% w/w). The w/o droplets were transformed into microparticles by the glutaraldehyde and stirred at 1000 rpm for a duration of 2 h to ensure thorough mixing. The resultant lidocaine NaCMC/gelatine formulation was stored at 2–4°C in a laboratory refrigerator (Liebherr-Great Britain Ltd, Biggleswade, UK) for a period of 4 hours to allow for the separation of residual paraffin liquid (organic layer) from a dense lidocaine NaCMC/gelatine formulation layer. The organic layer was cloudy in appearance as compared with the lower dense layer. After refrigeration, the organic layer was syringe removed. The refrigerated lidocaine was mixed with an organic solvent, n-hexane (50% v/v) for the subsequent removal of residual organic solvent. Any remaining residual organic solvent was oven dried under vacuum at 40°C to enhance solvent evaporation (Technico, Fistreem International Ltd, Loughborough, UK). Finally, any unbound lidocaine was removed through filter washing with DI water. The grade 3 filter (Whatman International Ltd, Oxon, UK) that was used for the formulation washing stage had an average pore size of 6 µm. The lidocaine NaCMC/gelatine hydrogels were collected in amber vials and characterised for PD and MN assisted skin permeation.

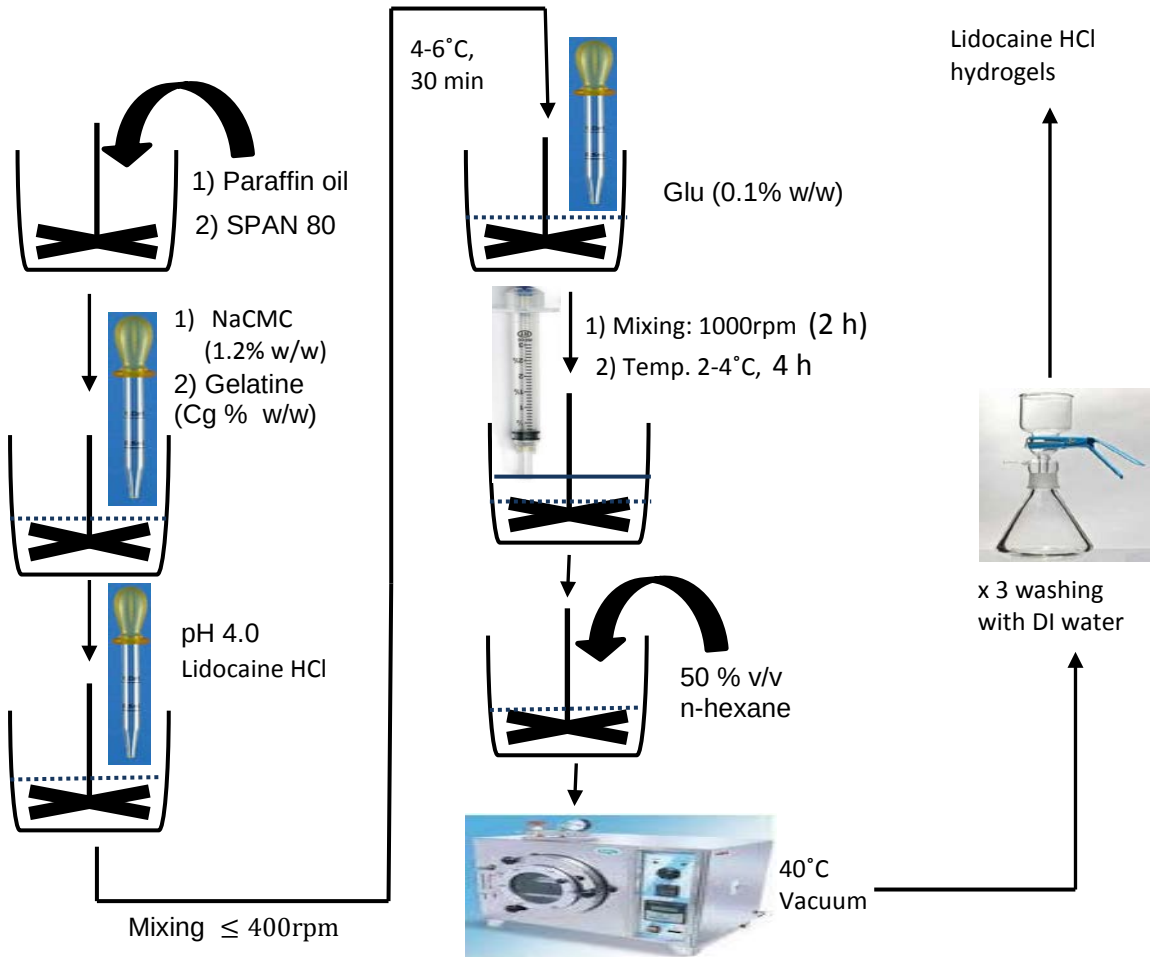

Figure 3.2: Batch processing of lidocaine NaCMC:gelatine hydrogel formulation

Table 3.1: Composition of reagents used in formulating distinct lidocaine NaCMC/gelatine (NaCMC/G) hydrogels

Drug Formulation	Lidocaine HCl (% w/w)	DI water (% w/w)	cG (% w/w)	Paraffin oil (% w/w)	SPAN 80 (% w/w)	Na-CMC (% w/w)	Acetic acid (~ %w/w)	Glutaraldehyde (% w/w)
Lidocaine NaCMC/G hydrogel	2.4	26.1	2.0	66.7	0.5	1.2	1.0	0.1
		25.6	2.5					
		25.3	2.8					
		24.9	3.2					

Table 3.1: Continued

Drug Form-ulation	Lido-caine HCl (% w/w)	DI water (% w/w)	cG (% w/w)	Paraffin oil (% w/w)	SPAN 80 (% w/w)	Na-CMC (% w/w)	Acetic acid (~ %w/w)	Glutar-alde-hyde (% w/w)
Lidocaine NaCMC/G 1:1.6 hydrogel	1.2	27.3	2.0	66.7	0.5	1.2	1.0	0.1
	2.4	26.1						
	2.8	25.8						
	7.0	21.5						
Lidocaine NaCMC/G 1:2.3 hydrogel	1.2	26.5	2.8					
	2.4	25.3						
	2.8	25.1						
	7.0	20.7						
Unloaded NaCMC/G 1:2.3 hydrogel	0	27.7	2.8					

3.2.3 Different loading of drug lidocaine in hydrogel of constant NaCMC/gelatine mass ratio

The plausible effect of varying lidocaine concentration on constant NaCMC/gelatine mass ratios is necessary in exploring significant changes in pseudoplasticity and microparticle dispersion. In this case, the preparation methods and conditions were replicated as those adopted for constant lidocaine encapsulation experiments described earlier. Also the outlined batch process was the same (Figure 3.2). However, on this occasion, the initial lidocaine concentration in the NaCMC/gelatine hydrogel was varied in the range 1.2–7.0% w/w prior to achieving a hydrogel of certain NaCMC/gelatine mass ratio. Lidocaine NaCMC/gelatine with 1:1.6 and 1:2.3 mass ratios of microparticles were prepared to evaluate visco-elasticity and Zeta potential effects for a variable lidocaine encapsulated concentration (Table 3.1).

3.2.4 The unloaded NaCMC/gelatine 1:2.3 mass ratio hydrogel

The effect of varying pH on Zeta potential for unloaded NaCMC/gelatine 1:2.3 mass ratio hydrogel was used as a drug free control in this study to explore the ideal pH conditions for microparticle dispersion. Unencapsulated gelatine to NaCMC mass ratio of 2.3 for hydrogel microparticles, which were devoid of lidocaine were replicated from the same methods and conditions as for the constant lidocaine encapsulation to evaluate the Zeta potential effects (Table 3.1).

3.2.5 *In vitro* permeation of lidocaine from NaCMC/gelatine microparticles

An FDC for vitro skin permeation was used in exploring and understanding the pharmacokinetics of lidocaine prepared with different NaCMC/gelatine mass ratios. The FDC is a common method for TD permeation studies. It has two compartments which comprises of a donor (open cylinder lid) and a receptor. The skin sample is sandwiched between the two compartments (Küchler et al., 2013). The donor compartment represents the interface between the drug component and skin surface (Karadzovska et al., 2013). In particular, this research infers the receptor compartment is the interface between lower VE/upper dermis regions of porcine skin with deeper dermis layer of skin in the water plasma, receptor compartment (Karadzovska et al., 2013). In this work, MN assisted diffusion of lidocaine NaCMC/gelatine (Figure 3.3) were studied using full thickness porcine skin.

All skin samples were excised from an ear auricle with approximate dimensions of 20.0 x 20.0 x 0.73 mm which were acquired from 4 to 5 months old piglets and stored at −20.0°C. The procurement of swine auricles were confirmed to be pre−washed in plain water and purchased in a non-mutilated condition from swine cadaver. An approximate force of 0.57 N per array perpendicular to the base was directed on AdminPatch MNs (Nano-biosciences, Sunnyvale, CA, USA) pre-fabricated from stainless steel with arrow head geometry.

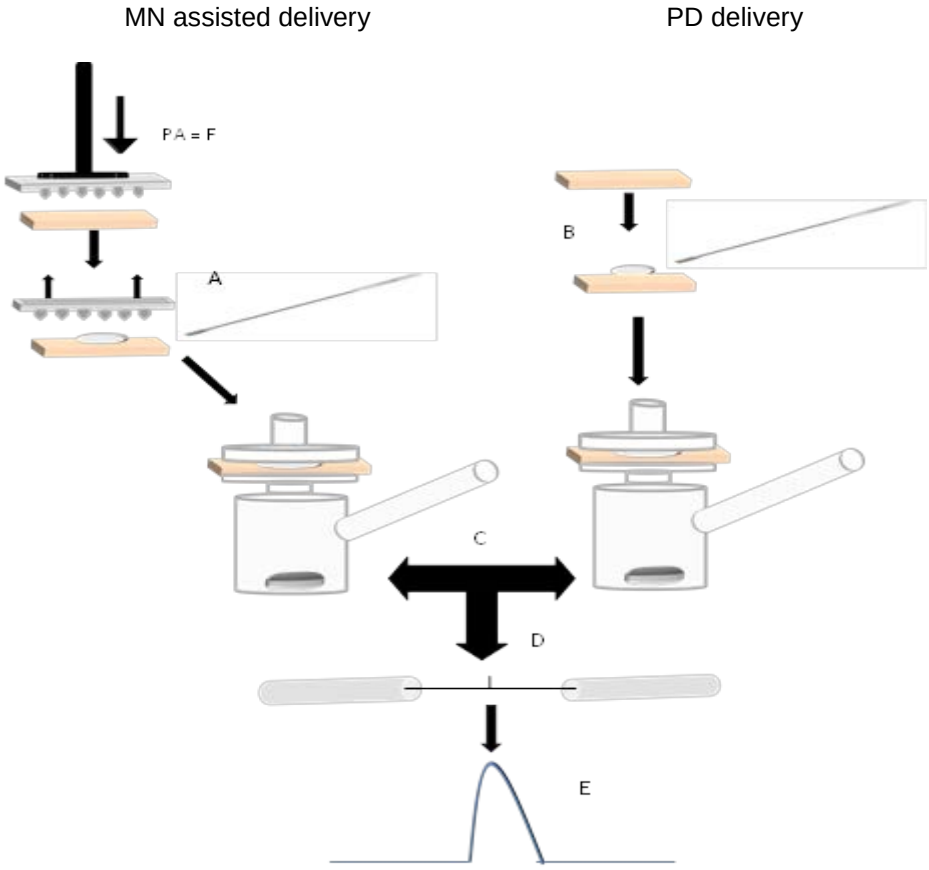

Figure 3.3: Pathways for miconeedle assisted and PD studies of lidocaine NaCMC/gelatine on porcine skin via FDCs. Porcine skin was treated with microneedles before the addition of lidocaine NaCMC/gelatine (A) for FDC. The direct addition (B) of lidocaine NaCMC/gelatine is the start of the PD pathway. Sample lidocaine NaCMC/gelatine (C) added to skin undergoes FDC experimentation for both microneedle and PD delivery. The FDC receptor amount was removed and centrifuged (D). The supernatant removed was then analysed using liquid chromatography – diode array (LC-DA) (E). Inset is a stainless steel micrnoneedle array with needle aspect ratio of 1:4 and a tip to tip needle spacing of 1100 μm.

The MNs were applied on the skin for a total duration of 5 min. This corresponds to the time duration we needed to pierce the skin without bending or damaging the MN. We wanted to ensure that each experiment with MN is conducted for a consistent time of application and thumb force. From our experiments (e.g, staining experiments) we found that it was necessary to apply the MNs for about 5 min on

the skin sample before we obtained detectable holes on the MN. Many MNs (e.g., those which are coated with drugs or biodegradable in nature) are designed to stay in the skin for longer duration (e.g., 30 min - 4 h) so that the drugs loaded on the MNs are released. This is not the case in this study and we apply the MNs for 5 min to create the holes on the skin. The force inducer supporting a flat based punch dye was lowered below the flat MN base before the application of forces was directed on the MN array by hand leverage. At the end of 5 min the applied force was released, the microneedle array was carefully removed and a constant mass of lidocaine formulation (0.10 ± 0.03 g) was placed on the skin. This technique is a two stage process commonly described as “poke and patch” (Van der Maaden et al., 2012) where the “patch” in this context is the applied hydrogel formulation.

It is known that the penetration depth of the MNs is less than the actual MN lengths. Further, the penetration depth depends on the MN density on the patch, and other factors (e.g., tissue) remaining the same. From the histology of the skin with and without MNs, we observe that the lengths of the holes created by the MN are roughly about 50–60% of the actual MN length for normal thumb force applied in this work. PD studies (Figure 3.3) using lidocaine NaCMC/gelatine hydrogel were conducted on the adjacent section of the same square skin section of precisely the same average dimensions as previously stated. The same mass of formulation (0.10 ± 0.03 g) was placed onto the middle of the skin to conduct the PD studies. The FDC set up with a receptor compartment aperture area of 1.93 ± 0.0005 cm^2 was connected to an instrument module in supporting water circulation and magnetic stirring induction used in measuring the permeation kinetics of lidocaine through the skin. The SC layer in skin was facing the donor lid and the dermis layer was facing the receptor aperture. The skin surface which is part of the SC layer was exposed to a room temperature of 20°C. A stretchable parafilm seal (Fisher Scientific, Loughborough, UK) placed on the open aperture lid of the donor

compartment prevented air influx to the receptor compartment during syringe removal of DI water. The receptor compartment which has a volume of 5.3 ± 0.05 ml contained DI water at 37.0°C stirred at 300 rpm to represent a well-mixed liquid. Unlike most clinical studies concerning physiological pH mimicked by PBS (Heilmann et al., 2013), this work used DI water with respect to mimicking watery plasma in the lower VE layer of skin. The use of DI water is consistent with developmental stage of in vitro skin permeation studies (Han and Das, 2013). A receptor volume (1.5 ± 0.05 ml) was syringe removed (Cole-Palmer, Hanwell, UK) at 30 min and subsequent 1 h intervals. This amount was put in a centrifuge vial and centrifuged (1300 rpm) for 6 min and the clear supernatant was pipetted out into 2 ml vials for LC-DA (Agilent technologies, Wokingham, UK) analysis of lidocaine concentration.

All HPLC analyses were performed within 24 h of sample collection from the FDC receptor. The results were obtained in duplicate which were then used to determine average pharmacokinetic variables for further analysis. The permeation flux was calculated based on two data sets of mass ratio hydrogel formulations, plotted with error bars representing the random error at 90% confidence level. In this work, the in vitro permeation of lidocaine were interpreted by constructing a profile of cumulative amount of the drug against time as distinct charts in the section for both microneedle assisted and PD. A percentage adjustment of 28.0% was calculated from taking the 1.5 ml syringe removal volume as the numerator and the 5.3 ml receptor compartment volume as the denominator in obtaining a percentage from a fraction. This percentage adjustment (28.0%) from the previous dilution was added to the next detected concentration during a lapsed time period in obtaining a cumulative concentration profile. The cumulative concentration detected was interpreted into a more tangible parameter of cumulative amount permeated when taking into account of the receptor compartment's distinct aperture. The cumulative

amount permeated (*Q*) was determined by equation (3.1) (Auner and Valenta, 2004; Zhao et al., 2006) with coefficient, C_x, the lidocaine concentration in receiver compartment at the specific time (h), *V* is the volume of DI water in receptor compartment (ml) and *A* is the cross sectional diffusion area of receptor aperture (cm^2).

$$Q = \frac{C_x V}{A} \tag{3.1}$$

The flux permeation at steady state (*Js*) was determined by Fick's first law using equation (3.2) with coefficients, $\Delta m/\Delta t$, the amount of drug permeating through the skin per incremental time at steady state (µg/h) (Kang et al., 2000; Poet and McDougal, 2002).

$$J_s = \frac{\Delta m}{A \Delta t} \tag{3.2}$$

3.2.6 Analysis of particle size distribution

The particle size distributions in the hydrogel were analysed using laser diffraction particle size analyser (Series 2000, Malvern Instruments, Malvern, UK). A sample hydrogel volume ~ 10 ml was dispensed inside the instrument sample fask containing DI water (100 ml). Low shear was gradually increased and maintained upto a spped of 200 rpm. The instrument lasers were aligned and ready to take sample readings of the hydrogel. The data were obtained in duplicate per repeated hydrogel mass ratio sample via superimposition of data points and the particle size distributions were plotted as particle diameter against percentage particle volume. Particle diameters were compared at 10% (d10), 50% (d50) and 90% (d90) regions of total percentage particle volume. The refractive index of water as the continuous phase medium was adapted in determining hydrogel microparticle sizes for the particle size analyser.

3.2.7 Optical micrography of microparticles in lidocaine NaCMC/gelatine hydrogel

The microparticles in lidocaine NaCMC/gelatine hydrogel are visible optically and the increasing mass of gelatine in the lidocaine NaCMC/gelatine hydrogel provides a significant trend in microparticle morphology. A sample volume of ~30 µl containing the microparticles of lidocaine NaCMC/gelatine hydrogel was pipetted onto a slide placed on the stage of an optical microscope (BX 43, Olympus, Southend-on-Sea, UK) which was used to obtain the micrographs. The micrograph scale was calibrated with a certified external slide graticule using Imagej. ImageJ is a Java based open source image processing and analysis program developed at the National Institute of Health (NIH), USA.

3.2.8 Determination of lidocaine encapsulation efficiency (EE)

The experimentally determined amount of lidocaine contained in a sample of NaCMC/gelatine micro-particles was interpreted in terms of encapsulation efficiency (EE). For the purpose of determining lidocaine EE, a sample weight (5.0%) of lidocaine NaCMC/gelatine microparticles from the overall lidocaine bipolymeric hydrogel batch was measured. DI water representing excess watery plasma (20.0 ml ± 0.1 ml) was pipetted into the weighed lidocaine hydrogel sample and heated to 37.0 ± 1°C in a pre-heated bath (Grant Instruments Ltd, Shepreth, UK). This sample was then sonicated using a vessel sonifier (Fisher Scientific, Loughborough, UK) at 35 W for 10 min. It was then filtered using Nylon 6,6 membranes of 0.1 µm pore size (Posidyne membranes, Pall Corporation, Portsmouth, UK) under gentle vacuum using a Buchner filter setup (Fisher Scientific, Loughborough, UK). The filtrate was immediately dispensed into a HPLC vial of volume 1.5 ml. The HPLC results were obtained in triplicate which were then used to determine the mean percentage encapsulation efficiency by using equation 3.3 (Naidu and Paulson, 2011; Al-Kahtani and Sherigara, 2009).

$$\% \text{ EE} = \frac{\text{actual } 5.0\% \text{ wt of lidocaine from polymeric ratio sample (g)}}{5.0\% \text{ theoritical encapulsaion wt of lidocaine (g)}} \text{ x } 100 \qquad (3.3)$$

3.2.9 Zeta potential analysis

The measurement of Zeta potential provides a valid indication for microparticle dispersion with respect to charged particle repulsion between microparticles, and as such, the Zeta potential of the microparticles was measured in this study. Ideal Zeta potential thresholds will be discussed in detail later. The Zeta potential of lidocaine loaded microparticles was measured using a Zetasizer (Malvern 3000 HAS, Malvern, Malvern, UK). The microparticles in the developed lidocaine NaCMC/gelatine hydrogel (2.0 ± 0.5 g/ml) diluted in DI water were injected into the sample port, temperature maintained at 20.0°C and the results were obtained in duplicate. Unloaded NaCMC/gelatine 1:2.3 mass ratio hydrogels without any lidocaine were also subject to Zeta potential analysis. Likewise, the temperature was maintained at 20.0°C and the results were obtained in duplicate.

3.2.10 Measurement of viscosity

The overall viscoelastic property of lidocaine NaCMC/gelatine hydrogel formulation requires investigation so as to maintain consistency of the formulation and since the rheological properties of the hydrogel affects its flow through the holes created by the MNs. In this case, we used a rotational viscometer (Haake VT 550, Thermo Fisher Inc, Massachusetts, USA) for determination of bulk (average) dynamic viscosity of the samples of lidocaine NaCMC/gelatine hydrogels (maximum volume 25 ml). An NV cup and rotor segment (dimensions of length: 60 mm and radius: 20.1 mm) with a gap of 0.35 mm was acquired after a brief qualitative observation of samples as a thick, semi-solid texture. The shear rate was ramped from 1 s^{-1} to 200 s^{-1} and held constant at 200 s^{-1} for 30 s. The viscosity measurement experiments were carried out at ambient condition of 20°C. NaCMC/gelatine

hydrogel is not a thermoresponsive polymer, so the effects of viscosity against temperature at different, shear rates were not considered in this thesis. Rheological properties of the hydrogel in this thesis represent the normal condition for storage at ambient temperature and not the body temperature.

3.2.11 Analysis of lidocaine concentration using HPLC

Lidocaine concentrations were analysed by using HPLC. The mobile phases for eluting lidocaine were acetonitrile (HPLC grade) and 10 mM ammonium bicarbonate solution (pH 7.5), respectively, in an isocratic ratio of 50:50. The flow rate of 0.4ml/min and column temperature of 20.0°C (Perkin Elmer, Series 1100, Cambridgeshire, UK) was kept constant. Lidocaine molecule was detected by a diode array detector with the wavelength set at 210 nm (Agilent, Series 1100, Berkshire, UK). The system's tube lines were purged after eluent degrassing with helium. The baseline corrections were performed before the injection of 5 µl of lidocaine standard and a characteristic peak was identified and recorded. Standard solutions of lidocaine HCl were prepared in ultrapure water with concentrations ranging from 1.0 to 64.0 µg/ml from a stock solution of 1.0 mg/ml. Each standard solution was analysed by HPLC in duplicate to obtain a linear profile of known concentration against mean area under curve of the integrated lidocaine peak. The HPLC column specifications are Gemini-NX 3 µm particle size of reverse phase, C18 compound composition and physical dimensions of 100 x 2 mm, which was purchased from Phenomenex, Cheshire, UK. The mean area under signal peak corresponding to serial standard concentrations for lidocaine (0.5–64.0 ppm) was plotted with a linear regression analysis (R^2 = 0.999) which showed very good agreement with the data points.

3.3 Results

Desirable trends and outlines of results are organised with subheadings concerning lidocaine NaCMC/gelatine hydrogel MN-assisted permeation of lidocaine formulation and pharmacokinetics of lidocaine permeation through the skin with relation to therapeutic levels.

3.3.1 Encapsulation of lidocaine in NaCMC/gelatine microparticles

The mean percentage of lidocaine encapsulated in the NaCMC/gel microparticles as a function of mass ratio of NaCMC to gelatine is plotted in Figure 3.4. Lidocaine 2.4% w/w NaCMC/gelatine 1:2.7 mass ratio showed the highest encapsulation efficiency of 32% (SD = 1.2%) as compared with the microparticles of lower NaCMC/gelatine polymeric ratios.

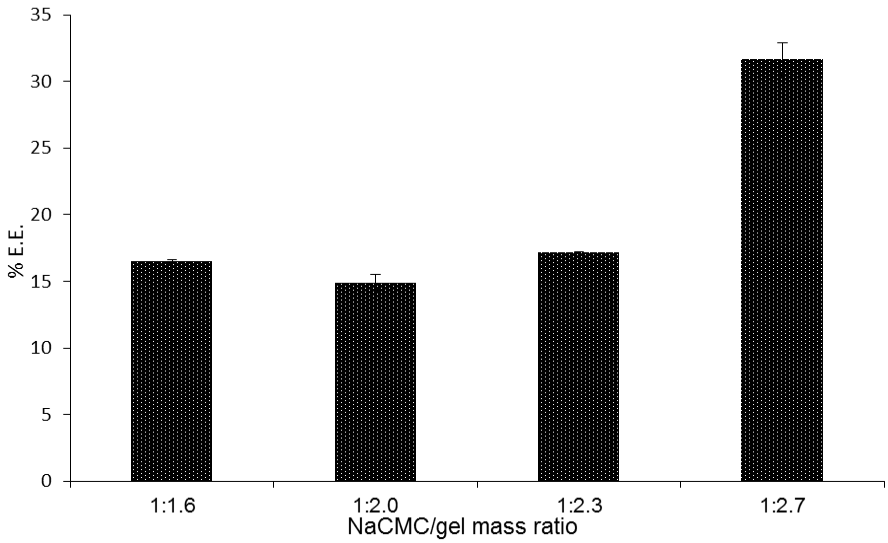

Figure 3.4: Percentage encapsulation efficiency of lidocaine in hydrogel particles as a function of NaCMC/gelatine (NaCMC/gel) mass ratio. The concentration of lidocaine in the initial emulsion was 2.4% w/w (Results represent arithmetic mean ± SD values based on data from there reproduced hydrogel samples per mass ratio).

3.3.2 Viscoelasticity of lidocaine NaCMC/gelatine hydrogel

The results in this work (Figure 3.5a) suggest that the increase in lidocaine concentration had no significant effect on the average dynamic viscosity of the

hydrogel. In particular, the data points after the shear rate of 100 s^{-1} outlined a single asymptote and they super imposed well (Figure 3.5a). The minimum dynamic viscosity of constantly encapsulated lidocaine NaCMC/gelatine hydrogels (Figure 3.5b) from the shear range 100 to 200 s^{-1} asymptote is found to be 0.14 Pa.s for lidocaine NaCMC/gelatine 1:2.0 mass ratio, which may provide a low pseudo plasticity to the hydrogel. Within the shear range 100 to 200 s^{-1} asymptotes of 0.28 and 0.31 Pa.s are found for lidocaine NaCMC/gelatine 1:2.3 and 1:2.7 mass ratios, respectively and they account for little difference in pseudo-plasticity. But a marked difference in pseudo-plasticity is observed when lidocaine NaCMC/gelatine 1:2.0 mass ratio is compared with lidocaine NaCMC/gelatine 1:2.7 mass ratio (Figure 3.5b). Substantially, there is no significant difference in shear thinning dynamic viscosity induced by a constant maximum shear of 200 s^{-1} when comparing lidocaine 2.4% w/w NaCMC/gelatine variable mass ratio hydrogels. This outlines very good reproducibility with SD of 0.02 for each lidociane NaCMC/gelatine hydrogel mass ratios (Figure 3.6).

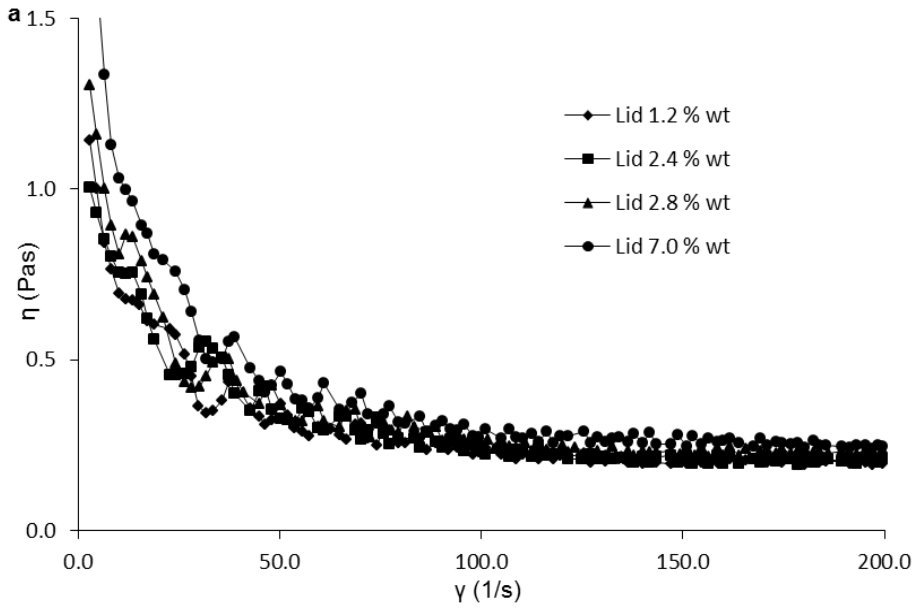

Figure 3.5: (continued to next page).

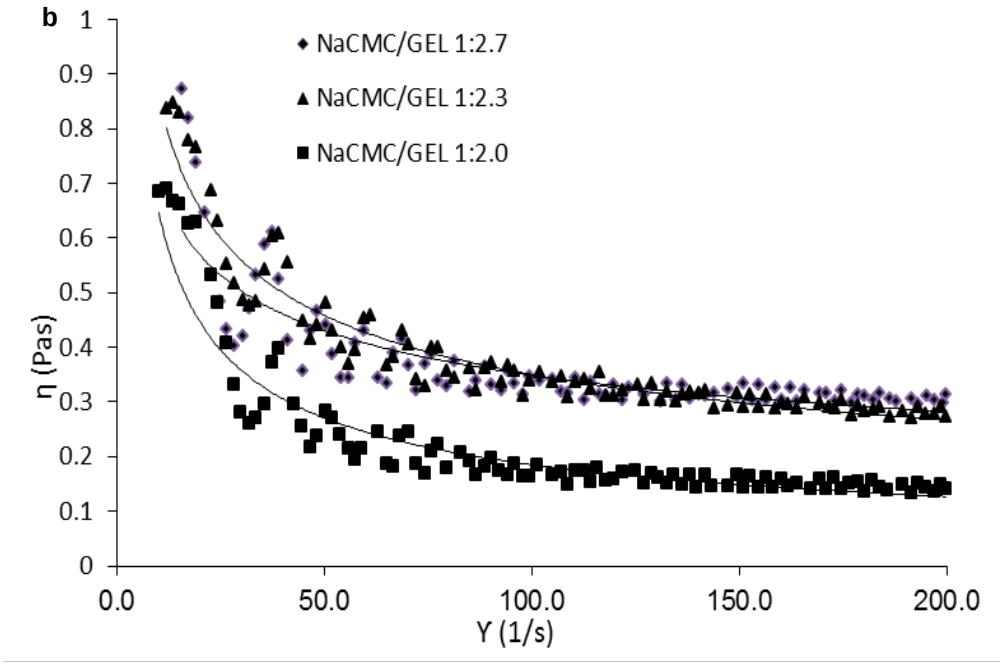

Figure 3.5: (a) Dynamic viscosity of lidocaine NaCMC/gelatine (NaCMC/GEL) hydrogels as a function of shear rate. (b) Dynamic viscosity of lidocaine 2.4 % w/w in NaCMC/gelatine hydrogels as a function of shear rate (Results represent data points from individual hydrogel samples per mass ratio).

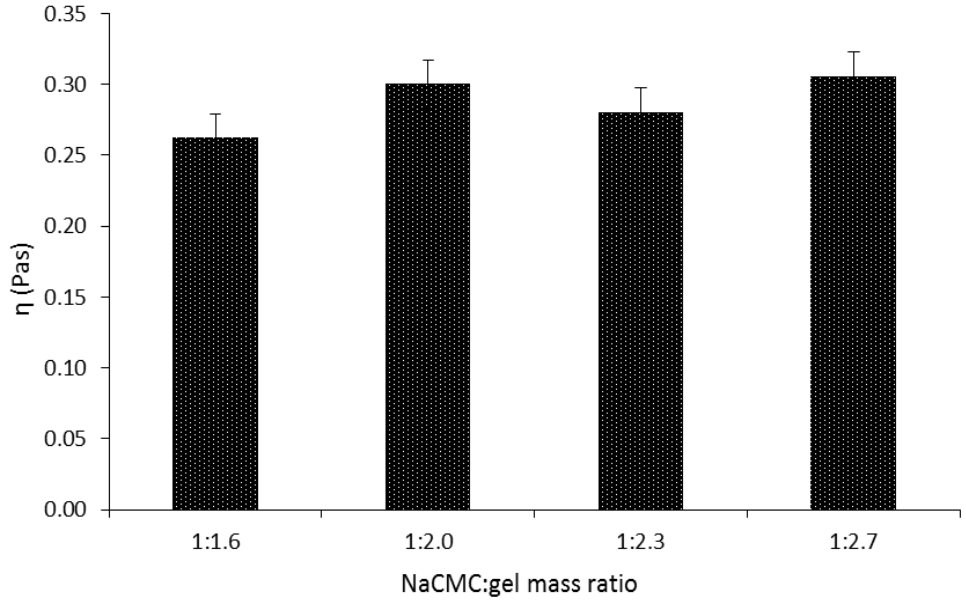

Figure 3.6: Constant shear induction (200 s^{-1}) for lidocaine 2.4 % w/w NaCMC/gelatine (NaCMC:gel) hydrogel as a function of mass ratio NaCMC to gelatine (Results represent arithmetic mean ±SD values based on data from two reproduced hydrogel samples per mass ratio).

3.3.3 Distribution of microparticles in lidocaine NaCMC/gelatine hydrogel

The particle size distribution curves were noticeably similar for lidocaine 2.4% w/w NaCMC/gelatine 1:2.3 and 1:2.7 mass ratios with the same mean particle diameter of 140 µm (Figure 3.7) for each one. As found, the d10 values were 29 µm and 35 µm for lidociane NaCMC/gelatine 1:2.3 and 1:2.7 mass ratios, respectively. Also, the d90 values were 305 µm and 277 µm for lidocaine NaCMC/gelatine 1:2.3 and 1:2.7 mass ratios, respectively (Figure 3.7). The particle size distribution was considerably left skewed, less broad in describing the peak outline for lidocaine 2.4% w/w NaCMC/gelatine 1:1.6 mass ratio with a mean particle diameter of 98.65 µm where d10= 19.3 µm and d90 = 301.78 µm were recorded (Figure 3.7).

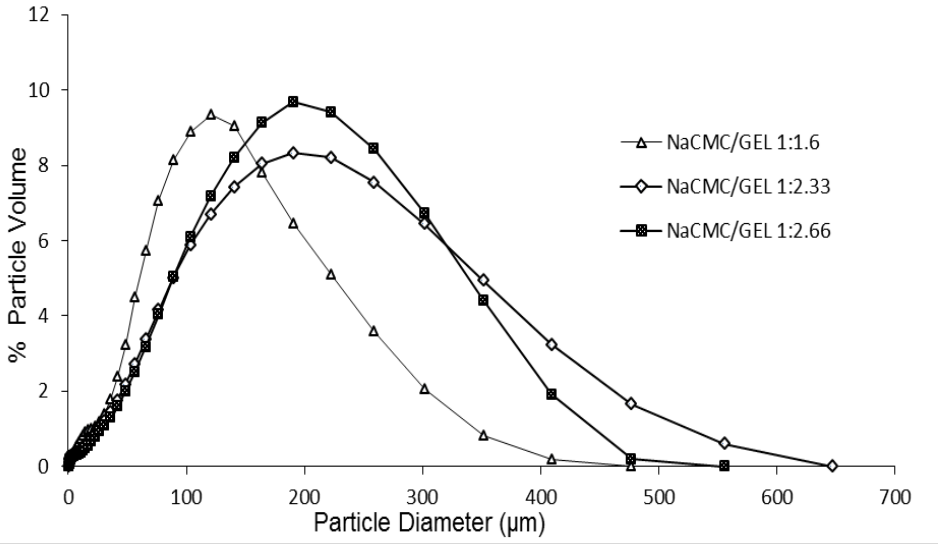

Figure 3.7: Lidocaine 2.4 % (w/w) NaCMC/gelatine (NaCMC/GEL) particle size distribution as a function of mass ratio of the two polymers (Results represent superimposed data points of each repeated hydrogel sample from a total of six individual hydrogel samples).

3.3.4 Zeta Potential of lidocaine NaCMC/gelatine mass ratio and pH effects in micro-particles

In developed microparticles, lidocaine loading ranges from 1.2–2.8% w/w for NaCMC/gelatine 1:1.6 mass ratio resulted in no significant change in Zeta potential

(SD=0.09) and showed excellent reproducibility in comparison to the high Zeta potential values and poor reproducibility of lidocaine 7.0% w/w NaCMC/gelatine 1:1.6 mass ratio (SD=1.84) (Figure 3.8a).

Lidocaine 2.4% w/w and 2.8% w/w, loaded each in NaCMC/gelatine 1:1.6 and 1:2.3 mass ratios showed good reproducibility (SD=0.10 and SD=0.05 respectively) and desirably low Zeta potential values approaching −40 mV (Figure 3.8b). Lidocaine 2.4% w/w NaCMC/gelatine 1:1.6 till 1:2.3 mass ratios provided desirably low Zeta potential values approaching -40 mV and good reproducibility (SD=0.76) compared with lidocaine NaCMC/gelatine 1:2.7 mass ratio in which the Zeta potential was undesirably high and, hence, agglomeration was more significant due to the high gelatine concentration (Figure 3.8c).

The hydrogel microparticles may have unbound gelatine flocculating and diverting the innermost negative charge boundaries of defined lidocaine loaded NaCMC/gelatine microparticles. Lidocaine 2.4% and 2.8% w/w encapsulated NaCMC/gelatine 1:2.3 mass ratio depict desirable and stable Zeta potential values close to −40 mv despite lidocaine 2.8% w/w loaded NaCMC/gelatine 1:2.3 mass ratio outlining a slightly lower reproducibility (SD=0.80) (Figure 3.7d). Also lidocaine 7.0% w/w encapsulated NaCMC/gelatine 1:2.3 mass ratio depicted a repeat of the high Zeta potential behaviour in terms of an undesirably high and slightly more agglomeration effect due to high loading of lidocaine (Figure 3.8d). The effect of pH on NaCMC/gelatine 1:2.3 resulted in a minima point near -60 mV on the experimental curve observed at pH 4.0 (Figure 3.8e). Buffering the continuous phase containing bi polymeric microgels at pH 4.0 is favourable in allowing larger microparticle dispersion in the media.

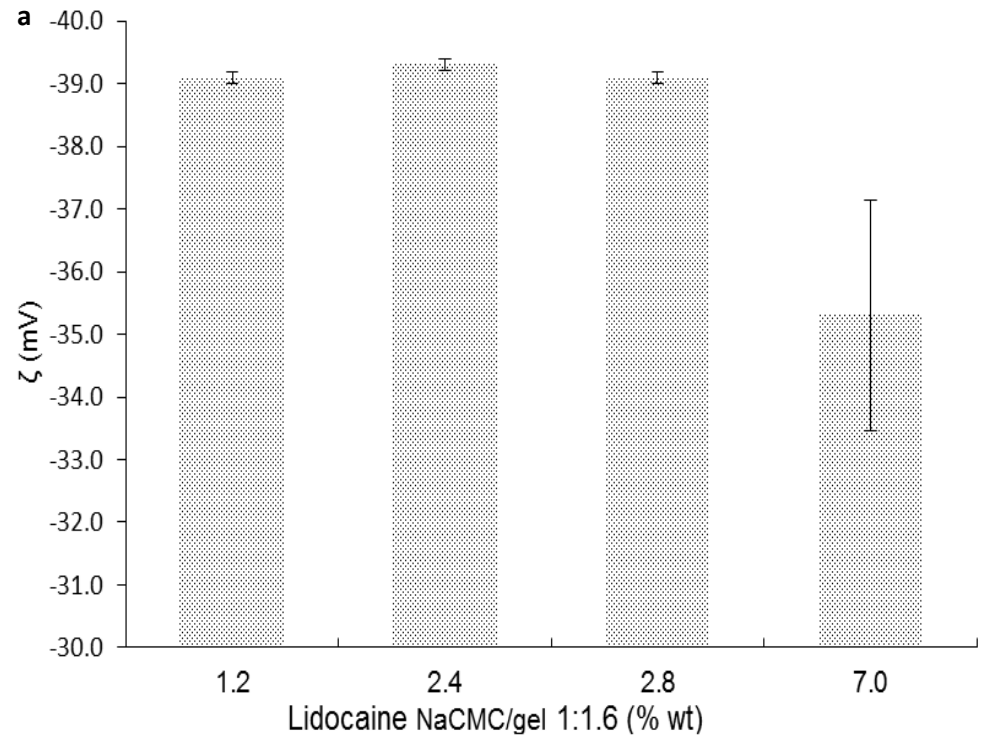

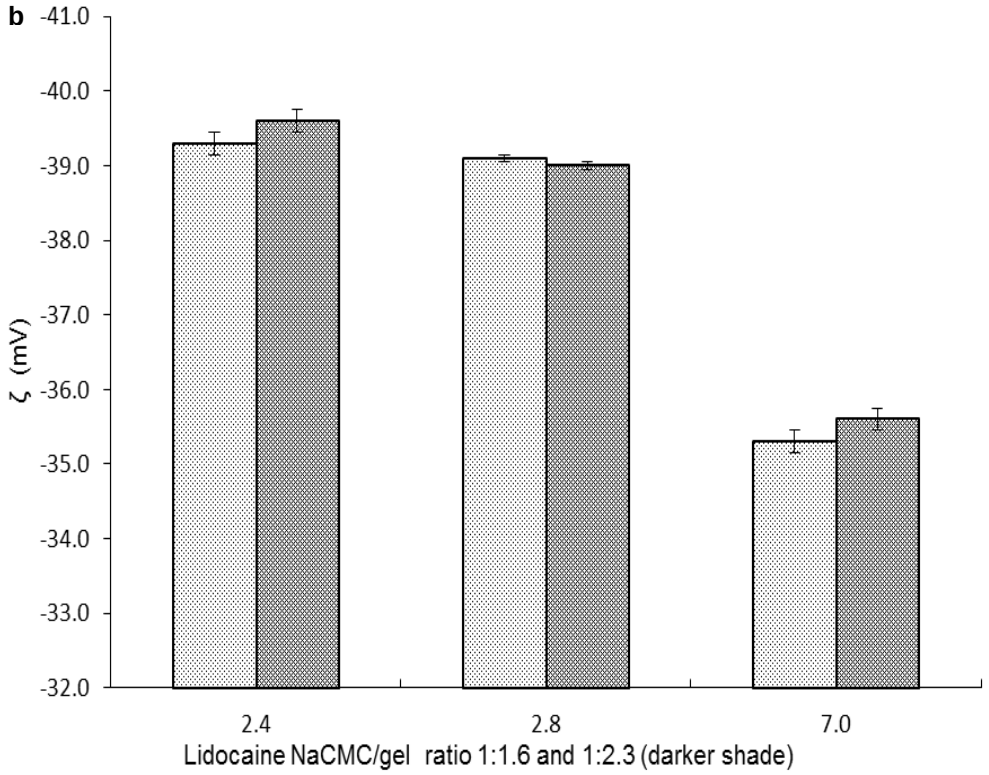

Figure 3.8: (Continued to next page).

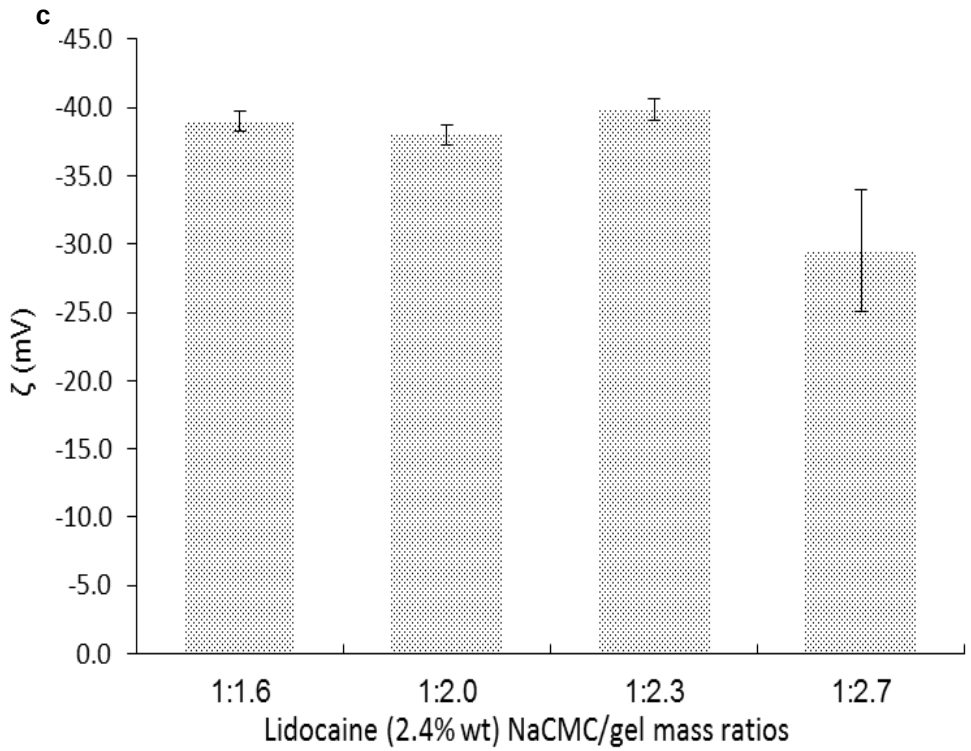

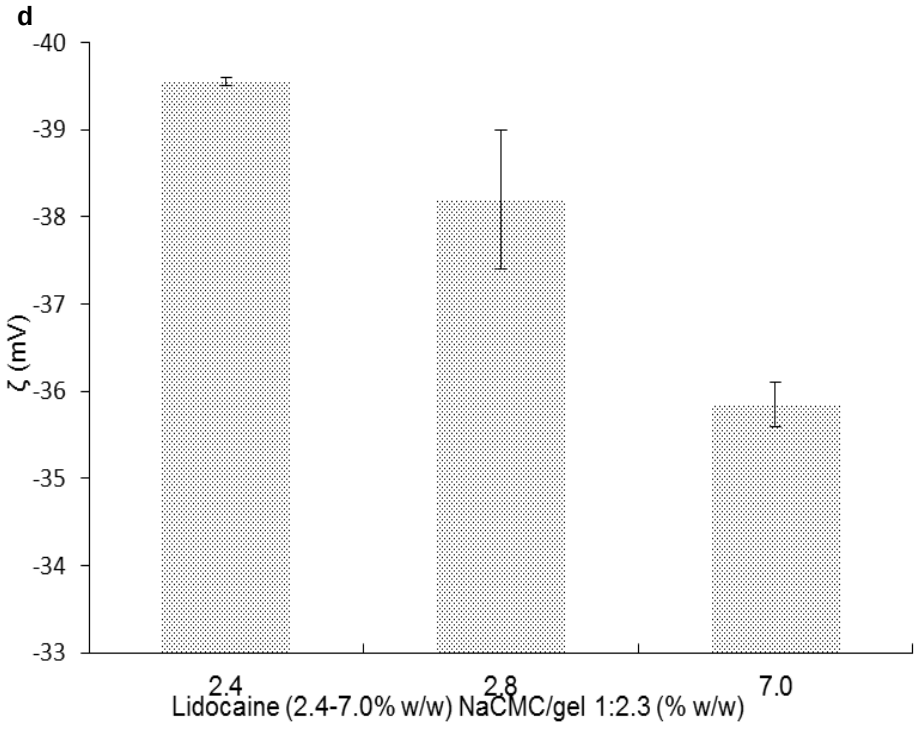

Figure 3.8: (Continued to next page).

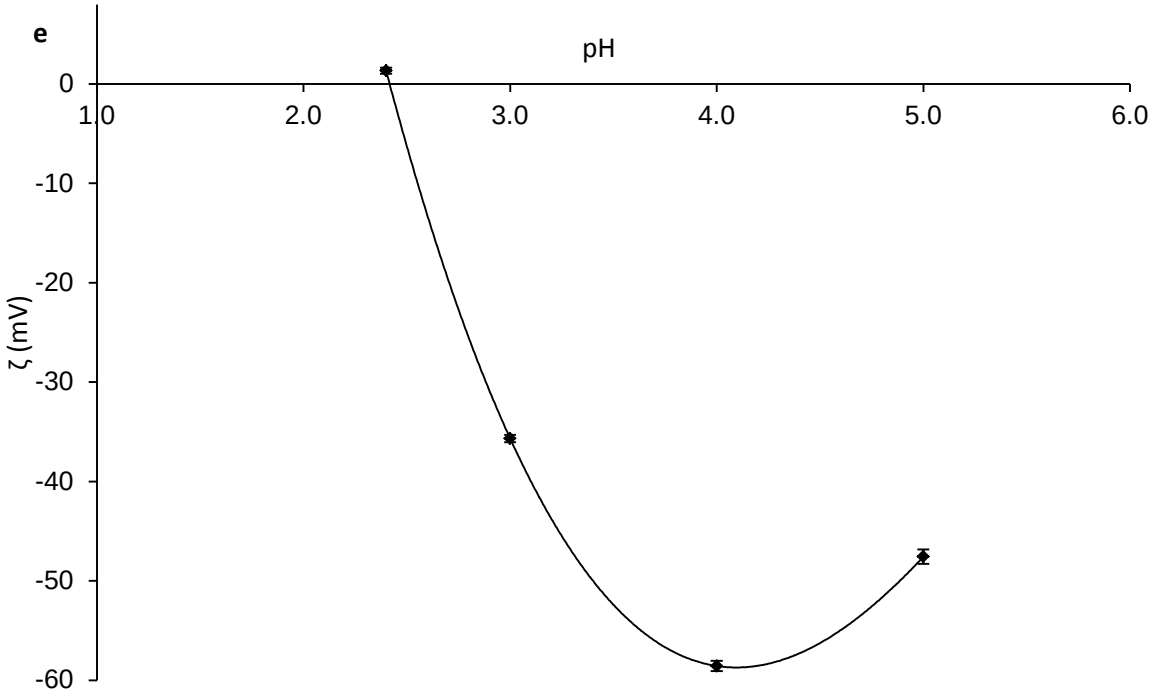

Figure 3.8: (a) Zeta potential of lidocaine NaCMC/gelatine (NaCMC:gel) 1:1.6 mass ratio microparticles. Values 1.2-7.0 are lidocaine loaded yields in % w/w. (b) Zeta potential of lidocaine (2.4-7.0 % w/w) NaCMC/gelatine mass ratio 1:1.6 and 1:2.3 microparticles. Values 2.4-7.0 are lidocaine loaded yields in % w/w. (c) Zeta potential of lidocaine (2.4 % w/w) NaCMC/gelatine mass ratio 1:2.3 microparticles. (d) Zeta potential of lidocaine NaCMC/gelatine mass ratio 1:2.3 microparticles. (e) pH effects on unloaded NaCMC/gelatine 1:2.3 microparticles as a function of Zeta potential. Values 2.4-7.0 are lidocaine loaded yields in % w/w (results represent arithmetic mean ± SD values based on data from two reproduced hydrogel samples per mass ratio or concentration).

3.3.5 Morphology of microparticles in lidociane NaCMC/gelatine hydrogel

The micro-particles of lidocaine 2.4% w/w NaCMC/gelatine 1:1.6 to 1:2.7 mass ratio were found to be spherical. However they show small areas of agglomeration with respect to microparticulate hydrogel morphology (Figure 3.9a-d). The microparticles in lidocaine 2.4% w/w NaCMC/gelatine 1:1.6, 1:2.3 and 1:2.7 mass ratios appear slightly more distinct spherically and dispersed with less agglomeration compared with lidocaine 2.4% w/w NaCMC/gelatine 1:2.0 mass ratio. More significantly in the quantity with regards to larger microparticle sizes were observed for lidocaine 2.4% w/w NaCMC/gelatine 1:2.7 mass ratio hydrogel (Figure 3.9d).

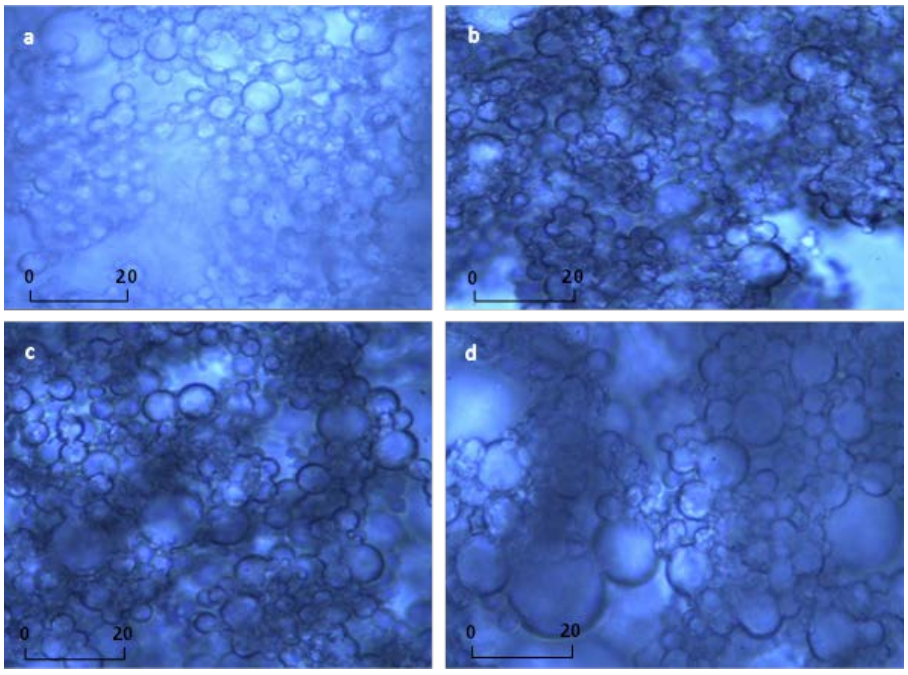

Figure 3.9: Micrograph of lidocaine 2.4 % w/w NaCMC/gelatine microparticles prepared using different polymeric ratios: (a) 1:1.6, (b) 1:2.0, (c) 1:2.3, (d) 1:2.7 (Scaling bar units: μm).

3.3.6 Microneedle-assisted and passive diffusion of lidocaine from NaCMC/gelatine hydrogel

Clinical research has shown that lidocaine in hypodermal plasma fluid is able to sustain localised drug action at a normal threshold range of 1.2 to 5.5 μg/ml or 3.11 μg/cm^2 to 14.25 μg/cm^2 after conversion into cumulative permeated amounts for lidocaine (Stenson et al., 1971; Greco, 2011). MN assisted diffusion of lidocaine NaCMC/gelatine 1:2.3 mass ratio showed a fast time taken for the cumulative amount permeated at 1.1 h after crossing the minimum lidocaine therapeutic level. Comparatively, the same lidocaine formulation used for PD studies showed the fastest time in crossing the minimum therapeutic level regarding the cumulative amount permeated was 1.5 h (Figure 3.10a). During the MN assisted diffusion of lidocaine NaCMC/gelatine, 1:1.6 and 1:2.0 mass ratios both outlined faster times taken for the cumulative amount permeated past 1.25 h when extrapolated towards a minimum lidocaine therapeutic level. Comparatively the PD of lidocaine NaCMC/gelatine 1:1.6 mass ratio and PD of lidocaine NaCMC/gelatine 1:2.0 mass

ratios crossed the minimum therapeutic level at 2 h and 3 h, respectively (Figure 3.10a). The SD error bars from duplicate data sets showed very good reproducibility (Figure 3.10a). Permeated rates of MN assisted lidocaine NaCMC/gelatine hydrogels recorded in the first 0.5 h, were significantly bigger for 1:2.3 mass ratio with a 20.5 fold increase when compared with PD and low for 1:2.0 mass ratio with a 1.4 fold increase compared with PD (Figure 3.10b). Likewise as discussed, the error bars from duplicate data sets showed good reproducibility (Figure 3.10b). Lidocaine NaCMC/gelatine 1:1.6 mass ratio formulation represented the lowest MN assisted permeation flux of 3.8 µg/ cm^2/ h (Figure 3.10c) despite a low microparticle size diameter of nearly 99 µm compared with other NaCMC/gelatine mass ratio formulations. In theory smaller microparticles should allow greater ease in passing skin pores and diffusing water plasma in the lower regions of the skin. Nevertheless the Zeta potential results with respect to a very low Zeta correlating to greater dispersion than agglomeration of microparticles is the main supporting concept for high permeation flux. The random error of permeation flux for the duplicate data sets showed good reproducibility (Figure 3.10c).

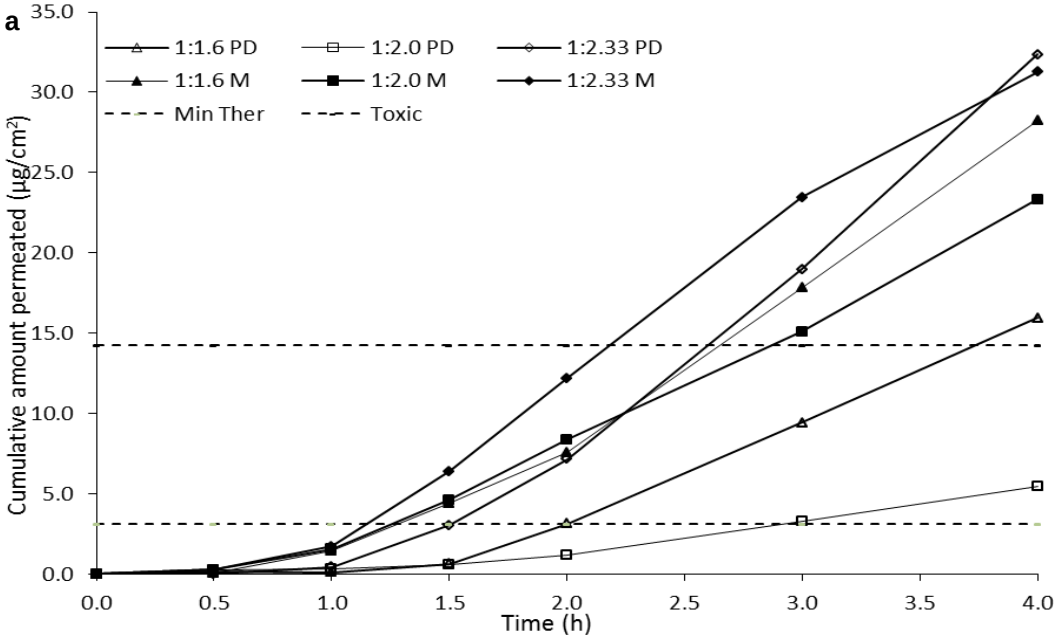

Figure 3.10: (Continued to next page).

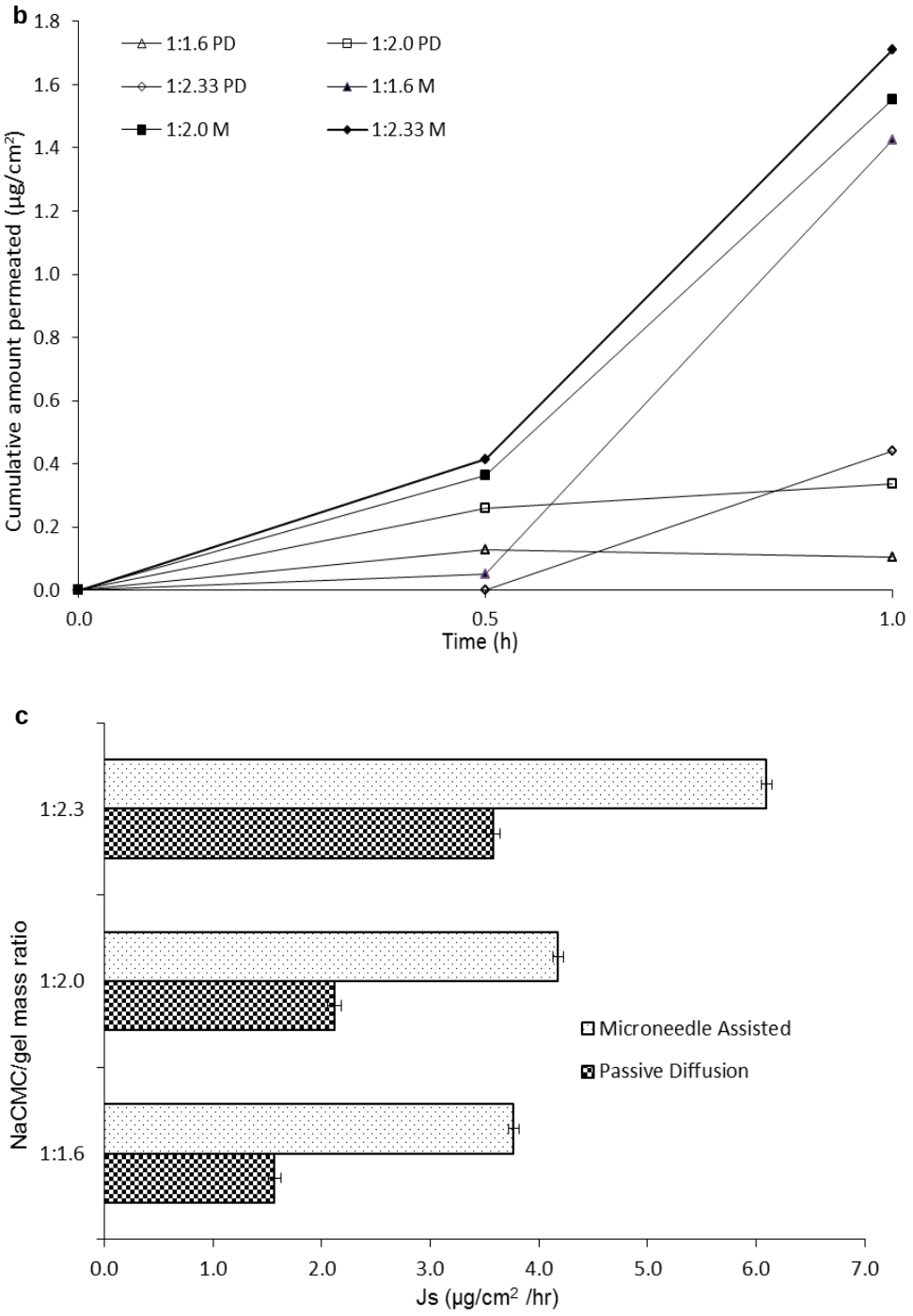

Figure 3.10: (a) Cumulative amount of lidocaine permeated through skin from NaCMC/gelatine with a four hour period. (b) Cumulative amount of lidocaine permeated through skin from NaCMC/gelatine with a 1 hour period. (results represent arithmetic mean ± SD values based on data from two reproduced hydrogel samples per mass ratio). (c) Lidocaine (2.4 % w/w) NaCMC/gelatine flux permeation through skin (results represents random error of two reproduced mass ratio samples for PD and microneedle values based on 90 % confidence level).

3.4 Discussion

3.4.1 Surfactant and oil based continuous phase medium in emulsion stage preparation

Paraffin oil as the continuous phase mixed with non-ionic surfactant, SPAN 80, for stabilising aqueous emulsion droplets possessed ideal properties (Marquez, 2007). Comparatively SPAN 20, SPAN 40 and SPAN 60 series were unsuitable surfactants because SPAN 80 is the most hydrophobic (Marquez, 2007). Paraffin oil, continuous phase medium aided the dispersion of polar droplets before further addition of glutaraldehyde for microparticle formation. The n-octonol/water partition coefficient of paraffin oil is noted, log P >3.5 (Fisher Scientific Ltd, Loughborough, UK) and the non-polarity is attributed to the high interfacial tension and lower dielectric constant in terms of percentage w/w solubilisation (El-Mahrab Robert et al., 2008). The formation of a NaCMC/gelatine polymeric hydrogel network is to entrap and crosslink a linear polymeric structure with a more branched structure in considering covalent bonding interactions to a lesser extent, thus permitting intermolecular dissociation in a continuous phase such as water (Chikh et al., 2011; Jenkins et al., 1996). Glutaraldehyde was used for fixing and strengthening the crosslinking of a polymer and co-polymer to form spherically shaped microparticles (Kajjari et al., 2011).

3.4.2 The effect of increasing gelatine concentration on encapsulation efficiency of lidocaine NaCMC/gelatine

Gelatine in greater concentrations in hydrogel NaCMC/gelatine microparticles influences the gelling properties of the hydrogel matrix with respect to crosslinking with NaCMC at low pH via electrostatic charges and hypothetically creating a more complex intertwined mesh to trap lidocaine molecules. In order to gain a better insight into the reason for a substantially valid increase in EE from 1:2.3 mass ratio

NaCMC/gelatine to 1:2.7 mass ratio requires electro-analytical research with respect to overall ionic charge distribution effects. However this is not within the scope of this thesis.

3.4.3 Viscoelastic and particle diameter properties of lidocaine NaCMC/gelatine hydrogel

Lidocaine is a weakly acidic and the positively charged tertiary amide on it has no effect on influencing the pseudoplasticity of the NaCMC/gelatine hydrogel (Figure 3.5a). Increasing the gelatine mass ratio component in the lidocaine polymeric hydrogel microparticles slightly increases the pseudoplasticity of the hydrogel formulation caused by gelling thus appearing more pronounced with respect to lidociane NaCMC/gelatine 1:2.3 and 1:2.7 mass ratios. This has an influence on creating bigger microparticle sizes as discussed later in particle size distribution (Figure 3.7). Mild pseudoplasticity is a common viscoelastic property for lidocaine NaCMC/gelatine hydrogels despite low values pointing to shear thinning at a maximum shear of 200 s^{-1} (Figures 3.5a and 3.6). The reduced hydrogel matrix properties caused by a much lower gelatine mass ratio for lidociane NaCMC/gelatine hydrogel despite a constant high shear of 1000 rpm during the formulation preparation stages has a significantly profound decrease of mean particle size diameter when comparing NaCMC/gelatine 1:1.6 mass ratio with NaCMC/gelatine 1:2.3 and 1:2.7 mass ratios (Figure 3.7). Morphologically larger microparticles in lidocaine NaCMC/gelatine hydrogel are distinctly represented for the 1:2.7 mass ratio with respect to the highest concentration of gelatine co-polymer (Figure 3.9). A similar polymeric gelatine microparticle study (Rokhade et al., 2006) obtained volume mean particle size range from 247–535 μm for 1:4 and 1:9 NaCMC/gelatine ratio non-steroidal anti-inflammatory drug (NSAID) mainly because of low overhead stirring speeds of 400 rpm, high viscosity grade NaCMC (500–800 mPas) and higher copolymer, gelatine concentration in the ratio mixture.

3.4.4 Polyelectrostatic lidocaine NaCMC/gelatine and unloaded NaCMC/gelatine microparticles on Zeta potential

A high concentration of weakly acidic lidocaine in a low polycationic gelatine weight ratio NaCMC/gelatine hydrogel formulation is likely to influence slightly more agglomeration of microparticles. Also the high lidocaine concentration disrupted the complex coacervate formation before the permanent fixation and assembly of droplets into defined spherical microparticles by glutaraldehyde (Figure 3.8a). Low agglomeration was already deduced from low Zeta potential values and there was no significant difference for further reduced agglomeration and metastable particle stability when lidocaine 2.4% w/w or 2.8% w/w is encapsulated in either NaCMC/gelatine 1:1.6 or 1:2.3 mass ratios, respectively (Figure 3.8b). However lidocaine 7.0% w/w loaded in NaCMC/gelatine 1:1.6 and 1:2.3 mass ratios showed significantly higher, positive, Zeta potential values and therefore slightly more agglomeration of microparticles (Figure 3.8b). The Zeta potential effect of charged particles with a charge distribution density on the inner core provides a good indication of a metastable and non-agglomerated particulate hydrogel in the empirically determined range of −31.0 to −40.0 mV (Schramm, 2005; Riddick, 1968). The surface charges in the microparticles of lidocaine NaCMC/gelatine hydrogel are negative due to dissociation of acidic groups on gelatine and lidocaine contributing to an acidic environment in forming a spherical core shell structure in conjunction to electronegative DI water molecules, basic carboxylate groups in NaCMC and conjugate base of acetic acid contribute to the outermost shell boundary (Riddick, 1968; Koul et al., 2011).

Zeta potential is a fairly common and valid analytical technique for determining the lidocaine NaCMC/gelatine microparticles in dispersal from weak acid medium of pH 4.0 to a near neutral plasma pH medium. Placebo NaCMC/gelatine hydrogel microparticles outline the minima ($d\zeta/d(pH)=0$) which is representative of the lowest

Zeta value showed the most desirable pH value at −58.6 mV (Figure 3.8e) so pH 4.0 was the ideal and adapted pH for NaCMC/gelatine overall hydrogel media in the encapsulation of lidocaine. Above acidic conditions of pH 4.0 for the placebo NaCMC/gelatine 1:2.3 mass ratio resulted in a gradual increase in Zeta potential which is likely caused by reduction in dissociated polycationic gelatine and polyanionic NaCMC, and microparticle agglomeration is more defined.

3.4.5 Lidocaine from NaCMC/gelatine hydrogels as a transdermally permeating agent

The minimum therapeutic level for In Vitro studies is a prediction of the concentration or permeated amount of drug with the potential to invoke a therapeutic response. The minimum therapeutic and toxic level permeation threshold values were taken from references (Stenson et al., 1971; Greco, 2011), converted from micrograms per millilitre concentration of lidocaine into micrograms per square centimetres for permeated concentration using equation 3.1 and expressed using constants derived from FDC receptor compartment volume and receptor area of aperture in equation (3.4).

$$\mathrm{Q} = \frac{5c}{1.93} \tag{3.4}$$

Commercially acquired AdminPatch MNs (Nanobiosciences, Sunnyvale, CA, USA) created hypothetical channels and widened skin pores for the drug to bypass the SC layer and diffuse into the VE layer. Staining techniques have shown similar length AdminPatch MNs to penetrate beyond the SC layer of skin from a recent study (Han and Das, 2013). Imperatively the use of MNs is to allow the drug to diffuse just above the minimum therapeutic levels at lower recorded time durations than PD which is devoid of any needles. The effective diffusional area in considering the barrier diffusing membrane properties of skin was adapted from Fick's first law for explaining the permissible trends for PD and microneedle assisted cumulative diffusion of lidocaine NaCMC/gelatine hydrogels through the

skin. The lidocaine 2.4% w/w NaCMC/gelatine hydrogels are permeating the uppermost layer, highly lipophilic layer of skin very slowly for upto 30 min (Figure 3.10b). This highly lipophilic layer is suitable for the passive diffusion of small molecular weight lipophilic drugs for which lidocaine HCl is not the case. After 30 min, the permeating amount of lidocaine diffuses at a much faster rate because the lower section layer of skin is less lipophilic and pseudo steady state conditions are observed for all lidocaine NaCMC/gelatine hydrogels after 1.5 h (Figure 3.10a).

Lidocaine NaCMC/gelatine microparticles enter the opened MN treated skin cavity while for PD the hair follicles and sweat pores are the natural cavities for these microparticles (Todo et al., 2010). The natural cavities in skin are considerably smaller openings when compared with post MN ones (Todo et al., 2010). Excised skin used in vitro will generally have lower moisture content because of high trans-epidermal water loss (TEWL) values and microparticles will tend to cause a reservoir effect in VE or dermis layers of skin (Victoria Klang et al., 2013). After 30 min, the permeating amount of lidocaine diffuses at a much faster rate because the lower section layer of skin is less lipophilic and pseudo steady state conditions are observed for all lidocaine NaCMC/gelatine hydrogels after 1.5 h. The cumulative skin permeation of the three lidocaine 2.4% w/w NaCMC/gelatine hydrogels depicted good overall high rates than compared with PD, especially past the time of 0.5 h (Figure 3.10a and b). Emerging plateau levels of cumulative permeation amounts through skin were already documented post 4.5 h. However, the aim for a higher lidocaine amount permeated past minimum therapeutic levels were particularly targeted at the most plausible shorter time duration than a long sustained release profile hence comparative cumulative permeation studies were conducted in a short time range. Increasing the gelatine concentration in a lidocaine 2.4% w/w NaCMC/gelatine hydrogel outlined an increase in permeation flux for both PD and MN assisted permeation (Figure 3.10c). Lidocaine 2.4% w/w

NaCMC/gelatine mass ratio 1:2.3 showed a highly favourable permeation flux with respect to MN assisted delivery of lidocaine.

The EE of lidocaine 2.4% w/w NaCMC/gelatine mass ratios are similar and therefore cannot explain the effect of increasing lidocaine release rates when the gelatine mass ratio is increased in the hydrogel vehicle in terms of correlating with an unchanged EE just above 15%. However, lidocaine 2.4% w/w NaCMC/gelatine mass ratio 1:2.7 provided a substantially high EE of 32% and a reciprocally poor, highly insignificant, low value skin permeation flux which was interpreted as a no result. A high gelatine mass weight of 3.3% w/w in lidocaine 2.4% w/w NaCMC/gelatine mass ratio 1:2.7 hydrogel provided for a more compacted gelling and adsorbing properties, thus preventing the release of a detectable quantity of lidocaine. The high gelation of lidocaine 2.4% w/w NaCMC/gelatine mass ratio 1:2.7 microparticles are responsible for agglomeration by high Zeta potential (Figure 3.8c). However, lidocaine 2.4% w/w NaCMC/gelatine mass ratio 1:2.3 had a slightly higher and a favourably closer Zeta potential to −40 mV and therefore the permeation flux for PD and MN assistance is influenced to be highest because of less microparticulate agglomeration or clustering effect.

3.5 Chapter summary

Lidocaine NaCMC/gelatine is a highly potential and promising hydrogel formulation requiring MN assisted delivery to excel low PD flux rates by relatively significant proportions. MN assisted lidocaine 2.4%w/w NaCMC/gelatine mass ratio 1:2.3 hydrogel is found to be the most ideal formulation for exceeding the minimum therapeutic permeation threshold of 3.11 μg/cm^2 just after 70 min but requiring removal before 140 min. A seventy minute duration for pseudo steady state permeation, concerning lidocaine 2.4% w/w NaCMC/gelatine mass ratio 1:2.3 is highly beneficial in numbing the immediate skin region in a hypothetical case of

multiple lacerations in close proximity that require wound cleaning and suturing. Lidocaine 2.4% w/w is the most ideal loading concentration for NaCMC/gelatine 1:1.6 and 1:2.3 mass ratio hydrogel because of reproducible and stable approaching values of −40.0 mV Zeta potential. A buffered pH 4.0 was essential in the induction of an anionic polymer and cationic co-polymer polyelectrolyte interaction and facilitation of dispersed hydrogel microparticles as measured by a Zeta of −58 mV. There are significant differences in visco-elasticity caused by polymeric ratios of NaCMC and gelatine than the constant loading concentration of lidocaine when an ideal polymeric mass ratio 1:2.3 is implemented.

Chapter 4

Lidocaine carboxymethylcellulose with gelatine co-polymer hydrogel delivery by combined microneedle and ultrasound

Chapter overview

A study that combines MNs and sonophoresis pre-treatment was explored to determine their combined effects on percutaneous delivery of lidocaine from a polymeric hydrogel formulation. Varying ratios of NaCMC/gelatine ranges 1:1.6–1:2.66 loaded with lidocaine were prepared and characterized for Zeta potential and particle size. Additionally, variations in the formulation drying techniques were explored during the formulation stage. In vitro permeation studies using FDCs measured lidocaine permeation through porcine skin after pre-treatment with stainless steel MNs and 20 kHz sonophoresis for 5 and 10 min durations. A stable formulation was related to a lower gelatine mass ratio because of smaller mean particle sizes and high Zeta potential. Lidocaine permeability in skin revealed some increases in permeability from combined MN and ultrasound pre-treatment studies. Furthermore, up to 4.8 fold increase in the combined application was observed compared with separate pre-treatments after 30 min. Sonophoresis pre-treatment alone showed insignificant enhancement in lidocaine permeation during the initial 2 h period. MN application increased permeability at a time of 0.5 h for up to ~17 fold with an average up to 4 fold. The time required to reach therapeutic levels of lidocaine was decreased to less than 7 min. Overall, the attempted approach promises to be a viable alternative to conventional lidocaine delivery methods involving painful injections by hypodermic needles as mentioned in Chapter 3. The mass transfer effects were fairly enhanced and the lowest amount of lidocaine in skin was 99.7% of the delivered amount at a time of 3 h for lidocaine NaCMC/gelatine 1:2.66 after low-frequency sonophoresis and MN treatment.

4.1 Introduction

This chapter is concerned with the delivery of lidocaine HCl, a common anaesthetic, from a lidocaine carboxymethylcellulose with gelatine co-polymer hydrogel formulation such as discussed recently by Nayak et al. (2014a). Lidocaine HCl, termed as lidocaine, is a water soluble weak acid, fully ionized at pH 5.0 and administered into the plasma rich layer under the skin surface (Igaki et al., 2013). However, this administration is conventionally performed via hypodermic needles as a low cost and fast acting method (Hedge et al., 2011; Kim et al., 2012b). This is known to cause significant pains as mentioned in section 2.2. Alternatives, such as EMLA, topical lidocaine, require at least an hour of application to achieve effective analgesia, thus limiting its use especially in emergency situations (Nayak and Das, 2013). Therefore, there are important rationales for the pursuits of alternative lidocaine administration (Nayak and Das, 2013; Nayak et al., 2014a). This can be evidenced in the European paediatric drug legislation which backs innovation to develop ‘‘easy to administer’’ and ‘‘minimally invasive’’ drug delivery methods (Shah et al., 2011). The alternative rationales for lidocaine delivery include increased safety amongst the patients and healthcare providers, increased compliance with those who possess a fear of needles, reduced discomfort and pain especially in the case of applying anaesthetics as well as improved ease of delivery (Giudice and Campbell, 2006; Gill and Prausnitz, 2007; Li et al., 2010). The initial goal of this chapter is to further discuss enhanced lidocaine skin permeation from a NaCMC:gelatine hydrogel via an Ultrasound treatment, MN poke and skin coat technique as compared with lidocaine hydrogel application alone.

Low bioavailability of some drugs limits the therapeutic target effect (De Boer et al., 1979; Huet and Lelorier, 1980; Benet et al., 1996; Shipton, 2012). Lidocaine’s oral bioavailability is approximately reduced by 65–96% by digestive enzymes (Fen-Lin et al., 1993; Fasinu et al., 2011). In principle, innovative percutaneous delivery

could overcome the barriers associated with direct injection and oral drug administration (Polat et al., 2011) such as lidocaine. The rate of PD of drugs by percutaneous delivery depends on the molecular structure, size and hydrophobicity in conjunction with the drug concentration gradients. However, many studies have used combinations of PD and non-invasive techniques with varying success, e.g. MNs and ultrasound (Chen et al., 2010; Han and Das, 2013). This is the topic of this chapter and it is discussed in more detail below.

MNs are needle like structures of the size order of microns commonly arranged in a matrix (Gill and Prausnitz, 2007; Olatunji et al., 2014; Zhang et al., 2014). The lidocaine NaCMC/gelatine hydrogels pseudo-plasticity property permits seepage into MN cavities to bypass the SC skin layer compared with PD (Nayak et al., 2014a). Research has shown significant increases in skin permeability using optimized MNs when considering factors of MN length, number of MNs, the length and width aspect ratio and surface area (Al-Qallaf and Das, 2008, 2009; Olatunji et al., 2012, 2013; Guo et al., 2013). It has been suggested that MNs can be adapted to aid lidocaine delivery yielding many fold increase in delivery rate (Kwon, 2004; Li et al., 2008; Wilson et al., 2008; Zhang et al., 2012a, b; Kochhar et al., 2013; Ito et al., 2013; Nayak et al., 2014a). A number of studies have successfully delivered numerous active molecules using MNs, e.g. hepatitis B vaccine (Guo et al., 2013), Solaraze® gel in extending pore opening (Ghosh et al., 2013b) and naltrexone co-drug with diclofenac drug (Banks et al., 2011). In another recent study, it has been shown that MNs can be combined with ultrasound for increasing the delivery rate of a large macromolecular drug (Han and Das, 2013). These studies have directed the hypothesis that MNs and ultrasound combination could be used for greater epidermal lidocaine delivery in order to determine the significance of optimum sonophoretic power related effects on lidocaine permeation.

In this context, it is important to state that sonophoresis is generally based on ultrasound frequency. The low frequency sonophoresis (LFS) is defined to be within 20–100 kHz and the high frequency sonophoresis is usually for above 0.7MHz (Polat et al., 2011). The mechanism by which enhanced permeability is achieved via ultrasound can be linked to a number of physical phenomena, including thermal effects, formation of cavitation, mechanical effects and convective localized fluid velocities in skin. However, in the ultrasound pre-treatment experiment, it is generally accepted that inertial cavitation is the largest contributor to the enhancement in skin permeability. It is more so with LFS as described by Merino et al. (2003) due to larger bubble size at low frequency range. Inertial cavitation occurs due to pressure variations induced by ultrasound, resulting in rapid growth and collapse of bubbles formed in the coupling medium. The collapsing of the aforementioned bubbles near skin surface will cause micro-jets due to asymmetrically release of energy. These micro-jets have been confirmed as the main contributors to the permeability increment (Wolloch & Kost, 2010). The effects of ultrasound have been studied for the enhancement of TD lidocaine delivery with significant results for both pulsed and continuous output mode of LFS (Ebrahimi et al., 2012). However, as far as we are aware of, these techniques are yet to be combined and studied for permeability enhancement levels, particularly for lidocaine. The potential for MN assisted lidocaine delivery via hydrogel microparticles was discussed to summarise that there is significant commercial potential for lidocaine MNs (Zhang et al., 2012a, b; Nayak et al., 2014a). Polymeric hydrogel microparticles are good for the purpose of controlling spreading (i.e. controllable spreading radius, droplet height and contact angle) of the drug formulation over skin (Nayak et al., 2014a).

In this particular study, the drug vehicle for lidocaine encapsulation is polyanionic, carbohydrate based NaCMC cross-linked with polycationic, protein based gelatine

in forming a hydrogel (Nayak et al., 2014a). Previously lidocaine formulation bypassing the SC epidermal layer was outlined, the viscoelastic properties in adapting a NaCMC/gelatine network hydrogel prevent slippage of the drug formulation when applied to the skin and the possibility of non convective flow through the opened cavities of the skin from MN treatment (Milewski and Stinchcomb, 2011; Ghosh et al., 2013a). To try and exploit this potential, the main aim of the study is to combine the techniques in MN array and ultrasound technology as a pre-treatment to meet the definition of an ideal anaesthetic delivery method. A major advantage is that an extended release is possible using this approach. A carbohydrate based visceral hydrogel formulation was prepared as a model anaesthetic as this provides flexible properties and ability to encapsulate considerable amounts of liquid drug, lidocaine in this instance (Milewski and Stinchcomb, 2011), as discussed in the following section. Furthermore, the spreading behaviour of the prepared formulation was studied and compared with the spreading behaviour lidocaine solution as a Newtonian liquid. Unlike numerous studies performed using synthetic substrates, this study implements porcine skin as a lipophilic substrate as was attempted by Chow et al. (2008).

4.2 Materials and methods

NaCMC and gelatine emulsion was cross-linked to form hydrogels with encapsulated lidocaine as described in section 3.2. This formulation setup is highly beneficial because of fairly efficient preparation times in achieving a finished drug formulation in adaptation of green chemistry.

4.2.1 Materials

The reagents used in the preparation of lidocaine NaCMC/gelatine hydrogels were the exact specification as outlined in section 3.2.1. Methylene blue (50% v/v) was purchased from Sigma Aldrich Ltd (Dorset, UK). The column and and reagents

used in HPLC analysis were also taken from sections 3.2.1 and 3.2.11. Amputated porcine ears (age of pig: 5-6 months) were processed as mentioned in section 3.2.5. Also, 10mm x 10mm squares of same porcine skin were dissected as a substrate for droplet spreading. MN patch used is mentioned in section 3.2.5. Branson Digital Sonifier 450 (Danbury, CT) was chosen as the ultrasound output system. This ultrasound system includes an auto-calibrated transducer and a digital output controller. The frequency of the ultrasound is fixed at 20 kHz but the output powers are adjustable between 4 and 400 W. The equipment for droplet spreading studies was AVT Pike F-032 high-performance camera (Allied Vision Technologies UK), Camera i-speed LT high speed video (Olympus, UK).

4.2.2 Formulation of lidocaine NaCMC/gelatine hydrogel

The formulation of lidocaine NaCMC/gelatine hydrogel was taken from section 3.2.2. Each variation of the hydrogel formulation was coded with a letter F and outlined in Table 4.1. In the case of F5 residual paraffin and n-hexane were removed by rotary evaporation (Heidolph Instruments, Essex, UK) instead of the vacuum oven method from section 3.2.2.

Table 4.1: Lidocaine NaCMC/gelatine (gel) hydrogel mass ratio with particle size values

Sample ID	NaCMC (% w/w)	gel (c % w/w)	NaCMC:gel ratio	Drier type	Mean particle diameter ± S.D. (μm)	Particle diameter range (μm)
F1	1.2	2.0	1:1.6	Vacuum	5.89 ± 0.0026	1 - 13
F2		2.4	1:2.00	Vacuum	6.04 ± 0.0027	1 - 14
F3		2.8	1:2.33	Vacuum	6.81 ± 0.0029	2 - 17
F4		3.2	1:2.67	Vacuum	7.42 ± 0.0029	3 - 17
F5		3.2	1:2.67	Rotary Evap.	14.60 ± 0.0067	4 - 31

4.2.3 Zeta potential of lidocaine NaCMC/gelatine hydrogel

The samples for Zeta potential were analysed as described in section 3.2.8. The results were obtained in triplicate. The Zeta potential (ζ) was measured in terms of electrophoretic mobility (*μ*) via an optical technique, and ζ (mV) (Park et al., 2005) of the diluted hydrogel was computed from the Smoluchowski equation (equation 4.1), where μ is the referenced with latex ($m^2v^{-1}s^{-1}$), η is the DI volume viscosity (m^2s^{-1}), ε_0 and ε_r are the permittivity in a vacuum and relative permittivity of DI water as medium, respectively (Sze et al., 2003).

$$\zeta = \frac{4\pi\mu\eta}{(\varepsilon_r\varepsilon_0)} \tag{4.1}$$

4.2.4 Viscometric analysis of lidocaine NaCMC/gelatine hydrogel

The viscometric analysis of lidocaine NaCMC/gelatine hydrogel was characterised as in section 3.2.9.

4.2.5 Optical micrographs of lidocaine NaCMC/gelatine hydrogel

Micrographs were taken as described in section 3.2.10. Micrographs were pictured in triplicate for each formulation. Image processing software (ImageJ) was adapted in pixel measurement via graticule calibration to interpret particle size diameters from a random selection of 50 microparticles per image.

4.2.6 Controlled release of lidocaine from NaCMC/gelatine hydrogel

Lidocaine NaCMC/gelatine hydrogel (0.1 ± 0.05 g) was placed in an amber vial and 25.0 ml of DI water was dispensed before the sample was placed in a pre-heated thermostat bath at 37.0 ± 0.5˚C (Grant Instruments, Cambridge, UK). Subsequently, 1 ± 0.0005 ml of heated sample removed by autopipette (Eppendorf, Stevenage, UK), filtered using Nylon membranes (Posidyne, 0.1 μm) and analyzed for lidocaine

content using HPLC instrumentation. The results were measured in triplicate and the standard deviation from sample mean was taken.

4.2.7 *In vitro* skin permeation study of lidocaine NaCMC/gelatine hydrogel

The in vitro skin permeation for PD and MN characterisation was adopted as in section 3.2.5. The FDC receptor chamber volume was 5.0 ml. The aperture surface area was 1.33 cm^2. In vitro experiments were grouped as PD, MNs only pre-treatment, LFS only pre-treatment, MNs and LFS pre-treatment. The continuous viscoelastic properties of skin are unlikely to allow for MNs to penetrate beyond 200 mm when considering 1500 mm needle length rollers penetrating a depth of 150 mm (Roxhed et al., 2007; Badran et al., 2009). MNs were carefully applied to the skin ensuring penetration and held in place using a constant pressure device comprising a pneumatic piston (0.05 MPa) for 3 or 5 min. LFS was supplied for pre-treatment only using a probe set to 20 kHz frequency for 5–10 min. Continuous mode of ultrasound was chosen due to no significant difference being observed during pre-treatment applications (Herwadkar et al., 2012). The inter-coupling distance between the skin and probe was set to 2mm with coupling medium of DI water. In the case of MNs combined with ultrasound pre-treatment, the MN patch is applied before the ultrasound treatment. A minimum lidocaine concentration of 1.5 µg/ml was deduced from the literature as the permissible effective drug therapeutic value in plasma (Grossman et al., 1969; Schulz et al., 2012).

4.2.8 Spreading of lidocaine NaCMC/gelatine 1:2.33 across porcine skin

The setup for measurement of spreading radius, droplet height and apparent contact angle of droplet was similar to Chao et al. (2014). A square section of porcine skin (10mm x 10 mm) was placed flat in a closed sample box. A sample droplet (3.0 ± 0.5 ml) was dispensed on the porcine skin, camera frame rate capture of 1.85 frames per second (fps) was maintained and the results recorded.

Results were obtained in duplicate for the optimum particle size-controlled formulation and compared with a duplicate set of lidocaine solution of the same lidocaine loading weight (2.44 % w/w).

4.2.9 Histological study

The determination of MN insertion depth into skin by post MN treatment of skin was adapted from Cheung et al. (2014). First, the skin sample is pre-treated using 1100 mm MN patch for 5 min. Then, the porcine skin sample is stained using methylene blue (50% v/v) and merged into embedding compound (Bright Cryo-m-Bed, Huntingdon, UK) which is filled in a cuboid mould. The whole sample is then put inside the microtome (Bright Cryostat 5030, Huntingdon, UK) to solidify. The frozen sample is cut into 15 µm slices and analyzed under the microscope for the histology.

4.3 Results and discussions

4.3.1 Lidocaine NaCMC/gelatine hydrogel microparticle size diameters and morphology

Lidocaine encapsulated hydrogel microspheres based on NaCMC and gelatine were prepared using glutaraldehyde in transforming emulsion droplets to defined microparticles. As the mechanisms for ionic interactions in forming spherical microparticles are known (Gupta and Ravi Kumar, 2000; Berger et al., 2004), it is not discussed in detail in this thesis. The morphological observations of lidocaine NaCMC/gelatine microparticles are spherical, well-formed and slightly agglomerated for a significant number of them (Figure 4.1a and b). Mean particle size diameters (Table 4.1) in the formulation ranged from 5.89 to 14.60 mm depending on the formulation with an increase in mean particle size observed with an increased gelatine ratio. This is the likelihood of increased gelatine component

of the hydrogel, producing larger droplets during the w/o emulsification and subsequent hardening after the addition of glutaraldehyde. The rotary evaporation method yielded significantly larger particle sizes in comparison to vacuum drying. Interestingly, a positively skewed particle size distribution was observed for all lidocaine hydrogel formulations (Figure 4.2).

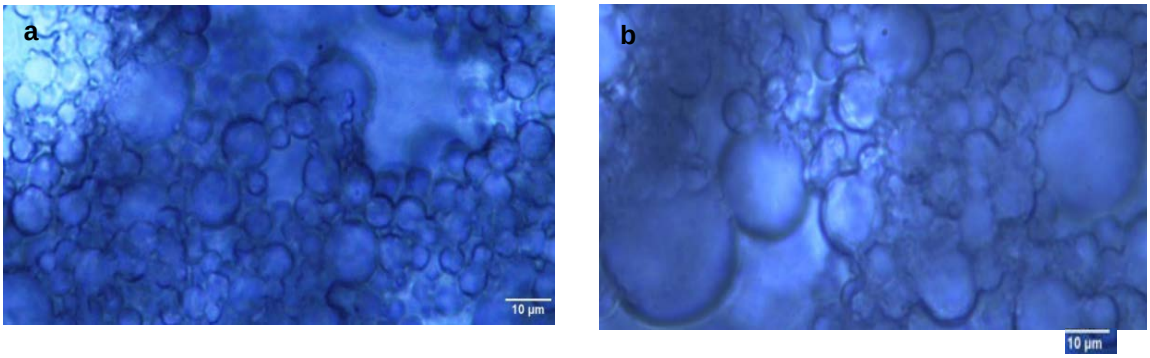

Figure 4.1: (a) lidocaine NaCMC/gelatine 1:2.33 hydrogel showing distinctly formed microparticles. (b) lidocaine NaCMC:gelatine 1:2.66 hydrogel showing larger and slightly more agglomerated microparticles.

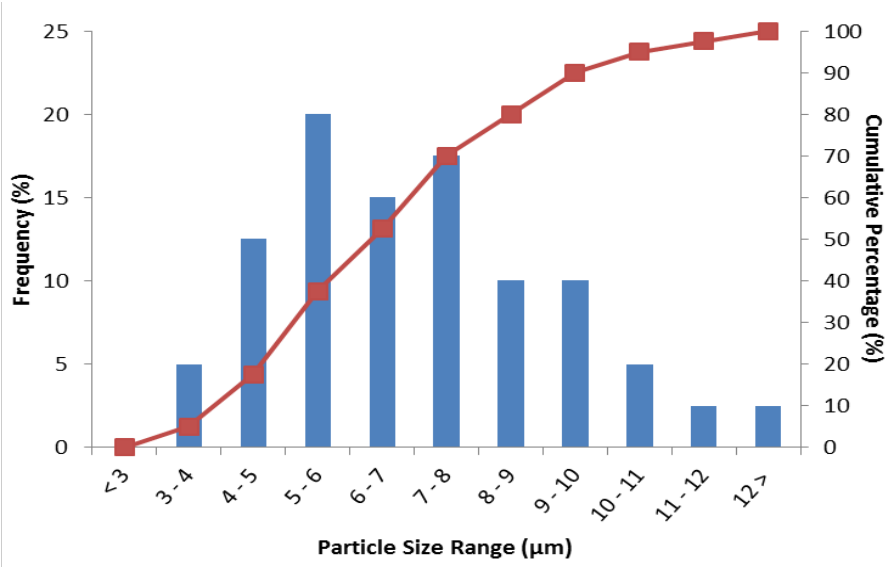

Figure 4.2: Particle size distribution of lidocaine NaCMC/gelatine hydrogels.

4.3.2 Dispersion of lidocaine NaCMC/gelatine hydrogel microparticles

Zeta potential studies in lidocaine NaCMC/gelatine hydrogels demonstrated a stable and fairly dispersed microparticulate system. The results (Figure 4.3)

expressed a trend of decreasing stability with an increase in the gelatine ratio, which in theory should impact a greater level of microparticle agglomeration thus likely affecting the permeability through skin. The pH of all formulations was kept constant and therefore it should not have affected the Zeta potential although the slight decline of ζ-potential in the positive direction is linked to the increase in gelatine ratio caused by gelatine in conjunction to lidocaine possessing a positively charged tertiary amide group at pH 4.0 and thus contributing to the increasing negative surface charge. The anionic polymer, NaCMC has a ζ-potential value of -30mV (Ducel et al., 2004) and electric charge neutralization did not occur or was not significantly induced by gelatine or lidocaine, so the overall lidocaine NaCMC/gelatine hydrogel charge was greater than -30mV. Nevertheless, reduced agglomeration is the result of a medium pKa, higher dielectric constants in comparison to a polymeric hydrogel components converging to significantly low overall ζ-potential range of -35 to -40mV and the effect of electrostatic particle repulsion (Xu et al., 2007).

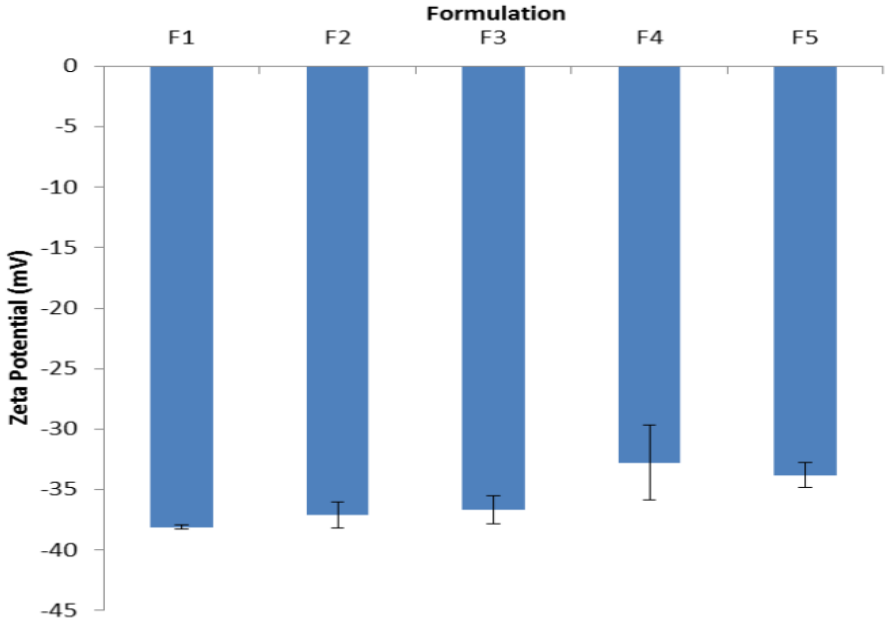

Figure 4.3: Lidocaine NaCMC/gelatine 1:1.6-1:2.66 (F1-F4) and lidocaine NaCMC/gelatine 1:2.66 by rotary evaporation preparation (F5) for Zeta potential.

4.3.3 Viscoelasticity of lidocaine NaCMC/gelatine hydrogel

Viscosity determination (Figure 4.4) revealed a lenient pseudoplastic nature for the formulation with lidocaine NaCMC/gelatine hydrogel with good correlative best fit curves observed for individual set of data points (R^2 > 0.93). The dynamic viscosity plots showed similar mild pseudo-plastic behaviour between the formulations with lidocaine NaCMC/gelatine 1:2.66 hydrogel being marginally higher when considering the upper viscosity range of 0.5–0.6 Pa.s at a starting shear of 25 s^{-1} and then more defined shear thinning behaviour observed above 100 s^{-1}. Lidocaine with NaCMC as a polyanionic vehicle alone will not be sufficient in enhancing pseudo-plastic properties and a recent study has shown that the profile of a dynamic viscosity plot is Newtonian (Alaie et al., 2013).

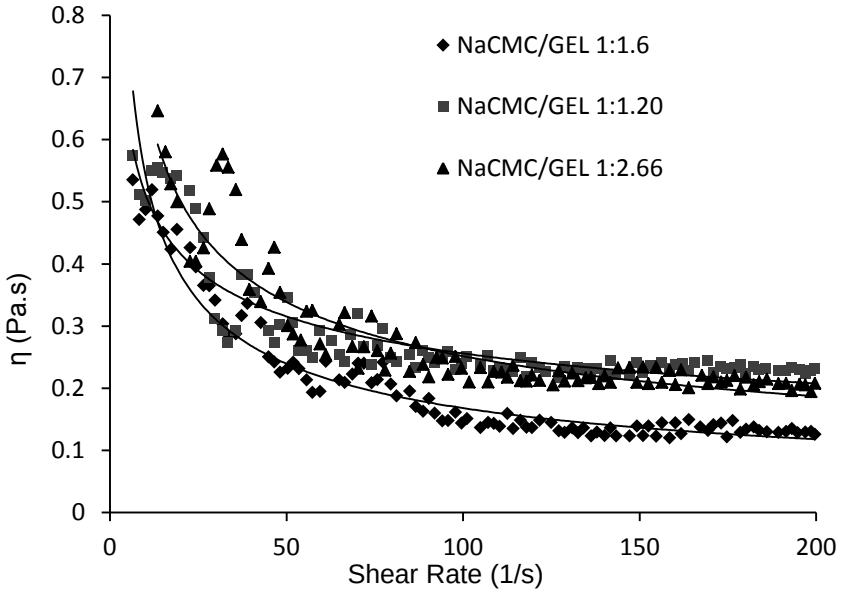

Figure 4.4: Lidocaine 2.44% w/w NaCMC/gelatine (NaCMC/gel) ratio pseudoplasticity.

4.3.4 Control of lidocaine NaCMC/gelatine 1:2.33 spreading on porcine skin

The spreading radius and height of lidocaine NaCMC/gelatine 1:2.33 outline significant control on its spreading behaviour compared with lidocaine solution of the same mass loading (Figure 4.5a and 4.5b). The beginning of the plateau effect is observed after 10 s and therefore, there is expected to be a localization effect on

the skin surface (Figure 4.5a and 4.5b). The dynamic contact angles of lidocaine NaCMC/gelatine 1:2.33 droplets are considerably higher than the lidocaine solution contact angle droplets, near to the skin impact time of 0 s (Figure 4.5c). Dynamic contact angle stability is noticed after 40 s (Figure 4.5c). Our results also show that the lidocaine solution is a Newtonian liquid that can spread much faster than lidocaine NaCMC/gelatine microparticles.

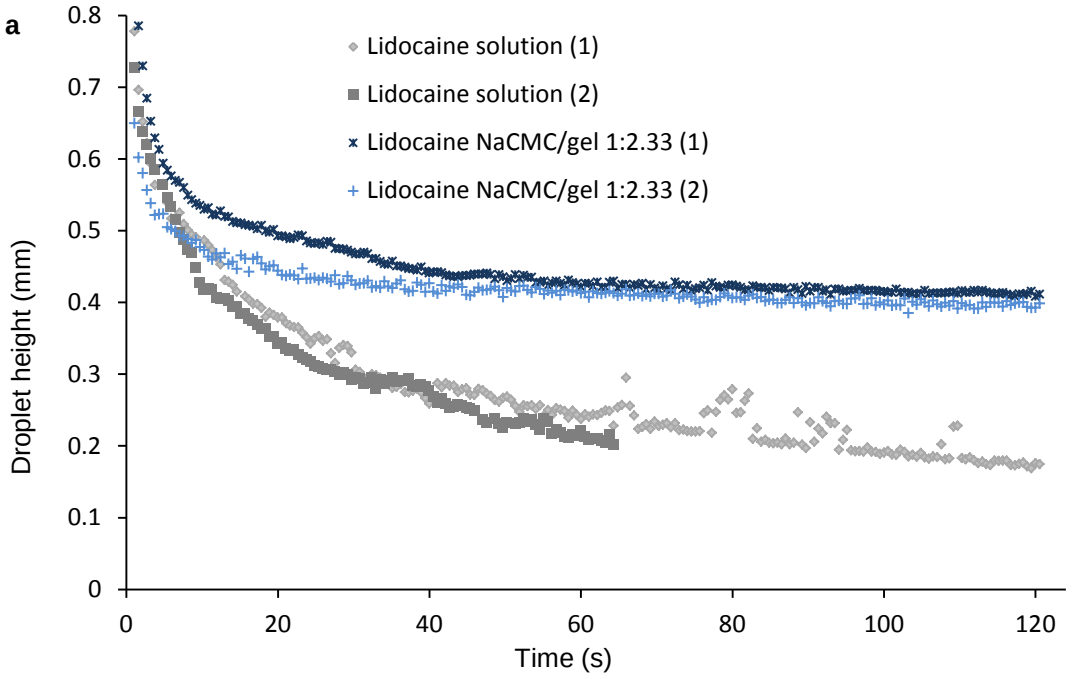

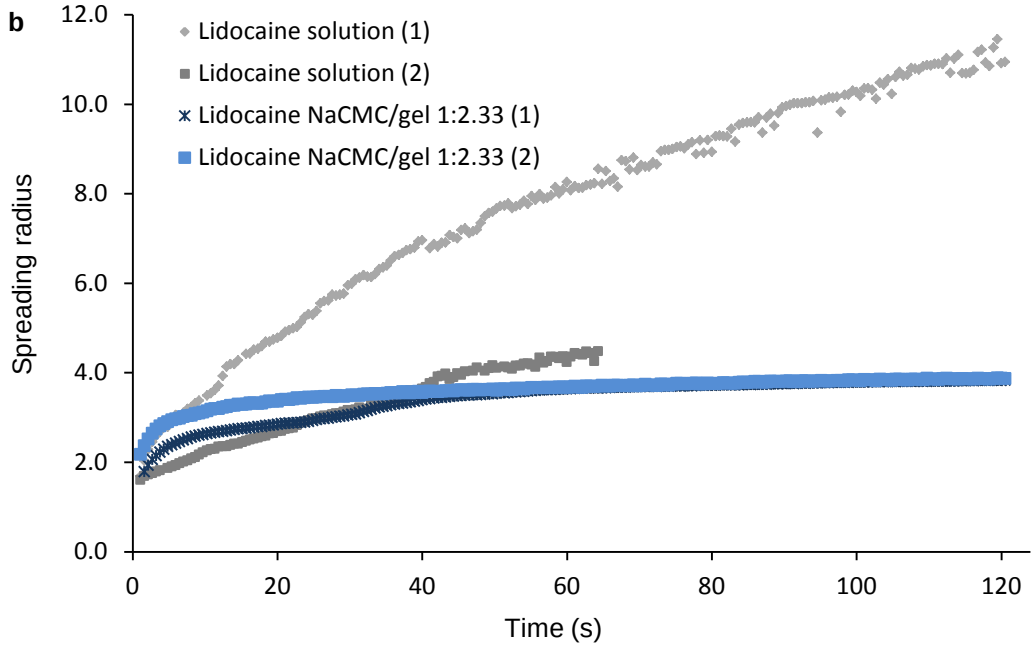

Figure 4.5: (Continued to next page).

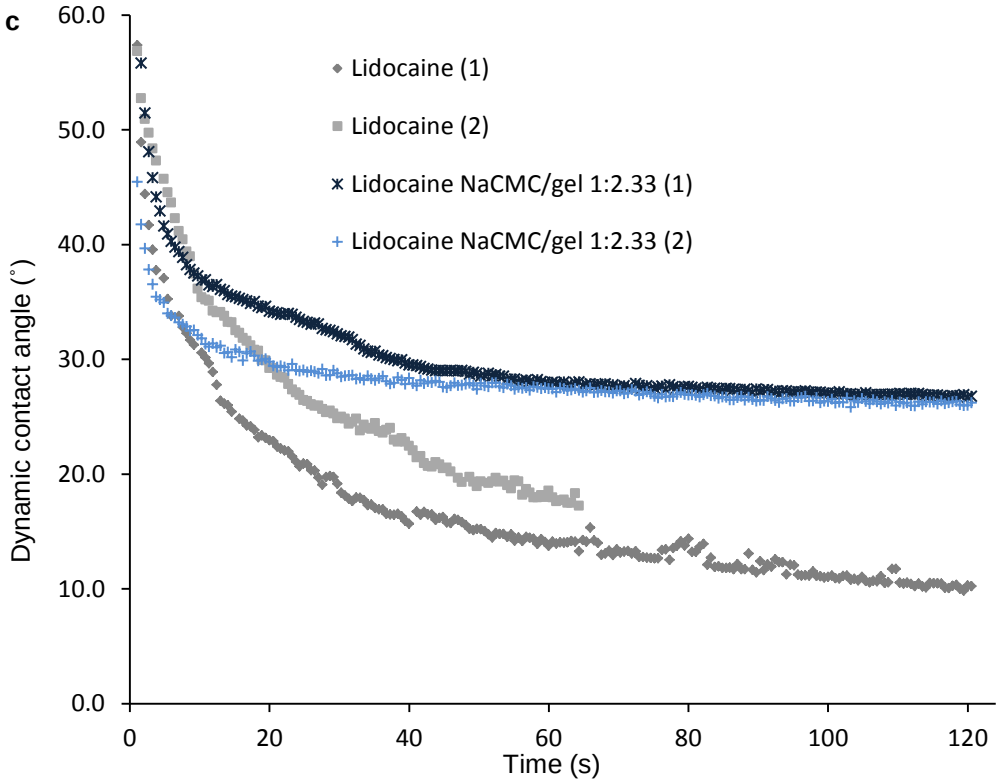

Figure 4.5: Lidociane NaCMC/gelatine (NaCMC/gel) 1:2.33 comparison with Newtonian liquid solution according (a) droplet heights (b) spreading radii (c) dynamic contact angles. The results suggest that the spreading of lidocaine NaCMC/gelatine 1:2.33 on the skin surface much more predictable/ controllable as compared with lidocaine solution.

4.3.5 The percentage release of lidocaine from controlled release of lidocaine

All four lidocaine NaCMC/gelatine hydrogels outline rapid release of lidocaine directly in DI water during the first 1 h with steady state conditions observed in the next 3 h (Figure 4.6a). A 0.3 fold decrease in cumulative release is observed in the first hour when comparing lidocaine NaCMC/gelatine 1:1.6 with lidocaine NaCMC/gelatine 1:2.66 as the highest releasing outline. Also, a 0.1 fold decrease in cumulative release was observed in the next three hours when comparing lidocaine NaCMC/gelatine 1:1.6 with lidocaine NaCMC/gelatine 1:2.66. This shows that the variation between hydrogel ratios is not significantly large as permeation release

profiles explained in the following sections. The percentage release of lidocaine from NaCMC/gelatine hydrogels was determined by the following:

$$\text{Percentage drug release} = \frac{M_s - M_t}{M_s} \times 100 \qquad (4.2)$$

where M_s is the maximum mean cumulative steady state concentration of drug and M_t is the mean cumulative concentration of lidocaine taken specifically at release time. The highest amount of lidocaine released was from NaCMC/gelatine 1:1.6 hydrogel in which 32.3% was detected in the DI water media in one hour (Figure 4.6b). This is because the smaller particles sizes of lidocaine NaCMC/gelatine 1:1.6 ratio allow for a greater surface area and encapsulated lidocaine thus rapidly dissolves in DI water. The lidocaine NaCMC/gelatine 1:2.66 ratio comprises larger microparticles and therefore a smaller surface area is exposed for DI water dissolution so the percentage of lidocaine released was 17.4% in one hour. Significantly less amounts of lidocaine is released for all NaCMC/gelatine hydrogel formulations after 1 hour reflecting the steady state conditions of the hydrogel as the DI water media becomes a saturated solution.

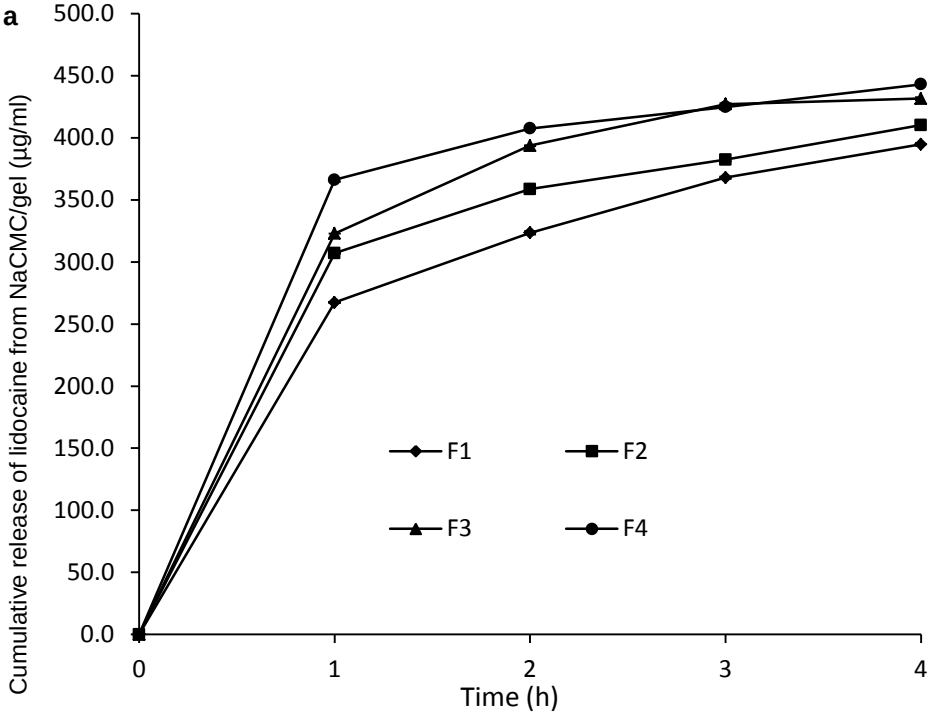

Figure 4.6: (Continued to next page).

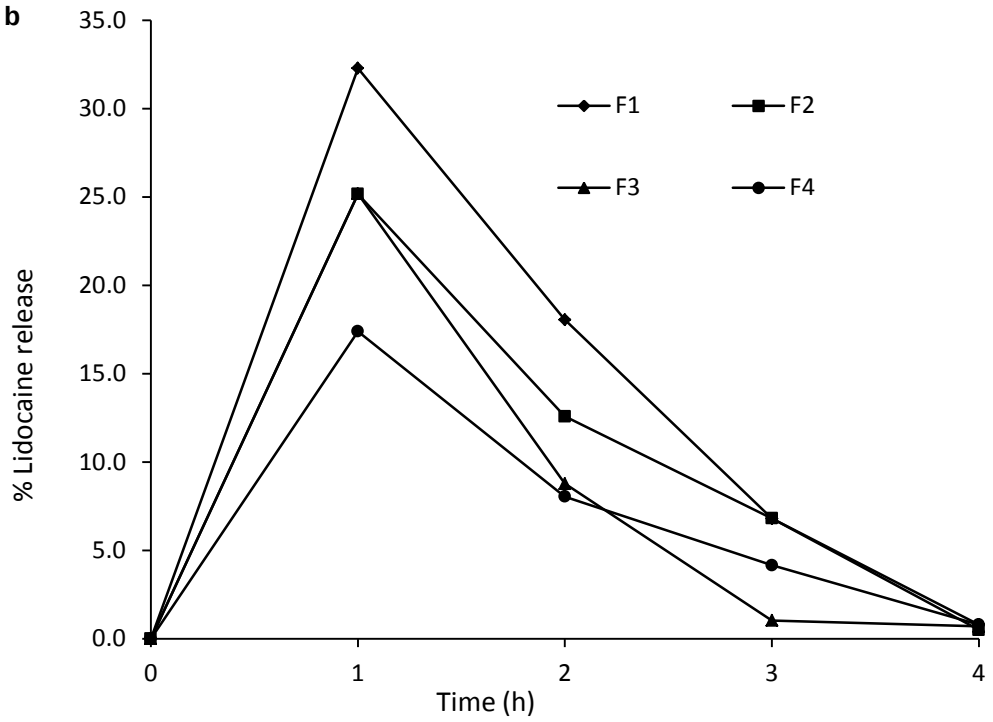

Figure 4.6: The controlled release of lidocaine 2.44% w/w loaded (a) NaCMC/gelatine 1:1.6 (F1), NaCMC/gelatine 1:2.0 (F2), NaCMC/gelatine 1:2.33 (F3) and NaCMC/gelatine 1:2.66 (F4). (b) as a percentage into DI water medium from NaCMC/gelatine 1:1.6 (F1), NaCMC/gelatine 1:2.0 (F2), NaCMC/gelatine 1:2.33 (F3) and NaCMC/gelatine 1:2.66 (F4). The error bars in (a) the standard deviation of mean represents the error (b) No error bards indicated.

4.3.6 Histological analysis on the MNs

The MNs that are employed in the histological experiment are 1100 mm in length. The purpose of the histological experiment is to determine the insertion depth of this MN patch under thumb pressure for which post MN treated skin is micrograph imaged (Figure 4.7). According to Figure 4.7, the insertion depth is between 300 and 400 mm which are much lower than the real length of MNs. This is caused by several reasons, such as the viscoelastic properties of the skin, the geometry of the MNs and the insertion force. This reduced insertion depth can further affect the permeation results.

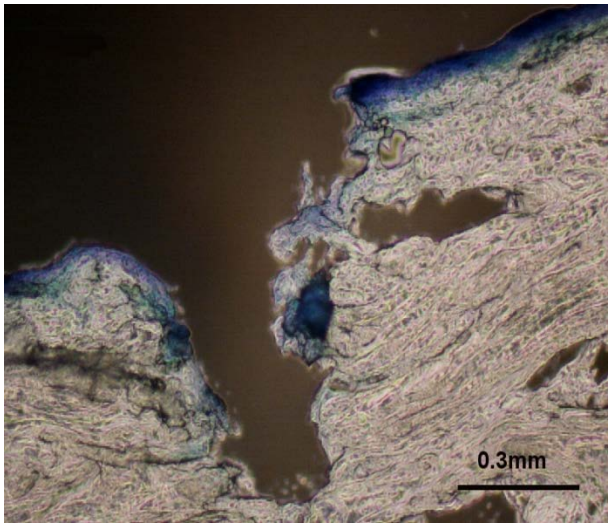

Figure 4.7: The MN insertion depth of skin sample using 1100µm MNs under thumb pressure. The histological studies show that although the MNs are 1100µm, for the MN density in the array and force applied, they create holes of approximately 400µm.

4.3.7 Passive diffusion of lidocaine NaCMC/gelatine hydrogel

Skin PD experiments were carried out in order to provide a control from which any pre-treatment enhancement results can be compared and contrasted. The lowest polymeric microparticle ratio 1:1.6 of lidocaine (Figure 4.8a) outlines the most desirable cumulative permeation for lidocaine in crossing the minimum threshold therapeutic level after 0.57 h. This is the shortest lag time for reaching the pain receptors for lidocaine in the deep dermis region rich in watery plasma and nerves. The hydrogel microparticle chemistry is a combination of significantly high negative Zeta potential and smaller mean particle size contributing to an increased permeation.

All lidocaine NaCMC/gelatine ratio hydrogels have demonstrated a very low initial permeation at a maximum of 0.3 µg/ml reached in 0.5 h. This is the normal lag time because of a longer path length for microparticle permeation when considering the topmost SC layer surface area bigger than the accessible VE layer microcavities. However, lidocaine NaCMC/gelatine 1:2.0 and lidocaine NaCMC/gelatine 1:2.66

hydrogels are the next two favorables after the most desirable formulation containing a polymeric mass ratio 1:1.6 for bypassing the minimum therapeutic threshold at a shorter time interval. Initially, lidocaine is diffusing through the fresh skin because of microparticulate disruption to the hydrogel formula caused by natural skin moisture hence the low initial concentration rates proceeding upto 0.5 h. Due to the requirements of lidocaine as an fast acting anaesthetic, the current results confirm enhancement of permeation is required if minimum therapeutic threshold of lidocaine (1.5 µg/ml) are to be reached within a suitable time frame for this technique to be of practical use. The lag time to cross a minimum therapeutic level is slightly greater than 1 h in lidocaine NaCMC/gelatine 1:2.33 hydrogel and just over 2 h for lidocaine NaCMC/gelatine 1:2.66 hydrogel, a rotary evaporation method with respect to PD alone which is considerably a long, unreasonable waiting time for a promising polymeric hydrogel ointment drug. The cumulative lidocaine thresholds tend to stabilize post 4 h, where equilibrium is reached and no more drug is released into the concentrated dermal region. This means that the lidocaine hydrogel ointment can be washed off the skin.

FDCs are in vitro glass cells in which soluble drugs can dissolve in a known volume of liquid solvent before timed removal and replacement of fresh solvent. The challenges in using FDCs are minimizing the occurrence of trapped air during the replaced of a volume of dissolved drug solution with fresh solvent (Sintov & Shapiro, 2004). Also large trapped air bubbles may be observed sometime while placing sectioned skin sample across the aperture of the receptor chamber. Overfilling the receptor aperture by 0.4 ml minimizes the introduction of large air bubbles. Lidocaine NaCMC/gelatine hydrogel was compared with lidocaine solution permeation from the literature (Sekkat et al., 2004). Prior to this PD comparison with lidocaine solution PD, the permeation units of µg/ml were converted into µg/cm^2 by the product of the known receptor volume followed by the quotient of the

adjustment factor value of 2.36 (3.14 cm^2/1.33 cm^2) due to the increase in FDC diffusion area when comparing a similar study using a smaller aperture diameter (Sekkat et al., 2004). The current lidocaine NaCMC/gelatine 1:1.6 hydrogel crosses the minimum therapeutic threshold by 1.8 fold than lidocaine solution on similar full thickness skin despite lidocaine solution permeating initially at 1.4 fold faster before a half an hour time frame and not anywhere near the minimum therapeutic threshold (Sekkat et al., 2004). Most FDC techniques appear a common place for PD studies and there is still a relatively big gap in adopting FDCs for MN based permeation studies. Lidocaine NaCMC/gelatine 1:2.66 and lidocaine NaCMC/gelatine 1:2.66 hydrogel formulated by rotary evaporation were chosen to be studied for further enhancement via pre-treatment. The factor of permeation enhancement can be deduced when making this comparison.

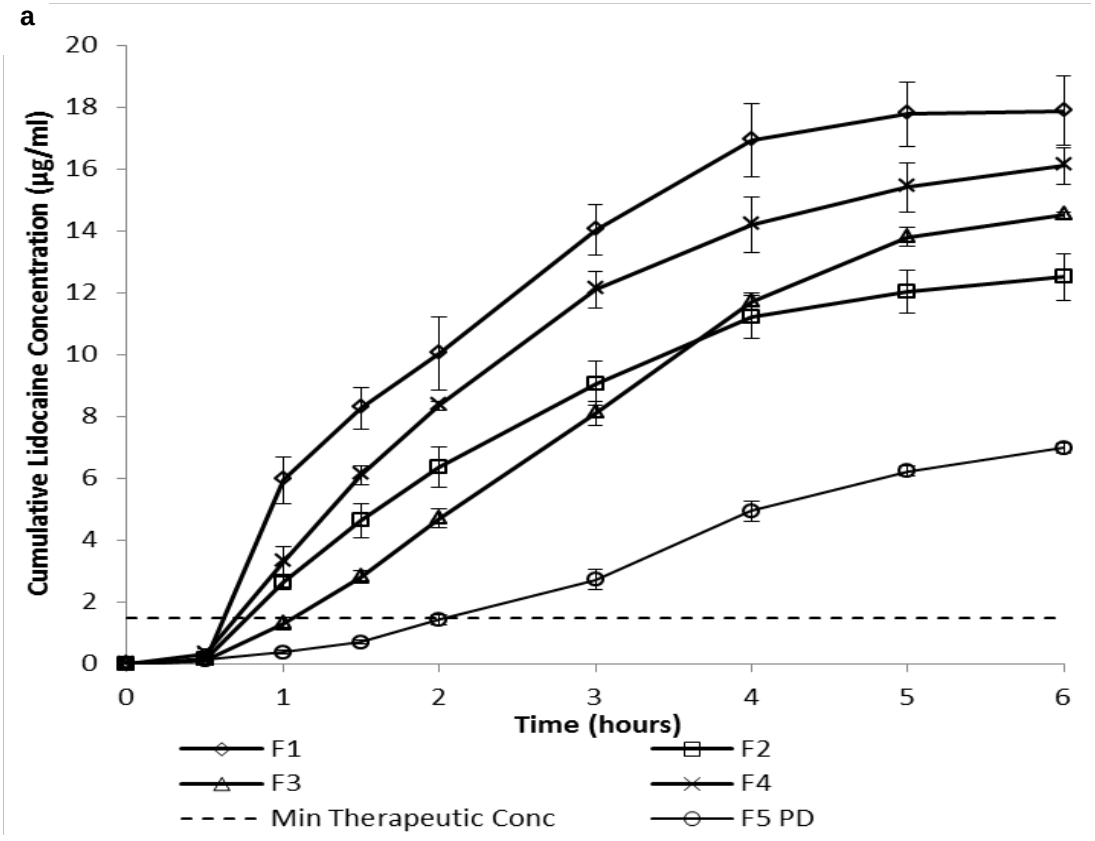

Figure 4.8: (Continued to next page).

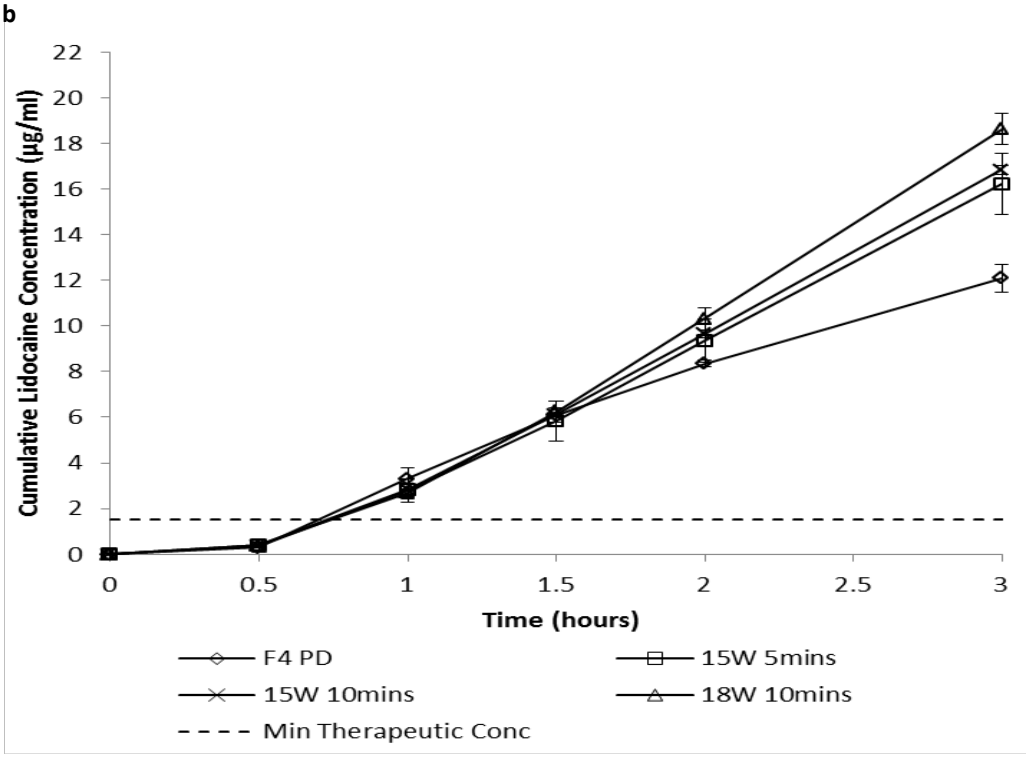

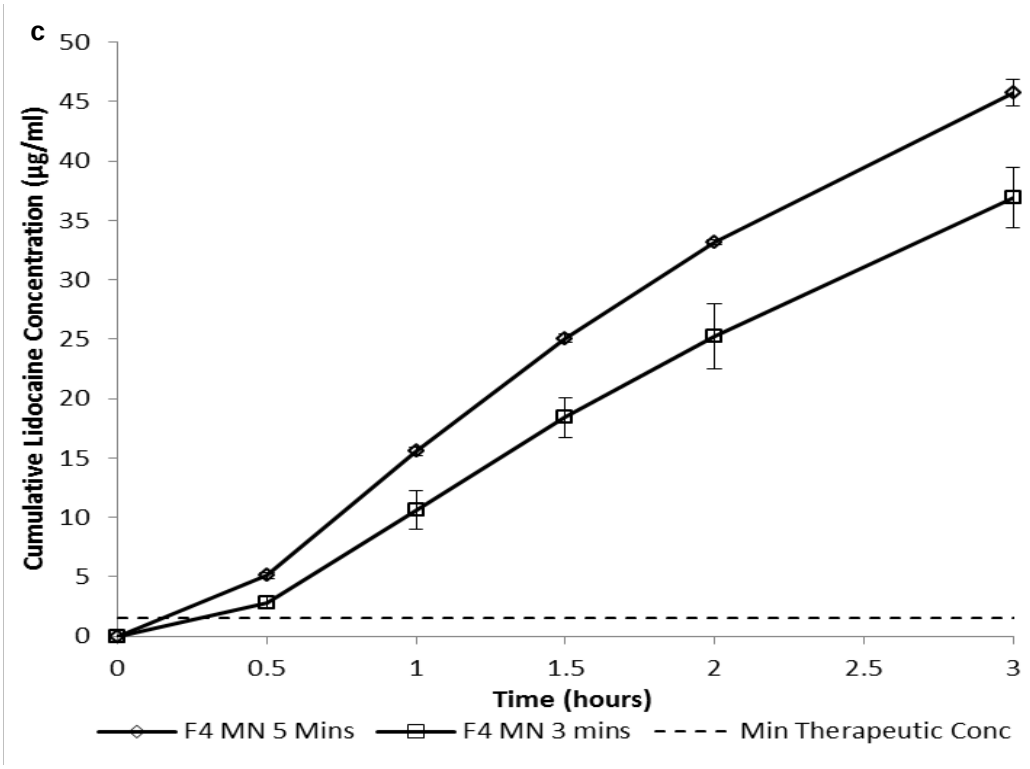

Figure 4.8: (Continued to next page).

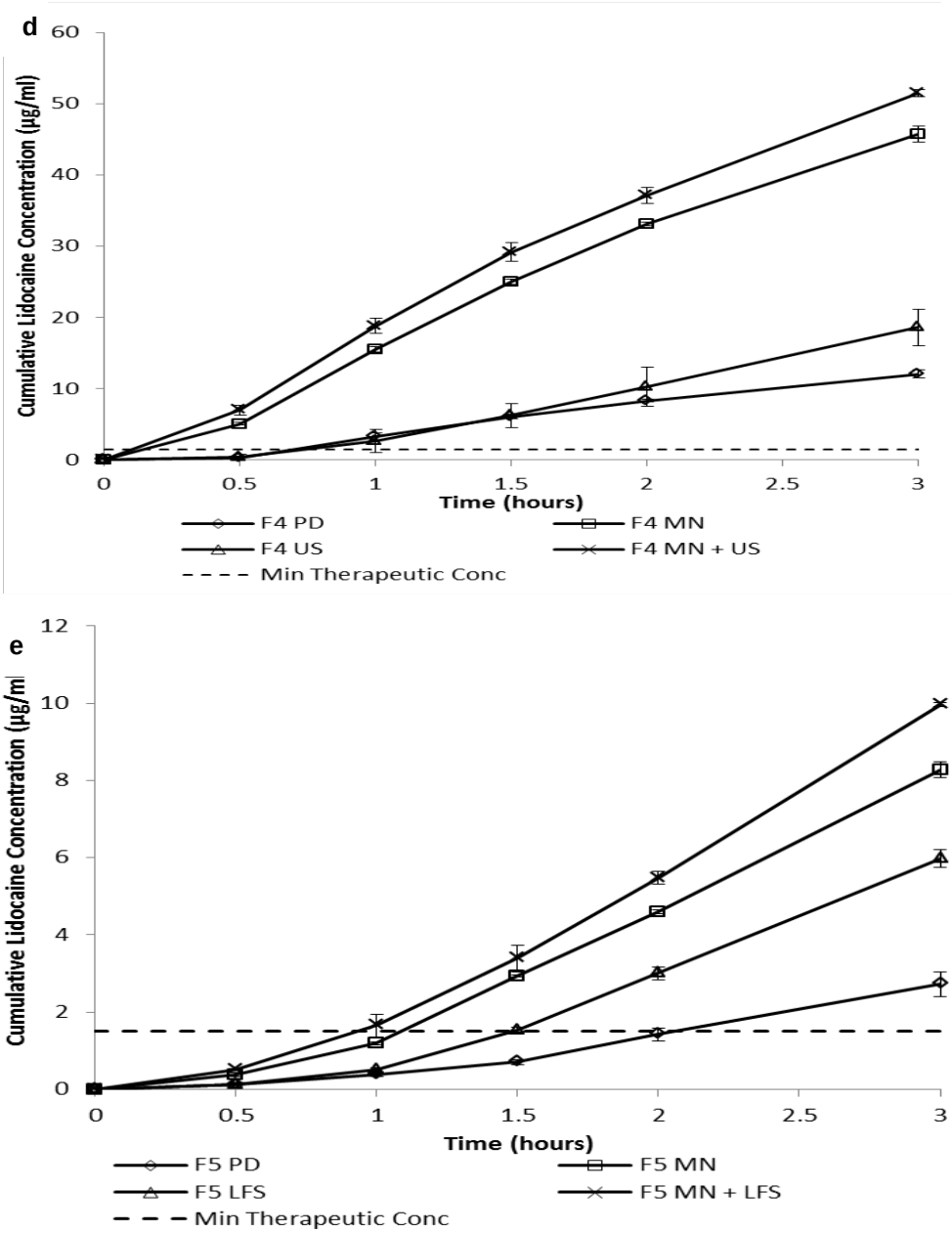

Figure 4.8: Cumulative lidocaine permeation from lidocaine (a) NaCMC/gelatine 1:1.6 (F1), NaCMC/gelatine 1:2.0 (F2), NaCMC/gelatine 1:2.33 (F3) and NaCMC/gelatine 1:2.66 (F4) and PD, NaCMC/gelatine 1:2.66 by rotary evaporation prep stage (F5). (b) F4 PD and comparative pre-treatment with ultrasound at 15 W and 18 W for 5 and 10 min, respectively. (c) F4 adapting MN patch for a 3 min and 5 min pre-treatment duration for lidocaine NaCMC/gel 1:2.66. (d) F4 adapting NaCMC/gelatine 1:2.66 (F4 PD), NaCMC/gelatine 1:2.66 (F4 US, 18W 10 min), NaCMC/gelatine 1:2.66 (F4 MN, 5 min) and NaCMC/gelatine 1:2.66 (F4 MN 5 min and US 18W 10 min). (e) NaCMC/gelatine 1:2.66 (F5 PD), NaCMC/gelatine 1:2.66 (F5 LFS, 18W 10 min), NaCMC/gelatine 1:2.66 (F5 MN, 5 min) and NaCMC/gelatine 1:2.66 (F5 MN 5 min, LFS, 18W 10 min).

4.3.8 Ultrasound only pre-treatment of lidocaine NaCMC/gelatine ratio 1:2.66 hydrogel

To observe the effect of power and application time of LFS has on permeation, LFS was applied continuously with varying power and exposure time as shown in Figure 4.8b. Theoretically, the exposure of LFS should form inertial cavities in the coupling medium and develop micro-jets toward the skin surface to aid permeation. However, lidocaine transport through the skin saw no significant enhancement up to 2 h after which a significant enhancement, especially power induction, 18 W at 10 min for lidocaine NaCMC/gelatine 1:2.66 (T-test $p < 0.026$) outlined a greater permeation profile. The results conclude that an increase in power has a greater enhancement effect compared with an increase in LFS exposure time; however, no significant increase in lidocaine transport through the skin was observed during the initial stages after varying respective power induction and time durations while maintaining constant NaCMC/gelatine ratios of lidocaine hydrogel drug application. It is predicted that a higher LFS power level would further increase diffusion; however, the risk of thermal effects would be too high for this to be of practical use.

4.3.9 MN pre-treatment of lidocaine NaCMC/gelatine ratio 1:2.66 hydrogel

PD permeation (Figure 4.8d) and MN assisted permeation (Figure 4.8c) with a post application time limit of 3 and 5 min concurrently were compared altogether. MN only pre-treatment of lidocaine NaCMC/gelatine 1:2.66 hydrogel generated a substantial increase in lidocaine permeation for both the 3 and 5 min post MN duration (Figure 4.8c). A statistically significant difference ($p < 0.04$) was observed for MN application duration. Initial (t=0.5 h) permeation for the 3 and 5 min patch duration resulted in increases of 9 and 17 fold, respectively. An average 3 fold increase in permeation was observed for the 3 min MN application and comparatively an increase by 4 fold for a 5 min MN application. The results indicate that therapeutic levels of lidocaine could be reached within 0.15 h or 9 min post application MN, in comparison to no pre-treatment requiring 40 min (Figure 4.8c

and 4.8d). The reason for this short lag time is due to lidocaine microparticles traveling at a shorter path length to the deep dermis layer. The SC layer has been bypassed by artificial MN cavities. MN assisted cumulative release study with respect to lidocaine formulations has not been performed *In vivo* to date. However, *in vivo* release studies have been performed using non degrading polymeric MN array coating of lidocaine alone, sustained approximately 15 min of delivery thus proven successful for rapid emergency anaesthesia (Zhang et al., 2012a,b). In vivo release studies with ex vivo cumulative release studies are completely incomparable due to obvious differences in experimental procedures and removal of active drug for characterization. The lidocaine NaCMC/gelatine 1:1.6 ratio (Figure 4.8a) hydrogel crosses the therapeutic level at significantly slower time duration, greater than 30 min in lidocaine NaCMC/gelatine 1:2.66 ratio in comparison of MN and LFS treatment. This is due to the fact that MNs and ultrasound are involved in either cavity engulfing of larger sized hydrogel microparticles.

4.3.10 MN and ultrasound (dual) pre-treatment of lidocaine NaCMC/gelatine ratio 1:2.66 hydrogel

Both pre-treatments (dual) were combined and studied for further permeation enhancement in comparison to MN or LFS pre-treatment only. Lidocaine NaCMC/gelatine 1:2.66 hydrogel in which combining a 10 min application of 18W LFS after a 5 min application of MNs demonstrated an initial faster permeation by 23 fold with an average 4.8 fold increase over 30 min of application when compared with separate device treatments and PD (Figure 4.8d). Therapeutic levels of lidocaine could theoretically be reached after 7 min post application in terms of reaching the deep dermis layer of skin as the target. A general increase in permeation throughout the period of experimentation can be noticed rather than post 2 h as seen with LFS pre-treatment only, this could be due to efficiency of LFS pre-treatment is further enhanced on porous skin sample formed via the MN patch.

4.3.11 Dual pre-treatment of lidocaine NaCMC/gelatine 1:2.66 hydrogel via a rotary evaporation method

Lidocaine NaCMC/gelatine 1:2.66 hydrogel with the rotary evaporation method as described earlier, favoured an additional time of nearly 0.9 h or 50 min after the application of 18W LFS at 10 min ($p < 0.04$) to reach minimum therapeutic level in conjunction to a two fold average increase in permeation after 1 h, compared with the same formulation without rotary evaporation method (Figure 4.8d and 4.8e). This was the likelihood of higher heating temperatures compromising the glutaraldehyde fixation and thus resulting in larger microparticle as previously reported. Higher heating temperatures were required in the large volume removal of n-hexane and paraffin oil mixture by solvent evaporation. A 5 min application of the MN array led to an initial increase by 2.8 fold and subsequently an average 3.4 fold increase was observed with respect to the deep dermis layer skin target. Combining the two pre-treatments resulted in an initial permeation increase by 3.8 fold followed by an average increase by 4.1 fold in comparison to PD only (Figure 4.8d and 4.8e). Therapeutic levels of lidocaine were reduced from just over 2 h to less than 1 h on average.

4.3.12 Mass transfer of lidocaine from NaCMC/gelatine 1:2.66 hydrogel

The percentage of lidocaine remaining inside ex vivo skin was determined by the subtraction of the mass of lidocaine initially encapsulated during formulated preparation (125 000 µg) by the cumulative amount detected in DI water from controlled release studies. The purpose of using controlled release studies is to determine the amount of lidocaine contained in the vehicle as mass balance before the subtraction of the mass of lidocaine in the receptor in which the DI water in the receptor is the deep dermis. All mass balances were carried out in µg and converted from cumulative concentration units of µg/ml before the percentage of lidocaine remaining inside the skin was determined (Figure 4.9). Overall the mass

transfer of lidocaine with respect to all treatment applications appeared to outline a gradual, a slow process of diffusing through the full thickness appendage. However, there is a fairly substantial decline in the percentage of lidocaine remaining inside the skin when MN and ultrasound treatment (LFS) method was applied. This can be interpreted as diffusion of lidocaine molecules through skin cells and layers before clearance into the blood stream. The lowest percentage of lidocaine remaining in the skin is 99.7% after a time of 3 h (Figure 4.9).

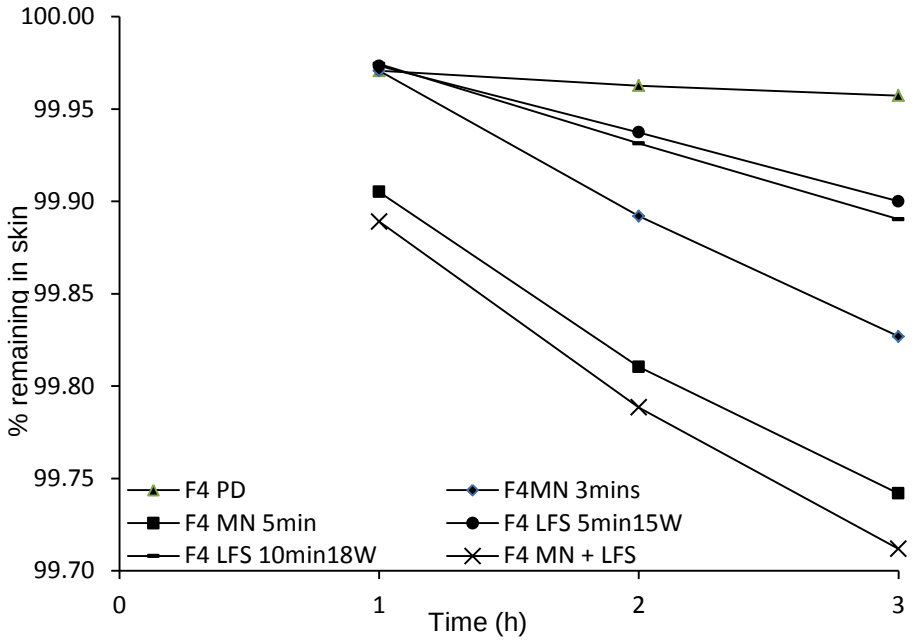

Figure 4.9: Percentage of lidocaine contained in (F4) NaCMC/gelatine 1:2.66 (PD), (MNs, 3 min), (MNs, 5 min), (LFS 5 min 15W), (LFS 10 min 18W), (MN + LFS). Error bars outline a random error range of 0.005%)

4.4 Chapter summary

This study aimed to use LFS and MNs as a pre-treatment to skin in order to enhance permeation of lidocaine encapsulated in a formulation. A significantly more microparticle stability was found with lower gelatine ratios (1:1.6); however, all formulations were sufficiently stable (Zeta potential: ≥ -30 mV). Our diffusion

experiments revealed a small increase in diffusional permeation when LFS was used in combination with a MN array pre-treated skin. However rotary evaporation during the final polymeric drug formulation stage caused significant reductions in lidocaine permeation levels. Nota bene that the main purpose for utilizing rotary evaporation was for reduced time in the removal of a large volume of residual paraffin and n-hexane as the final operative method compared with vacuum oven drying (data not shown).

Lidocaine NaCMC/gelatine 1:2.66 and lidocaine NaCMC/gelatine hydrogel 1:2.66 formulated by rotary evaporation showed a decreased time required to reach minimum therapeutic levels of lidocaine by 5.7 and 2 fold, respectively. Generally, lidocaine permeation was significantly increased with higher sonophoresis power and increasing exposure duration demonstrated a minor increase in the permeation rate for lidocaine NaCMC/gelatine hydrogel formulations. Also, the MN application time duration of 5 min resulted in a highly favourable increase in lidocaine permeation. Furthermore, combining MN and LFS pre-treatments allowed for the time to reach minimum therapeutic lidocaine levels to be significantly reduced, For example, in the case of lidocaine NaCMC/gelatine, 1:2.66 hydrogel therapeutic thresholds of lidocaine were reached within 7 min of application. The mass transfer effects in which the percentage of lidocaine remained in the full skin depicted the gradual movement of drug in targeting pain receptors below the SC layer. The lidocaine NaCMC/gelatine 1:2.66 hydrogel treated by MNs and LFS shows a greater mass transfer profile. The US and MN treated lidocaine NaCMC/gelatine 1:2.66 has a 0.18% mass transfer of lidocaine through skin within 2 h compared with 0.01% mass transfer of lidocaine through skin. Therefore, this method is promising and could be of medical use as a painless, easy to administer technique for drug delivery overcoming the time constraints associated with delivery of lidocaine. The resources and materials in developing a lidocaine NaCMC/gelatine

1:2.66 hydrogel without rotary evaporation is economical on a batch scale at present. Lidocaine NaCMC/gelatine 1:2.33 formulation with defined morphological appearance is able to remain on the surface of the skin for longer durations compared with a lidocaine solution of the same mass loading.

Chapter 5

Lidocaine permeation from a lidocaine NaCMC/gelatine microgel formulation in microneedle-pierced skin: vertical (depth averaged) and horizontal permeation profiles

Chapter overview

Common local anaesthetics such as lidocaine are administered by the hypodermic parenteral route but it causes pain or anxiety to patients. Alternatively, an ointment formulation may be applied which involves a slow drug diffusion process. In addressing these two issues, this chapter aims to understand the significance of the 'poke and patch' MN treatment on skin in conjunction to the lidocaine permeation, and in particular, the vertical (depth averaged) and horizontal (e.g. lateral) permeation profiles of the drug in the skin. The instantaneous pharmacokinetics of lidocaine in skin was determined by a skin denaturation technique coupled with FDC measurements of the drug pharmacokinetics. All pharmacokinetic profiles were performed periodically on porcine skin. Three MN insertion forces of 3.9, 7.9 and 15.7 N were applied on the MN to pierce the skin. For the smaller force (3.9 N), post MN treated skin seems to provide an 'optimum' percutaneous delivery rate. A 10.2 fold increase in lidocaine permeation was observed for a MN insertion force of 3.9 N at 0.25 h and similarly, a 5.4 fold increase in permeation occurred at 0.5 h compared to PD delivery. It is shown that lidocaine permeates horizontally beyond the area of the MN treated skin for the smaller MN insertion forces, namely, 3.9 and 7.9 N from 0.25 to 0.75 h, respectively. The lateral diffusion/permeation of lidocaine for larger MN treated force (namely, 15.7 N in this work) seems to be insignificant at all recorded timings. The MN insertion force of 15.7 N resulted in lidocaine concentrations slightly greater than control (PD) but significantly less than 3.9 and 7.9 N impact force treatments on skin. We believe this likelihood is due to the skin

compression effect that inhibits diffusion until the skin had time to relax at which point lidocaine levels increase.

5.1 Introduction

The specific nomenclature expressed in chapter 4, lidocaine HCl, to be called as lidocaine herein, is a drug which is used as a local anaesthetic for superficial skin wounds (Smith et al., 1999; Quinn et al., 2014). Traditionally, lidocaine is delivered by hypodermic injection for parenteral administration. This causes pain and often trepidation coupled with patient phobia, which may obstruct the successful delivery of the drug (Nir et al., 2003; Kim et al., 2014). Other traditional methods of lidocaine delivery involve the use of topical ointment (e.g., AnestenTM, Haim International, Seoul, Korea) and TD patch (e.g., Lidoderm® patch, 2013). However, they have a disadvantage of taking a longer time for the drug to diffuse into the dermis layer through the SC layer of skin (Singh and Morris, 2011). In percutaneous lidocaine delivery, the formidable challenge is to bypass the SC. This layer is 10-15 μm thick and it is the skin's uppermost barrier to foreign particulate entry into skin (Akhtar, 2014; Sivamani et al., 2005). This chapter carries forward the formulated lidocaine NaCMC:gelatine 1:2.3 microgel for a direct, depth averaged, In Vitro skin analysis via the poke and coat technique. Common conventional FDC methods are severly restricted to deep dermal and systemic clearance diffusion of drugs.

In general, the mass flux due to diffusion of drug molecules through the SC is affected by the molecular hydrophilicity and the concentration gradient across different skin depths (Allen, 2002). FDC is typically adopted to determine the in vitro mass transport properties of the active molecules passing the SC (Raphael et al., 2013) or the whole skin thickness (Nayak et al., 2014a; Nayak et al., 2014b). Depending on the direction of concentration gradient and permeability, an active molecule can, however, diffuse both vertically and horizontally in skin tissues. In the

present context, horizontal permeation is taken in a broad sense. It may imply both lateral and transverse permeation in a cartesian coordinate system or radially for circular co-ordinate system.

The migration of the active molecules due to a concentration gradient from the skin surface is the most commonly accepted in vitro vertical (depth averaged) TD delivery. The meaning depth average is the average depth of full thickness skin sections devoid of SC. The depth average of full thickness skin cannot be deduced metrologically accurate because of the known elastic property of skin. These molecules bypass the VE and dermis layer before appearing into the receptor compartments of FDC. In a similar manner, the horizontal permeation of the drug molecules is achieved from in vitro skin biopsy. Following this, a direct drug transport quantification technique in the lateral (x-direction), transverse (y-direction) or radial (r-direction) directions at different distances from an epicentre of the skin (Figure 5.1a) provided the drug transport can be determined analytically. In the case of MN treated skin, e.g., 'poke and patch' type delivery (Bal et al., 2010), the origin of a drug can be the outermost (e.g., skin surface) and/or the inner locations of the skin (e.g., micro-cavity). As far as we are aware, there are few or no studies relating to the migration of a drug molecule in both vertical and horizontal directions in MN pierced skin, and in particular, lidocaine delivery using MNs. This issue can be particularly important for distribution of lidocaine delivered in skin via the implementation of this direct depth averaged biopsy technique.

Skin can be interpreted as a complex hydrophobic membrane because of the inherent barrier property against most exogenous molecules. In most cases, small, hydrophobic molecules migrate by intracellular and intercellular routes inside the skin. At a given time, biopsied sections of the skin can be homogenised and denatured for the purpose of disrupting the skin tissue structure and releasing the

active molecules into sample vials for determining their concentrations, e.g. analyses using HPLC (Peira et al., 2014). The homogenisation and denaturing of skin is discussed further in this chapter.

In a number of recent studies, it has been discussed that MN assisted percutaneous delivery of lidocaine may be beneficial in numbing a larger surface area of skin and minimising possible clearance from predominate vertical permeation of the drug (Nayak et al., 2014a; Nayak et al., 2014b; Zhang et al., 2012a; Mitragotri, 2003). Parenteral administration of lidocaine may increase the chances of clearance resulting in its depleted levels in the systemic circulation (Bari, 2010). Hypodermic needles in parenteral administration are common in reaching systemic circulation depths because of their macroscopic dimensions. Therefore hypodermically delivered lidocaine will clear in blood circulation. Lidocaine is metabolised in the systemic circulation by various enzymes, and additional medications such as statins and chemotherapeutic agents can potentially increase the clearance of lidocaine influenced by the metabolism (Olkkola et al., 2005; Gudin, 2012). Furthermore, the diffusion of hydrophobic and hydrophilic molecules in SC layer has been reported to be faster laterally than vertically across the skin because of the continuous nature of the intercellular pathway (Johnson et al., 1997; Schwindt et al., 1998). As far as we know, there is only one reported experimental study on horizontal permeation of lidocaine in full thickness skin (Zhang et al. 2012a). In this study, a method of dip coating MNs with lidocaine and single patch application was attempted. After skin samples were enzymatically digested, it was found that therapeutic thresholds could be sustained for short durations and higher lidocaine concentrations could be obtained for longer durations when combined with a vasoconstrictor epinephrine after treatment with dip coated liquid crystalline polymer MNs (Zhang et al., 2012a).

As a drug delivery method, MNs have been reviewed significantly in the literature and therefore, they are not discussed in length in this chapter (Nayak and Das, 2013; Cheung et al., 2014; Cheung and Das, 2014). The MNs can be constructed from silicon, metals or polymers (Allen et al., 2002; Nayak and Das, 2013; Olatunji et al., 2014). Hypodermic needles are restricted to metallic materials which is normally medical grade stainless steel. In principle, they should pierce past the SC layer to form micro-cavities in the skin before drug application or pre-loaded with drugs at the point of application. In other cases, the MNs dissolve once in the skin releasing the drug to allow increased permeation rates (Yeu-Chun et al., 2012). The re-sealing time of MN induced cavities in skin has evoked interest when considering the poke and patch technique (Bal et al., 2010) and, drug pharmacokinetic thresholds have been found to be affected when pore closure is considered. For example, Brogden et al. (2012) expressed the half-life of pore closure from placebo MNs at 18.2 h and 87.5–97 % of microcavities were closed between 54.7–91.2 h. In the case of lidocaine application with the help of MN, time duration of 45 min to 1 h may be short in attempting to relate the possible effects on pore closure time with micro-cavity drug permeation; however, there is little or no evidence in this regards at the moment.

Recently, a lidocaine NaCMC/gelatine bipolymeric formulation has been suggested for controlled permeation of lidocaine in MN pierced skin (Nayak et al., 2014a; Nayak et al., 2014b) where the authors have used a poke and patch approach for percutaneous delivery of lidocaine. Subsequently, the permeation profiles of the MN pierced skin for various mass ratios of NaCMC/gelatine with lidocaine were determined. The MN pierced skin showed faster lidocaine permeation than untreated MN skin for vertical layer skin profiles. Lidocaine was released into the skin from the formulation and it bypassed the SC layer because of the MN cavities. Transverse microsliced, treated skin imaged microscopically initially showed the

irregular morphology of artificial micro-cavities. This irregular morphological outline is very different from a rounded natural pore micro-cavity. From skin micrographs, the penetration depths were accurately measured. Furthermore, the physico-chemical properties of the formulations, encapsulation efficiency, Zeta potential, mean particle size and morphology have been studied. In principle, the MN treatment of skin allows further increase in the efficacy of lidocaine permeation as well as controlled spreading of the drug formulation along the skin surface as demonstrated in the above studies.

In general, homogenisation of skin adopts mechanical forces of shearing and compression of skin into shredded tissue components. For example, a rotor component of a rotor/stator homogeniser may be used which creates low pressure areas, moving suspension material (e.g., skin tissue debris) towards a sub 500 μm gap between the rotor and stator, shearing any trapped suspension material (Goldberg, 2008). However, the adaptation of a rotor/stator homogeniser is unsuitable for shredding dissected thin skin slices below 500 μm thickness. This is due to the skin not being properly sheared if it enters and exits the rotor/stator. An alternative homogeniser is a glass tissue grinder (e.g., constructed from Teflon) and comprising of a specialist mortar test tube (Akin and Norred, 1976). Sharp blade-based shear homogenisation is not a regular process for skin tissue samples despite not requiring external power sources. An example application of this can be found in cutting of porcine ear tissue before denaturation by dimethylsulfoxide solution (Peira et al., 2014).

Another method which involves the pestle and mortar skin homogenisation (Entenman, 1961) without the need for direct current or alternating current supply was adopted in our study. There have been a relatively small number of publications outlining the details of this technique for skin homogenisation prior to

drug quantification in skin layers. Conceptually, the method aims to increase the amount of ruptured cells and dissemble the organised cell packing in skin tissues randomly. There is a likelihood of tissue sections that have not been exposed to sufficient shear forces. Therefore, this alone cannot suffice for the purpose of drug detection and, hence, a second step of cellular denaturation is required to release the drug molecules for subsequent detection. The second stage of enzymatic protein denaturation of skin specimens are outlined in examples of quantification of hydroxyproline as a byproduct of α-chymotrypsin hydrolysis from fragmented collagen (Fligiel et al, 2003) and the quantification of combined chemical enhancers such as 5-aminolevulinic acid with glycerol monooleate in epidermal skin delivery (Steluti et al., 2005). However, diode array detection and peak area quantification of active macromolecules eluting at similar detection wavelengths ranges to enzyme and skin protein by products is unachievable by LC-DA analysis alone. Therefore, heat denaturation technique may be used.

High temperatures above 50 °C for a long period allow for intra and extracellular denaturation of skin proteins (Viglianti et al., 2014). Denaturation temperature of human skin at 38.5 °C allows the appearance of imino acid residues in protein breakdown (222 imino residue parts per 1000 part amino acids) (Bornstein and Piez, 1964). Collagen based porcine skin has a denaturation temperature of 37 °C (Lui et al., 2007; Nagai, 2002). Also, dry heating (e.g., a thermal effect generated by passing hot air) at temperature ranging from 100 to 315 °C on skin surfaces result in the weakening of mechanical properties and disorder of keratin network of the skin (Park et al., 2008). Adaptation of dry heat ablation of skin at high temperatures occurred during micro second time frames as longer durations would have denatured more skin proteins below the upper layers (Park et al., 2008). Also, prolonged dry heat ablation would burn skin into powdered carbon ash and

lidocaine will be undetectable by LC-DA methods as the chemical structure would be changed completely.

Keeping the above discussed points in mind, lidocaine permeation rates have been analysed in the vertical and horizontal directions in this chapter specifically for lidocaine NaCMC/gelatine bipolymeric formulation. Alternatively, to Zhang et al. (2012a), enzymatic denaturation technique, homogenisation followed by heat denaturation of the in vitro skin biopsy was performed to determine the horizontal permeation profile in the MN pierced skin from the epicentre location. FDC was used to determine the vertical permeation profiles into clearance. For the purpose of this work, a poke and patch technique was adopted using fixed MN insertion forces (Cheung et al, 2014; Olatunji et al., 2014; Milewski et al., 2013) with the purpose to obtain reproducible artificial micro-cavities and to enhance the percutaneous lidocaine delivery in bypassing the SC layer of skin. Constant MN insertion forces from a pneumatic pressure based force device are applied and held for fixed time duration to allow the MNs to pierce the skin as uniformly as possible (Cheung et al., 2014). This also ensures that the MN cavities are formed so as to just pierce past the SC providing small MN holes for percutaneous drug delivery.

In the context of this chapter, we aim to relate the effects of MN insertion forces with the instantaneous pharmacokinetic distribution of lidocaine towards vertical (depth averaged) and horizontal permeation in skin. Ideally, the lag time for therapeutic level of lidocaine permeation needs to be the shortest possible for affecting the skin target region. Nevertheless, a sustained therapeutic level for up to 45 min is considered to be most ideal in numbing the area, for example, in the treatment of skin wounds or localised biopsy of abnormal skin tissue. Procedures such as ablative skin resurfacing requiring at least 60 min for uniform anaesthetic effect can potentially be shortened to 45 min duration maximum for regaining

complete local sensation in the area and reducing patient waiting time (Sobanko et al., 2012). Within this work, a method of measuring the vertical diffusion coefficient through porcine skin is also attempted. This required first the use of a FDC followed by centroid and diametric from centroid punching of the square sectioned skin which were subsequently homogenised mechanically and heat denatured. It is expected that this chapter would allow better understanding of vertical and horizontal permeation of lidocaine in MN pierced skin.

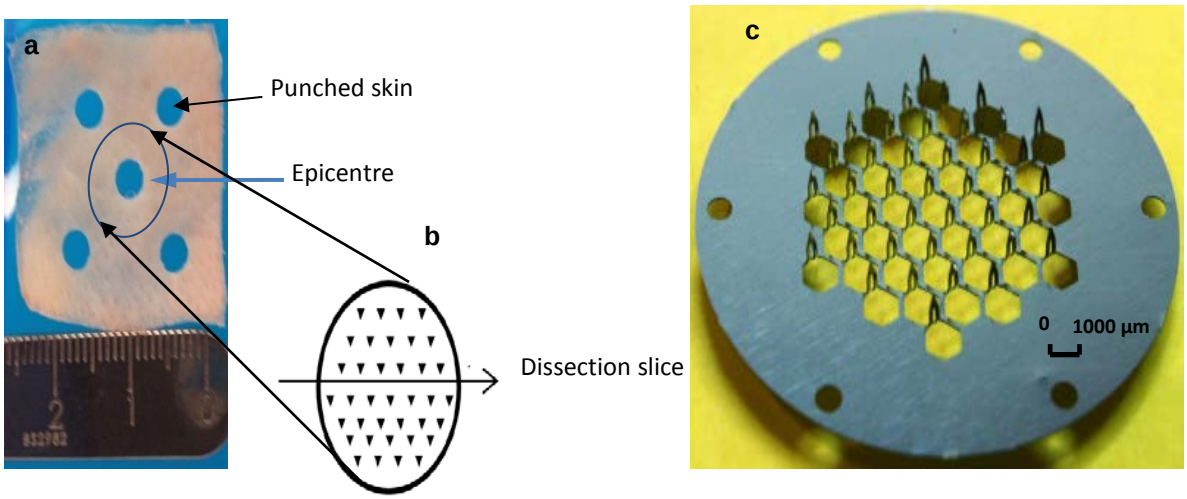

Figure 5.1: Schematic diagram a) the epicentre punch where the blue circle shows the area/size of the chosen microneedle patch b) the orientation of microneedle imprints in obtaining a slice in quantifying micro-cavity pathlengths. c) pre-fabricated microneedles adopted (AdminPatch®, Sunnyvale, USA) for 'poke and patch' drug delivery in this work.

5.2 Material and methods

5.2.1 Materials

The reagents used in the preparation of lidocaine NaCMC/gelatine hydrogels were the exact specification as outlined in section 3.2.1. The column and reagents used in HPLC analysis were also taken from section 3.2.1 and 3.2.11. However the buffering reagent for HPLC was replaced with trifluoroacetic acid (>99 % assay)

purchased from Sigma-Aldrich Ltd, Dorset, UK. The purpose for using trifluoroacetic acid was to further reduce peak broading of lidocaine which is detected in acidic conditions. Skin was acquired as mentioned in section 3.2.5. Essential materials for stainless steel MNs (AdminPatch®1200, nanoBioSciences PLC, California, USA) and FDCs (Logan Instruments Inc., 'FDC-6', New Jersey, USA) were already available.

5.2.2 Preparation of lidocaine NaCMC/gelatine microgels

The optimum lidocaine NaCMC/gelatine 1:2.3 microgels were prepared exactly as outlined from the methods stated in Nayak et al. (2014a) devoid of the rotary evaporation method. The principle of rotary evaporation is removal of excess water and organic solvent mixture containing paraffin oil and n-hexane. The reason for choosing NaCMC/gelatine 1:2.3 as the optimum vehicle was due to the ideal physico-chemical properties outlined in Chapter 3.

5.2.3 Percentage encapsulation efficiency

The characterised percentage EE for our lidocaine microgel formulation (equation 3.3) was calculated as discussed earlier (Nayak et al., 2014a; Nayak et al., 2014b).

A 5 % of the mean total sample weight was used to save time in preparation of new batches of formulation for one set of tests. Lidocaine microgels formulated on a batch scale was a time consuming process and complete samples were not tested here. The lidocaine hydrogels were diluted with 20 ml of ultrapure water as excess solvent heated to 40 ± 0.5 °C and sonicated (Branson Digital Sonifier 450, USA) at 15–20W for 2 min. This allows lidocaine to dissolve in ultrapure water. Normal sonication frequencies cut approximately 24 h maximum time required to disrupt the electrostatic and covalently held microparticle interactions between NaCMC and gelatine by high temperature denaturation without boiling the drug (Banerjee et al.,

2012). Also the time for sonication here was a fifth less than the one performed in section 3.2.7. This was because a probe device directed ultrasonic waves directly into the medium than a bath arrangement with a constant power of 35 W (Fisher Scientific, Loughborough, UK). The 'dissolved lidocaine' was filtered using Nylon 6,6 membranes of 0.1 µm pore size (Posidyne membranes, Pall Corporation, Portsmouth, UK) before quantification by HPLC analysis.

5.2.4 Microgel morphology and microparticle diameters

The morphology of lidocaine NaCMC/gelatine 1:2.3 microgels was characterised as described in section 3.2.10 and analysed via ImageJ software as described in section 4.2.5.

5.2.5 *In vitro* permeation studies

The amounts of lidocaine in the VE layer and systemic layer (receptor of FDC) were determined from in vitro studies. The pharmacokinetics was subsequently deduced from in vitro quantification for vertical and horizontal permeation of lidocaine assuming homogeneity of the VE layer for molecular diffusion, i.e. isotropic diffusion profiles (Naegel, 2013).

5.2.6 Skin preparation

As recommended in Meyer et al, (2007), whole porcine auricle squares of 4.0 cm^2 were laterally thin sliced and the cartilage, connective tissue and fatty components were discarded. All visible hair was removed using scissors to minimise any obstruction with the placement of lidocaine microgel on skin. MNs (AdminPatch® 1200) were applied on the skin for up to 5 min. Each needle was preset to 1100 µm length with a MN density of 43 in 1 cm^2 surface area. MNs fabricated at 1000 µm length have the same pain scores from a visual analogue scale on human subjects in comparison to the borosilicate glass material extruded at 500 µm length when a

saline volume of up to 0.6 ml was delivered in the dermis layer of skin (Gupta et al., 2011b). Normally, the entire length of MNs from base to tip does not penetrate the skin with the needle base touching the skin surface because of the elastic folding effect of skin (Allen et al., 2002). A full thickness skin piercing using 1100 μm length MNs and the MNs density resulted in approximately 400 μm deep cavities (Nayak et al., 2014b). However, we controlled the MN cavities to a much smaller length so as to just pierce the SC in this work as discussed below.

5.2.7 Application of MN insertion force

In order to ensure that uniform force is applied to pierce the skin, the MN patch was applied on the skin samples at 0.5, 1.0 and 2 bar pressures equating to forces of 3.9, 7.9 and 15.7 N, respectively. The minimum insertion force achievable using an in-house pressure/force device (Cheung et al., 2014) was 3.9 N. The three insertion forces adopted here were constant forces as a hypothetical standard if an applicator device were to be fabricated to insert the MNs into skin. Thumb pressure, as often done to insert MN on skin, was not applied as they may introduce some variability in the forces applied. Furthermore, the forces were chosen so as to just pierce the skin keeping in mind the percutaneous delivery of lidocaine where the MNs cavities are small rather than large which facilitate TD permeation of the drug. The insertion forces were applied via a vertically arranged pressure/force impact device (SMC Pneumatics Ltd., Buckinghamshire, UK; serial: CD85N16-50-B) as adopted from Cheung et al, (2014). The insertion force was calculated using equation 5.1:

$$F = \frac{p\pi d^2}{4} \tag{5.1}$$

Where *F* is the force (N), *p* is the pressure (N/mm^2), and *d* is the piston bore diameter (mm). As the piston rod is lowered far down the cylinder compartment so that the punch unit touches the MN substrate, the outstroke impact of a double-

acting cylinder is the dominating force in a double acting pressure device (Padmanabhan et al., 2014). Independent air pressures at 0.5-2 bar ranges were impacting on the bore area of the lowered piston rod. The bore area was contained inside a closed piston chamber so that compressed air could not escape the piston chamber and impact the tissue directly. Therefore, equation 5.1 is implemented in determining the vertical compression force.

5.2.8 Colour dye of skin samples

Skin samples were dyed to show qualitative MN piercing patterns through skin in plan (top) view as a quick method to determine if MNs have pierced the skin. As in in vitro studies, the device outlined by Cheung et al. (2014) was used to treat skin samples at 3.9, 7.9 and 15.7 N for up to 5 ± 0.1 min. Samples were observed after dyeing with a natural blue food colouring (Sainsbury's, Loughborough, Leicestershire, UK).

5.2.9 Characterisation of microcavities

Similar MN impact forces and time taken as mentioned in sections 5.2.7 and 5.2.8 were subjected on the skin samples. The largest cross sectioned row of channels was viewed by micro-dissecting strips in plane to MN path as shown in Figure 5.1b. An image of a MN patch (AdminPatch®) adopted for the poke and patch method throughout this study is shown in Figure 5.1c. As described in Section 4.2.9, the skin samples were cyroglued prepared, cryotomed (5 µm), dyed in methylene blue solution (0.5 % w/v) (Sigma-Aldrich, Dorset, UK), observed under the microscope (Ceti S035, Chalgrove, Oxfordshire, UK) and scaled using an image processing software (ImageJ, National Institute of Health (NIH), USA) with a certified graticule. Unlike in the previous method of using proprietary food colouring, the distinct blue colour density between SC and VE layer can only be observed by methylene blue dye. Methodology for this was adapted from Chueng et al, (2014). Additionally,

flash freezing was adopted to preserve pierced holes created as compared with slow 24 h freezing at −30 °C in a cryotome. As stated above, the SC layer is accepted to be the topmost (first) ~15 µm thick skin layer in accordance with literature e.g., Sivamani et al, (2005). It was also confirmed by dissecting 5 µm transverse slices of skin and studying under the microscope after dying the skin surface with methylene blue solution (0.5% w/v) (Sigma-Aldrich Ltd., Dorset, UK). The recommended concentration of methylene blue solution and the approximate time in allowing dye diffusion through skin was adopted from Singh and Banga, (2013) and Kalluri and Banga, (2011).

5.2.10 Permeation study

Lidocaine permeation studies were performed using MN treated skin, which were compared with PD profiles of the drug. The FDC setup was similar to section 3.2.5. The lidocaine loaded in the microgel was 2.44% w/w. The FDC receptor orifice was measured 0.679 cm^2. Lidocaine formulations were dispensed on the epicentre of the skin (Figure 5.1a) (Nayak et al., 2014a; Nayak et al., 2014b). The total receptor volume was 5.0 ± 0.025 ml. Receptor volumes (1.5 ± 0.5 ml) were removed at 0.25 h intervals. The total duration of in vitro study was 1 h. After the FDC experiments, the epicentre and diametrically opposite regions of the skin was biopsied (Figure 5.1a) (RS International, Nottinghamshire, UK). The epidermis of punched skin was temporarily bonded using Cryo-M-bed inert glue (Bright Instrument Company Ltd., Cambridgeshire, UK) onto pre-chilled sample holders frozen in a cryotome (−30 °C) for 30 min (Bright Instrument Company Ltd., Cambridgeshire, UK). Horizontal SC layer micro dissection followed and first 15 µm thick layer was accepted as the SC layer (Swindle, 2008) with the remaining skin layer saved as VE for lidocaine quantification. The VE and dermis boundary was not possible to separate accurately as compared to the SC and VE boundary by cryotome dissection.

The depth resolved mass transfer of lidocaine through the skin involved treated skin samples separated into the VE and systemic layer as clearance. The SC layer was discarded because the amount of lidocaine was found to be inconclusive and, we are primarily interested in the permeation from the micro-cavities created by the MNs. There is a likelihood of parts per billion amounts of lidocaine that cannot be traced by LC-DA methods as adopted in this work.

The VE samples were homogenised in a pestle and mortar containing pipetted 1.5 ± 0.03 ml DI water (ThermoFisher Scientific, Loughborough, Leicestershire, UK) before being denatured in a water bath (Nickel-electro Ltd., Somerset, UK) at 60 °C for 1.5 h. Conceptually, lidocaine HCl readily dissolved in the excess solvent water due to the thermolabile nature of proteins and onset of denaturation at 40 °C (Lepock et al., 1993). After centrifugation at 4443g (8500 rpm) (Eppendorf Minispin, Hamburg, Germany), the supernatant was filtered using polyethersulfone (PES) membranes (Pall Life Sciences, Portsmouth, UK) with a trapping MW of 1 kDa in preventing excess skin proteins and polypeptides contaminants accumulating with the released lidocaine. HPLC (PerkinElmer 1200, Abingdon, Oxfordshire) protocol was then implemented to analyse the lidocaine allowing deduction of permeation kinetics (Nayak et al., 2014b). This study was performed in triplicate. In addition to the in vitro studies under taken, several synergistic characterisations were performed as discussed in the subsequent sub-sections.

The appearance of lidocaine in “other”, biopsied skin region and clearance compartments is an overall mass transfer correlation expressed as a percentage. The correlation of lidocaine in the “other” compartment, VE layer (vertical), VE layer (lateral) and systemic clearance were calculated as the percentage lidocaine. The VE (lateral) was the sum total of lidocaine from all four diametric regions of skin. The percentage lidocaine was the total lidocaine detected just after a period of one

hour. The "other" compartment refers to the percentage lidocaine in drug vehicle and the remaining non-biospied skin which was discarded. Systemic clearance displayed the unit's μg/ml. All values reported in μg/ml were converted into μg/g of lidocaine from the maximum amount released under control after a period of 1 hour (g). The percentage lidocaine contained in each compartment is from the total amount of drug released from the lidocaine NaCMC/gelatine microgel.

5.2.11 Determination of lidocaine diffusion in skin

The exploration of lidocaine diffusional pharmacokinetics such as apparent diffusion coefficient and permeation flux are obtained from Fick's diffusion law as shown in equation 2.2. When MNs are inserted to pierce of skin, the concept is to increase the diffusion coefficient D_m effectively so that there is an increase in mass transfer through the SC into the VE layer. If this is achieved, MN poke and patch would decrease the dependence on hypodermic needles and improve on the current use of creams.

For an infinite donor solution, the concentration of active molecules in a drug vehicle is constant and can be adopted from equation 2.2.1 by replacing ΔC_{vs} with C_i in which is the concentration of active molecules in a drug vehicle is constant. The infinite donor method describes a practice of dispensing the drug on the donor area for increased reproducibility (Wagner et al., 2000). In this case, the source of the lidocaine is from NaCMC/gelatine microgels (Nayak et al., 2014a; Nayak et al., 2014b).

Graphically, the cumulative amount of active molecule or drug permeated is plotted against time and the linear region of the slope in a polynomial based function graph is the permeation rate of drug at steady state (Moser et al., 2001). Due to the insignificant number of nociceptive receptors in the SC layer, the VE and dermis (D)

are defined as the target layers where lidocaine is required for effective anaesthetic action. A minimum therapeutic lidocaine concentration of 1.5 μg/ml (Ghafari et al., 2012) is defined to be necessary in the VE and dermis layers for this to be the case. Separating the VE layer from the dermis is only possible through histological detection of the boundary between cell morphological changes. As mentioned earlier, the VE and dermis layer cell boundaries could not be detected uniformly and efficiently. The dermis layer skin thickness can vary from 200 to 350 μm (Liu and Bergstrom, 1996). However, there is no distinct, fast procedure for VE and dermis layer boundary identification, followed by micro dissection according to fundamental histological changes in strata.

5.3 Results and discussions

5.3.1 Effects of insertion forces on MN cavities in skin

As we mentioned earlier, we controlled the MN insertion forces directed on the skin surface to ensure reproducible and minimum variability of path lengths for the cavities. MN impact forces ranging from 3.9–15.7 N were used in this work. All forces were applied for 5 min durations and, in each case, the MNs pierced skin (Figure 5.2 and 5.3). In the figures, the dark blue spots were due to liquid dye pooling and increased diffusing into the MN micro-cavity's viable strata. The skin images did not show all of the MNs that had punctured the skin at 90° to a horizontal plane, as in a small number of cases the regular array triangular based pattern could not be identified (Figure 5.3). This effect was caused by needles not entering into the skin vertically due to the elastic nature and inherent roughness of the skin. The SC layer emerged as a dark blue band along a transverse slice of skin as highlighted by a yellow line (Figure 5.3). Initial dissecting of skin at 15 μm thickness showed some blade skin stretching due to the applied shear forces resulting in some SC thicknesses greater than 30 μm. Thinner transverse slices at 5

μm minimised any substantial blade stretching. An average SC thickness of 18.6 μm was deduced. Although this is marginally larger than the 15 μm conventional depth taken in in vitro studies, it was decided that due to the likelihood of minor blade stretching of the skin during dissection, the 15 μm would be retained as the average thickness of the SC in this study as mentioned in several literature sources. Blade stretching effects on 5 μm sliced skin was fairly evident when compared with a 15 μm sliced skin that resulted in up to 33 μm SC layers. This means that the insertion forces should be designed so as to enable the MNs to pierce 15 μm on top of the skin.

After analysis of the skin samples (n=6) corresponding to each MN insertion force, the average cavity lengths corresponding to each MN insertion force are calculated which are shown in figure 5.4. As expected, increasing the force increases the path length. A direct proportionality relationship between the insertion force and cavity length (e.g., doubling the force resulting in a doubling of cavity length) was not observed.

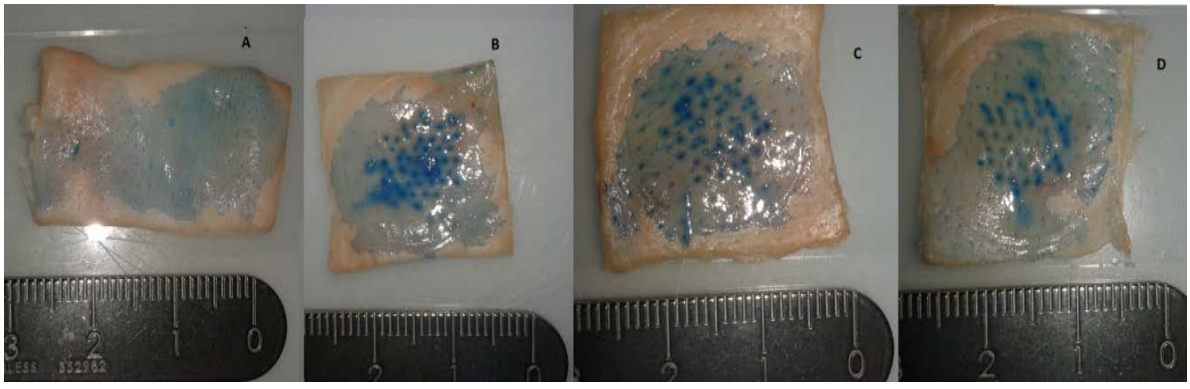

Figure 5.2: Typical surface images a) Non-treated skin sample. b) MN treated skin with insertion force of 3.9 N. c) MN treated skin with insertion force of 7.9 N. d) MN treated skin with insertion for of 15.7 N, all after a constant application time of 5 min. The dye

(blue colour) is from Spirulina used in the food colouring (Sainsbury's, Loughborough, Leicestershire, UK).

The cavity length increased 18.4 and 15.8 % from 3.9 to 7.9 and 7.9 to 15.7 N, respectively. This suggests that increasing force decreases potential cutting effect through the skin. This is likely caused by a resultant force skin compression effect from the excess perpendicular force on the skin. As the skin compresses, it may become more dense (e.g., higher viscoelasticity) and harder to penetrate deeper into the skin. In fact, the increasing force may cause more deformation of the skin. This may cause the entering needles to buckle and therefore, they may be unable to penetrate as deeply as expected into the skin. Other factors have been shown to affect the size of cavities that can be made by MNs such as the viscoelasticity of the microgels filling the cavities. This is discussed further by Cheung et al. (2014).

5.3.2 Optimum lidocaine NaCMC/gelatine 1:2.3 microgel

A favourable mass ratio microgel vehicle according to strong physico-chemical interactions between NaCMC and gelatine was chosen for this study. The optimum gelatine to NaCMC mass ratio of 2.3 for lidocaine derives from the previous studies on Zeta potential and particle sizes by Nayak et al. (2014a).

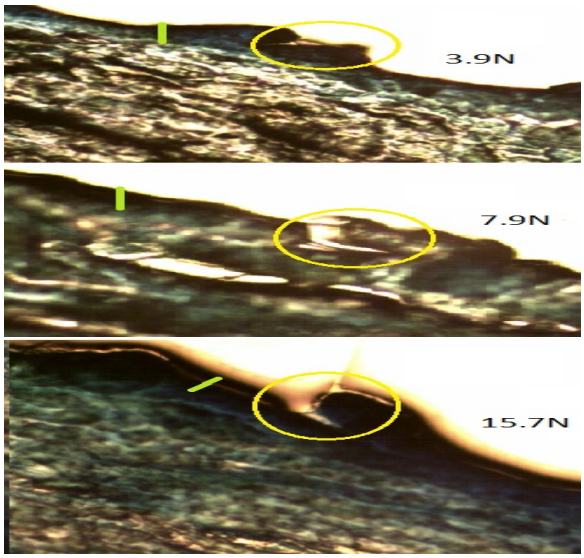

Figure 5.3: Typical microscope images of MN cavities (yellow circle) in micro-dissected skin for different MN insertion forces.

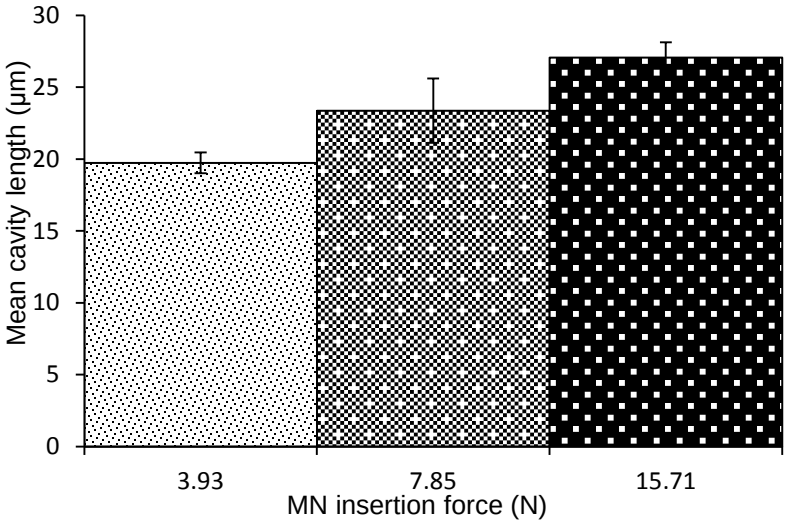

Figure 5.4: Average lengths of MN cavity in skin for different MN insertion forces (n=6 per force). The results show that the cavity lengths are slightly bigger than the top layer of the skin (SC). These are relevant for percutaneous delivery of lidocaine.

This section expresses comparisons with particle morphology and outlines the challenge in controlling the encapsulation efficiency of microgels. Lidocaine NaCMC/gelatine 1:2.3 microgels were observed to be spherically defined and polydisperse (Figure 5.5).

An average of 53 % encapsulation efficiency was deduced for lidocaine encapsulation. In comparison to Nayak et al. (2014a) this was slightly higher. The observed microparticles range was 1.7-8.0 µm (Figure 5.5) in this work had a smaller range than in Nayak et al. (2014a) which would contribute a greater encapsulation efficiency because of larger microparticle surface areas (Figure 5.5). The polydispersity of the applied formulation was less than in Nayak et al. (2014a) because the difference in microgel diameter was 15 µm compared with our current study of 6.3 µm microgel diameter.

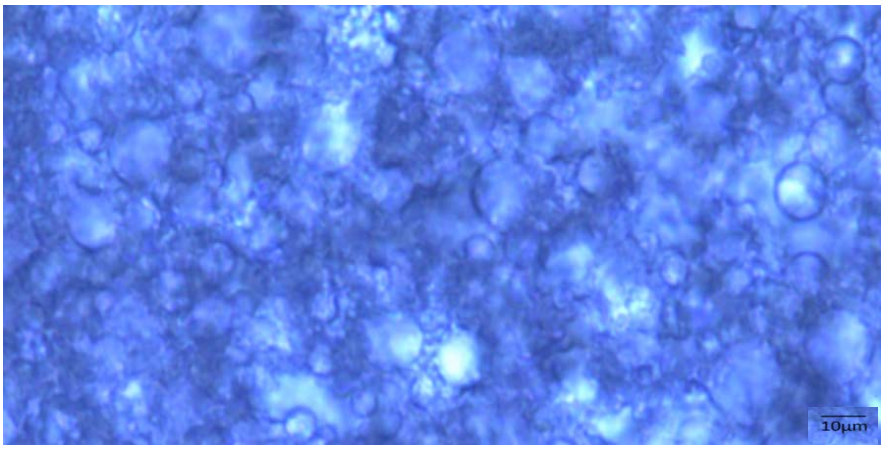

Figure 5.5: Lidocaine NaCMC/gelatine 1:2.3 microgels.

5.3.3 Vertical percutaneous lidocaine permeation

The trend on the effects of MN insertion force, cavity depths and permeation of lidocaine vertically (depth averaged) through the skin are discussed in this section. The VE layer is the main focus for lidocaine permeation because we consider this to be the target region in skin. It seems that a small force such as an MN impact force of 3.9 N was the most favourable for lidocaine permeation through the vertical VE layer. A 10.2 fold increase in permeation was observed for a 3.9 N force at 0.25 h and similarly a 5.4 fold increase in permeation occurred at 0.5 h compared with PD permeation (Figure 5.6a). The lidocaine permeated in the VE layer for 7.9 and 15.7 N MN treated skin was less than the 3.9 N treated skin. This result, at first, may appear to be a contradiction to increasing trends because the longer the cavity path length, the shorter time and greater concentration of drug in reaching the VE layer. However, we believe that the elasticity of the skin causes a cushioning effect for the MN arrays and higher MN insertion force does not necessarily allow the whole set of MNs in the array sequence to penetrate the skin at double or treble depths of proportional MN force (Figures 5.2 and 5.4). This could be worsened by a 'bed of nails effect' in which the MNs are close enough together to spread the force causing it to compress the skin rather than penetrating it. Once compressed, the diffusion coefficient (D_m) (equation 2.2) of the skin could be decreased, making it

more difficult for the molecule to diffuse through the skin despite the increased path length (Olatunji et al., 2012).

The error bars representing standard deviation outline good reproducibility, especially for the MN permeation results up to t=0.75 h (samples n=3) (Figure 5.6). Overall, for the MN chosen, the smallest force (i.e., the force of 3.9 N) showed a more favourable transient permeation profile because of substantial increases in lidocaine in the VE layer epicentre and a slight plateau effect emerging just after 0.5 h (Figure 5.6a). The largest MN insertion force, namely, 15.7 N, also shows a favourable transient profile with respect to a plateau appearing after 0.25 h but the amount of lidocaine permeated in the VE layer is 2.0 and 2.8 folds less than the amounts observed for 3.9 N at timings of 0.25 and 0.5 h, respectively (Figure 5.6a).

The main target skin layer for local anaesthesia is the VE layer as outlined in the introduction. Figure 5.7 outlines the instantaneous lidocaine permeation profile in blood plasma clearance, namely, the receptor cell of FDC (n=3). The Grubb's test (British Standards, 2002) identified outliers from pooled data sets and all outliers were eliminated. A coefficient of variance (*CoV*) identified other possible random errors (equation 5.2).

$$\mathrm{CoV} = \frac{SD}{\overline{x}} \tag{5.2}$$

Where SD is standard deviation and $\overline{x}$ is the arithmetic mean of data points. A threshold of up to 30% *CoV* was taken to justify disregarding any data that caused significant increases in SD. The lowest *CoV* values were taken in triplicate. In cases where results were seen to be anomalous, it was likely to be caused by errant skin proteins that partially denatured or passed through the pores of the ultrafine PES membranes during the released drug filtration stage (permeation study section). The concentration of lidocaine (μg/ml) detected in the epicentre VE layer was

converted to permeation-based concentrations (μg/cm^2) using equation 3.1, which were subsequently used to compute the diffusion coefficients according to equation 2.2.1. The denominator of equation 3.1 is 0.679 cm^2.

In the VE layer of skin, all three MN insertion forces (3.9-15.7 N) (Figure 5.6b) helped bypassing the minimum lidocaine therapeutic level of 1.5 μg/ml (Ghafari et al., 2012). This was achieved in a small fraction of 15 min despite the control samples appearing to reach that level slightly longer. On a dry skin surface, the likelihood of slow PD is a balance in stability between electrostatic interactions of polymers, lidocaine and covalent Schiff's base interaction by glutaraldehyde (Nayak et al., 2014a).

With improved formulation giving a greater concentration gradient, this may allow therapeutic levels to be reached in a relatively short period of time. The permeation of lidocaine into the clearance plasma compartment showed favourable trends for all three MN insertion forces and control within 0.75 h (Figure 5.7).

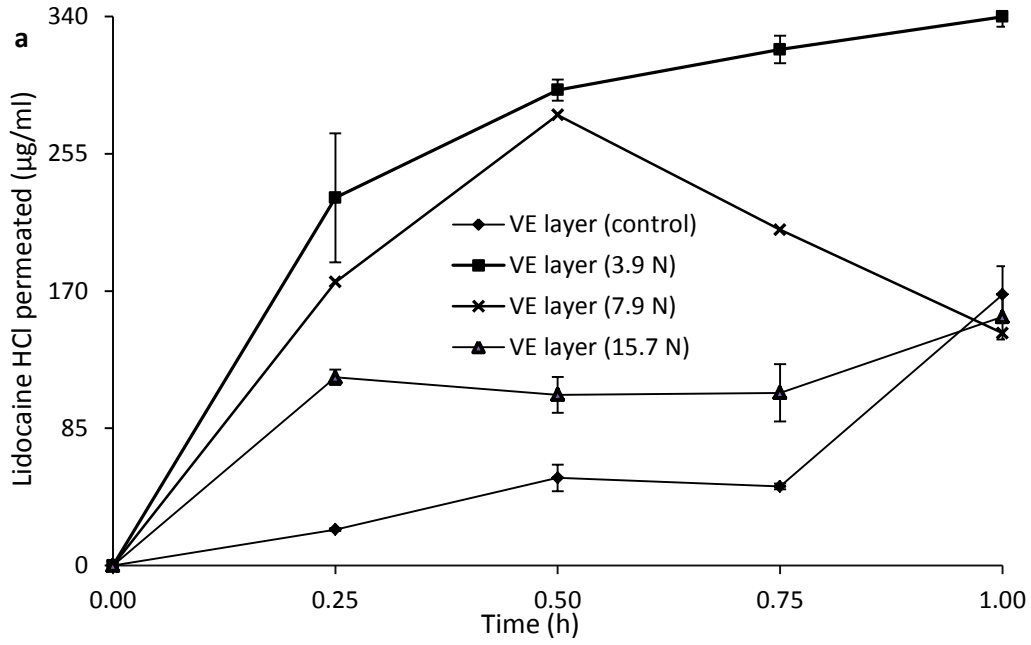

Figure 5.6: (Continued to next page).

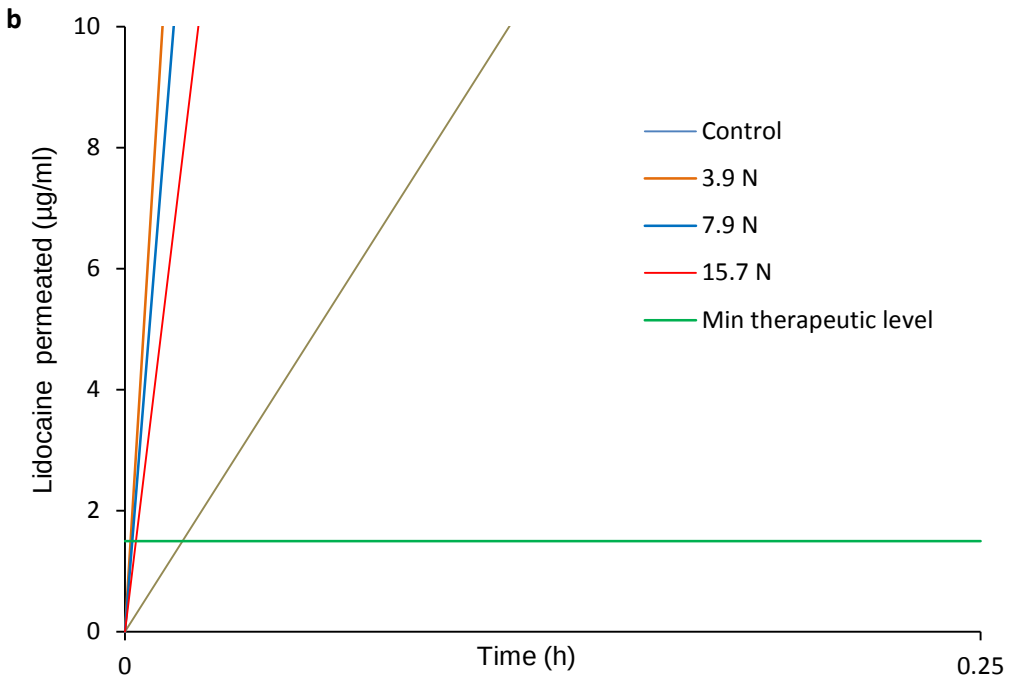

Figure 5.6: Lidocaine permeated into VE skin layer vertically. a) Control and microneedle pierced skin at given force induced depths. b) Control and microneedle pierced skin crossing the minimum therapeutic level for lidocaine before 0.25 h.

The smallest force of 3.9 N showed the lidocaine crossing over the toxic plasma level of lidocaine (5 µg/ml) at a time of nearly 1 h. Usually, a range of 5 to 10 µg/ml is considered to be a toxic concentration for lidocaine in blood plasma (Woodruff et al., 2010).

5.3.4 SC layer permeation

The SC layer has the potential to bind certain drug molecules despite not being a target region of lidocaine and other local anaesthetics. It is fairly important to outline if a significant amount of lidocaine has remained in this layer, and if not, it can then be defined that the applied lidocaine has permeated into the lower skin layers (Nayak et al., 2014b).

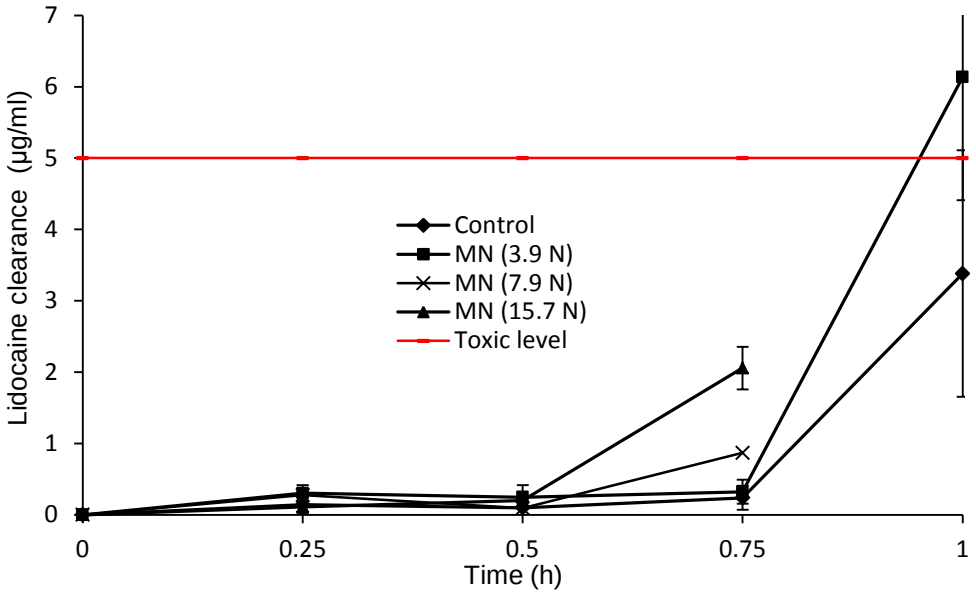

Figure 5.7: Lidocaine clearance in control, microneedle treated skin forces (3.9 to 15.7 N) and the toxic level for lidocaine in plasma clearance concentration.

In this work, the SC layer contained no lidocaine, irrespective of instantaneous MN treatment or PD. The results of numerous 'no result' and occasional very small (~60 x 10^{-5} µg/cm^2) lidocaine detected in the SC lead to CoV >30 % and also high standard deviations of the results. In any case, the SC layer concentration detected and amount permeated retained in the SC was taken as negligible. Although the SC layer is the major barrier to diffusion into the skin, it does not retain large quantities of hydrophilic molecules in the present context. The rate limiting step appears evident in PD of lidocaine into the VE layer as there is a 5.2 fold permeation decrease at 0.25 h as compared to MN 15.7 N treated skin. However, due to the lack of nociceptive receptors, anaesthesia will not be affected by this and minimum therapeutic levels as stated in the introduction are non-applicable. For this reason, the SC layer permeation will not be discussed further within this thesis.

5.3.5 Horizontal permeation of lidocaine in VE layer

The horizontal permeation for lidocaine was depicted as a square apex in the VE layer which is outlined and explained according to MN treated skin. The mass

transfer of lidocaine was expressed from knowing the mass released for lidocaine in excess DI water. The lidocaine concentration and mass transfer observed were deduced as favourable with respect to crossing the minimum therapeutic levels. The minimum therapeutic level of lidocaine is reported to be 100 μg/g by Zhang et al. (2012a). The aim is to understand the shortest possible lag time for horizontal permeation of lidocaine. The horizontal permeation colour charts of lidocaine permeating at a maximum distance of 1 cm from the epicentre were outlined as localised concentration (Figure 5.8) and mass transferred (Figure 5.9). Both figures outline completely different minimum therapeutic level trends for lidocaine observed in the VE layer. The mass of lidocaine (M) was computed according to equation 5.3.

$$\mathrm{M} = \frac{C_s V}{M_t} \tag{5.3}$$

The coefficients C_s and V are the same as in the numerator for equation 3.1. In the denominator, M_t is the calculated mass of lidocaine released from the NaCMC/gelatine 1:2.3 vehicle from known periodic timings from controlled release studies Nayak et al., (2014a). Full skin thicknesses were an average 670 μm (± 50 μm) thick.

When considering the concentration of lidocaine permeated in VE layer, all regimens including control showed horizontal permeation at minimum therapeutic levels (Figure 5.8). A more substantial concentration of horizontal permeation was observed for the smallest MN insertion force (3.9 N) from 0.25 to 1 h. This is because the same concentration range was observed for all four corners of the permeation square. The second most favourable horizontal permeation trend was observed for control as concentration equal to or greater than 10 μg/ml was sustained from 0.50 to 1 h. However, as expected the horizontal permeation in skin for 3.9 and 7.9 N forces showed greater drug concentrations in three to four corners of a square as compared with control (Figure 5.8). The mass transfer of lidocaine

horizontally is favourable for MN treated skin at 3.9 and 7.9 N because of high distributions of lidocaine from 0.25 to 0.75 h. Unlike the previous concentration-based colour profiles (Figure 5.8), the horizontal diffusion (control) and permeation of lidocaine (MN treated 15.7 N) showed below therapeutic mass transfers of lidocaine (Figure 5.9). Usually, lidocaine administered by injection potentially results in faster permeation dependent on injection depth which is variable, initial drug volume from average loading dose of solution and pressure related liquid flow rates into site of delivery (Zhang et al., 2012a; Gupta et al., 2011b). The injection of 0.6 ml or greater volume of a fluid such as saline requires applied pressures greater than 1000 mmHg (Gupta et al., 2011b).

The poke and patch method used in this study allows the pseudoplastic microgel drug to permeate into the microcavities by pooling and without the need of flow. In a similar lateral based study by Zhang et al, (2012a), the lidocaine mass transfer was maintained successfully for up to 15 min and two biopsied areas from a total of three showed therapeutic levels when considering a distance of 1 cm from the epicentre and full thickness skin up to 4000 µm.

5.3.6 The partitioning, flux rate and diffusion coefficient of VE layer for lidocaine permeation

The pharmacokinetics relating to the permeation of lidocaine affected by the MN treatment at the chosen forces is outlined and explained in this section. It is evident that lidocaine concentration for 3.9 N insertion force increases after 0.25 h as the VE layer concentration is increased. This is because the concentration gradient is the driving force for mass transfer into the clearance layer. In the last 0.25 h of the experiment, the lidocaine is permeating into systemic circulation at a greater concentration than in any previous time interval (Figure 5.7).

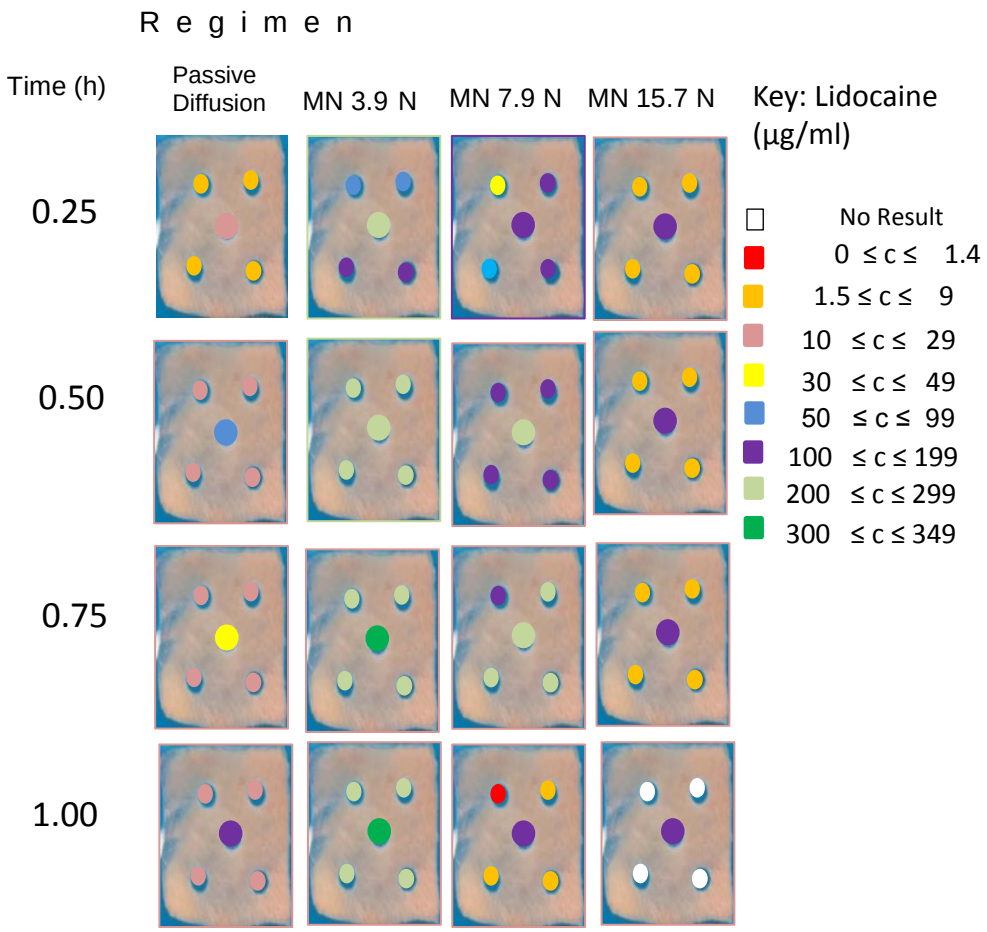

Figure 5.8: Colour codes to outline the local area and distance for drug permeation (horizontal) in the VE layer of skin according to concentration of lidocaine.

The concentration driving force permits lidocaine molecules to disperse across cellular structures inside skin both vertically (within epicentre) and laterally, also known as horizontally. The slow dispersion of lidocaine molecules within skin is ideal for observing low lidocaine contentrations within 0.5 h in systemic clearance, expecially with MN treated skin regimens (Figure 5.7).

The MN assisted permeation of lidocaine at the small (3.9 N) and medium (7.9 N) forces outline increasing partition coefficients (K), especially 3.9 N treated samples as more lidocaine is detected in the skin than the bipolymeric vehicle (Figure 5.10).

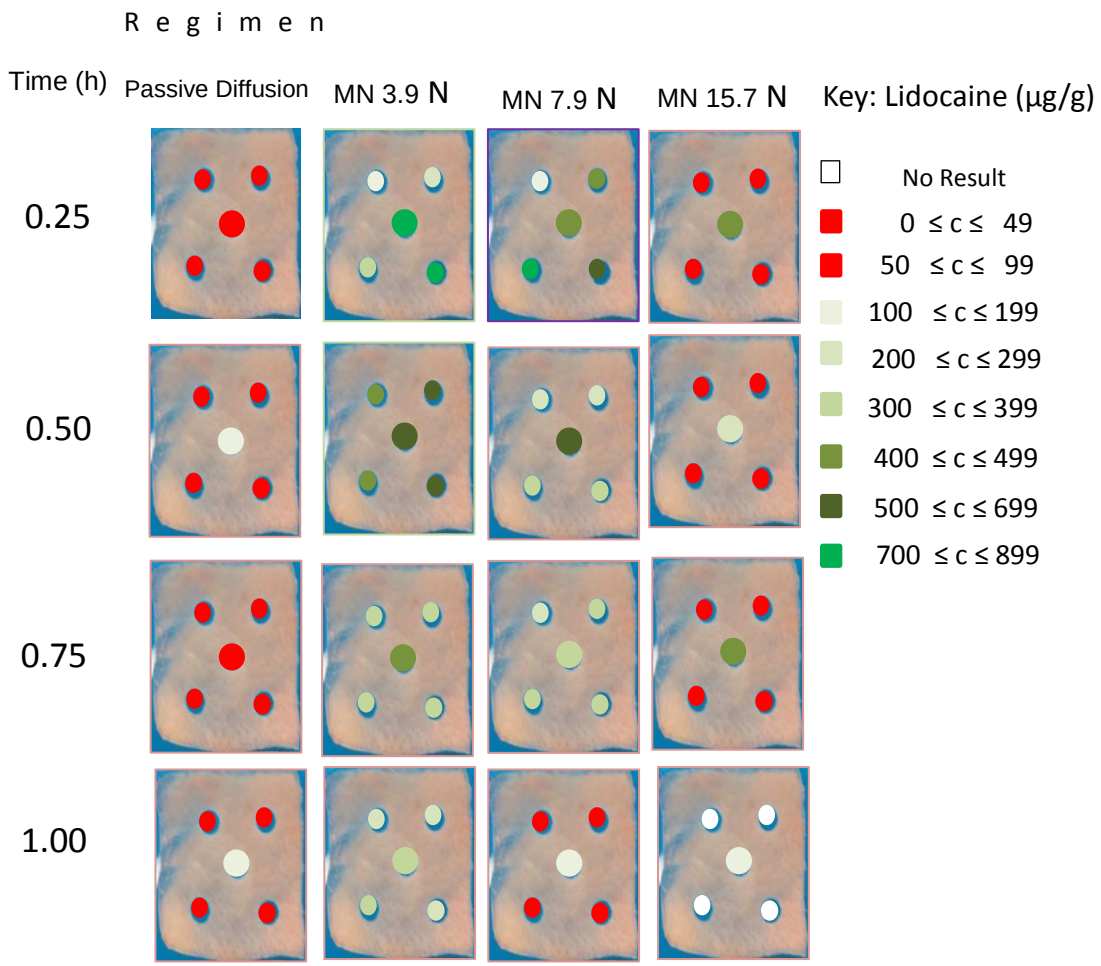

Figure 5.9: Coloured contrast circles to outline the local area and distance for drug permeation (horizontal) in the VE layer of skin according to the mass of lidocaine.

Nevertheless, all three MN pierced skin samples outlined K for lidocaine to be significantly greater than the control samples. Normally, K is deduced at observed steady state regions of charts at specific time duration in order to derive a constant K value as a point of reference. We define pseudo steady state at smaller time step, and K values were calculated for different time (Figure 5.10). At a time over 0.75 h the maximum partition, K of 0.58 was deduced for the 3.9 N treated samples as compared with other treatment technique (Figure 5.10). Drug based partition coefficients are normally fractions because the vehicle drug loaded mass is greater than the drug in a defined layer of skin.

The lidocaine permeation flux outlines a very consistent increasing trend for 3.9 N treated skin than control and 15.7 N treated VE layer of skin (Figure 5.11a). As expected, the flux was a lot higher for 3.9, 7.9 and 15.7 N MN treated VE skin than control (Figure 5.11a). Comparatively, the 3.9 N MN treated VE skin resulted in flux values of 13.9 and 10.5 folds greater than control at times of 0.25 and 0.50 h (Figure 5.11a). This is because of lidocaine bypassing the rate limiting SC layer of MN treated skin and diffusing through the VE layer faster. The permeation flux for all treatment regimens in the clearance layer of skin show lower lidocaine flux rates from 0.25 to 0.75 h (Figure 5.11b). The permeation flux for 7.9 N treated skin show significantly greater clearance levels than control, 3.9 and 15.7 N treated skin (Figure 5.11b). The likelihood is because of horizontal permeation as observed previously otherwise clearance flux rates would be just as high as VE layer flux when considering vertical permeation alone.

The apparent diffusion coefficient derived from rearranging Fick's first law in terms of coefficient D_m was taken from equation 2.2.1. Assuming pseudo steady state conditions, the 3.9 N treated VE layer outlines high lidocaine apparent D_m with good consistency as compared with control and 15.7 N (Figure 5.12). A relatively high lidocaine apparent D_m of 0.02 cm^2/h was observed for 15.7 VE treated skin at t=0.75 h which corresponds to the highest flux of lidocaine permeated (Figure 5.11a and 5.12). Like K based profiles (Figure 5.10), D_m is deduced at observed steady state in deriving a constant D_m value for reference.

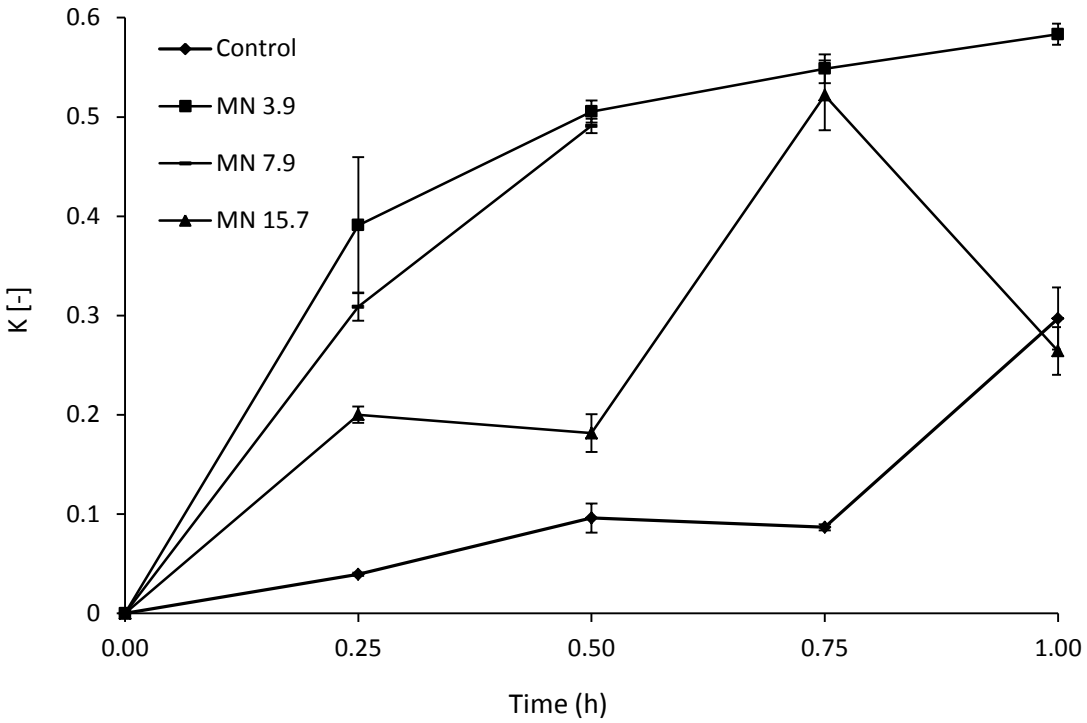

Figure 5.10 The partition coefficient (K) of lidocaine between vehicle and VE layer.

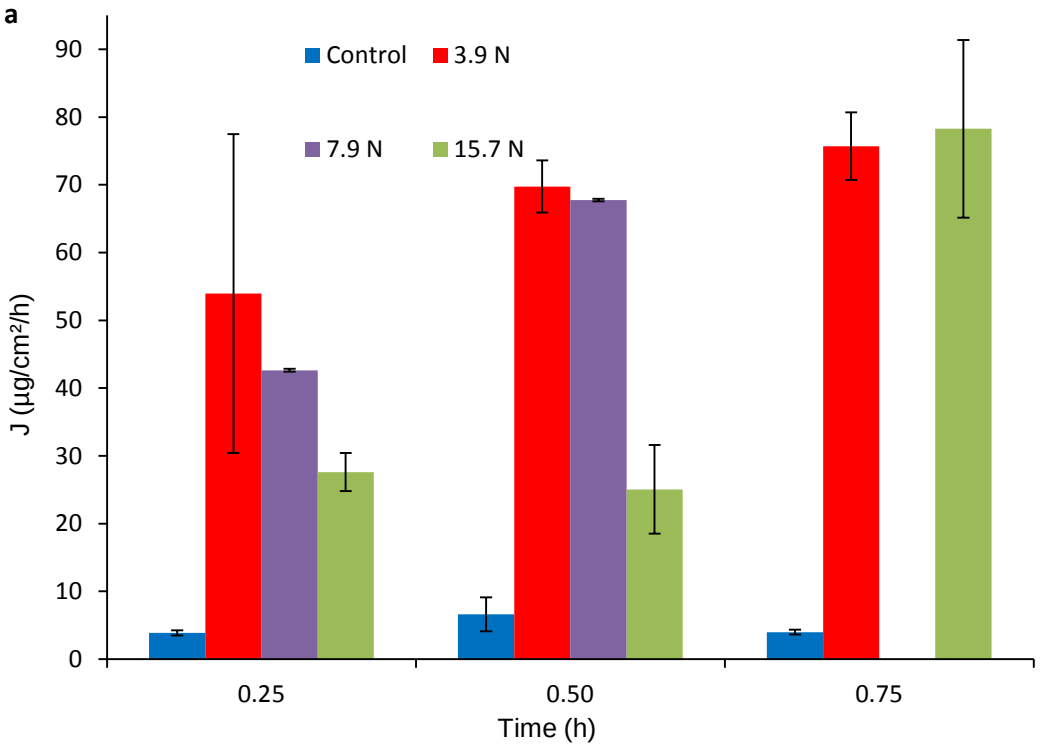

Figure 5.11: (Continued to next page).

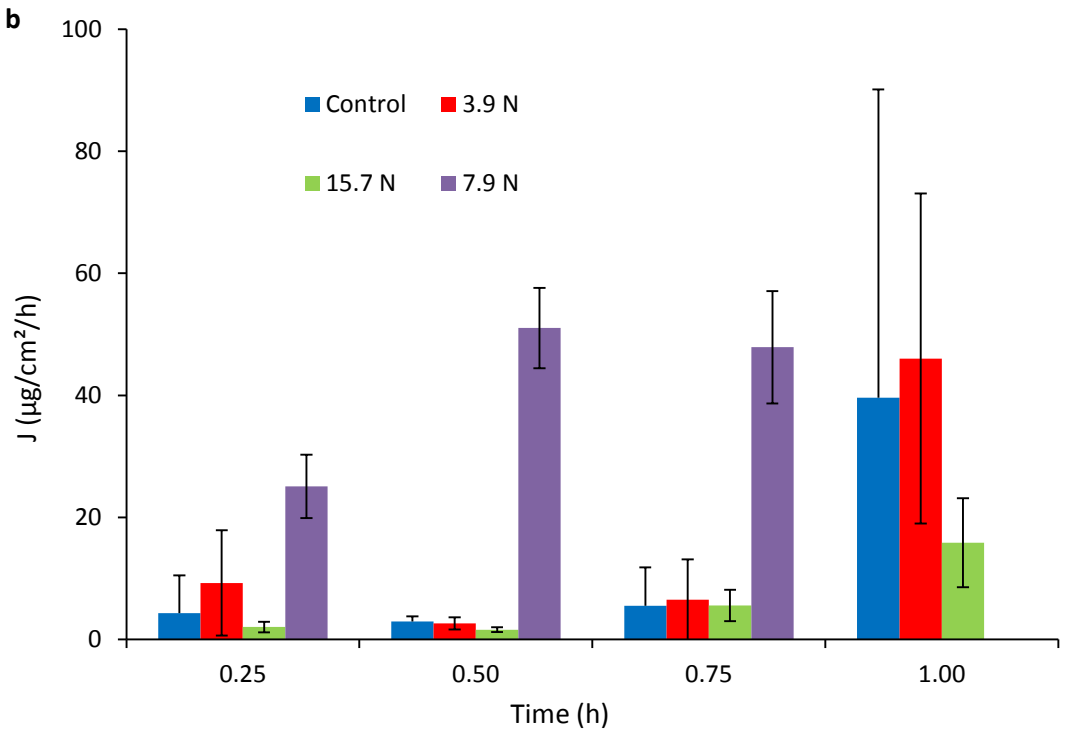

Figure 5.11: The permeation flux of lidocaine in a) VE skin layer b) clearance component (receptor cell in FDC).

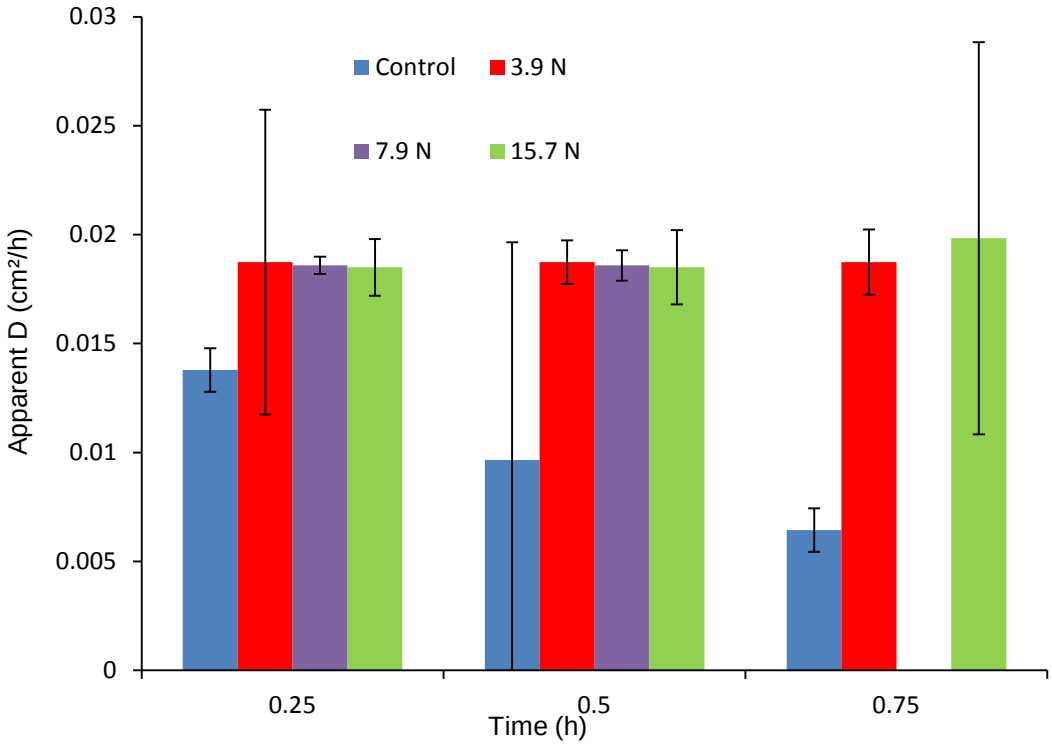

Figure 5.12: The apparent diffusion coefficients of lidocaine (vertical permeation).

5.3.7 The percentage correlation of Lidocaine in specific compartments

A total compartmental based correlation as a percentage of lidocaine from NaCMC:gelatine 1:2.3 microgel was performed. This provides an overall idea of lidocaine residing in specific compartments or regions of the skin. Lidocaine slowly diffuses or permeates through the skin from a microgel vehicle to the systemic layer down a concentration gradient. Most Lidocaine molecules are trapped inside the skin as a substantial amount was detected in both the lateral and vertical region of biosiped skin (Figure 5.13). The error bars in Figure 5.13 represent mean SD. Relatively small percentages of lidocaine are detected in the clearance compartment as higher amounts of lidocaine are traaped inside skin within 1 hour (Figure 5.13). Lidocaine in MN 3.9 and 7.9 treated skin outlines higher content percentages in both vertical and horizontal layers (Figgure 5.13). This is more because of easier access for lidocaine filling the artificial micropores caused by MNs. Also lateral layer permeation shows higher lidocaine percentages regarding MN 3.9 and 7.9 N than vertical layer permeation (Figure 5.13).

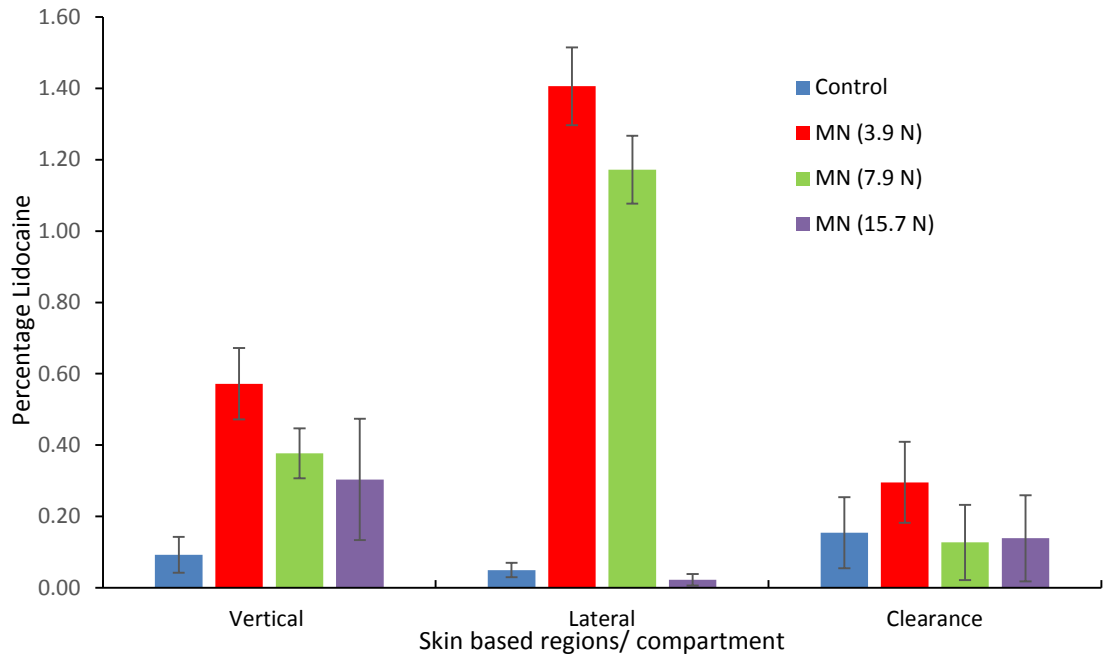

Figure 5.13: The percentage lidocaine contained in the vertical, lateral VE layer of skin and systemic circulation according to poke and coat and control treatment with lidocaine microgel.

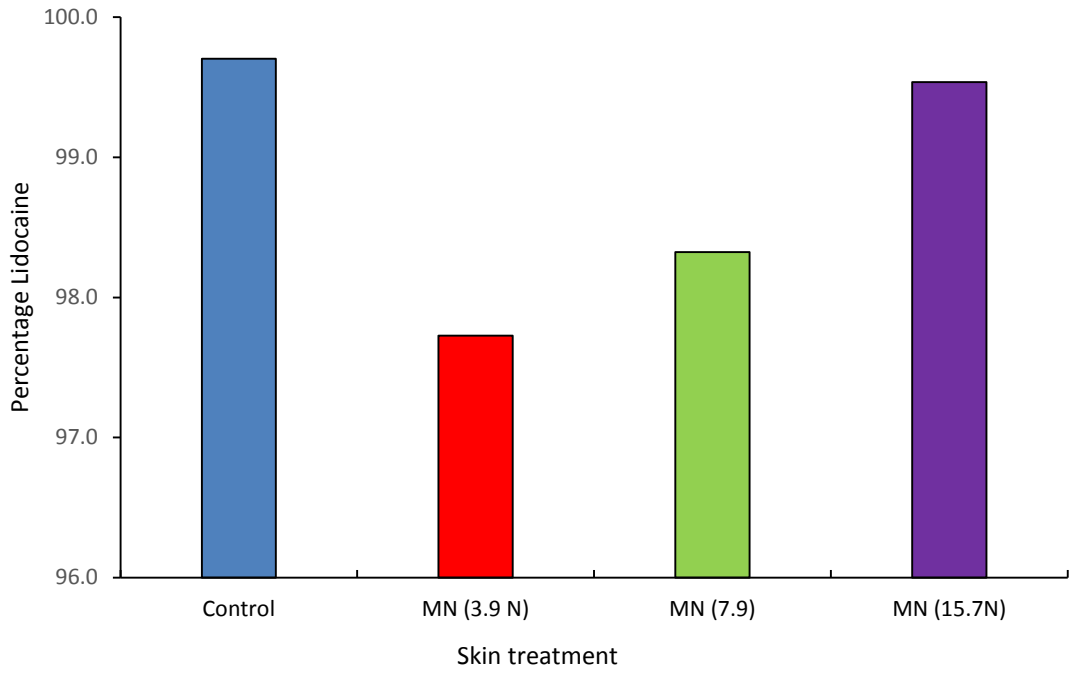

Figure 5.14: The percentage lidocaine contained NaCMC:gelatine 1:2.3 microgel vehicle and other regions of skin according to poke and coat and control treatment.

The percentage of lidocaine detected in skin even via the MN 3.9 N skin treatment, appears very small in a much broader concept. In terms of prilimary inspection, it appears that high percentages of lidocaine in “other” compartments infer high non-bioavailability and wastage of drug. This prilimary inference can be grossly misleading because a very high lidocaine percentage, especially in the clearance compartment is likely to pertain towards drug toxicity. These “other” compartments were described ealier in section 5.2.10. The control shows the highest percentage of lidocaine, 99.7 %, in “other” compartments as compared with all microneedle treated skin regimens adopted (Figure 5.14). The lowest percentage lidocaine in “other” compartments is from the 3.9 N, MN treated skin regimen at 97.7 % (Figure 5.14).

5.4 Chapter summary

The initial assumption of a 15 μm deep SC layer was confirmed as acceptable when examining the SC layer under microscope image gave an average of 18.6 μm. Therefore, the experimental value is in close agreement with the commonly

accepted average depth of 15 μm. Transverse skin slicing showed that even the lowest pressure of MNs impact penetrated the skin rather than simply deforming it. The initial premise that increasing the pressure, and therefore the force on MN treatment, was confirmed when cavity length studies showed approximately 18 and 16 % increases from 3.93 to 7.85 to 15.71 N.

In vitro studies of lidocaine diffusion gave slight mixed results as compared to PD; the samples treated with MNs at 3.9 N force had consistently larger concentrations of lidocaine in the VE layer. There was a steady increase in this concentration beyond 0.5 h, showing a significantly high mass transfer drug permeation at this time. Also, the increasing partition coefficient trend at increasing time for 3.9 NMN treated skin, VE layer, is very favourable for lidocaine bipolymer. In comparison to conventional creams, this is a great improvement and with an improved formulation or a MN array that does not suggest the bed of nails effect.

The horizontal permeation of lidocaine from adopted regimens of PD to MN-assisted 15.7 N treatment. All regimens show complete favourable trends at therapeutic level above 1.5 μg/ml solely for direct concentration results without further calculations with lidocaine controlled release adjustments in obtaining mass transfer profiles. The PD and a higher MN insertion force (15.7 N) are the most unfavourable regimens for horizontal permeation-based transfer of lidocaine in VE layer. This is because the mass transfer of lidocaine is below the minimum predicted therapeutic mass transfer for local anaesthesia in skin. The MN assisted 3.9 and 7.9 N delivery of lidocaine horizontally in VE layer are the most favourable regimens. This favourability was due to lidocaine permeating at 100 μg/g and higher from 0.25 till 0.75 h.

Chapter 6

Spreading of lidocaine NaCMC/gelatine 1:2.3 hydrogels on microneedle treated skin

Chapter overview

The spreadability of a liquid drug formulation on skin is an indication of it either remaining stationary or distributing (spreading) as a droplet. Factors determining droplet spreadability of the formulation are spreading area, diameter of the droplet base, viscosity of the liquid, contact angle, volume of droplet on skin and any others. The creation of microcavities from the application of microneedle (MN) has the potential to control droplet spreading, and hence, target specific areas of skin for drug delivery. However, there is little work that demonstrates spreading of liquid drug formulation on MN treated skin. Below, spreading of a lidocaine hydrogel formulation and lidocaine solution (reference liquid) on porcine skin is investigated over MN treated skin. Controlled spreadability was achieved with the lidocaine hydrogel on MN treated skin as compared with lidocaine solution. It was observed that the droplet spreading parameters such as spreading radius, droplet height and dynamic contact angle were slightly lower for the lidocaine hydrogel than the lidocaine solution on skin. Also, the lidocaine hydrogel on MN treated skin resulted in slower dynamic reduction of droplet height, contact angle and reduced time taken in attaining static advancing droplets due to the MN microcavities.

6.1 Introduction

Percutaneous absorption/permeation of a drug molecule (e.g., lidocaine) through skin depends on the contact between the formulation and skin properties through which the drug molecules are absorbed into different skin layers. The possibility of the drop of a liquid drug formulation either remaining static or distributing

(spreading) horizontally on the skin surface relies on its spreadability. If the droplet is capable of spreading, then the contact line between the formulation and skin moves over the skin. The rate of movement of the contact line can be defined as the spreadability of the formulation.

Spreadability has significant importance in localised application and efficacy of topical drugs (Chow et al., 2007). However, the characteristic time scales for spreading of a drug formulation on skin (~seconds to minutes) is significantly smaller than the characteristic time scales for drug absorption/permeation into skin (~10s of minutes to hours). Therefore, most studies of percutaneous or transdermal drug delivery do not characterise spreading behaviour of the drug formulation over skin. Spreadability is primarily determined by the area/diameter of the formulation droplet on a substrate (e.g., skin below), viscosity of the formulation, contact angle, the volume of a droplet (permeant amount) (Jelvehgari and Montazam, 2011), and any others.

Over recent years a number of researchers have discussed the possibility of enhanced permeation of lidocaine (a common anaesthetic) via a ‘poke and patch’ approach with the help of solid MN arrays (Banks et al., 2011; Hamzah et al., 2012; Nayak et al., 2014a,b). This approach involves treating the skin with well-defined MNs to create micro-cavities in skin followed by the deposition of a droplet of lidocaine solution on the MN treated area. For example, Nayak et al. (2014a,b, 2015) demonstrated this approach using a lidocaine NaCMC/gelatine 1:2.3 hydrogel formulation and determined the permeation profiles of lidocaine in porcine skin. While the lidocaine droplets spread over the skin, the lidocaine molecules also permeate through the treated area (Nayak et al., 2014a,b; Nayak et al., 2015). The duration of lidocaine hydrogel droplet spreading is in seconds, which is much faster as compared with that for drug permeation which normally takes about an hour to

reach equilibrium lidocaine concentration in skin. It is known that MNs have been primarily developed to control the mass transfer distance and time as a drug molecule is absorbed in the skin. However, the creation of microcavities using MN to accelerate penetration in the skin (Figure 6.1) allows controlling of spreading of the drug formulation droplet on skin and, hence, targeting a specific skin area over which the drug absorption/permeation can take place. On the other hand, a liquid droplet on a normal skin (i.e. untreated skin) is likely to spread in a low controlled manner, with low reproducibility and more rapidly as compared with a MN treated skin. At the moment, there is little or no study that specifically analyses in detail such spreading dynamics of drug formulation on MN pierced skin and the role that the MN cavities play in determining the formulation spreading behaviour. This work aims to address this gap in this chapter.

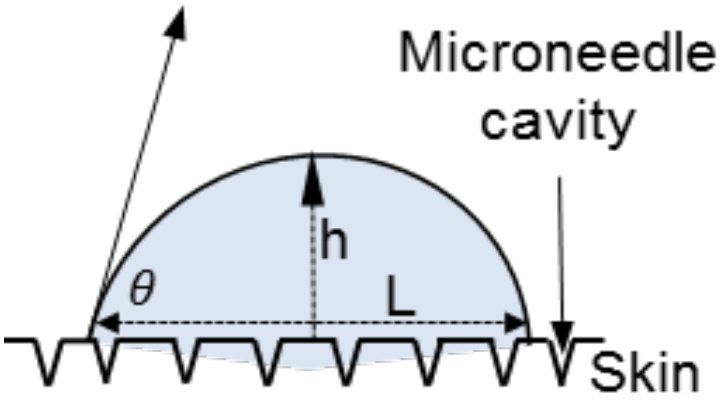

Figure: 6.1 A liquid droplet on microneedle treated matrix and percolation of liquid into microcavities. The arrows illustrate droplet spreading (horizontal), droplet height (vertical) and contact angle (slanting). The letter L represents the droplet spreading radius.

Below, lidocaine was loaded in a hydrogel biopolymer with a gelatine to NaCMC mass ratio of 2.3 as discussed earlier in Nayak et al. (2014a,b) and Nayak et al.

(2015). This mass ratio represents optimum drug and vehicle physico-chemical properties for a formulation (Nayak et al., 2014a,b). For the developed approach, controlling the spreadability of lidocaine hydrogel on skin is important to acquire liquid distribution of a liquid over the skin surface. A slower droplet spreading on skin coupled with a faster time in attaining static advancing contact angle is a favourable outcome in ensuring localised permeation of lidocaine at the treatment site.

Lidocaine NaCMC/gelatine 1:2.3 hydrogel is a non-Newtonian liquid at standard room temperatures and pressure (Nayak et al., 2014a). The Ostwald de Waele power law (equation 6.1) can be used to describe the pseudoplastic behaviour of for such a fluid as follows:

$$\eta = k(\gamma)^{\mathrm{n}-1} \tag{6.1}$$

Where η is the apparent viscosity, γ is the shear rate, k is the consistency constant of the substance and n is the power law or flow index. A log-log plot of viscosity (η) on shear rate (γ) for lidocaine NaCMC/gelatine 1:2.3 taken from Nayak et al. (2014a) provides an index value n = 0.392. As the index value is less than 1, the fluid is identified as pseudoplastic (Fang and Hanna, 1999). Its physical property can be exploited in quantifying and controlling the spreading of a lidocaine hydrogel droplet on an untreated flat skin surface without the need for manual rubbing across the whole area. For example, the pseudoplastic properties of the hydrogel is likely to provide a better control in droplet spreading as discussed earlier by Nayak et al. (2014b).

Below a comparison of spreadability between lidocaine NaCMC/gelatine 1:2.3 hydrogel (higher viscosity) and lidocaine solution (lower viscosity) is conducted in order to understand the spreading behaviour. The loading dosage of lidocaine in both the hydrogel and solution form containing water was 2.4% w/w. The objective

of the study is to examine the spreadability of lidocaine NaCMC/gelatine 1:2.3 hydrogel droplets on MN treated and untreated skin in relation to the viscosity of the formulation. Surface layers of skin treated with MN contain microcavities, which allow controlling the spreading of the lidocaine hydrogel and achieving static advancing contact angles and decreased spreading radius faster as compared with untreated skin. Three different MN types are applied to the skin samples in order to create controlled cavity depths past ~ 15μm thick stratum corneum (SC) layer of skin. Evaporation of the droplet is defined to be negligible due to the high boiling point of residual paraffin content in the lidocaine hydrogel, and relatively short duration of the spreading experiments. Our study specifically focuses on a drug formulation spreading on MN treated skin, which is the first attempt to investigate this process to the best of our knowledge.

6.2 Materials and methods

A lidocaine NaCMC/gelatine 1:2.3 hydrogel formulated by Nayak et al. (2014a) was adopted for characterising spreadability on porcine skin. The method of preparation of the hydrogel can be found in Nayak et al. (2014a,b) and Nayak et al. (2015). As stated earlier, the gelatine to NaCMC mass ratio of 2.3 was chosen for this study because of a faster permeation of lidocaine into the skin. The lidocaine NaCMC/gelatine 1:2.3 hydrogels were formulated using the vacuum oven method during final stage evaporation of excess paraffin dissolved in n-hexane as described in Nayak et al. (2014a,b). To prepare lidocaine solution, lidocaine HCl (> 98% assay) was added to deionised water (DI) and heated gently to ensure a dissolved solution at 2.4% w/w. However, no lidocaine permeability experiments were conducted in this chapter. This work is focussed on determining the spreading radii, droplet heights, dynamic contact angles and characteristic spreading times of lidocaine hydrogel and solution (i.e., lidocaine dissolved in DI water) on both porcine skin and an artificial skin membrane, namely, Strat-M.

6.2.1 Reagents and materials

Lidocaine HCl (Sigma Aldrich UK, Dorset, UK), lidocaine NaCMC:gelatine 1:2.3 hydrogels, autopipette 0-10 µl (Thermofisher Ltd, Warrington, UK), Camera i-speed LT high speed video (Olympus, Essex, UK), MNs (AdminPatch, California, U.S.A), porcine skin (local butcher, UK), piston enabled pressure/ force device (SMC pneumatics Ltd, Buckingham-shire, UK), synthetic transdermal membrane (Strat-M™, Merck Millipore, Hertfordshire, UK), temperature and humidity probe (Standard, Maplin Electronics, Leicestershire, UK) were used 126 in experiments below.

6.2.2 Preparation of skin for spreading experiments

The procedures for skin preparation were similar to the ones used for FDC experiments for determining drug permeation in skin, e.g., please see method stated in chapter 3. Briefly, these procedures involved the following steps: (i) either fresh porcine skin pieces originating from the porcine ears were washed in DI water and dried using a tissue, or frozen porcine skin pieces originating from the porcine ears were thawed at room temperature, washed in DI water and dried using a tissue; (ii) the cartilage, subcutaneous fat, blood vessels and connective tissue were removed from the underlying dermis sections of all skin samples; (iii) the skin samples were dissected further into 10 mm x 10 mm square pieces; (iv) the skin was placed on microscope slides with SC layer facing upwards for observation of the spreading dynamics.

6.2.3 MN treatment of skin

Stainless steel MNs of two lengths (1100µm and 600µm) were placed in the centre of a prepared porcine skin sample. A perpendicular piston barrel device (SMC pneumatics Ltd, serial: CD85N16-50-B) was used for transmission of controlled pressure induced force onto the chosen MN as described by Cheung et al. (2014).

Using the system, constant pressures of 0.5 bar, 1.0 bar and 2.0 bar equating to impact forces of 3.9 N, 7.9 N and 15.7 N were held for five minutes on the base of the MN (Nayak et al., 2015; Cheung et al., 2014). The forces (3.9 N, 7.9 N and 15.7 N) used to treat the skin with the MNs (Nayak et al., 2015). The MN patch was removed from the porcine skin prior to droplet spreading experiments.

6.2.4 Spreading of lidocaine NaCMC/gelatine 1:2.3 over skin surface

The experimental procedures for studying the spreading of lidocaine hydrogel droplet on porcine skin were adapted from Chao et al. (2014). A lidocaine hydrogel droplet (volume of 3.0 ± 0.5 µl) was deposited using a pipet onto a piece of skin resting on a microscope slide as carefully as possible to prevent splashing or fast inertial spreading. The i-speed LT high speed camera (Olympus, UK) recorded 1.85 frames per second until a stationary droplet profile or full disappearance was reached. The procedure was repeated twice for the control lidocaine solution. The real time capture of stages of the droplet spreading by camera configurations (i-speed, LT high speed) focused on the droplet is presented in Figure 6.2. This arrangement is based on liquid spreading and imbibition experiments for Newtonian liquids (Chao et al., 2014).

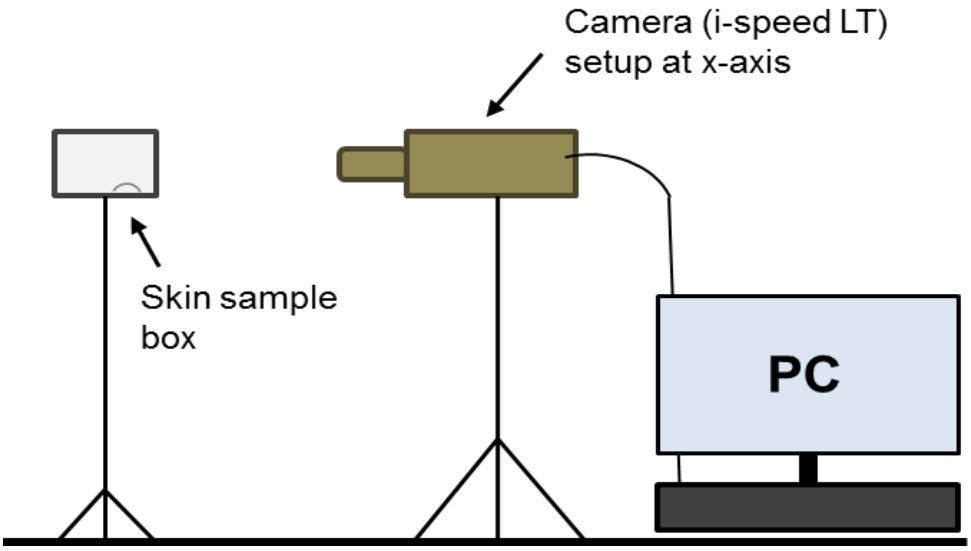

Figure: 6.2 A diagram of experimental setup for the capture of droplet spreading.

6.2.5 Spreading of lidocaine NaCMC/gelatine 1:2.3 hydrogels on the surface of artificial skin Strat-M membrane

Besides porcine skin, synthetic membrane which is sometimes used as a substitute for skin in transdermal in vitro studies were used as a substrate. These are composed of polyether-sulfone and polyolefin and are known by the trade name Strat-M (Merck Millipore Ltd, Hertfordshire, UK). Strat-M membranes were chosen as control matrices for spreadability studies because of a relatively uniform flat surface as compared with the less uniform and rough surfaces of natural skin samples. The characterisation of droplet spreading parameters, especially contact angles, was adopted from Chao et al. (2014). A square section of membrane substrate (15 mm x 15 mm) from a larger section was cut and taped to an edge of the glass side. This allows closer distance and improved resolution between the droplet and the camera lens. A hydrogel droplet of volume 3.0 ± 0.5 µl was immediately deposited on the membrane in the same way as in the case a natural skin. The recording procedure was identical to that described in the previous section. The droplet images of all formulations used were processed using Vision Builder software (National Instrument, UK) to determine droplet spreading parameters: contact angle, droplet height and spreading radius.

6.2.6 The measurement of relative humidity and temperature

The percentage relative humidity (% RH) and temperature of the droplet environment were recorded using an electronic probe (Standard, Maplin Electronics, Leicestershire, UK). The data were acquired in triplicate.

6.3 Results and discussion

Comparative trends for lidocaine droplet spreading on porcine skin samples and Strat-M membrane were deduced starting with lidocaine solution as a control sample. The results are discussed below.

6.3.1 Spreadability of lidocaine 2.4 % w/w solution (lidocaine dissolved in DI water)

The spreading of lidocaine 2.4% w/w solution droplets on normal skin (i.e., untreated porcine skin) were significantly more rapid and showed an almost linear dependence of spreading radius on time as compared with those for MN treated skin (Figure 6.3a). Likewise, the droplet heights of lidocaine solution droplets showed faster reduction and the droplet heights at static profiles was achieved after approximately 130 seconds (Figure 6.4a). The dynamic contact angle for the same case showed a faster reduction reaching the static advancing contact angle approximately of 11° after 130 seconds (Figure 6.5a). A sharp reduction in the contact angle was observed within the first 40 seconds for the lidocaine solution on the untreated skin. This suggests a slightly steeper reduction profile as compared with that for the lidocaine solution on 3.9 N MN treated skin for MNs of 600 and 1100µm lengths, respectively (Figure 6.5d). The microcavity depths for both 600µm and 1100µm long MNs are expected to be shallow for the force applied on the MNs (Nayak, et al., 2015) and, therefore, significantly less reduction in the contact angles was observed when compared with those for non-MN treated skin (Figure 6.5c).

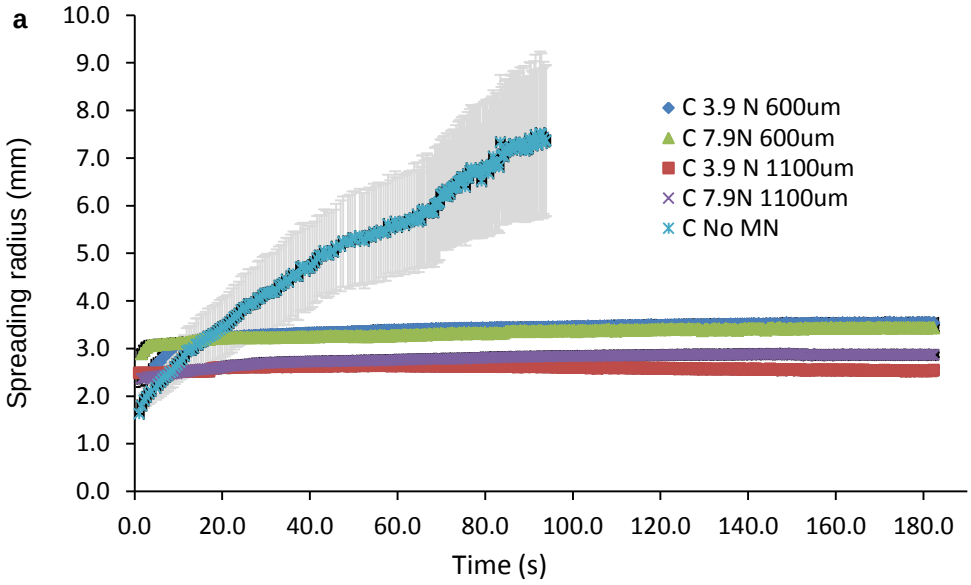

Figure 6.3: (Continued to next page).

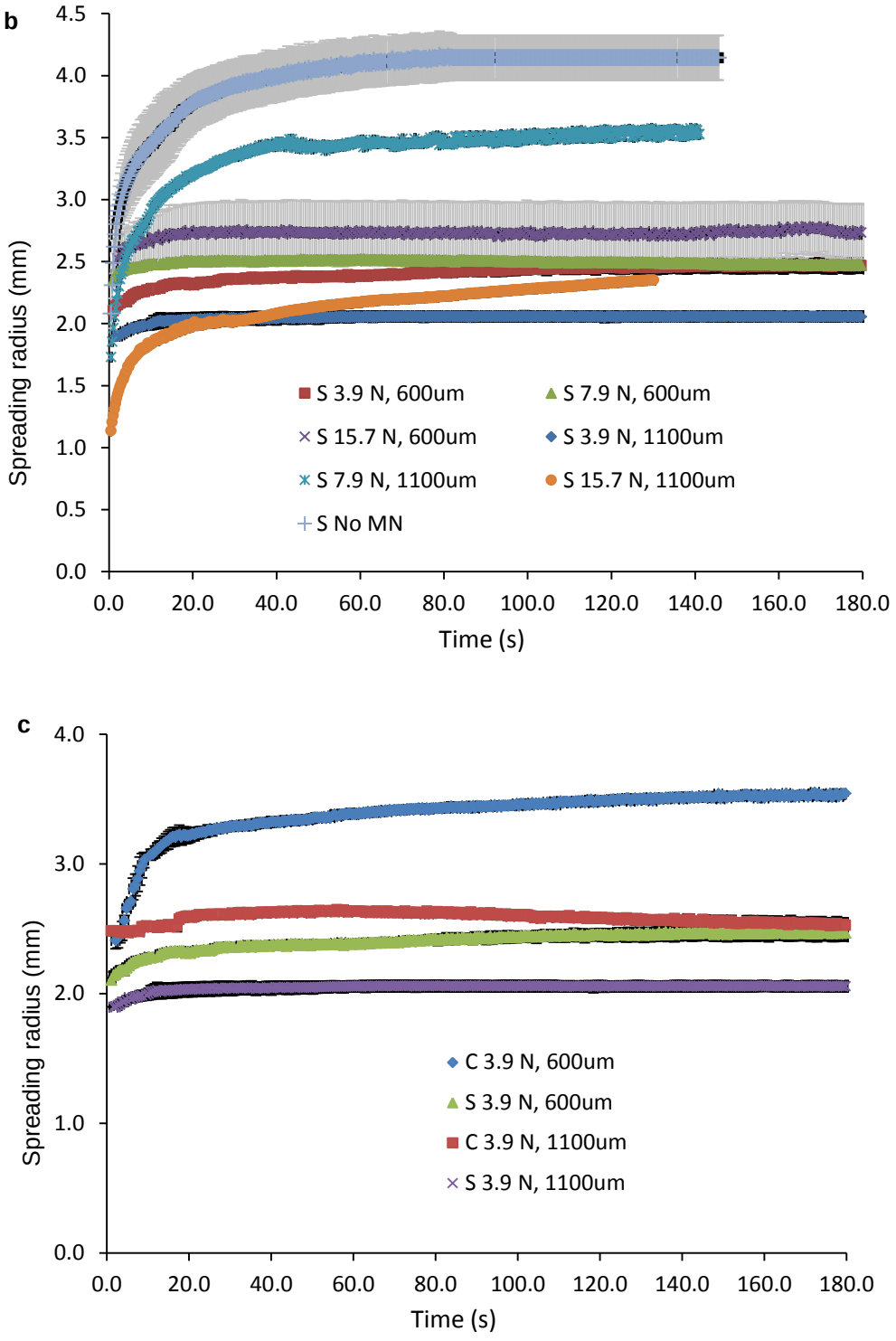

Figure 6.3 Time evolutions of droplet spreading radius for a) lidocaine solution on microneedle and non-microneedle treated skin b) lidocaine microgels on microneedle treated skin c) lidocaine solution and lidocaine microgels on microneedle treated skin. The abbreviation C is control lidocaine solution and S is sample lidocaine hydrogel.

Droplets of the lidocaine solution have an initial contact angle of 57.1° at the moment of deposition (t≅0) on the non-MN treated skin. The viscosity of lidocaine solution is very similar to DI water and both are Newtonian fluids. However, the initial contact angle was near 90° for DI water on non-MN treated skin as reported earlier by Elkhyat et al. (2004), which is significantly higher than observed for the lidocaine solution. The high contact angle of DI water was caused by the low sebum content on skin and there is a big variation in the initial contact angle depending on skin location (Elkhyat et al., 2004). Sebum is a natural mixture of lipids. Lidocaine solution on non-MN treated skin is devoid of artificial cavities and excess liquid cannot retain inside cavities and slow down droplet spreading.

The 1100 μm long MN induced microcavity depths for 3.9 N, 7.9 N and 15.7 N forces are reported to be 19.5 μm, 23.1 μm and 26.7 μm, respectively (Nayak et al., 2015). The mean microcavity depths using 600 μm long MN for the same forces are small but they are not easily detectable for transverse visualisation of skin microcavities as the forces applied are relatively small (implying smaller microcavity length). However, AdminPatchTM microneedles at 600μm length are shown to increase drug permeation. For example, drug permeability studies by Kaur et al. (2014) demonstrated a 14.3 fold increase in permeation flux as compared with PD for the transdermal delivery of an anti-hypertensive agent, thus implying that microcavities were formed in skin. These depths cross the typical SC layer depth of 15 μm (Nayak et al., 2015).

The dynamic contact angles of lidocaine solution on 7.9 N force treated MN skin outlines slow decreases in contact angles, which is especially more significant for the 1100 μm long MNs (Figure 6.5a). The spreading radius and droplet height of lidocaine solution are significantly less for 7.9 N force treated skin (Figures 6.3a and 6.4a). This is because of deeper MN cavities capturing excess liquid during droplet

spreading of lidocaine solution. Nevertheless, it was not possible to determine using conventional cryotome techniques if a large quantity of MN in a patch created a uniform depth microcavity for both specific MN lengths. MNs were impacted on skin for 5 minutes maximum using one specific force, so an assumption that most MNs have successfully pierced skin at significant microcavity depths will be made here.

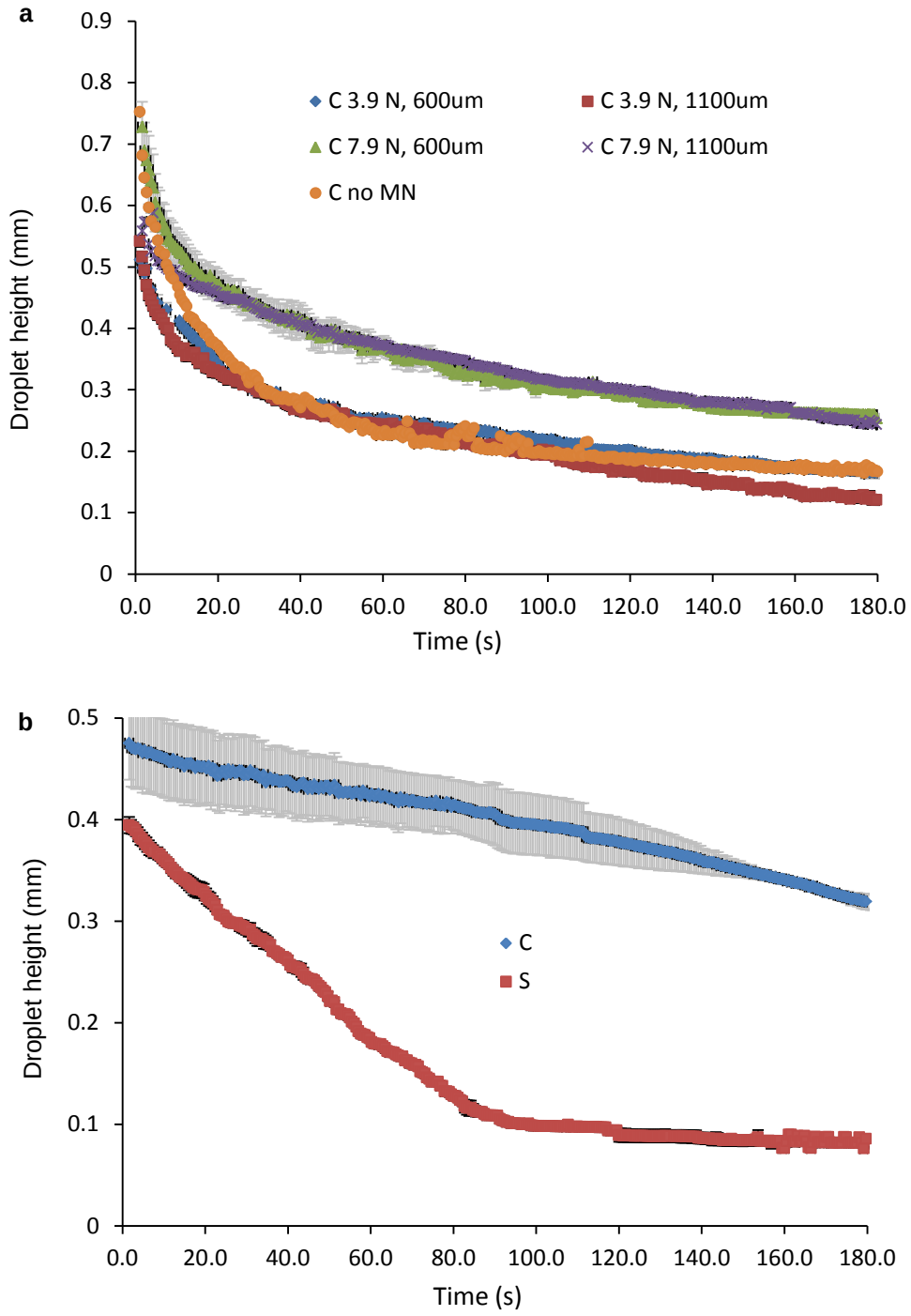

Figure 6.4: (Continued to next page).

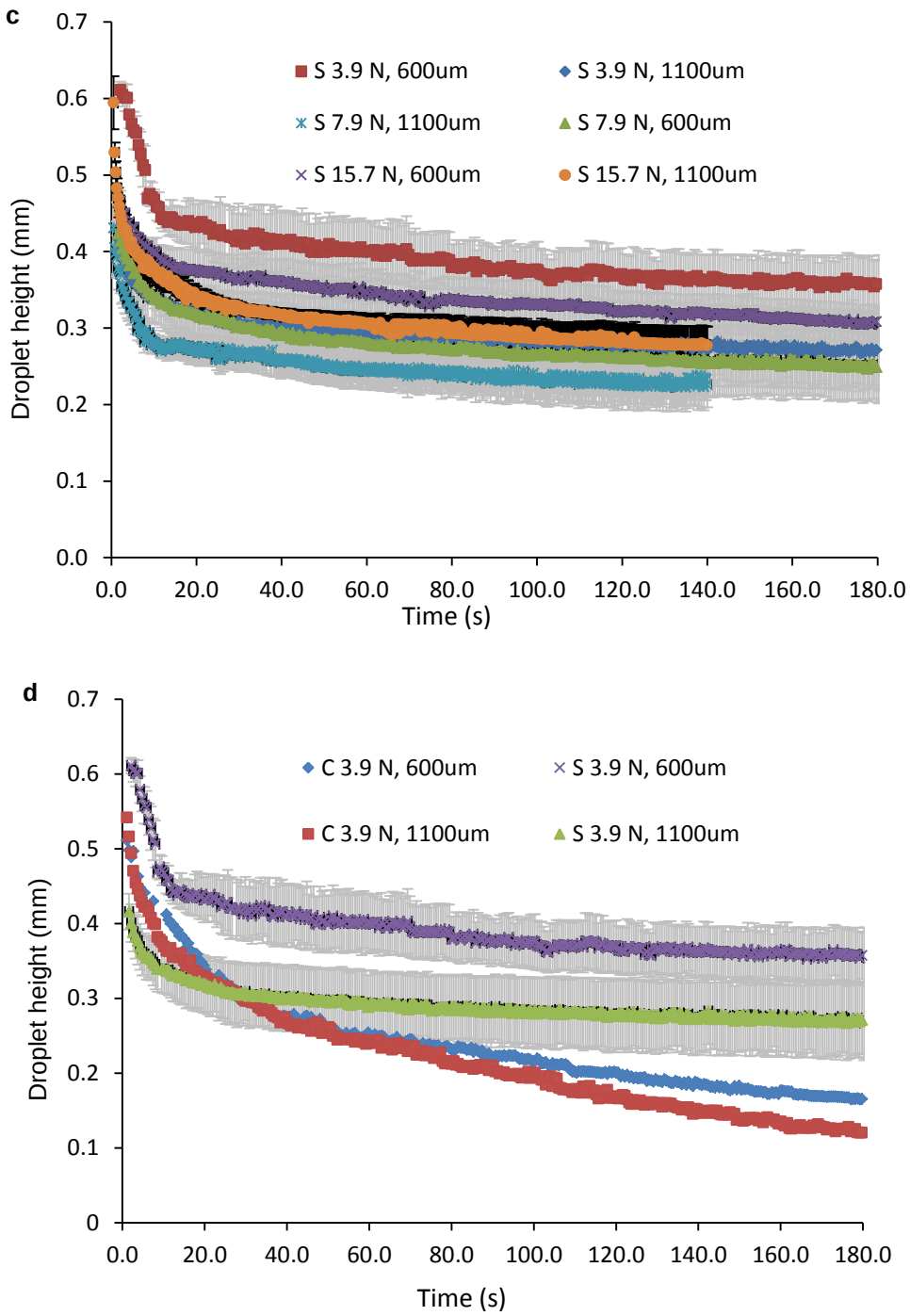

Figure 6.4 Time evolutions of droplet height for a) lidocaine solution on microneedle and non-microneedle treated skin b) lidocaine solution and lidocaine microgels on Strat-M membrane c) lidocaine microgels on microneedle and non-microneedle treated skin d) lidocaine solution and lidocaine microgels on microneedle treated skin. The abbreviation C is control lidocaine solution and S is sample lidocaine hydrogel.

6.3.2 Spreadability of lidocaine NaCMC/gelatine 1:2.3 hydrogel

The spreading of lidocaine NaCMC/gelatine 1:2.3 hydrogel show similar trends for 600µm long MN treated skin, particularly closer for 3.8 N and 7.8 N forces (Figure 6.3c). The fluid properties of the formulation which affect the spreading behaviour have been discussed earlier (Nayak et al., 2014a, b).

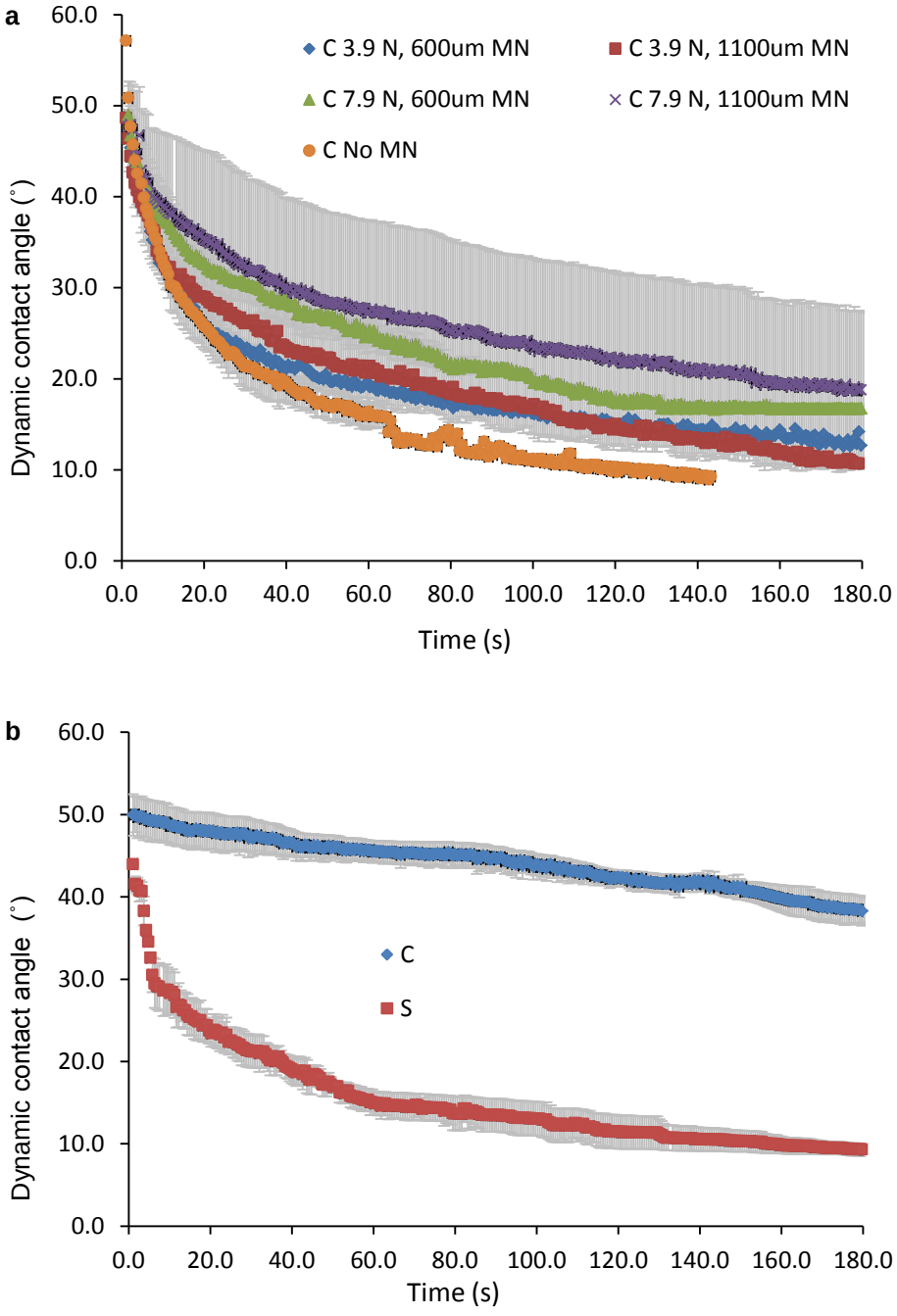

Figure 6.5: (Continued to next page).

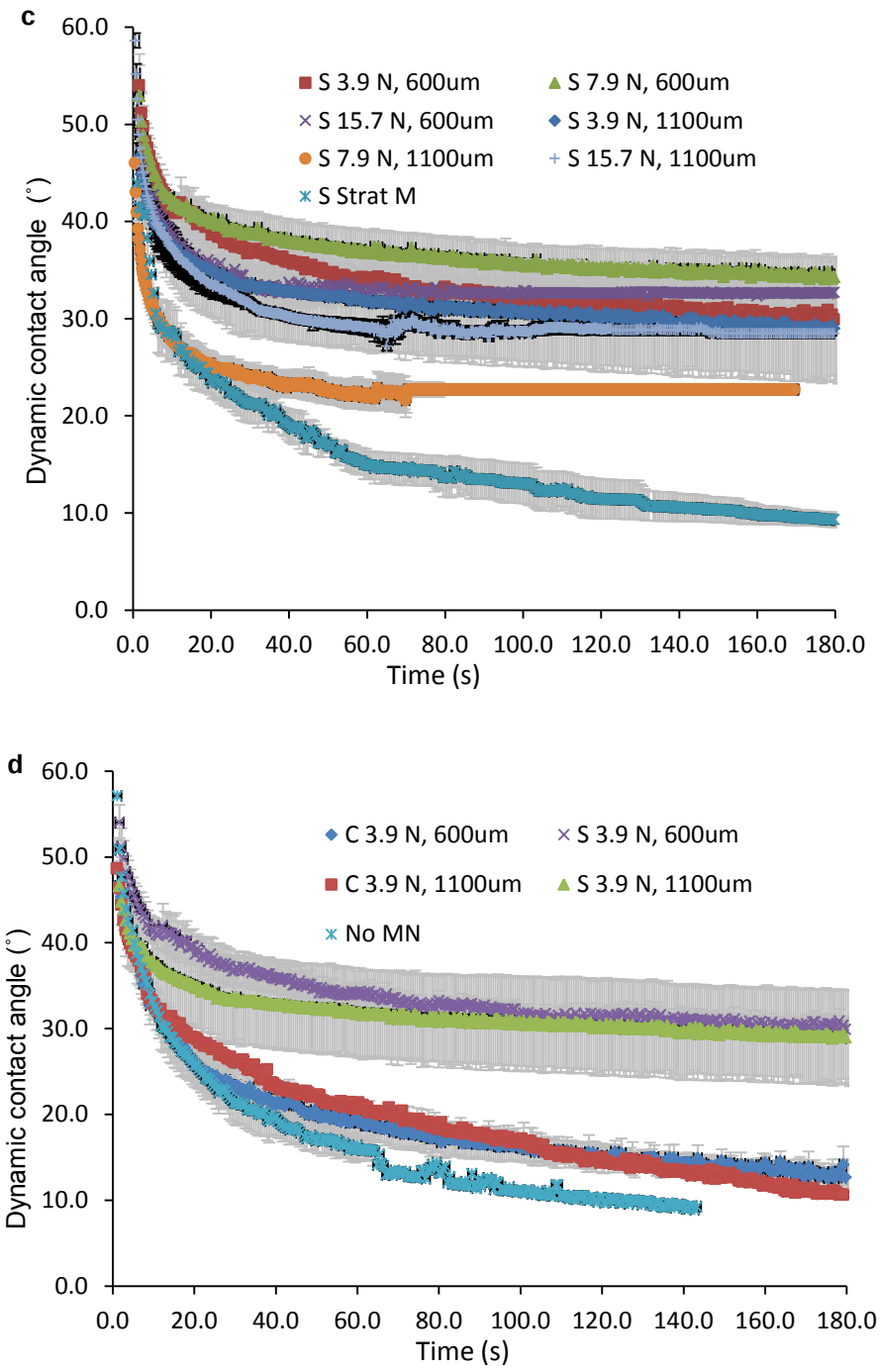

Figure 6.5 Time evolutions of dynamic contact angle for a) lidocaine solution on microneedle and non-microneedle treated skin b) lidocaine solution and lidocaine microgels on Strat-M membrane c) lidocaine microgels on microneedle and non-microneedle treated skin d) lidocaine solution and lidocaine microgels on microneedle treated skin. The abbreviation C is control lidocaine solution and S is sample lidocaine hydrogel

The 15.7 N force on a 600μm MN patch treated skin showed increasing spreading radius than 3.9 N as compared with the lowest force of the same MN length (Figure 6.3c). This is because the MN cavity depths are likely not to be deep enough. The reason is because of an observable reduction in spreading radius caused by deeper micro-cavities from higher MN forces. Lidocaine hydrogel droplets for the insertion forces of 3.9 N, 7.9 N and 15.7 N for 1100 μm long MNs provide less rapidly increasing spreading radius, less rapidly decreasing droplet heights and less rapidly decreasing dynamic contact angles (Figures 6.3c, 6.4c and 6.5c) before static profiles were reached. Nevertheless, there were minor contradictions in reporting lower spreading radii when droplet heights were not decreasing rapidly because of the mild pseudoplastic properties of the lidocaine hydrogel (Nayak et al., 2014a). For example, lidocaine hydrogel from 3.9 N, 600μm treated skin should hypothetically outline faster spreading than 7.9 N, 1100μm on skin because the latter usually possess deep microcavites (Figure 6.3c). Skin microcavities created by MNs do not produce exact replicates of microcavity lengths as shown in transverse section micrographs due to variability in the viscoelastic property of skin (Nayak et al., 2015). Further, lidocaine hydrogel droplets were sometimes difficult to dispense with accurate volumes within ± 0.05 μl because of the viscous nature of the formulation.

The results show that the lidocaine solution spreading radii for 3.9 N and 7.9 N forces of 1100 μm long (longer MNs) MN is distinctly different as compared to the lidocaine hydrogel spreading radii (Figures 6.3a and 6.3c). However, no significant difference in droplet spreading radii was observed when comparing 3.9 and 7.9 N force of 600 μm long MN (shorter MNs) for lidocaine solution (Figure 6.3a). In further scrutinising spreading patterns the lidocaine solution showed rapid spreading, faster decrease in droplet height and rapid decrease in dynamic contact

angle as compared with lidocaine hydrogel when the same forces, namely, 3.9 N force was applied on the skin (Figure 6.3d).

The artificial membrane (Strat-M), which is normally implemented in drug based in vitro PD studies, was a control for skin because of a relatively smooth surface (Uchida et al., 2015). The spreading radii of lidocaine solution and hydrogel droplets could not be measured reliably with a good repeatability because of the horizontal placement of camera and liquid percolation through the pores in the membrane. However, there is a slight decrease in droplet height and dynamic contact angle for lidocaine solution droplets (Figures 6.4b and 6.5b). This slight decrease can be attributed to the percolation of lidocaine solution into Strat-M pores despite no significant change in droplet spreading radius.

Lidocaine hydrogel droplets showed significant change in spreading radius, droplet height and dynamic contact angle (Figures 6.4b, 6.5b) on Strat-M. The droplet spreading was likely to be caused by the lower surface tension of lidocaine hydrogel on the hydrophobic surface of Strat-M. Lidocaine hydrogel contains residual paraffin of low surface tension properties as compared with water.

Lidocaine hydrogels and lidocaine solution droplets snapshots outline spreading in terms of observed changes in droplet shape at three distinct timings (Figures 6.6 and 6.7). Lidocaine solution droplets have dome shape at the initial time of placement as compared with slightly flattened dome shaped droplets for lidocaine hydrogel (Figures 6.6 and 6.7). After a duration of 10 seconds, the lidocaine hydrogels spread more than the lidocaine solution, especially on skin treated with 600 µm long MNs (Figures 6.6 and 6.7). In most cases, lidocaine solution shows distinct droplet with respect to 7.9 N force with 1100µm long MN treated skin and Strat-M membrane after 180 seconds (Figure 6.6). The remaining MN treated skin

variables appear not to retain more lidocaine solution droplets in the microcavities (Figure 6.6). After the duration of 180 seconds, the droplet outline is distinctly notable for lidocaine hydrogel after 1100µm MN treatment on skin (Figure 6.7).

The relative humidity and temperature of the surrounding vicinity for droplet spreadability was 48.6 ± 4.31% at 20.1° ± 2.40°C, respectively. The standard deviation for relative humidity is observed because the surroundings are not an isolated system preventing the transfer of heat.

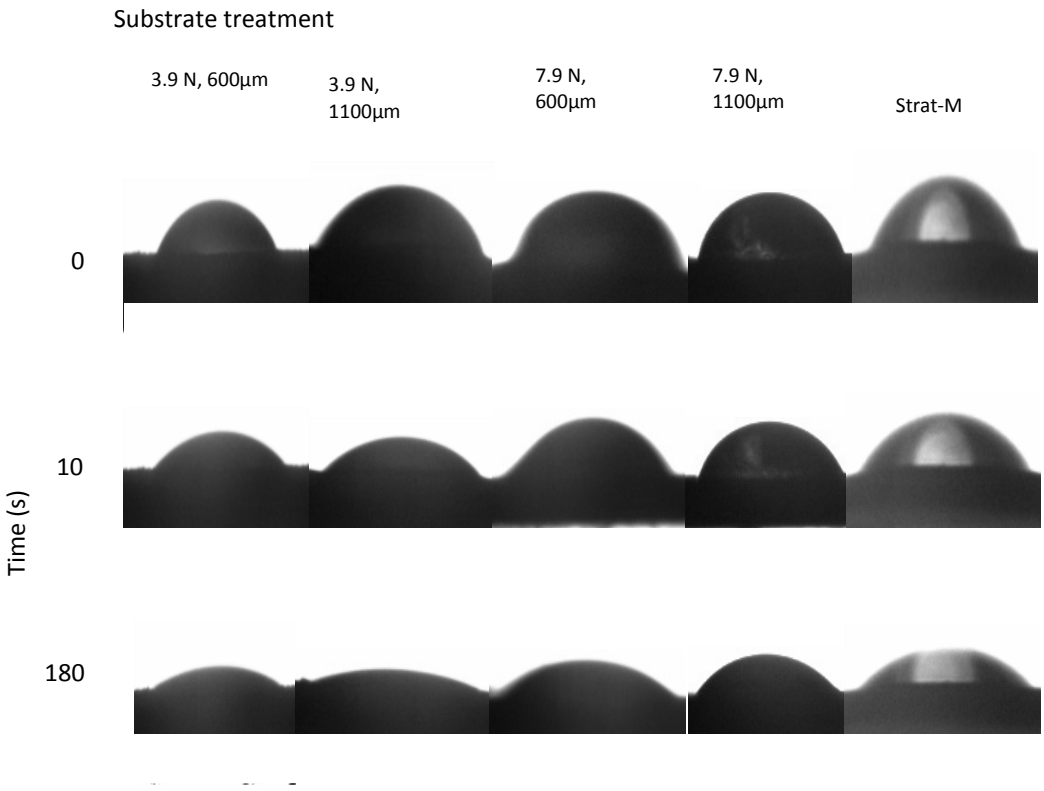

Figure 6.6 Captured images of lidocaine solution droplets (C) on a substrate (skin or membrane) at three different time points. The figure shows the droplet morphology at the substrate for different forces of MN insertion and MN lengths which were used to treat the skin.

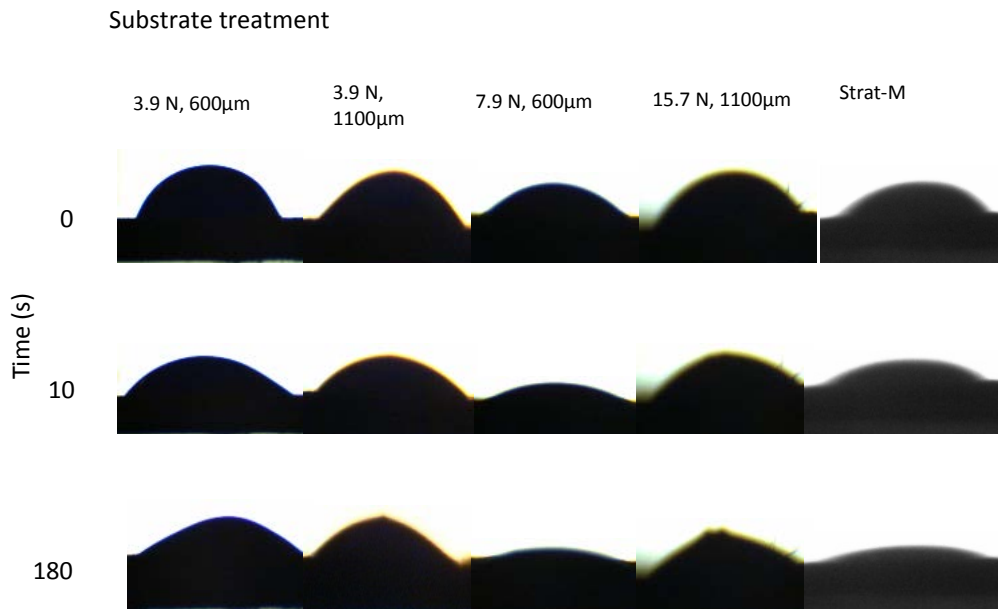

Figure 6.7 Captured images of lidocaine NaCMC/gelatine 1:2.3 hydrogel droplets (S) on a substrate (skin or membrane) at three different time points. The figure shows the droplet morphology at the substrate for different forces of MN insertion and MN lengths which were used to treat the skin.

Normal environmental changes in relative humidity were expected because the duration of experiments were conducted upto 3 minutes and relative humidity can fluctuate in a matter of seconds. The reading of relative humidity of 48.6% is near average at a low room temperature. The likelihood of evaporation is low for these surrounding conditions and the short duration of the experiments.

6.3.3 Dimensionless spreading parameters of lidocaine hydrogel and solution

The spreading dynamics of lidocaine NaCMC/gelatine 1:2.3 hydrogel and solution are represented in this section in terms of dimensionless parameters, namely, dimensionless spreading radius $\left(\frac{L_t}{L_m}\right)$, dimensionless contact angle $\left(\frac{\theta_t}{\theta_m}\right)$, dimensionless droplet height $\left(\frac{h_t}{h_m}\right)$, dimensionless spreading time $\left(\frac{t}{t^*}\right)$ and dimensionless droplet volume $\left(\frac{V_t}{V_{max}}\right)$. For the above five dimensionless parameters, the numerators, namely, L_t, θ_t, h_t, V_t and t, are the droplet spreading radius, contact

angle, height, volume and measured time periodically at different time intervals. On the other hand, the denominators of the fractions are the droplet base showing the maximum spreading radius, maximum contact angle, maximum droplet height, maximum droplet volume and static advancing droplet time. The dimensionless numbers, namely, $\frac{L_t}{L_m}, \frac{\theta_t}{\theta_m}, \frac{h_t}{h_m}$ and $\frac{V_t}{V_{max}}$ are plotted as function of $\frac{t}{t^*}$ for various circumstances (Figure 6.8). Analyses of these parameters provide understanding of the time evolution of these parameters and give some generality to the results (e.g., see Chao et al., 2014). Figure 6.8 shows that the time evolutions of these dimensionless parameters are different implying that the spreading behaviour is different in different cases. These are discussed below.

The lidocaine hydrogel spreading on 3.9 N and 7.9 N force treated skin with 1100 µm and 600 µm long MN showed short durations in increasing dimensionless spreading profiles, thus attaining closeness to a plateau of dimensionless value of 1.0 at a shorter time interval (Figure 6.8a). The lidocaine solution on non-MN treated skin could not be reported as dimensionless spreading because a linear profile was observed and L_m could not be deduced because of no plateau (Figure 6.3a).

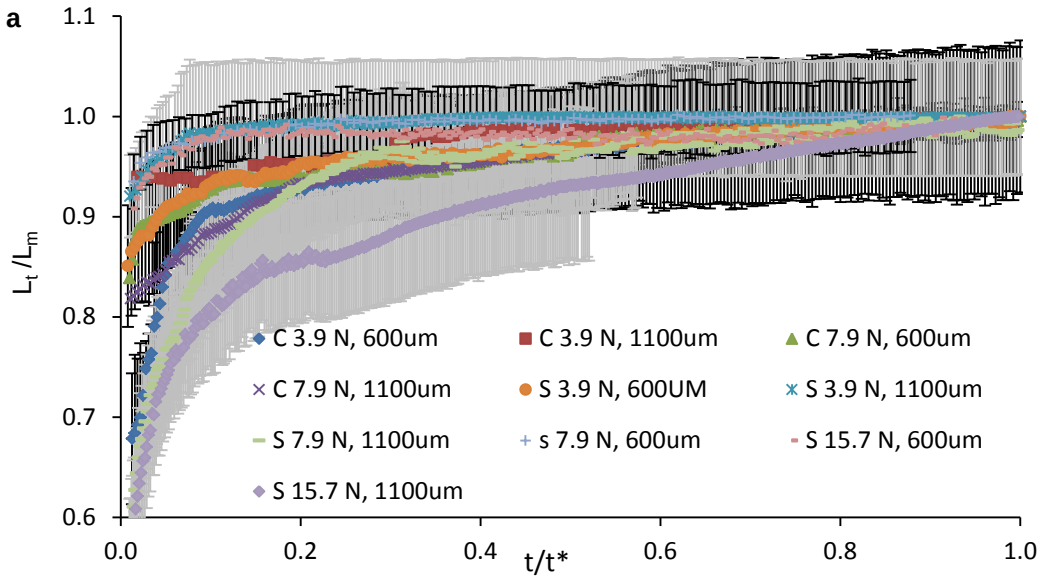

Figure 6.8: (Continued to next page)

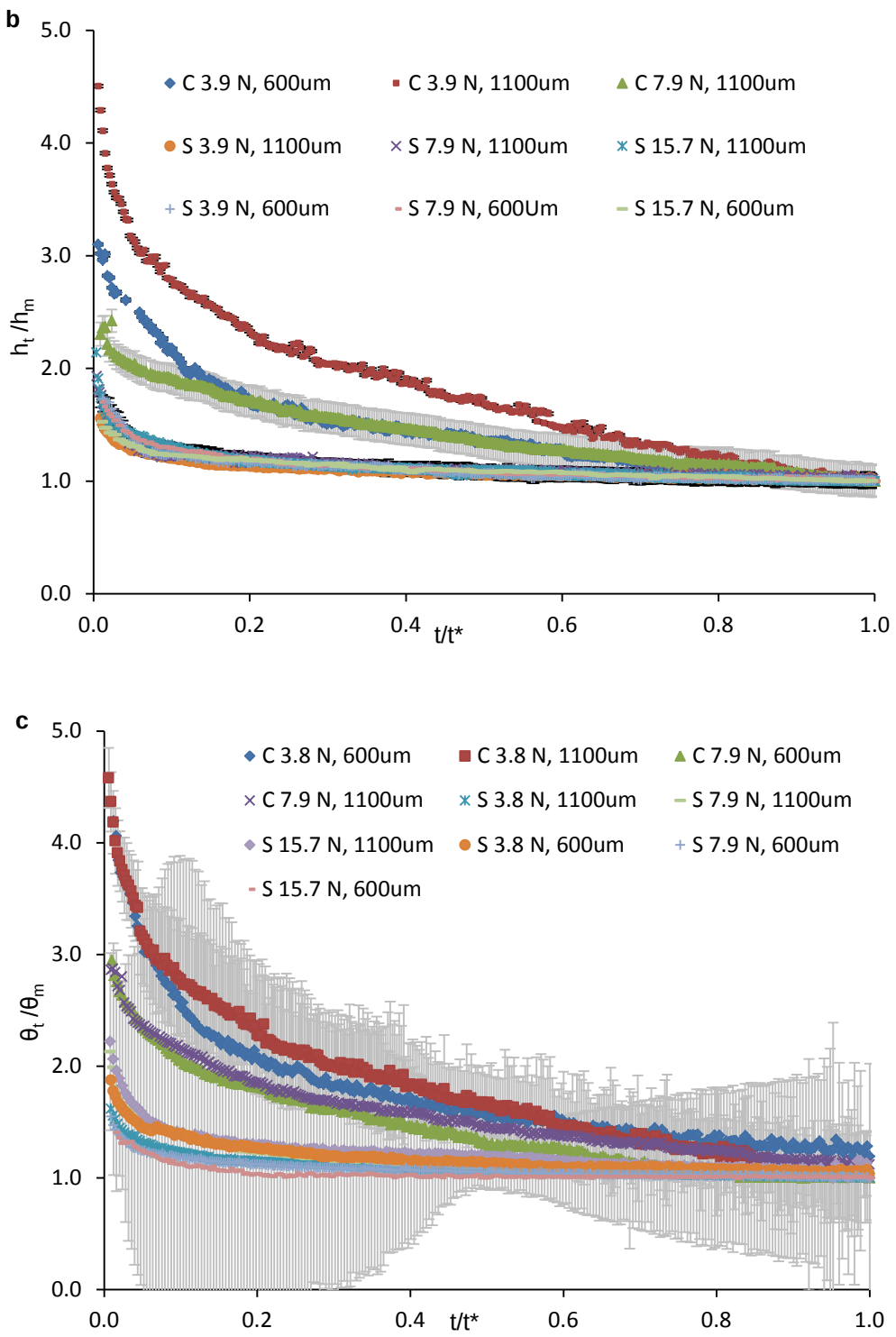

Figure 6.8. The lidocaine droplet plots outlining dynamic variation in a) spreading of hydrogel (S) or solution (C) on microneedle and non-microneedle treated skin b) droplet height of hydrogel (S) or solution (C) on microneedle and non-microneedle treated skin c) contact angle of hydrogel (S) or solution (C) on microneedle and non-microneedle treated skin.

The spreading of lidocaine hydrogels on 7.9 N and 15.7 N force treated skin with 1100 µm long MN showed a long durations in increasing spreading radius; thus, attaining closeness to dimensionless value 1.0 above the fractional time of 0.90 (Figure 6.8a). A short duration in increasing dimensionless spreading means a less dynamic spreading across the skin. As mentioned earlier in this chapter, the lidocaine hydrogel fill the skin microcavities and the spreading of the hydrogel slow down.

All lidocaine hydrogels droplets on MN treated skin outlined slower reduction of dimension-less droplet height as the liquid fills the microcavities on MN treated skin (Figure 6.8b). Comparatively, the lidocaine solutions showed faster dynamic height reduction from maximum spreading height (t = 0) because of high initial droplet height fractions and faster spreading (Figure 6.8b).

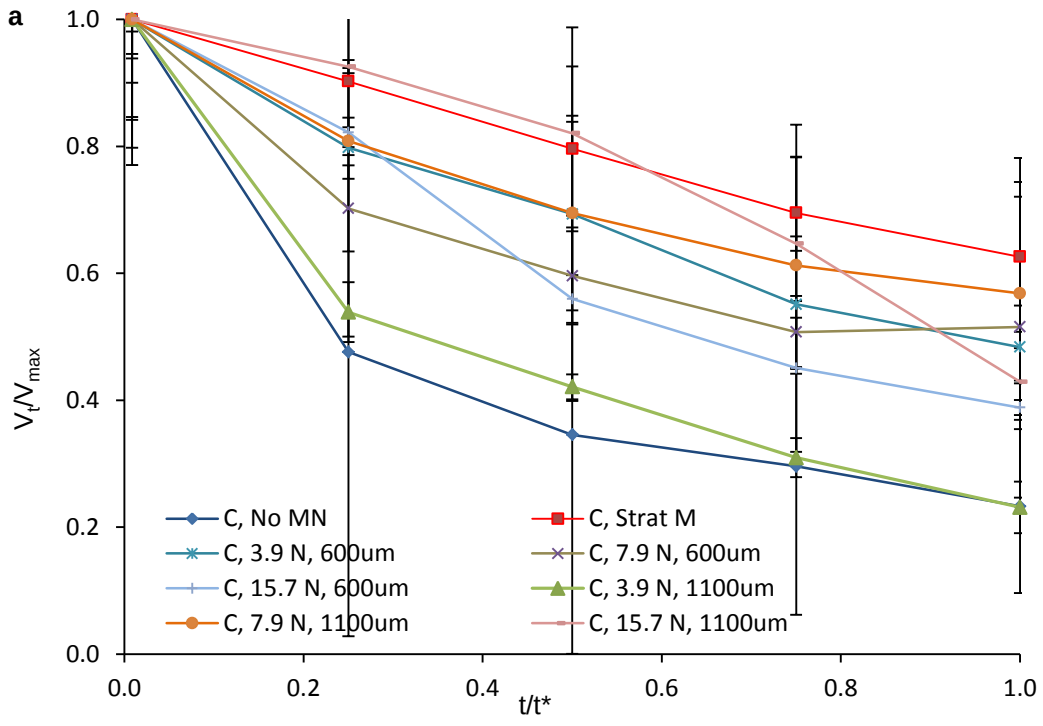

Figure 6.9: (Continued to next page).

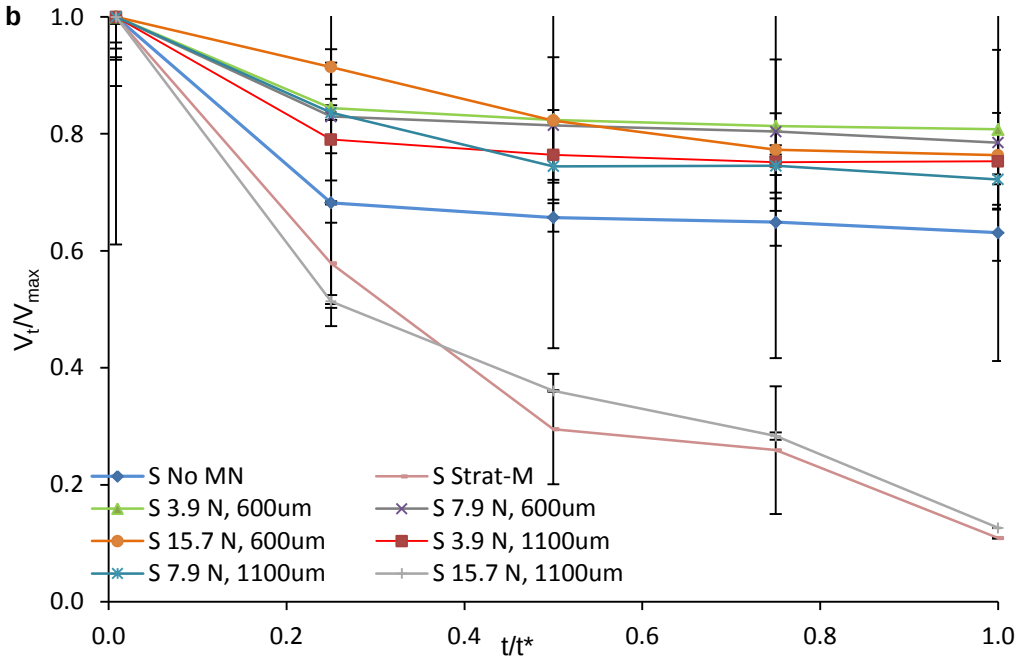

Figure 6.9 The non-dimensional droplet volume on top of skin sample a) for lidocaine solution b) lidocaine NaCMC/gelatine 1:2.3. The abbreviation C is control lidocaine solution and S is sample lidocaine hydrogel.

Slower dynamic reduction of contact angle was observed for all lidocaine hydrogel droplets on MN treated skin (Figure 6.8c). The lidocaine hydrogel on 3.9 N of 1100 µm length, 7.9 N and 15.7 N of 600 µm treated skin showed slightly slower reductions in fractional contact angles (Figure 6.8c). Nevertheless, lidocaine hydrogel on 7.9 N and 15.7 N treated skin samples with 1100 µm long MN outlined slightly faster reductions in the dimensionless contact angle (Figure 6.8c). Static advancing droplets were found to arrive at shorter fractional timings for lidocaine hydrogels because of the viscous property of the hydrogel and presence of numerous MN microcavities as liquid percolates into the microcavity spaces.

The lidocaine solution droplets show significantly more dynamic volume decreases as compared with lidocaine hydrogel droplets (Figure 6.9 a,b), which is due to the fact that the lidocaine solution percolates into the MN holes faster than the lidocaine

hydrogel droplets. The lidocaine hydrogels outline low droplet volume reductions in microneedle treated skin and fast appearance of static droplet volumes (Figure 6.9b). There was a faster reduction in droplet volume for Strat-M and 15.7 N, 1100 μm treated skin (Figure 6.9b). The roughness of skin and the pseudoplastic properties of the hydrogel are two factors in explaining the likelihood for the observed static advancing droplet profiles. Non-microneedle treated skin and Strat-M membrane surfaces appear smooth, so there appears to be faster droplet volume decreases in those two substrate control parameters.

6.4 Chapter summary

The spreading of a liquid drug formulation, namely, lidocaine NaCMC/gelatine 1:2.3 hydrogel, on MN treated skin is studied. The results of the study show improved control of the formulation spreadability as compared to those for lidocaine solution (lidocaine dissolved in DI water) alone. Lidocaine NaCMC/gelatine 1:2.3 hydrogel show a slightly lower spreading radius, sight decrease in droplet height and smaller, controlled decrease in dynamic contact angle as compared with lidocaine solution. The slower dynamic reduction of droplet height and contact angle and convergence to static advancing droplet at short initial timings for lidocaine NaCMC/gelatine 1:2.3 hydrogel are indication of the seepage of the liquid inside MN microcavities in skin.

Chapter 7

Conclusion and future work

7.1 Conclusion

In this PhD research, a natural bi-polymeric hydrogel was formulated with lidocaine and a microneedle (MN) “poke and patch” method was adopted for studying percutaneous drug delivery on porcine skin. The summary of the work which was outlined in various chapters have been directly mentioned in those chapters. Therefore, this chapter outlines the overall conclusions and main contributions of this PhD research.

The work centres around the fact that both sodium carboxymethylcellulose and gelatine, which are natural polymers, are suitable for encapsulating lidocaine. A lidocaine sodium carboxymethylcellulose and gelatine bi-polymeric hydrogel was successfully formulated to encapsulate lidocaine molecules. The optimum mass ratio achieved to encapsulate lidocaine was gelatine to NaCMC of 2.3. Solid microneedle assisted delivery of this lidocaine bi-polymeric hydrogel through skin provided highly desirable permeation kinetics. Gelatine is ideal for forming ionic interactions with sodium carboxymethylcellulose, which permits good encapsulation and release properties for lidocaine. The mass ratio between these two polymers permits an intermolecular charge distribution with encapsulated lidocaine and therefore the lowest Zeta potential value corresponding to a greater hydrogel microparticle dispersion. This microparticle dispersion provides an occurrence of surface repulsion between hydrogel microparticles which is negative in our case. A low Zeta potential pertaining to low potential differences on the hydrogel particle surface repels neighbouring particle surface charges, which explains the decrease of particle agglomeration.

In this work the developed bipolymeric hydrogel showed an optimum mass ratio of 1:2.3. The encapsulation efficiency of 53% for lidocaine NaCMC/gelatine 1:2.3 was a considerable improvement from previous encapsulation efficiency of 17.2% of the same mass ratio bi-polymeric lidocaine. This was due to batch formulation processing accuracy and low recorded particle sizes despite significant polydisperisity. The pseudoplasticity of lidocaine NaCMC/gelatine 1:2.3 was significant to further explore the spreadability of this hydrogel on skin. The gelatine component leads to formulation gelation and, thus contributes to the pseudoplasticity of the bipolymeric hydrogel.

Lidocaine from NaCMC/gelatine 1:2.3 permeated at a minimum therapeutic level of 1.2 µg/ml after 1.1 h post microneedle treatment on skin. Comparatively lidocaine passive diffusion showed time duration of 1.36 fold greater in bypassing the minimum therapeutic level with respect to the same hydrogel formulation mass ratio. A second result for lidocaine PD's therapeutic advance was 0.4 h lower than the first PD result of 1.5 h. Here, the lidocaine detected was in the receptor compartment of the Franz diffusion cell (FDC) which represented the hypodermis. Full thickness skin was calculated at 670 ± 50 µm deep and therefore the receptor level depth has a bigger range and is greater than this. The passive diffusion (PD) of lidocaine from NaCMC/gelatine 1:2.66 was just under 0.75 h in reaching minimum therapeutic level. There is a large variability in lidocaine reaching the hypodermis level by PD. This can be attributed to the depth range or path length that lidocaine molecules travel past skin before detection.

In taking lidocaine NaCMC/gelatine 1:2.66 as the favourable hydrogel, MN treated skin outlined 0.17 h in bypassing the minimum therapeutic level. This can be attributed to a high encapsulation efficiency of 32 % as mentioned in Chapter 3. However lidocaine NaCMC/gelatine 1:2.66 was not selected for further permeation

based studies because of large particle sizes and unfavourable Zeta potential results. The selection of lidocaine NaCMC/gelatine 1:2.3 successfully outlined depth averaged vertical and horizontal permeation of MN treated skin, bypassing therapeutic lidocaine levels at 0.25 h. This time accurate MN forces were implemented on skin with 3.9 and 7.9 N forces more favourable for sustained therapeutic lidocaine delivery within viable skin consisting of VE and dermis layer. The mass transfer of lidocaine regarding skin's depth averaged vertical and horizontal permeation provided accurate results of lidocaine's presence within viable skin because the known periodic lidocaine release quantities were subtracted.

Already knowing the mild pseudoplastic properties of lidocaine NaCMC/gelatine 1:2.3 hydrogel paved the way for spreadability based research. The spreadability of lidocaine NaCMC/gelatine 1:2.3 hydrogel on MN treated skin successfully showed spreading control. The static advancing contact angle was achieved at a lower time as compared with lidocaine solution on non-MN treated skin. The shorter the time for static advancing contact angle of lidocaine hydrogel droplets on skin means the longer the localised redency for percolation of liquid into microcavities. Also, manual rubbing or spreading the lidocaine formulation with fingers is not required.

Overall lidocaine NaCMC/gelatine 1:2.3 hydrogel in tandem with solid microneedle assisted drug delivery shows a successful outcome in drug formulation development and percutaneous permeation kinetics. Also, the time taken for lidocaine to appear in the viable epidermis layer of skin was significantly less than conventional passive diffusion by lidocaine hydrogel alone.

7.2 Future work

In the current work no focus was given to control and reduce the microgel polydispersity because the reduction in gelation and increase in covalent crosslinking reagents such as glutaraldehyde in the formation of polymeric microparticles may alter the current hydrogel properties of the formulation. However, we recognise that lidocaine NaCMC/gelatine hydrogel as an ideal painless, local anaesthetic formulation is likely to be an advancing area in the future. Therefore, further developmental work to reduce residual paraffin oil content, smaller micron-scale particle sizes and subsequently higher encapsulation efficiency could be the focus of further studies. In the context of electro-ionic interactions concerning the formulation, there is no significant quantitative study on ionic interactions between NaCMC, gelatine and lidocaine with respect to potentiometric measurements, pH thresholds and polarography analysis. These are fairly important parameters for relating ionic properties but Zeta potential analysis looks into the dispersion of microparticles in the hydrogel as a result of the degree in like charge repulsion which is discussed later.

A Phase 1 double blind clinical study on human volunteers is the next stage in the proof of concept in percutaneous anaesthesia. Optimum lidocaine 1:2.3 mass ratio hydrogel with coat and poke method shall justify the attainment of fast minimum therapeutic levels below the SC layer of skin. Following current successful in vitro based studies in proving fast vertical and lateral permeation of lidocaine, the need for implementing in vivo studies is imperative. In deducing the lidocaine pharmacokinetics to be successfully desirable and reproducible in the application of emergency anaesthesia, further commercial based goals can be satisfied in achieving a new commercial microneedle product.

References

Ahmed E.M., (2015). Hydrogel: Preparation, characterization, and applications, *J Adv Res*, **6**: 105-121

Akhtar N., (2014). Vesicles: a recently developed novel carrier for enhanced topical drug delivery, *Curr Drug Deliv*, **11**: 87-97

Akin F.J., Norred W.P., (1976). Factors affecting measurement of aryl hydrocarbon hydroxylase activity in mouse skin, *J Invest Dermatol*, **67**: 709-712

Alaie J., Vasheghani-Farahani E., Rahmatpour A., Semsarzadeh M.A., (2013). Gelation rheology and water absorption behavior of semiinterpenetrating polymer networks of polyacrylamide and carboxymethylcellulose, *J Macromolecular Sci B*, **52**: 604-613

Al-Kahtani A.A., Sherigara B.S., (2009). Controlled release of theophylline through semi-interpenetrating network microspheres of chitosan- (dextran-g-acrylamide), *J Mater Sci: Mater Med*, **20**: 1437-1445

Al-Qallaf B., Das D.B., (2008). Optimization of square microneedle arrays for increasing drug permeability in skin, *Chem Eng Sci*, **63**: 2523-2535

Al-Qallaf B., Das D.B., (2009). Optimizing microneedle arrays to increase skin permeability for transdermal drug delivery, *Ann New York Acad Sci*, **1161**: 83-94

Allen L.V., Popovich N.G., Ansel H.C., (2005). Ansel's pharmaceutical dosage forms and drug delivery systems, 8th edition, Baltimore: *Lippincott Williams & Wilkins*, 131

Allen M., Prausnitz M., McAllister D., Cros F., Microneedledevices and methods of manufacture and use thereof, *United States of America Patent US 6334856 B1*, January 1, 2002

Alvarez-Lorenzo C., Blanco-Fernandez B., Puga A.M., Concheiro A., (2013). Crosslinked ionic polysaccharides for stimuli-sensitive drug delivery, *Adv Drug Deliv Rev*, **65**: 1148-1171

Ameri M., Fan F.C., Maa Y.F., (2010). Parathyroid hormone PTH (1–34) formulation that enables uniform coating on a novel transdermal microprojection delivery system, *Pharm Res*, **27**: 303-313

Ami Y., Tachikawa H., Takano N., Miki N., (2011) Formation of polymer microneedle arrays using soft lithography, *J Micro Nanolithogr MEM*, **10**: 011503. doi:10.1117/1.3553393

Armani D.K., Liu C., (2000). Microfabrication technology for polycaprolactone, a biodegradable polymer, *J Micromech Microeng*, **10**: 80-84

Arora A., Prausnitz M.R., Mitragotri S., (2008). Micro-scale devices for transdermal drug delivery, *Int J Pharm*, **364**: 227-236

Auner B.G., Valenta C., (2004). Influence of phloretin on the skin permeation of lidocaine from semisolid preparations, *Eur J Pharm Biopharm*, **57**: 307-312

Badran M.M., Kuntsche J., Fahr A., (2009). Skin penetration enhancement by microneedle device (Dermaroller®) in vitro: dependency on needle size and applied formulation, Eur J Pharm Sci, **36**: 511-23

Bal S., Kruithof A.C., Liebl H., Tomerius M., Bouwstra J., Ladermann H., Meinke M., (2010). In vivo visualization of microneedle conduits in human skin using laser scanning microscopy, *Laser Phys Lett*, **7**: 242-246

Banerjee S., Siddiqui L., Bhattacharya S.S., Kaity S., Ghosh A., Chattopadhyay P., Pandey A., Singh L., (2012). Interpenetrating polymer network (IPN) hydrogel microspheres for oral controlled release application, *Int J Biol Macromol*, **50**: 198-206

Banks S.L., Paudel K.S., Brogden N.K., Loftin C.D., Stinchcomb A.L., (2011). Diclofenac enables prolonged delivery of naltrexone through microneedle-treated skin, *Pharm Res*, **28**: 1211-1219

Bari H., (2010). A prolonged release parenteral drug delivery system—an overview, *Int J Pharm Sci Rev Res*, **3**: 1-11

Bariya S.H., Gohel M.C., Mehta T.A., Sharma O.P., (2011). Microneedles: an emerging transdermal drug delivery system, *J Pharm Pharmacol*, **64**:11-29

Becker D.E., Reed K.L., (2012). Local anaesthetics: Review of pharmacological consideration, *Anesth Prog*, **59**: 90-102

Bekhit M.H., (2011). The essence of analgesia and anagesics, Chapter 67, Lidocaine for neural blockade, *Editors, Sinatra RS, Jahr JS, Watkins-Pitchford JM, Cambridge University Press*, 280-281

Benet L.Z., Oie S., Schwartz J.B., (1996). Design and optimisation of dosage regimens: Pharmacokinetic data, In The pharmacological basis of therapeutics, Editors Hardman J.G., Limbard L.E., Molinoff P.B., Rudon R.W., Gilman A.G., *McGraw Hill: New York*, 1707-1792

Berger J., Reist M., Mayer J.M., Felt O., Peppas N.A., Gurny R., (2004). Structure and interactions in covalently and ionically crosslinked chitosan hydrogels for biomedical applications, *Eur J Pharm Biopharm*, **57**: 19-34

Bhattacharyya R., Ray S.K., (2014). Enhanced adsorption of synthetic dyes from aqueous solution by a semi-interpenetrating network hydrogel based on starch, *J Ind Eng Chem*, **20**: 3714-3725

Bodhale D.W., Nisar A., Afzulpurkar N., (2010). Structural and microfluidic analysis of hollow side-open polymeric microneedles for transdermal drug delivery application, *Microfluid Nanofluid*, **8**: 373-392

Bornstein P., Piez K.A., (1964). A biochemical study of human skin collagen and the relation between intra and intermolecular cross-linking, *J Clin Invest*, **43**: 1813-1823

Braga D., Chelazzi L., Greprioni F., Dichiaranta E., Chierotti M.R., Gobetto R., (2013). Molecular salts of anaesthetic lidocaine with dicarboxylic acids: Solid-state properties and a combined structural and spectroscopic study, *Cryst Growth Des*, **13**: 2564-2572

Brazel C.S., Peppas N.A., (2000). Modeling of drug release from swellable polymers, *Eur J Pharma Biopharm*, **49**: 47-58.

British, Standards ISO 5725-2 (2002). International Standard, *Standards Board*

Brogden N.K., Milewski M., Ghosh P., Hardi L., Crofford L.J., Stinchcomb A.L., (2012). Diclofenac delays micropore closure following microneedle treatment in human subjects, *J Control Release*, **163**: 220-229

Buhus G., Poap M., Desbrieres J., (2009). Hydrogels based on carboxymethylcellulose and gelatin for inclusion and release of chloramphenicol, *J Bioact Compat Pol*, **24**: 525-45

Cai Y., Shen W., Leng Loo S., Krantz W.B., Wang R., Fane A.G., Hu X., (2013). Towards temperature driven forward osmosis desalination using Semi-IPN hydrogels as reversible draw agents, *Water Res*, **47**: 3773-3781

Capellan O., Hollander J.E., (2003). Management of lacerations in the emergency department, *Emerg Med Clin North Am*, **21**: 205-31

Carter Fox S., Li B., Xu D., Edgar K.J., (2011). Regioselective esterification and etherification of cellulose: A review, *Biomacromolecules*, **12**: 1956-1972

Cepeda M.S., Tzortzopoulou A., Thackrey M., Hudcova J., Gandhi P.A., Schumann R., (2010). Adjusting the pH of lidocaine for reducing pain on injection, *Cochrane Database of Systematic Reviews, The Cochrane Collaboration, John Wiley & Sons Ltd*, **12**: doi:10.1002/14651858

Chale S., Singer A.J., Marchini S., McBride M.J., Kennedy D., (2006). Digital versus local anesthesia for finger lacerations: A randomized controlled trial, *Acad Emerg Med*, **13**: 1046-1050

Chang C., Duan B., Cai J., Zhang L., (2010). Superabsorbent hydrogels based on cellulose for smart swelling and controllable delivery, *Eur Polym J*, **46**: 92-100

Chang C., Zhang L., (2011). Cellulose-based hydrogels: Present status and application prospects, *Carbohyd Polym*, **84**: 40-53

Chao T.Z., Trybala A., Starov V., Das D.B., (2014). Influence of haematocrit level on the kinetics of blood spreading on thin porous medium during blood spot sampling, *Colloids Surf A: Physicochem Eng Aspects*, **451**: 38-47

Chen B., Wei J., Iliescu C., (2010). Sonophoretic enhanced microneedles array (SEMA) – improving the efficiency of transdermal drug delivery, *Sens Actuators B: Chem*, **145**: 54–60

Chen B., Wei J., Tay F.E.H., Wong Y.T., Iliescu C., (2008). Silicon microneedles array with biodegradable tips for transdermal drug delivery, *Microsyst Technol*, **14**: 1015-1019

Cheung K., Das D.B., (2014). Microneedles for drug delivery: trends and progress, Drug Deliv, doi:10.3109/10717544.2014.986309 (In press)

Cheung K., Han T., Das D.B., (2014). Effect of force of microneedle insertion on the permeability of insulin in skin, *J Diabetes Sci Technol*, **8**: 444-452

Chikh L., Delhorbe V., Fichet O., (2011). (Semi-) Interpenetrating polymer networks as fuel cell membranes, *J Membrane Sci*, **368**: 1-17

Choi N.S., Kim C.H., Cho K.Y., Park J.K., (2002). Morphology and hydrolysis of PCL/PLLA blends compatibilized with P(LLA-co-ε CL) or P(LLA-b-ε CL), *J Appl Polym Sci,* **86**: 1892-1898

Chow K.T., Chan L.W., Heng P.W.S., (2008). Characterization of spreadability of nonaqueous ethylcellulose gel matrices using dynamic contact angle, *J Pharm Sci*, **97**: 3467-3481.

Chu L.Y., Choi S.O., Prausnitz M.R., (2010). Fabrication of dissolving polymer microneedles for controlled drug encapsulation and delivery: bubble and pedestal microneedle designs, *J Pharm Sci*, **99**: 4228-4238

Cleary G.W., (1993) Transdermal Delivery Systems: A Medical Rationale, in Topical Drug Bioavailability, Bioequivalence, and Penetration, *Editors: Shah V.P., and Maibach H.I., New York*, Plenum, 17-68

Columb M.O., Ramsaran R., (2010). Local anaesthetic agents, *Anaesthe Intensive Care Med*, **11**: 113-117

Conroy P.H., O'Rourke J., (2013). Tumescent anaesthesia, *The Surgeon*, **11**: 210-221

Costa J.C.S., Neves J.S., de Souza M.V.N., Siqueira R.A., Romeiro N.C., Boechat N., e Silva P.M.R., Martins M.A., (2008). Synthesis and antispasmodic activity of lidocaine derivatives with reduced local anesthetic action, *Bioorg Med Chem Lett*, **18**: 1162-1166

Costa-Júnior E.S., Barbosa-Stancioli E.F., Mansur A.A.P., Vasconcelos W.L., Mansur H.S., (2009). Preparation and characterization of chitosan/poly(vinyl alcohol) chemically crosslinked blends for biomedical applications, *Carbohyd Polym*, **76**: 472-481

Coutinho D.F., Sant S.V., Shin H., Oliveira J.T., Gomes M.E., Neves N.M., Khademhosseini A., Reis R.L., (2010). Modified Gellan Gum hydrogels with tunable physical and mechanical properties, *Biomaterials*, **31**: 7494-7502

Couto A., Fernandes R., Natália Cordeiro M.S., Reis S.S., Ribeiro R.T., Pessoa A.M., (2014). Dermic diffusion and stratum corneum: A state of the art review of mathematical models, *J Control Release*, **177**: 74-83

Dai W., Zhu J., Shangguan A., Lang M., (2009). Synthesis, characterization and degradability of the comb-type poly(4- hydroxyl-ε-caprolactone-co-ε-caprolactone)-γ-poly(L-lactide), Eur Polym J, **45**: 1659-1667

Danhier F., Ansorena E., Silva J.M., Coco R., Le Breton A., Préat V., (2012). PLGA-based nanoparticles: an overview of biomedical applications, *J Control Release*, **161**: 505-522

Dash T.K., Konkimalla B.V.B., (2012). Polymeric modification and its implication in drug delivery: poly-ε-caprolactone (PCL) as a model polymer, *Mol Pharm*, **9**:2365-2379

Davis S.P., Prausnitz M.R., Allen MG., (2003). Fabrication and characterization of laser micromachined hollow microneedles, *Transducers*, *IEEE*: 1435-1438

De Boer A.G., Breimer D.D., Mattie H., Pronk J., Gubbens-Stibbe J.M., (1979). Rectal bioavailability of lidocaine in man: partial avoidance of ‘‘first-pass’’ metabolism, *Clin Pharmacol Ther*, **26**: 701-709

Del Campo A., Greiner C., (2007). SU-8: a photoresist for high aspect-ratio and 3D submicron lithography. *J Micromech Microeng* **17**: R81-R95

Desai M.J., Radhika S., Wang D., (2008). Treatment of pain in Dercum’s disease with Lidoderm® (Lidociane 5% Patch): a case report, *Pain Med*, **9**: 1224-1226

Devi N., Kumar M.T., (2009). Preparation and evaluation of gelatin/sodium carboxymethyl cellulose polyelectrolyte complex microparticles for controlled delivery of isoniazid, *APPS PharmSciTech*, **10**: 1412-1419.

Djabri A., Guy R.H., Delgado-Charro M.B., (2012). Transdermal iontophoresis of ranitidine: an opportunity in paediatric drug therapy, *Int J Pharm*, **435**: 27-32

Donnelly R.F., Singh T.R.R., Tunney M.M., Morrow D.I.J., McCarron P.A., O' Mahony C., Woolfson A.D., (2009). Microneedle arrays allow lower microbial penetration than hypodermic needles in vitro, *Pharm Res*, **26**: 2513-2522

Donnelly R.F., Singh T.R.R., Woolfson A.D., (2010). Microneedle based drug delivery systems: microfabrication, drug delivery and safety, *Drug Deliv*, **17**: 187-207

Donnelly R.F., Majithiya R., Singh T.R.R., Morrow D.I.J., Garland M.J., Demir Y.K., Migalska K., Ryan E., Gillen D., Scott C.J., Woolfson A.D., (2011). Design, optimization and characterisation of polymeric microneedle arrays prepared by a novel laser-based micromoulding technique, *Pharm Res*, **28**: 41-57

Ducel V., Richard J., Saulnier P., Popineau Y., Boury F., (2004). Evidence and characterization of complex coacervates containing plant proteins: application to the microencapsulation of oil droplets, *Colloids Surf A*, **232**: 239-247

Ebrahimi S., Abbasnia K., Motealleh A., Kooroshfard N., Kamali F., Ghaffarinezhad F., (2012). Effect of lidocaine phonophoresis on sensory blockade: pulsed or continuous mode of therapeutic ultrasound? *Physiotherapy*, **98**: 57-63

El-Mahrab-Robert M., Rosilio V., Bolzinger M.A., Chaminade P., Grossiord J.L., (2008). Assessment of oil polarity: Comparison of evaluation methods, *Int J Pharm*, **348**: 89-94

Elkhyat A., Courderot-Masuyer C., Mac-Mary S., Courau S., Gharbi T., Humbert P., (2004). Assessment of spray application of Saint GERVAIS® water effects on skin wettability by contact angle measurement comparison with bidistilled water, *Skin Res Tech*, **10**: 283-286

Entenman C.T., (1961). The preparation of tissue lipid extracts. Lectures of the 1961 short course on newer lipid analyses, *J Am Oil Chem Soc*, 534-535

Fang Q., Hanna M.A., (1999). Rheological properties of amorphous and semicrystalline polylactic acid polymers, *Ind Crop Prod*, **10**: 47-53.

Fasinu P., Viness P.V., Ndesendo V.M.K., du Toit L.C., Choonara Y.E., (2011). Diverse approaches for the enhancement of oral drug bioavailability, *Biopharm Drug Dispos*, **32**: 185-209

Fen-Lin W., Razzaghi A., Souney P.F., (1993). Seizure after lidocaine for bronchoscopy: case report and review of the use of lidocaine in airway anesthesia, *Pharmacotherapy*, **13**: 72-78

Fiala S., Brown M.B., Jones S.A., (2011). Dynamic in situ eutectic formation for topical drug delivery, *J Pharm Pharmacol*, **63**: 1428-1436

Fligiel S.E., Varani J., Datta S.C., Kang S., Fisher G.J., Voorhees J.J., (2003). Collagen degradation in aged/photodamaged skin in vivo and after exposure to matrix metalloproteinase-1, *In Vitro. Soc Invest Dermatol*, **120**: 842-848

Fredenberg S., Wahlgren M., Reslow M., Axelsson A., (2011). The mechanisms of drug release in poly(lactic-co-glycolic acid)-based drug delivery systems - a review, *Int J Pharm*, **415**: 34-52

Fujita H., (1997). A decade of MEMS and its future, *IEEE 10th Annual International Workshop on Micro Electro Mechanical Systems*: 1-8. doi:10.1109/MEMSYS.1997.581729

Fundueanu G., Constantin M., Ascenzi P., (2009). Poly(N-isopropylacrylamide-co-acrylamide) cross-linked thermoresponsive microspheres obtained from preformed polymers: Influence of the physico-chemical characteristics of drugs on their release profiles, *Acta Biomater*, **5**: 363-373

Gabor F., Ertl B., Wirth M., Mallinger R., (1999). Ketoprofenpoly(DL-lactic-co-glycolic acid) microspheres: influence of manufacturing parameters and type of polymer on the release characteristics, *J Microencapsul*, **16**: 1-12

Garland M.J., Migalska K., Mahmood T.M., Singh T.R., Woolfson A.D., Donnelly R.F., (2011) Microneedle arrays as medical devices for enhanced transdermal drug delivery, *Expert Rev Med Devices*, **8**: 459-482

Garland M.J., Migalska K., Tuan-Mahmood T.M., Singh T.R.R., Majithija R., Caffarel-Salvador E., McCarthy H.O., Woolfson A.D., Donnelly A.F., (2012) Influence of skin model on in vitro performance of drug-loaded soluble microneedle arrays, *Int J Pharm*, **434**: 80-89

Garlotta D., (2001). A literature review of poly(lactic acid), *J Polym Environ*, **9**: 63-83

Gerstel M.S., Place V.A., (1976). Drug delivery device. Alza Corporation, United States, Patent: 3,964,482

Gill H.S., Prausnitz M.R., (2007). Coated microneedles for transdermal delivery, *J Control Release*, 117: 227-237

Ginde R., Gupta R., (1987). In vitro chemical degradation of poly(glycolic acid) pellets and fibers, J Appl Polym Sci, **33**: 2411-2429

Gittard S.D., Chen B., Xu H., Ovsianikov A., Chichkov B.N., Monteiro-Riviere N.A., Narayan N.J., (2012). The effects of geometry on skin penetration and failure of polymer microneedles, *J Adhesion Sci Technol*, **27**: 227-243

Giudice E.L., Campbell J.D., (2006). Needle-free vaccine delivery, *Adv Drug Deliv Rev*, **58**: 68-89

Ghafari R., Baradari A.G., Firouzian A., Nouraei M., Aarabi M., Zamani A., Emami Zeydi A., (2012). Cognitive deficit in first-time coronary artery bypass graft patients: a randomized clinical trial of lidocaine versus procaine hydrochloride, *Perfusion*, **27**: 320-325

Ghosh P., Brogden N.K., Stinchcomb A.L., (2013a). Effect of formulation pH on transport of naltrexone species and pore closure in microneedle-enhanced transdermal drug delivery, *Mol Pharm*, **10**: 2331-2239

Ghosh P., Pinninti R.R., Hammell D.C., Paudel K.S., Stinchcomb A.L., (2013b). Development of a codrug approach for sustained drug delivery across microneedletreated skin, *J Pharm Sci*, **102**:1458-1467

Goldberg S., (2008). 2D PAGE: Sample preparation and fractionation. Volume 1, In: Posch A, editor.Mechanical/physical methods of cell disruption and tissue homogenization, *Part 1, Humana Press*: 10-11

Greco FA., (2011). Therapeutic drug levels, MedlinePlus. A service of the U.S. National Library of Medicine, http://www.nlm.nih.gov/medlineplus/ency/article/003430.htm. Accessed: 22/04/13

Grossman J.I., Cooper J.A., Frieden J., (1969). Cardiovascular effects of infusion of lidocaine on patients with heart disease, *Am J Cardiol*, 24: 191-197

Gudin J., (2012). Opioid therapies and cytochrome P450 interactions, *J Pain Symptom Manage*, **44**: S4-S13

Gulrez S.K.H., Al-Assaf S., Phillips G.O., (2011). Progress in Molecular and Environmental Bioengineering – From Analysis and Modeling to Technology Applications*. Editor Capri A., Chapter 5, In: Hydrogels: Methods of preparation, characterisation and applications, InTech*: 126-131

Guo L., Qiu Y., Chen J., Zhang S., Xu B., Gao Y., (2013). Effective transcutaneous immunization against hepatitis B virus by a combined approach of hydrogel patch formulation and microneedle arrays, *Biomed Microdevices*, **15**: 1077-1085

Gupta J., Gill H.S., Andrews S.N., Prausnitz M.R., (2011a). Kinetics of skin resealing after insertion of microneedles in human subjects, *J Control Release*, **154**:148-155

Gupta J., Park S.S., Bondy B., Felner E.I, Prausnitz MR., (2011b). Infusion pressure and pain during microneedle injection into skin of human subjects, *Biomaterials*, **32**: 6823-6831

Gupta K.C., Ravi Kumar M.N.V., (2000). Semi-interpenetrating polymer network beads of crosslinked chitosan–glycine for controlled release of chlorphenramine maleate, *J Appl Polym Sci*, **76**: 672-683

Gupta P., Vermani K., Garg S., (2002). Hydrogels: from controlled release to pH-responsive drug delivery, *Drug Discov Today*, **7**: 570-579

Hamzah A.A., Aziz N.A., Majlis B.Y., Yunas J., Dee C.F., Bais B., (2012). Optimization of HNA etching parameters to produce high aspect ratio solid silicon microneedles, *J Micromec Microeng*, **22**: 1-10

Han M., Kim D.K., Kang S.H., Yoon H.R., Kim B.Y., Lee S.S., Kim K.D., Lee H.G., (2009). Improvement in antigen-delivery using fabrication of a grooves-embedded microneedle array, *Sens Actuators B Chem*, **137**: 274–280

Han T., Das D.B., (2013). Permeability enhancement for transdermal delivery of large molecule using low-frequency sonophoresis combined with microneedles, *J Pharm Sci*, **102**: 3614-3622

Han T.Y., Park K.Y., Ahn J.Y., Kim S.W., Jung H.J., Kim B.J., (2012). Facial skin barrier function recovery after microneedle transdermal delivery treatment, *Dermatol Surg*, **38**: 1816-1822

Hedge N.R., Kaveri S.V., Bayry J., (2011). Recent advances in the administration of vaccines for infectious diseases: microneedles as painless delivery devices for mass vaccination, *Drug Discov Today*, **16**: 1061-1068

Heilmann S., Küchler S., Wischke C., Lendlein A., Stein C., Schäfer-Korting M., (2013). A thermosensitive morphine-containing hydrogel for the treatment of large-scale skin wounds, *Int J Pharm*, **444**: 96-102

Hennick W.E., van Nostrum C.F., (2012). Novel crosslinking methods to design hydrogels, *Adv Drug Deliv Rev*, **64**: 223-236

Henry S., McAllister D.V., Allen M.G., Prausnitz M.R., (1998). Microfabricated microneedles: a novel approach to transdermal drug delivery, *J Pharm Sci*, **87**:922-925

Herwadkar A., Sachdeva V., Taylor L.F., Silver H., Banga A.K., (2012). Low frequency sonophoresis mediated transdermal and intradermal delivery of ketoprofen, *Int J Pharm*, **423**: 289-296

Hoare T.R., Kohane D.S., (2008). Hydrogels in drug delivery: Progress and challenges, *Polym*, **49**: 1993-2007

Hoffman A.S., (2002). Hydrogels for biomedical applications, *Adv Drug Deliv Rev*, **54**: 3-12

Hogan M.E., VanderVaart S., Permapaladas K., Márcio M., Einarson T.R., Taddio A., (2011). Systematic review and meta-analysis of the effect of warming local anesthetics on injection pain, *Ann of Emerg Med*, **58**: 86-98

Hruby J.M., (2001). LIGA technologies and applications. M R S Bull [online]. 337-340. www.mrs.org/publications/bulletin

Hu X., Lu Q., Sun L., Cebe P., Wang X., Zhang X., Kaplan D.L., (2010). Biomaterials from ultrasonication-induced silk fibroin-hyaluronic acid hydrogels, *Biomacromolecules*, **11**: 3178-3188

Huet P.M., Lelorier J., (1980). Effects of smoking and chronic hepatitis B on lidocaine and indocyanine green kinetics. *Clin Pharmacol Ther*, **28**: 208-215

Huang Y., Yu H., Xiao C., (2007). pH-sensitive cationic guar gum/poly (acrylic acid) polyelectrolyte hydrogels: Swelling and in vitro drug release, *Carbohyd Polym*, **69**: 774-783

Igaki M., Higashi T., Hamamoto S., Kodama S., Naito S., Tokuhara S., (2013). A study of the behaviour and mechanism of thermal conduction in the skin under moist and dry heat conditions, *Skin Res Technol*, **20**: 43-49

Ito Y., Ohta J., Imada K., Akamatsu S.,Tsuchida N., Inoue G., Inoue N., Takada K., (2013). Dissolving microneedles to obtain rapid local anesthetic effect of lidocaine at skin tissue, *J Drug Target*, **21**: 770-775

Jacobs I.C., (2014). Semi-solid formulations, *Pediatric Formulations*, *Chapter 12, Editors Bar-Shalom D., Rose K., Springer, New York*, 171-172

Jelvehgari M., Montazam H., (2011). Evaluation of mechanical and rheological properties of metronidazole gel as local delivery system, *Arch Pharmacal Res*, **34**: 931-940

Jenkins A.D., Kratochvíl P., Stepto R.F.T., Suter U.W., (1996). Glossary of basic terms in polymer science, *Pure Appl Chem*, **68**: 2304-2305

Jeon O., Bouhadir K.H., Mansour J.M., Alsberg E., (2009). Photocrosslinked alginate hydrogels with tunable biodegradation rates and mechanical properties, *Biomaterials*, **30**: 2724-2734

Jeong W.L., Park J.H., Prausnitz M.R., (2008). Dissolving microneedles for transdermal drug delivery, *Biomaterials*, **29**: 2113-2124

Jin K.M., Kim Y.H., (2008). Injectable, thermo-reversible and complex coacervate combination gels for protein drug delivery, *J Control Release*, **127**: 249-256

Johnson M.E., Blankschtein D., Langer R., (1997). Evaluation of solute permeation through the stratum corneum: lateral bilayer diffusion as the primary transport mechanism, *J Pharm Sci*, **86**:1162-1172

Jonker A.M., Löwik D.W.P.M., van Hest J.C.M., (2012). Peptide- and protein-based hydrogels, Chem Mater, **24**: 759-773

Kaewprapan K., Inprakhon P., Marie E., Durand A., (2012). Enzymatically degradable nanoparticles of dextran esters as potential drug delivery systems, *Carbohydr Polym*, **88**: 875-881

Kajjari P.B., Manjeshwar L.S., Aminabhavi T.M., (2011). Semi-interpenetrating polymer network hydrogel blend microspheres of gelatin and hydroxyethyl cellulose for controlled release of theophylline, *Ind Eng Chem Res*, **50**: 7833-7840.

Kalluri H., Banga A.K., (2011). Formation and closure of microchannels in skin following microporation, *Pharm Res*, **28**: 82-94

Kalpan G., Shalini V.S., Jonnalagadda S., Kumar N., (2007). Fast degradable poly(L-lactide-co-ε-caprolactone) microspheres for tissue engineering: synthesis, characterization, and degradation behavior, *J Polym Sci*, **A1 (45)**: 2755-2764

Kamel S., Ali N., Jahangir K., Shah S.M., El-Gendy A.A., (2008). Pharmaceutical significance of cellulose: A review, *Express Polym Lett*, **2**: 758-778

Kamoun E.A., Chen X., Mohy Eldin M.S., Kenawy E.S., (2015). Crosslinked poly(vinyl alcohol) hydrogels for wound dressing applications: A review of remarkably blended polymers, *Arab J Chem*, **8**: 1-14

Kang L., Jun H.W., McCall J.W., (2000). Physicochemical studies of lidocaine menthol binary systems for enhanced membrane transport, *Int J Pharm*, **206**: 35-42

Karadzovska D., Brooks J.D., Monteiro-Riviere N.A., Riviere J.E., (2013). Predicting skin permeability from complex vehicles, *Adv Drug Dev Rev*, **65**: 265-77

Katz N.P., Gammaitoni A.R., Davis M.W., Dworkin R.H., (2002). Lidocaine patch 5% reduces pain intensity and interference with quality of life in patients with postherpetic neuralgia: an effectiveness trial, *Pain Med*, **3**: 324-332

Kaur M., Ita K.B., Popova I.E., Parikh S.J., Bair D.A., (2014). Microneedle-assisted delivery of verapamil hydrochloride and amlodipine besylate, *Eur J Pharm Biopharm*, **86**: 284-291.

Ke C.J., Lin Y.J., Hu Y.C., Chiang W.L., Chen K.J., Yang W.C., Liu H.L., Fu C.C., Sung H.W., (2012). Multidrug release based on microneedle arrays filled with pH-responsive PLGA microsphere, *Biomaterials*, **33**: 5156-5165

Khanna P., Luongo K., Strom J.A., Bhansali S., (2010). Sharpening of hollow silicon microneedles to reduce skin penetration force, J Micromech Microeng, **20**: 1-8

Kim B.J., Kim H.J., Jung S.M., Sung J.K., Lee H.H., (2009). Fabrication of microneedle using laser written PDMS mold for molecular transport into plant skin, *Biochip J*, **3**: 281-286

Kim J.K., Kim H.J., Chung J.Y., Lee J.H., Young S.B., Kim Y.H., (2014). Natural and synthetic biomaterials for controlled drug delivery, *Arch Pharm Res*, **37**: 60-68.

Kim J.T., Han S.P., Jeong M.Y., (2004). A modified DXRL process for fabricating a polymer microstructure, *J Micromech Microeng*, **14**: 256-262.

Kim M.Y., Jung B., Park J.H., (2012a). Hydrogel swelling as a trigger to release biodegradable polymer microneedles in skin, *Biomaterials*, **33**: 668-678

Kim N.W., Lee M.S., Kim K.R., Lee J.E., Park J.S., Matsumoto Y., Jo D.G., Lee H., Lee D.S., Jeong J.H., (2014). Polyplex-releasing microneedles for enhanced cutaneous delivery of DNA vaccine*, J Control Release*, **179**: 11-17

Kim S.W., Temperature sensitive polymers for delivery of macromolecular drugs, in *Advanced Biomaterials in Biomedical Engineering and Drug Delivery Systems* (1996) Ogata N., Kim S.W., Feijen J., et al. (Eds), *Springer, Tokyo*: 126-133

Kim Y.C., Park J.H., Prausnitz M.R., (2012b). Microneedles for drug and vaccine delivery. *Adv Drug Deliv Rev*, **64**: 1547-1568

Kissin I., (2012). How does the lidocaine patch (5%) relieve pain? *Pain*, **153**: 1332–1333

Klose D., Siepmann F., Willart J.F., Descamps M., Siepmann J., (2010). Drug release from PLGA-based microparticles: effects of the ‘‘microparticle:bulk fluid’’ ratio, *Int J Pharm*, **383**: 123-131

Kochhar J.S, Lim W.X.S, Zou S., Foo W.Y., Pan J., Kang L., (2013). Microneedle integrated transdermal patch for fast onset and sustained delivery of lidocaine, *Mol Pharm*, **10**: 4272-4280

Kolli C.S., Banga A.K., (2008). Characterization of solid maltose microneedles and their use for transdermal delivery, *Pharm Res*, **25**:104-112

Koul V., Mohamed R., Kuckling D., Adler H.J.P., Choudhary V., (2011). Interpenetrating polymer network (IPN) nanogels based on gelatin and poly(acrylic acid) by inverse miniemulsion technique: Synthesis and characterization, *Colloid Surface B*, **83**: 204-213

Küchler S., Strüver K., Wolfgang F., (2013). Reconstructed skin models as emerging tools for drug absorption studies. *Expert Opin Drug Met*, **9**: 1255-1263

Kundu J., Mohapatra R., Kundu S.C., (2011). Silk fibroin/sodium carboxymethylcellulose blended ilms for biotechnological applications, *J Biomat Sci Polym E*, **22**: 519-539

Kurland N.E., Ragland R.B., Zhang A., Moustafa M.E., Kundu S.C., Yadavalli V.S., (2014). pH responsive poly amino-acid hydrogels formed via silk sericin templating, *Int J Biol Macromol*, **70**: 565-571

Kwon S.Y., (2004). In vitro evaluation of transdermal drug delivery by a micro-needle patch, *Controlled Release Society 31st Annual Meeting Transactions*, TheraJect Inc. no. 115

Laftah W.A., Hashim S., Ibrahim A.N., (2011). Polymer Hydrogels: A Review, *Polym-Plast Technol*, **50**: 1475-1486

Lai P.L., Hsu C.C., Liu T.H., Hong D.W., Chen L.H., Chen W.J., Chu I.M., (2012). Mixed micelles from methoxy poly(ethylene glycol)–polylactide and methoxy poly(ethylene glycol)–poly(sebacic anhydride) copolymers as drug carriers, *React Funct Polym*, **72**: 846-855

Lee B.R., Oh E.S., (2013). Effect of molecular weight and degree of substitution of a sodium-carboxymethyl cellulose binder on Li4Ti5O12 anodic performance, *J Phys Chem*, **117**: 4404−4409

Lee J.W., Park J.H., Prausnitz M.R., (2008). Dissolving microneedles for transdermal drug delivery, *Biomaterials*, **29**: 2113-2124

Lee J.W., Choi S.O., Felner E.I., Prausnitz M.R., (2011a). Dissolving microneedle patch for transdermal delivery of human growth hormone, *Small*, **7**: 531-539

Lee K., Lee CY., Jung H., (2011b)., Dissolving microneedles for transdermal drug administration prepared by stepwise controlled drawing of maltose, *Biomaterials*, **32**: 3134-3140

Lee S.J., Lee I.W., Lee Y.M., Lee H.B., Khang G., (2004). Macroporous biodegradable natural/synthetic hybrid scaffolds as small intestine submucosa impregnated poly(DL-lactideco-glycolide) for tissue-engineered bone, *J Biomater Sci Polym E*, **15**: 1003-1017

Lee S.W., Lee S.S., (2008). Shrinkage ratio of PDMS and its alignment method for the wafer level process, *Microsyst Technol*, **14**: 205-208

Lepock J.R., Frey H.E., Ritchie K.P., (1993). Protein denaturation in intact hepatocytes and isolated cellular organelles during heat shock, *J Cell Biol*, **122**: 1267-1276

Lhernould M.S., Delchambre A., (2011). Innovative design of hollow polymeric microneedles for transdermal drug delivery, *Microsyst Technol*, **17**: 1675-1682

Li X., Ma X., Zhu C., Luo Y., Lui B., Chen L., (2014). A novel injectable pH/temperature sensitive CS-HLC/*β*-GP hydrogel: The gelation mechanism and its properties, *Soft Mater*, **12**: 1-11

Li X., Zhao R., Qin Z., Zhang J., Zhai S., Qui Y., Gao Y., Xu B., Thomas S.H., (2010). Microneedle pretreatment improves efficacy of cutaneous topical anesthesia, *Am J Emergency Med*, **28**: 130-134

Li X.G., Zhao R.S., Qin Z.L., Gao Y.H., Zhang J., Zhai S.D., Xu B., (2008). Painless microneedle transdermal patch enhances permeability of topically applied lidocaine, *Chinese J New Drugs*, **17**: 597-601

Li Y., McClements D.J., (2011). Controlling lipid digestion by encapsulation of protein-stabilized lipid droplets within alginate-chitosan complex coacervates, *Food Hydrocolloids*, **25**: 1025-1033

Lidoderm (lidocaine) patch, (2013). Current comprehensive medication information about marketed drugs. In: U.S. National library of medicine. *Daily Med*, http://dailymed.nlm.nih.gov/dailymed/ lookup.cfm?setid=5ffefcdc-ebfa-4dc8-b484-719658da9d6d (Accessed: 13/06/2014).

Lin C.C., Metters A.T., (2006). Hydrogels in controlled release formulations: Network design and mathematical modelling, *Adv Drug Deliver Rev*, **58**: 1379-1408

Lippmann J.M., Pisano A.P., (2006). In-plane, hollow microneedles via polymer investment molding. *Proceedings: IEEE Micro Electro Mechanical Systems Workshop*: 262-265

Lippmann J.M., Geiger E.J., Pisano A.P., (2007). Polymer investment molding: method for fabricating hollow, microscale parts, *Sens Actuators A Phys*, **134**: 2-10

Liu H.Y., Li D., Guo S.D., (2007). Studies on collagen fromthe skin of channel catfish (Ictalurus punctaus), *Food Chem*, **101**: 621-625

Liu P., Bergstrom T.K., (1996). Quantitative evaluation of aqueous isopropyl alcohol enhancement on skin flux of terbutaline (Sulfate). 2. Permeability contributions of equilibrated drug species across human skin in vitro, *J Pharm Sci*, **85**: 320-325

Loo S.C.J., Tan Z.Y.S., Chow Y.S., Lin S.L.I., (2010). Drug release from irradiated PLGA and PLLA multi-layered films, *J Pharm Sci*, **99**: 3060-3071

Lorenz H., Despont M., Fahrni N., La Bianca N., Renand P., Vettiger P., (1997). SU-8: a low-cost negative resist for MEMS, *J Micromech Microeng*, **7**: 121-124

Luo Y., Kirker K.R., Prestwich G.D., (2000). Cross-linked hyaluronic acid hydrogel films: new biomaterials for drug delivery, *J Control Release*, **69**: 169-184

Luckachan G.E., Pillai C.K.S., (2011). Biodegradable polymers-a review on recent trends and emerging perspective, *J Polym Environ*, **19**: 637-676

Marasso S.L., Canavese G., Cocuzza M., (2011). Cost efficient master fabrication process on copper substrates. *Microelectron Eng,* **88**: 2322-2324

Marquez A.L., (2007). Water in oil (w/o) and double (w/o/w) emulsions prepared with spans: microstructure, stability, and rheology, *Colloid Polym Sci*, **285**: 1119–1128

Martín del Valle E.M., Galán M.A., Carbonell R.G., (2009). Drug delivery technologies: The way forward in the new decade, *Ind Eng Chem Res*, **48**: 2475-2486

Martin C.J., Allender C.J., Brain K.R., Morrissey A., Birchall J.C., (2012). Low temperature fabrication of biodegradable sugar glass microneedles for transdermal drug delivery applications, *J Control Release*, **158**: 93-101

Martinenghi S., Caretto A., Losio C., Scavini M., Bosi E., (2015). Successful treatment of Dercum's disease by transcutaneous electrical stimulation, *Medicine*, **94**: 1-5

Matricardi P., Meo C.D., Coviello T., Hennink W.E., Alhaique F., (2013). Interpenetrating polymer networks polysaccharide hydrogels for drug delivery and tissue engineering, *Adv Drug Deliv Rev*, **65**: 1172-1187

Matteucci M., Fanetti M., Casella M., Gramaica F., Gaviolo L., Tormen M., Grenci G., De Angelis F., Di Fabrizio E., (2009). Poly vinyl alcohol re-usable masters for microneedle replication, *Microelectron Eng*, **86**: 752-756

Mattioli S., Kenny J.M., Armentano I., (2012). Plasma surface modification of porous PLLA films: analysis of surface properties and in vitro hydrolytic degradation, *J Appl Polym Sci*, **125**: E239-E247

Mazarro R., Cabezas L.I., De Lucas A., Garcia I., Rodríguez J.F., (2009). Study of different catalysts and initiators in bulk copolymerization of DL-lactide and glycolide, *J Macromol Sci A*, **46**: 1049-1059

Mehta R., Kumar V., Bhunia H., Upadhyay S.N., (2005). Synthesis of poly(lactic acid): a review, *J Macromol Sci Pol R*, **45**: 325-349

Merino G., Kalia Y.N., Delgado-Charro M.B., Potts R.O., Guy R.H., (2003). Frequency and thermal effects on the enhancement of transdermal transport by sonophoresis, *J Control Release*, **88**: 85-94

Meyer W., Kacza J., Zschemisch N.H., Godynicki S., Seeger J., (2007). Observations on the actual structural conditions in the stratum superficiale dermis of porcine ear skin, with special reference to its use as model for human skin, Ann Anat,**189**: 143-156

Microchem Corp. Material Safety Data Sheet (MSDS). www.microchem.com

Milewski M., Paudel K.S., Brogden N.K., Ghosh P., Banks S.L., Hammell D.C., Stinchcomb A.L., (2013). Microneedle-assisted percutaneous delivery of naltrexone hydrochrloride in yucatan minipig: in vitro-in vivo correlation, *Mol Pharm*, **10**: 3745-3757

Milewski M., Stinchcomb A., (2011). Vehicle composition influence on the microneedle-enhanced transdermal flux of naltrexone hydrochloride, *Pharm Res*, **28**: 124-134

Miller P.R., Gittard S.D., Edwards T.L., Lopez D.M., Xiao X., Wheeler D.R., Monteiro-Riviere N.A., Bozik S.M., Polsky R., Narayan R.J., (2011). Integrated carbon fiber electrodes within hollow polymer miconeedles for transdermal electrochemical sensing, *Biomicrofluidics*, **5**: 013415

Mitragotri S., (2003). Modeling skin permeability to hydrophilic and hydrophobic solutes based on four permeation pathways, *J Control Release*, **86**: 69-92

Miyano T., Tobinaga Y., Kanno T., Matsuzaki Y., Takeda H., Wakui M., Hanada K., (2005). Sugar micro needles as transdermic drug delivery system, *Biomed Microdev*, **7**: 185-188

Monheit G.D., Campbell R.M., Neugent H., Nelson C.P., Prather C.L., Bachtell N., Holmdahl L., (2009). Reduced pain with use of proprietary hyaluronic acid with lidocaine for correction of nasolabial folds: a patient-blinded, prospective, randomised controlled trial, *Dermatol Surg*, **36**: 94-101

Moreno E., Schwartz J., Larrañeta E., Nguewa P.A., Sanmartín C., Agüeros M., Irache J.M., Espuelas S., (2014). Thermosensitive hydrogels of poly(methyl vinyl ether-co-maleic anhydride) – Pluronic® F127 copolymers for controlled protein release, *Int J Pharm*, **459**: 1-9

Moser K., Kriwet K., Naik A., Kalia Y.N., Guy R.H., (2001). Passive skin penetration enhancement and its quantification in vitro, *Euro J Pharm Biopharm*, **52**: 103-112

Mu C., Guo J., Li X., Lin W., Lin D., (2012). Preparation and properties of dialdehyde carboxymethyl cellulose crosslinked gelatin edible films, *Food Hydrocolloid*, **27**: 22-9

Mueller R.S., Bergval K., Bensignor E., Bond R., (2012). A review of topical therapy for skin infections with bacteria and yeast, *Vet Dermatol*, **23**: 330-341

Mundargi R.C., Babu V.R., Rangaswamy V., Patel P., Aminabhavi T.M., (2008). Nano/micro technologies for delivering macromolecular therapeutics using poly(DL-lactide-co-glycolide) and its derivatives. *J Control Release* **125**: 193-209

Muzzarelli R.A.A., (2009). Genipin-crosslinked chitosan hydrogels as biomedical and pharmaceutical aids, *Carbohyd Polym*, **77**: 1-9

Naegel A., Heisig M., Wittum G., (2013) Detailed modeling of skin penetration—an overview, *Adv Drug Deliver Rev*, **65**: 191-207

Nagai T., Arakib Y., Suzukia N., (2002). Collagen of the skin of ocellate puffer fish (Takifugu rubripes), *Food Chem*, **78**: 173-177

Naidu B.V.K., Paulson A.T., (2011). A new method for the preparation of gelatin nanoparticles encapsulation and drug release characteristics, *J Appl Polym Sci*, **121**: 3495-500

Nayak A., Das D.B., Vladisavljević G.T., (2014a). Microneedle assisted permeation of lidocaine carboxymethylcellulose with gelatine co-polymer hydrogel, *Pharm Res*, **31**:1170-1184

Nayak A., Babla H., Han T., Das D.B., (2014b). Lidocaine carboxymethylcellulose with gelatine co-polymer hydrogel delivery by combined microneedle and ultrasound, *Drug Deliv*, **23**: 668-679

Nayak A., Das D.B., (2013). Potential of biodegradable microneedles as a transdermal delivery vehicle for lidocaine, *Biotechnol Lett*, **35**: 1351-1363

Nayak A., Short L., Das D.B., (2015). Lidocaine permeation from a lidocaine NaCMC/gel microgel formulation in microneedle pierced skin: vertical (depth averaged) and horizontal permeation profiles, *Drug Deliv Transl Res*, 5: 372-386

Nguyen M.K., Lee D.S., (2010). Bioadhesive PAA-PEG-PAA Triblock copolymer hydrogels for drug delivery in oral cavity, *Macromol Res*, **18**: 284-288

Nir Y., Paz A., Sabo E., Potasman I., (2003). Fear of injections in young adults: prevalence and associations, *Am J Trop Med Hyg*, **68**: 341-344

Nonoyama T., Ogasawara H., Tanaka M., Higuchi M., Kinoshita T., (2012). Calcium phosphate biomineralization in peptide hydrogels for injectable bone-filling materials, *Soft Matter*, **8**: 11531-11536

Olatunji O., Das D.B., (2010). Painless drug delivery using microneedles. Current technologies to increase the transdermal delivery of drugs (Editor: Joan Escober Chavez). *Bentham Science Publishers*, ISBN: 978-1-60805-191-5 (available online at http://www.benthamdirect.org/pages/b_getarticlebybook.php)

Olatunji O., Das D.B., (2011). Drug delivery using microneedles. Comprehensive biotechnology. In: Zhanfeng Cui. 2nd Edition, *Elsevier*, UK, ISBN: 13: 978-0-444-53352-4

Olatunji O., Das D.B., Garland M.J., Belaid L., Donnelly R.F., (2013). Influence of array interspacing on the force required for successful microneedle skin penetration: theoretical and practical approaches, *J Pharm Sci*, **102**: 1209-1221

Olatunji O., Das D.B., Nassehi V., (2012). Modelling transdermal drug delivery using microneedles: effect of geometry on drug transport behaviour, *J Pharm Sci*, **101**:164-175

Olatunji O., Igwe C.C., Ahmed A.S., Alhassan D.O.A., Asieba G.O., Das D.B., (2014). Microneedles from fish scale biopolymer, *J Appl Polym Sci*, **131**:1-10

Olkkola K.T., Isohanni M.H., Hamunen K., Neuvonen P.J., (2005). The effect of erythromycin and fluvoxamine on the pharmacokinetics of intraveneous lidocaine, *Anesth Analg*, **100**: 1352-1356

Orive G., Hernandez R.M., Gascon A.R., Dominguez-Gil A., Pedraz J.L, (2003). Drug delivery in biotechnology: present and future, *Curr Opin Biotech*, **14**: 659–664

Ouyang C.P., Ma G., Zhao S.X., Wang L., Wu L.P., Wang Y., Song C.X., Zhang Z.P., (2011). Preparation and characterization of the molecular weight controllable poly(lactide-co-glycolide), *Polym Bull*, **67**: 793–803

Padmanabhan M., Rahoof T.E., Vipin Raj V.M., Vivek K.K., (2014). Pneumatic stretcher chair device for paralysed patients, *IJRET*, **3**: 546-553

Park J.H., Choi S.O., Kamath R., Yoon Y.K., Allen M.G., Prausnitz M.R., (2007a). Polymer particle-based micromolding to fabricate novel microstructure, *Biomed Microdev*, **9**: 223-234

Park J.H., Davis S., Yoon Y.K., Prausnitz M.R., Allen M.G., (2003). Micromachined biodegradable microstructures. *In The 16th Annual International Conference on Micro Electro Mechanical Systems, IEEE*, Piscataway, NJ: 371-374

Park J.H., Lee J.W., Kim Y.C., Prausnitz M.R., (2008). The effect of heat on skin permeability, *Int J Pharm*, **359**: 94-103

Park J.H., Yoon Y.K., Choi S.O., Prausnitz M.R., Allen M.G., (2007b). Tapered conical polymer microneedles fabricated using an integrated lens technique for transdermal drug delivery, *IEEE Trans Biomed Eng*, **54**: 903-913

Park N., Kwon B., Kim I.S., Cho J., (2005). Biofouling potential of various NF membranes with respect to bacteria and their soluble microbial products (SMP): characterizations, flux decline, and transport parameters, *J Membr Sci*, **258**: 43-54

Patel S.R., Lin A.S.P., Edelhauser H.F., Prausnitz MR., (2011). Suprachoroidal drug delivery to the back of the eye using hollow microneedles, *Pharm Res*, **28**: 166-76

Peira E., Turci F., Corazzari I., Chirio D., Battaglia L., Fubini B., Gallarate M., (2014). The influence of surface charge and photo-reactivity on skinpermeation enhance property of nano-TiO2 in ex vivo pig skin model under indoor light, *Int J Pharm*, **467**: 90-99

Petrisor G., Ion R.M., Brachais C.H., Couvercelle J.P., Chambin O., (2012). Designing medical devices based on silicon polymeric material with controlled release of local anaesthetics, *J Macromol Sci A*, **49**: 439-444

Pietrzak W.S., Verstynen M.L., Sarver D.R., (1997). Bioabsorbable polymer science for the practicing surgeon, *J Craniofac Surg*, **8**: 2-92

Poet T.S., McDougal J.N., (2002). Skin absorption and human risk assessment, *Chem-Biol Interact*, **140**:19-34

Polat B., Hart D., Langer R., Blankschtein D., (2011). Ultrasound-mediated transdermal drug delivery: mechanisms, scope, and emerging trends, *J Control Release*, **152**: 330-348

Pregerson D.B., (2007). Suturing and wound closure: How to achieve optimal healing, *Consultant*, **47**: 1-7

Proprietary Prevelle Silk. www.mentorcorp.com [Accessed on 7/01/2013]

Proprietary Xylocaine. http://www.astrazeneca.co.uk/medicines/products-az/Product/xylocaine [Accessed on 7/01/2013]

Pushpamalar V., Langford S.J., Ahmad M., Lim Y.Y., (2006). Optimization of reaction conditions for preparing carboxymethyl cellulose from sago waste, *Carbohyd Polym*, **64**: 312-318

Qiu Y., Park K., (2012). Environment-sensitive hydrogels for drug delivery, *Adv Drug Deliv Rev*, **64**: 49-60

Quinn R.H., Wedmore I., Johnson E., Islas A., Anglim A., Zafren K., Bitter C., Mazzorana V., (2014). Wilderness medical society practice guidelines for basic wound management in the austere environment, *Wild Environ Med*, **25**: 295-310

Qvortrup K., Taveras K.M., Trastrup O., Nielsen T.E., (2011). Chemical synthesis on SU-8, *Chem Commun*, **47**: 1309-1311

Raphael A.P., Meliga S.C., Chen X., Fernando G.J.P., Flain C., Kendall M.A.F., (2013). Depth-resolved characterization of diffusion properties within and across minimally-perturbed skin layers, *J Control Release*, **166**: 87-94

Rokhade A.P., Agnihotri S.A., Patil S.A., Mallikarjuna N.N., Kulkarni P.V., Aminabhavi T.M., (2006). Semi-interpenetrating polymer network microspheres of gelatin and sodium carboxymethyl cellulose for controlled release of ketorolac tromethamine, *Carbohyd Polym*, **65**: 243-252

Roxhed N., Gasser T.C., Griss P., (2007)., Penetration-enhanced ultrasharp microneedles and prediction on skin interaction for efficient transdermal drug delivery, *J Microelectromecha Syst*, **16**: 1429-1440

Raphael A.P., Prow T.W., Crichton M.L., Chen X., Fernando G.J.P., Kendall M.A.F., (2010). Targeted, needle-free vaccinations in skin using multilayered, densely-packed, dissolving microprojection arrays, *Small*, **6**: 1785-1793

Rathna G.V.N., Chatterji P.R., (2003). Controlled drug release from gelatin-sodium carboxymethylcellulose interpenetrating polymer networks, *J Macromol Sci A*, **A40**: 629-639

Richter A., Paschew G., Klatt S., Lienig J., Arndt K.F., Adler H.J.P., (2008). Review on hydrogel-based pH sensors and microsensors, *Sensors*, **8**: 561-581

Riddick T.M., (1968) Control of colloid stability through zeta potential. *Zeta Meter Incorporated, New York, Volume 1*

Ro A.J., Falotico R., Davé V., (2012). Morphological and degradation studies of sirolimus-containing poly(lactide-coglycolide) discs, *J Biomed Mater Res B*, **100B**: 767-777

Roy T.B.V., Blanch H.W., Wilke C.R., (1982). Lactic acid production by Lactobacillus delbreuckill in a hollow fiber fermentor, *Biotechnol Lett*, **4**: 483-488

Ryu W.H., Vyakarnam M., Greco R.S., Prinz F.B., Fasching R.J., (2007). Fabrication of multi-layered biodegradable drug delivery device based on micro-structuring of PLGA polymers, *Biomed Microdevices*, **9**: 845-853

Safavieh R., Pla Roca M., Qasaimeh M.A., Mirzaei M., Juncher D., (2010). Straight SU-8 pins, *J Micromech Microeng*, **20**:1-9

Saliterman S.S., (2006). Fundamentals of bioMEMS and medical microdevices. *Wiley Interscience*: 531, ISBN: 0-8194-5977-1

Scheuplein R.J., Blank I.H., Brauner G.J., MacFarlane D.J., (1969). Percutaneous absorption of steroids, *J Invest Dermatol*, **52**: 63-70

Schramm L.L., (2005). Emulsions, foams, and suspensions, Chapter 5, in Colloid Stability, *Wiley-VCH, Verlag GmbH & Co*, 128-130

Schreiber S., Ronfani L., Chiaffoni G.P., Matarazzo L., Minute M., Panontin E., Poropat F., Germani C., Barbi E., (2013). Does EMLA cream application interfere with the success of venepuncture or venous cannulation? A prospective multicentre observational study, *Eur J Pediatr*, **172**: 265-268

Schulz M., Iwersen-Bergmann S., Andresen H., Schmoldt A., (2012). Therapeutic and toxic blood concentrations of nearly 1,000 drugs and other xenobiotics, *Crit Care*, **16**: R136

Schwindt D.A., Wilhelm K.P., Maibach I., (1998). Water diffusion characteristics of human stratum corneum at different anatomical sites in vivo, *J Invest Dermatol*, **111**: 385-389

Sekkat N., Kalia Y.N., Guy R.H., (2004). Porcine ear skin as a model for the assessment of transdermal drug delivery to premature neonates, *Pharm Res*, **21**: 1390-1397

Shah U.U., Roberts M., Orlu G.M., Tuleu C., Beresford M.W., (2011). Needle-free and microneedle drug delivery in children: a case for disease-modifying antirheumatic drugs (DMARDs), *Int J Pharm*, **416**:1-11

Shaikh V.R., Dagade D.H., Hundivale D.G., Patil K.J., (2011). Volumetric studies of aqueous solutions of local anesthetical drug compounds [hydrochlorides of procaine (PC HCl), lidocaine (LC HCl) and tetracaine (TC HCl)] at 298.15 K, *J Mol Liq*, **164**: 239-242

Shakeel M., Pathan Dilnawaz N., Ziyaurrrahman A.R., Akber B., Bushra S., (2011). Microneedle as a novel drug delivery system: a review, *Int Res J Pharm*, **2**: 72-77

Shipton E.A., (2012). Advances in delivery systems and routes for local anaesthetics, *Trends Anaesth Critic Care*, **2**: 228-33

Silva A., Santos D., Ferreira D., Souto E., (2007). Characterization of ibuprofen loaded solid lipid nanoparticles dispersed in semi-solid carbopol gels, *J Biotechnol*, **6**: S67-S68

Singh I., Morris A.P., (2011). Performance of transdermal therapeutic systems: effects of biological factors, *Int J Pharm Invest*, **1**: 4-9

Singh N.D., Banga A.K., (2013). Controlled delivery of ropinirole hydrochloride through skin using modulated iontophoresis and microneedles, *J Drug Target*, **21**: 354-366

Singh N.K., Lee D.S., (2014). In situ gelling pH- and temperature-sensitive biodegradable block copolymer hydrogels for drug delivery, *J Control Release*, **193**: 214-277

Sintov A.C., Shapiro L., (2004). New microemulsion vehicle facilitates percutaneous penetration in vitro and cutaneous drug bioavailability in vivo, *J Control Release*, **95**: 173-183

Sivamani R., Stoeber B., Wu G., Zhai H., Liepmann D., Maibach H., (2005). Clinical microneedle injection of methly nicotinate: stratum corneum penetration, *Skin Res Technol*, **11**: 152-156

Smith B.C., Wilson A.H., (2013). Topical versus injectable analgesics in simple laceration repair: An integrative review, *JNP*, **9**: 374-80

Smith D.W., Peterson M.R., DeBerard S.C., (1999). Regional anesthesia: nerve blocks of the extremities and face, *Postgrad Med*, **106**: 69-73

Sobanko J.F., Miller C.J., Alster T.S., (2012). Topical anesthetics for dermatologic procedures: a review, *Dermatol Surg*, **38**: 709-721

Song F., Zhang L.M., Yang C., Yan L., (2009). Genipin-crosslinked casein hydrogels for controlled drug delivery, *Int J Pharm*, **373**: 41-47

Sonia T.A., Sharma C.P., (2012). An overview of natural polymers for oral insulin delivery, *Drug Discov Today*, **17**: 784-792

Steluti R., Scarmato De Rosa F., Collett J., Tedesco A.C., Lopes Badra Bentley MV., (2005). Topical glycerol monooleate/propylene glycol formulations enhance 5-aminolevulinic acid in vitro skin delivery and in vivo protophorphyrin IX accumulation in hairless mouse skin, *Euro J Pharm Biopharm*, **60**: 439-444

Stenson R.E., Constantino R.T., Harrison D.C., (1971). Interrelationships of hepatic blood flow, cardiac output, and blood levels of lidocaine in man, *Circulation*, **43**: 205-211

Strat-M. Compound Correlation Tool. Lidocaine (Analgesic) http://fa24f31db0da67276cd1430be593b508d6f5ef1fdddadaa02b1fbea.r66.cf1.rackcdn.com/stratm2.html (Accessed: 08/04/2015).

Subedi R.K., Oh S.Y., Chun M.K., Choi H.K., (2010). Recent advances in transdermal drug delivery, *Arch Pharm Res*, **33**: 339-351

Sullivan S.P., Murthy N., Prausnitz M.R., (2008). Minimally invasive protein delivery with rapidly dissolving polymer microneedles, *Adv Mater*, **20**: 933-938

Swindle M., (2008). Porcine integumentary system models: part 1—dermal toxicology, *Sinclair Research Centre*

Sze A., Erickson D., Ren L., Li D., (2003). Zeta-potential measurement using the Smoluchowski equation and the slope of the current-time relationship in electroosmotic flow, *J Colloid Interface Sci*, **261**: 402-410

Tataru G., Popa M., Desbrieres J., (2011). Microparticles of hydrogel type based on carboxymethylcellulose and gelatin for controlled release of water soluble drugs, *Revue Roumaine de Chimie*, **56**: 399 +

Teeranachaideekul V., Souto E.B., Müller R.H., Junyaprasert V.B., (2008). Physicochemical characterization and in vitro release studies of ascorbylpalmitate-loaded semi-solid nanostructured lipid carriers (NLC gels), *J Microencapsul*, **25**: 111-120

Texmac Inc (USA). www.texmac.com [accessed on 14/12/2013]

Thaysen A.C., Morris A.R., (1947). The use of hydrofluoric acid in making glass microneedles, *J Gen Microbiol*, **221**: 641

Todo H., Kimura E., Yasuno H., Tokudome Y., Hashimoto F., Ikarashi Y., Sugibayashi K., (2010). Permeation pathway of macromolecules and nanospheres through skin, *Biol Pharm Bull*, **33**: 1394-1399

Tojo K., (2005). Mathematical models of transdermal and topical drug delivery, 2nd Edn. Japan: *Biocom systems Inc*

Trautmann A., Heuck F., Mueller C., Ruther P., Paul O., (2005). Replication of microneedle arrays using vacuum casting and hot embossing. *Transducers* **2**: 1420-1423

Tsioris K., Raja W.K., Pritchard E.M. Panilaitis B., Kaplan D.L., Omenetto F.G., (2012).

Fabrication of silk microneedles for controlled-release drug delivery, *Adv Funct Mater*, **22**: 330-335

Tzeng Y.S., Chen S.G., (2012). Tumescent technique in digits: a subcutaneous single-injection digital block, *Am J Emerg Med*, **30**: 592-596

Uchida T., Kadhum W.R., Kanai S., Todo H., Oshizaka T., Sugibayashi K., (2015). Prediction of skin permeation by chemical compounds using the artificial membrane, Strat-M™, Eur J Pharm Sci, **67**: 113-118

Ullah I., Baloch M.K., Durrani G.F., (2012), Solubility of lidocaine in ionic, nonionic and zwitterionic surfactants, *J Solut Chem*, **41**: 215-222

Valenta C., (2005). The use of mucoadhesive polymers in vaginal delivery, *Adv Drug Deliver Rev*, **57**: 1692-1712

Van der Maaden K., Jiskoot W., Bouwstra J., (2012). Microneedle technologies for (trans)dermal drug and vaccine delivery, *J Control Release*, **161**: 645-655

Van Vlierberghe S., Dubruel P., Schacht E., (2011). Biopolymer-based hydrogels as scaffolds for tissue engineering applications: A review, *Biomacromolecules*, **12**: 1387-1408

Venkata Prasad C., Sudhakar H., Yerri Swamy B., Reddy V., Reddy C.L.N., Suryanarayana C., Prabhakar M.N., Subha M.C.S., Chowdoji Rao K., (2011). Miscibility studies of sodium carboxymethylcellulose/poly(vinyl alcohol) blend membranes for pervaporation dehydration of isopropyl alcohol, *J Appl Polym Sci*, **120**: 2271-2281

Victoria Klang V., Schwarz J.C., Haberfeld S., Xiao P., Wirth M., Valenta C., (2013). Skin integrity testing and monitoring of in vitro tape stripping by capacitance-based sensor imaging, *Skin Res Technol*, **19**: e259-272

Viero Y., He Q., Mazenq L., Ranchon H., Fourniols J.Y., Bancaud A., (2012). Efficient prototyping of large-scale pdms and silicon nanofluidic devices using PDMS-based phase-shift lithography, *Microfluid Nanofluid*, **12**: 465-473

Viglianti B.L., Dewhirst M.W., Abraham J.P., Gorman J.M., Sparrow E.M., (2014). Rationalization of thermal injury quantification methods: applications to skin burns, *Burns*, **40**: 896-902

Wagner H., Kostka K.H., Lehr C.M., Schaefer U.F., (2000). Drug distribution in human skin using two different in vitro test systems: comparison with in vivo data, *Pharm Res*, **17**: 1475-1481

Wahit M.U., Akos N.I., Laftah W.A., (2012) Influence of natural fibers on the mechanical properties and biodegradation of poly(lactic acid) and poly(ε-caprolactone) composites: a review, *Polym Compos*, **33**: 1045-1053

Walraven J.A., (2003). Introduction to applications and industries for microelectromechanical systems (MEMS), *International Test Conference Proceedings IEEE*: 674-680

Wang M.W., Jeng J.H., (2009). Optimal molding parameter design of pla micro lancet needles using the taguchi method, *Polym Plast Technol*, **48**: 730-735

Wang X.L., Yang K.K., Wang Y.Z., (2003). Properties of starch blends with biodegradable polymers, *Polym Rev*, **43**: 358-409

Web of Knowledge, (2014). Search engine for obtaining specific scientific literature and citations. Thomson Reuters. http://apps.webof knowledge.com. [Accessed on 31/12/2014]

Wilson J.R., Kehl L.J., Beiraghi S., (2008). Enhanced topical anesthesia of 4% lidocaine with microneedle pretreatment and iontophoresis, *Northwest Dentistry*, **87**: 40-41

Wolloch L., Kost J., (2010). The importance of microjet vs shock wave formation in sonophoresis, *J Controlled Release*, **148**: 204-211

Woodruff C., Wieczorek P.M., Schricker T., Vinet B., Backman S.B., (2010). Atomised lidocaine for airway topical anaesthesia in the morbidly obese: 1 % compared with 2 %, *Anaesthesia*, **65**: 12-17

Woodruff M.A., Hutmaker D.W., (2010). The return of a forgotten polymer-polycaprolactone in the 21st century, *Prog Polym Sci*, **35**: 1217-1256

Xia Y., Chen E., Tibbits D.L., Reilley T.E., McSweeney T.D., (2002). Comparison of effect of lidocaine hydrochloride, buffered lidocaine, diphenhydramine, and normal saline after intradermal injection, *J Clin Anesth*, 14: 339-343

Xiangdong Ye., Liu H., Ding Y., Li H., Lu B., (2009). Research on the cast molding process for high quality PDMS molds, *Microelectron Eng*, **86**: 310-313

Xu R., Wu C., Xu H., (2007). Particle size and zeta potential of carbon black in liquid media, *Carbon*, **45**: 2806-2809

Yang K., Zhang L., Liang Z., Xhang Y., (2012a). Protein-imprinted materials: rational design, application and challenges, *Anal Bional Chem*, **403**: 2173-2183

Yang S., Feng Y., Zhang L., Chen N., Yuan W., Jin T., (2012b). A scalable fabrication process of polymer microneedle, *Int J Nanomed*, **7**: 1415-1422

York P., (1996). New materials and systems for drug delivery and targeting. *Spec Publ R Soc Chem* **178**: 1-10

Yeu-Chun K., Park J.H., Prausnitz M.R., (2012). Microneedles for drug and vaccine delivery, *Adv Drug Deliver Rev*, **64**:1547-1568

You X., Chang J.H., Ju B.K., Pak J.J., (2011). Rapidly dissolving fibroin microneedles for transdermal drug delivery, *Mat Sci Eng C*, **31**: 1632-1636

Youn S.W., Okuyama C., Takahasi M., Maeda R., (2008). A study on fabrication of silicon mold for polymer hot-embossing using focused ion beam milling, *J Mater Process Tech*, **201**: 548-553

Zhang D., Das D.B., Rielly C.D., (2014). Potential of microneedle-assisted micro-particle delivery by gene guns: a review, *Drug Deliv*, **21**: 571-587

Zhang J., Tan K.L., Gong H.Q., (2001). Characterization of the polymerization of SU-8 photoresist and its applications in micro-electro-mechanical systems (MEMS), *Polym Test*, **20**: 693-701

Zhang Y., Brown K., Siebenaler K., Determan A., Dohmeier D., Hansen K., (2012a). Development of lidocaine-coated microneedle product for rapid, safe, and prolonged local analgesic action, *Pharm Res*, **29**: 170-177

Zhang Y., Siebenaler K., Brown K., Dohmeier D., Hansen K., (2012b). Adjuvants to prolong the local anesthetic effects of coated microneedle products, *Int J Pharm*, **439**: 187-92

Zhao F., Qin X., Feng S., Gao Y., (2014). Preparation of microgel composite hydrogels by heating natural drying microgel composite polymers, *J Appl Polym Sci*, **131**: 1-7

Zhao J., Mayes R.H., Chen G., Chan P.S., Xiong Z.J., (2003). Polymer micromould design and micromoulding process, *Plast, Rubber Compos*, **32**: 240-247

Zhao X., Liu J.P., Zhang X., Li Y., (2006). Enhancement of transdermal delivery of theophylline using microemulsion vehicle, *Int J Pharm*, **327**: 58-64